PNL-10826
UC-721

Minimum Additive Waste Stabilization Using Vitreous Ceramics

Interim Progress Report

October 1994 - September 1995

X. Feng
W. K. Hahn
W. Gong*
L. Wang *
M. Gong
R. C. Ewing*

Pacific Northwest Laboratory
Richland, Washington 99352

*University of New Mexico
Department of Earth and Planetary Sciences
Albuquerque, New Mexico 87131

DISTRIBUTION OF THIS DOCUMENT IS UNLIMITED

MASTER

DISCLAIMER

This report was prepared as an account of work sponsored by an agency of the United States Government. Neither the United States Government nor any agency thereof, nor Battelle Memorial Institute, nor any of their employees, makes **any warranty, express or implied, or assumes any legal liability or responsibility for the accuracy, completeness, or usefulness of any information, apparatus, product, or process disclosed, or represents that its use would not infringe privately owned rights**. Reference herein to any specific commercial product, process, or service by trade name, trademark, manufacturer, or otherwise does not necessarily constitute or imply its endorsement, recommendation, or favoring by the United States Government or any agency thereof, or Battelle Memorial Institute. The views and opinions of authors expressed herein do not necessarily state or reflect those of the United States Government or any agency thereof.

PACIFIC NORTHWEST NATIONAL LABORATORY
operated by
BATTELLE
for the
UNITED STATES DEPARTMENT OF ENERGY
under Contract DE-AC06-76RLO 1830

Printed in the United States of America

Available to DOE and DOE contractors from the Office of Scientific and Technical Information, P.O. Box 62, Oak Ridge, TN 37831; prices available from (615) 576-8401.

Available to the public from the National Technical Information Service, U.S. Department of Commerce, 5285 Port Royal Rd., Springfield, VA 22161


This document was printed on recycled paper.

DISCLAIMER

Portions of this document may be illegible in electronic image products. Images are produced from the best available original document.

Abstract

Vitreous ceramic waste forms are being developed at Pacific Northwest Laboratory to complement glass waste forms in implementing the Minimum Additive Waste Stabilization (MAWS) Program to support the U.S. Department of Energy's environmental restoration efforts. These vitreous ceramics are composed of various metal-oxide crystalline phases embedded in a silicate-glass phase. This work extends the success of vitreous ceramic waste forms to treat wastes with both high metal and high alkali contents. Two successful approaches are discussed: developing high-durability alkali-binding crystals in a durable glassy matrix, and developing water-soluble crystals in a durable and continuous glassy matrix. Nepheline-vitreous ceramics were demonstrated for the immobilization of high-alkali wastes with alkali contents up to 21 wt%. The chemical durability of the nepheline-vitreous ceramics is better than the corresponding glasses, especially in over longer times. Vitreous ceramics with Cs_2O loading up to 35.4 wt% have been developed. Vitreous ceramic waste forms were developed from 90 and 100% Oak Ridge National Laboratory K-25 pond sludge. Heat treatment resulted in targeted crystal formation of spinels, potassium feldspar, and Ca-P phases. These K-25 pond sludge vitreous ceramics were up to 42 times more durable than high-level environmental assessment (EA) glass. The toxicity characteristics leach procedure (TCLP) concentration of LVC-6 is at least 2000 times lower than U.S. Environmental Protection Agency limits. Idaho Chemical Process Plant (ICPP) calcined wastes were immobilized into vitreous ceramics with calcine loading up to 88%. These ICPP-vitreous ceramics were more durable than the EA glass by factors of 5 to 30. Vitreous ceramic waste forms are being developed to complement, not to replace, glass waste forms. Usage of both glass and vitreous ceramics waste forms will make vitrification technology applicable to the disposal of a much larger range of nuclear and mixed wastes.

Summary

Vitreous ceramic waste forms are being developed to complement glass waste forms in implementing Minimum Additive Waste Stabilization (MAWS) Program to support the U.S. Department of Energy's (DOE) environmental restoration efforts. These vitreous ceramics are composed of various metal-oxide crystalline phases embedded in a silicate-glass phase. Glass is a homogeneous, amorphous solid. Both glass and vitreous ceramics are produced in vitrifiers (melters). The main difference between these two materials is the presence or lack of crystals.

The broad objective of this project is to support DOE's effort to apply the MAWS Program approach to remediate wastes across the DOE complex. The specific objective is to complement the compositions being developed for glass waste forms by using vitreous ceramics as waste forms to stabilize many types of waste. Achieving this objective will expand the range of waste streams to include those containing large amounts of scrap metals, high contents of metal compounds, and low-flux contents. The goal is to be able to blend multiple waste streams with minimum purchased additives to produce a durable vitreous ceramic waste form.

The vitreous ceramics produced are subject to characterization and testing to identify the destination of hazardous and radionuclide constituents in glass or in the crystalline phases to assess their long-term durabilities, and to determine the limitations of these waste forms.

This report summarizes the work performed at the Pacific Northwest Laboratory during the period of October 1994 to September 1995. This work is a continuation and expansion of the DOE-funded MAWS Programs. The work reported here expands the applicability of vitreous ceramic waste forms in the remediation of DOE mixed, low-level, and other wastes, with specific emphasis on waste streams with high alkalis, Oak Ridge National Laboratory (ORNL) and Idaho National Engineering Laboratory (INEL) wastes.

Work performed in 1995 extended the success of vitreous ceramic waste forms to treat wastes with both high metal and high alkali contents. This included two approaches: developing highly durable, alkali-binding crystals in a durable glassy matrix, and developing water-soluble crystals in a durable and continuous glassy matrix.

The development of low solubility alkali-binding crystalline phases includes phases free of SiO_2 and Al_2O_3 that bind alkalis, such as sodium-zirconium-phosphate (NZP), sodium-titanium-phosphate (NTP), alkali-containing perovskite, and other phosphate compounds that have low solubility in water; and phases incorporating Si, Al, and alkalis such as nepheline and acmite. Nepheline and acmite were successfully developed. Nepheline is more promising than acmite because of its high alkali-loading and low leachate pH. The long-term durability of nepheline-containing vitreous ceramics is much better than that of the corresponding glass with the same chemical compositions.

The development of durable vitreous ceramics that consist of isolated water-soluble alkali-binding crystals must satisfy the following conditions: the alkali-binding crystals have to be isolated in the waste form; the glassy matrix has to be enriched in network-forming elements such as SiO_2 and Al_2O_3 and be low in alkalis; and the glassy matrix has to be continuous. Samples LVC-2Q/LVC-2HT showed a microstructure consisting of 1000-nm-round particles scattered uniformly in the glassy matrix. The fine

particles are crystalline Na_3PO_4, and the glassy phase is enriched in SiO_2 and Al_2O_3. Although Na_3PO_4 is soluble in water, the durable glassy phase limits the access of water to Na_3PO_4, and the overall durability of this vitreous ceramic is very good. The normalized Na release from sample LVC-2Q is 0.504 g/m^2/7-day in a product consistency test, which is a factor of 13 times smaller than the 6.4 g/m^2/7-day of the high-level environmental assessment (EA) glass. The LVC-2Q has similar morphology as the LVC-2HT, but the size of the Na_3PO_4 crystalline phases was only about 150 nm and the longer term chemical durability was not as good as LVC-2HT. This is probably due to the shorter separation between Na_3PO_4 crystals in LVC-2Q and the less complete extraction of alkalis from the glassy matrix due to lack of heat treatment. The LVC-2 samples have a sodium loading of 24 wt% with good chemical durability. The heat-treated sample, LVC-2HT, further reduced the sodium release. Therefore, these types of waste forms can withstand a large variation in cooling rates during actual production, which provides more flexibility in terms of the product shape and production rate.

These results are significant because the range of waste streams that can be treated with VC waste forms will be expanded to include those with high alkali contents, especially those with high metal contents; the DOE vitrification technology will be applied to a wider range of DOE waste streams; and higher waste loading, smaller final waste volume, more flexible waste form productions, and larger remediation cost-savings will be realized.

Nepheline crystals in vitreous ceramics have been successfully formed between temperatures of 1500°C to 1600°C, followed by heat-treatment at a temperature between 850°C and 1050°C for 6 to 45 hours. The melting temperature is not critical for the formation of nepheline as long as the material is melted and is sufficiently fluid. However, the different heat-treatment schedules affected the product durability. For a six-hour heat-treatment at 850°C and 1050°C, time is sufficient for nepheline formation and also produces more durable nepheline-vitreous ceramics. The addition of a nucleation agent (TiO_2) seems to be unnecessary for the formation of nepheline in vitreous ceramics; the preferred approach is to replace the nucleation agent with excess SiO_2 to enhance product durability. This enhancement in durability is mainly achieved through increasing the SiO_2 content in the residual glass matrix. The residual glass phase in vitreous ceramics seems to control the overall waste form durability. The nepheline-vitreous ceramics are usually more durable than corresponding glass matrix with the same chemical composition, especially for longer test duration. The reaction acceleration in nepheline-vitreous ceramics is much slower compared to the corresponding glasses, probably due to the fact that nepheline crystals are thermodynamically more stable than the glasses with the same chemical compositions. The nepheline-vitreous ceramics also have lower leachate pH, which is believed to benefit the long-term durability of crystalline waste forms.

We conclude that nepheline-vitreous ceramics can be used to immobilize wastes with high alkali contents up to 21 wt%. The chemical durability of the vitreous ceramics is better than the corresponding glasses, especially in long-term chemical durability.

Vitreous ceramics with Cs_2O loading up to 35.4 wt% have been developed. These waste forms contain pollucite ($CaAlSi_2O_6$), and various Cs-Al-Si crystals such as $CsAlSi_5O_{12}$ and $CsAlSiO_4$. The data suggest that these crystals have similar stability (i.e. water solubility). The corrosion rates of these vitreous ceramics are up to 15 times lower than the corresponding glass waste form of the same chemical composition and are a factor of 8 better than EA glass. The similarity in normalized releases between short and long PCT tests suggests that the long-term durabilities of these vitreous ceramics are very good. This is probably due to the reaction affinity which is quite low throughout the test duration. This low reaction affinity can be maintained as a result of the thermodynamic stability of the crystals of pollucite

and other Cs-Al-Si compounds. The longer term durability of the corresponding glasses is expected to be much worse due to the possible precipitation and formation of more stable crystalline phases.

Vitreous ceramic waste forms were formulated from almost 100% ORNL K-25 pond sludge. Heat treatment resulted in targeted crystal formation of spinels (including trevorite and chromite, hosts for Ni and Cr), potassium feldspar (host for Cs^+), and Ca-P phases (host for Ce, a surrogate for U and Pu).

Sample LVC-5 was tested using the product consistency test (PCT), U.S. Environmental Protection Agency (EPA) TCLP test, and vapor-hydration test at 150°C for 28 days. The results showed a normalized PCT release of 0.38 g/m^2/7-days for Na, which is a factor of 18 lower than that of EA glass. The hazardous element releases in an EPA TCLP test are at least 476 times lower than the EPA limits. More significantly, the Ni concentration in the TCLP leachate is less than 0.02 ppm (the detection limit of ICP-AES), which is at least 16 times lower than the 0.32-ppm LDR limit. The vapor-hydration test sample showed almost no alteration by visual inspection; a thin "webby" clay layer was found under SEM. The extent of alteration of LVC-5 is much less than the alteration found on typical high-level waste glasses.

An improved formulation of LVC-6 at 90 wt% loading of K-25 pond sludge and 10 wt% ORNL soil, showed a PCT Na release of 0.16 g/m^2 which is 42 times lower than that of EA glass. The TCLP release concentrations of hazardous elements from LVC-6 are at least 2000 times lower than EPA limits. The vapor-hydration test again showed minimum corrosion to LVC-6. These data suggest that K-25 pond sludge can be immobilized with up to 100% waste-loading using vitreous ceramics. The vitreous ceramic waste form is more durable than typical high-level waste glasses and can be processed at temperatures of about 1425°C.

Idaho Chemical Process Plant (ICPP) calcined wastes were immobilized into vitreous ceramics. The waste loading was up to 100% if contaminated soil was used as a glass-forming additive. The highest calcine-loading achieved with alumina- and zirconia-calcines was 88%. Blending alumina- with zirconia-calcine increased calcine loading and increased vitreous ceramic durability, but reduced melting temperatures (for immobilizing alumina-calcine). These blended melts can be melted at 1500°C or below.

All of the vitreous ceramics passed the EPA TCLP concentration limits on hazardous elements; the alumina- and zirconia-calcine blended vitreous ceramics also passed the more restrictive land disposal limits on hazardous elements. The vitreous ceramics are factors of 5 to 30 more durable than the high-level EA glass when tested in a 7-day PCT. The leachate pHs of these vitreous ceramics were consistently lower than 10.

Even after corrosion in saturated water vapor at 150°C for 28 days, all of the vitreous-ceramics showed only minor alteration, characterized by thin alteration layers. Two types of surface layers were found on these altered vitreous ceramics. One formed in situ on the surface and grew into the inner zone of the sample. However, the crystalline phases, such as $Ca_3(PO_4)_2$, $(Fe^{2+}Ni,Mn)Fe^{3+}{}_2O_4$ (magnetite), $Ca(Al,Fe,Zr,Cr)_{12}O_{19}$ (hibonite), ZrO_2 (baddeyelite), $CaZrTi_2O_7$ (zirconolite), and Al_2O_3 (corrundum), are very durable and showed insignificant corrosion. The glass alteration usually stopped at the interface of the durable crystal and the glassy matrix. A more interesting observation is that durable hibonite in LVC-14 and corrundum formed three-dimensional internal barriers within the waste form, which may provide excellent long-term durability to these waste forms. The silicate phases, such as $KAlSi_3O_8$ (feldspar), $CaAl_2Si_2O_8$, $KAlSiO_4$ (leucite), and $CaFeSi_2O_6$ (pyroxene), are less durable than the above

crystals, but they are still more durable than most of the glasses.

Another type of surface layer is the precipitated layer formed through the solution deposition onto the original surface. The deposited materials came from the leached phases, such as Ca-high glass and fluorite. The hydroxylization of fluorite favors the glass corrosion. The common alteration products from these silicate phases are clay minerals, such as smectite-illite. Surface-precipitated phases developed well only on two samples, LVC-14 and LVC-15. They were identified as prehnite, $Ca_2Al_2Si_3O_{10}(OH)_2$.

One of the major differences between vitreous ceramics and glasses is that crystallization in vitreous ceramics is a preferred process, in fact, heat treatment or nucleation agents are added to promote such controlled crystallization. Crystallization in glass-making, or devitrification, is usually avoided.

Vitreous ceramics are suitable for waste streams with high metal contents but with low flux (alkalis and boron) content, while homogenous glass waste forms are suitable for waste streams with low metal content and sufficient flux content. Therefore, the vitreous ceramic waste form will encompass a different waste composition from that of homogenous glass waste forms.

The durability of a glass is mainly determined by the relative amount of structural-making elements of SiO_2 and Al_2O_3 to the total alkali. Glasses with more silica and alumina and less alkalis are usually more durable. The durability of the glassy phases in vitreous ceramics is determined by the same factors that are applicable to glass, but the glassy phase can usually have much higher SiO_2 and Al_2O_3 and much less alkali than normal glasses. The glassy phases in vitreous ceramics can usually be made more durable than normal glasses. The crystal phases in vitreous ceramics, such as $Ca_3(PO_4)_2$, magnetite, $(Fe^{2+}Ni,Mn)Fe^{3+}{}_2O_4$, hibonite, $Ca(Al,Fe,Zr,Cr)_{12}O_{19}$, baddeyelite, ZrO_2, zirconolite, $CaZrTi_2O_7$, and corrundum, Al_2O_3, are thermodynamically more stable than normal glasses and are also less soluble in water than glasses. Therefore, vitreous ceramics can be made very durable. This durability is better demonstrated in long-term PCTs or in vapor-hydration tests.

Use of vitreous ceramic waste forms allows MAWS Program technology to be applied to a much wider range of waste streams than those amenable to glass waste forms. The work in the MAWS Program has indicated that vitreous ceramics are good final waste forms based on their high chemical durability, especially the long-term durability (when properly formulated); its capability to incorporate large amounts of metal oxides; its capability to incorporate waste streams with low contents of flux components; its less-stringent requirements on processing parameters, such as viscosities, compared to glass waste forms; and its production requires little or no purchased additives, which means greater waste volume reduction and treatment cost-savings. High temperatures in the vitreous ceramic-making can destroy organic materials, enabling this technology to treat wastes containing large amounts of toxic organic contaminants.

The vitreous ceramics produced in the MAWS Program represent a class of waste forms that contain significant amounts of both vitreous and crystalline phases. The crystalline phases may account for up to 99% of the total volume of waste forms with high metal oxide loadings. Vitreous ceramics may be formulated in such a way that both crystalline and glass phases are very durable. Alternatively, vitreous ceramics can be made such that most of the hazardous and radioactive compounds are concentrated in crystalline phases. Vitreous ceramic compositions developed through crucible melts were also produced in a Retech pilot-scale plasma centrifugal furnace at Ukiah, California, with up to 100% waste loadings. These successful campaigns demonstrated the processibility of vitreous ceramics.

Vitreous ceramics waste forms are being developed to complement, not to replace, glass waste forms in implementing the MAWS Program. Use of both glass and vitreous ceramic waste forms will make vitrification technology applicable to the disposal of a much larger range of nuclear and mixed wastes.

Acknowledgement

We wish to acknowledge and thank D. E. McCready for X-ray diffraction analysis and experimental description; M. J. Schweiger and D. E. Smith for conducting durability and viscosity testing; Dr. P. R. Hrma, J. D. Vienna and Dr. H. Li for technical review. This work was sponsored by the Office of Technology Development and Landfill Stabilization Focus Area of the U.S. Department of Energy.

Contents

LIST OF TABLES

LIST OF FIGURES

1.0 Introduction

Vitrification to produce borosilicate glasses is the best demonstrated available technology within the DOE Complex for the treatment of low-volume, high-level radioactive wastes. Vitreous ceramics have been shown to be superior waste forms for wastes with high metal content (metallic or oxides of Ni, Cr, Fe, Ti, Zr, Cu, Cd, etc.) and low alkali contents (Feng 1994a; 1994b; 1994c; Wronkiewicz 1994). Vitreous ceramics (VC) have been used to complement homogeneous glass waste forms in the U.S. Department of Energy's (DOE) Minimum Additive Waste Stabilization (MAWS) Program for stabilizing mixed/low-level wastes (DOE 1993).

The MAWS concept provides an environmentally sound, cost-effective alterative for the vitrification of the vast amounts of low-level radioactive and mixed wastes that exist within the DOE complex. MAWS uses multiple waste streams as substitutes for glass-forming additives that would otherwise be necessary to produce a stable, high quality waste form. The result of substituting other waste streams for glass-forming additives is to lower the overall waste volume for disposal.

The objective of the MAWS program is to develop the technology to effectively remediate large quantities of multiple waste streams in a cost-effective manner. The first pilot-scale demonstration and evaluation of a complete vitrification system using the MAWS approach is underway at Fernald, Ohio; glass is produced as the final waste form (Pegg 1994).

This report summarizes the work performed at the Pacific Northwest Laboratory during the period of October 1994 to September 1995. This work is a continuation and expansion of the DOE-funded MAWS programs (Feng-1994c; 1995; Wronkiewicz 1995). The work reported here (sponsored by the Office of Technology Development and Landfill Stabilization Focus Area of the U.S. Department of Energy) expands the applicability of vitreous ceramic waste forms in the remediation of DOE mixed/low-level and other applicable wastes, with specific emphasis on waste streams with high alkalis, and Oak Ridge National Laboratory (ORNL) and Idaho National Engineering Laboratory (INEL) wastes.

Glass is a homogeneous, amorphous solid without long-range order. A properly formulated glass waste form can be relatively easy to produce and can resist aqueous corrosion. The glass matrix can have powerful solvating properties to incorporate a wide range and large amounts of hazardous and radioactive components. However, two limitations for the production of glass final waste forms restrict the application of the MAWS approach to produce acceptable glass waste forms: (1) a sufficient amount of fluxing components, such as alkalis, boron, or alkaline earths are required to attain a processible melt viscosity at a practical temperature; and (2) the solubilities of many metal waste components in the glass are low, so waste loadings may be unacceptably small. These limitations cause processing difficulties and the deterioration of glass waste forms.

Many DOE sites have large volumes of wastes that contain large amounts of scrap metals (e.g., 22 wt% of the buried wastes at the INEL Radioactive Waste Management Complex [RWMC] are metals) and metal oxides of Cr, Ni, Ti, and Fe (e.g., the 16 million kg of K-25 pond sludge/soil at the ORNL contains about 25 wt% iron oxides, 20 wt% alumina, and 20 wt% calcium oxides and 5% of NiO and Cr_2O_3). These wastes typically contain only small amounts of fluxing components. Because these metal oxides have relatively low solubilities in glass, moderate loadings of these waste streams can result in the formation of crystalline phases during vitrification. This uncontrolled crystallization in glass melts leads to difficulties in glass processing and uncertainties regarding glass durability. If this two-phase material is not an acceptable waste form, expensive additives must be used to dilute the metal oxides, thereby increasing the final waste volume and treatment costs.

The VC waste forms consist of metal oxide crystalline phases embedded in a silicate glass matrix. Recent work indicates that VC final waste forms exhibit advantages over both homogeneous glass and synrock waste forms (Feng 1994a; 1994b; 1994c; Wronkiewicz 1995). Properly formulated VC have chemical durabilities similar to Synrock™ waste forms and also have the processibility of glass waste forms. Vitreous ceramics can be economically produced in a vitrifier (Feng 1994d).

The objective of this project is to support DOE's effort to apply the MAWS approach to remediate wastes across the DOE complex. The specific objective is to complement the composition being developed for glass waste forms by using vitreous ceramics as waste forms to stabilize many types of waste. The project focus is on blending multiple waste streams that require remediation to produce a durable vitreous ceramic waste form with minimum purchased additives.

The vitreous ceramics produced are subject to characterization and testing to identify the destination of hazardous and radionuclide constituents between glass and crystalline phases within the vitreous ceramic; to assess the long-term durabilities of the waste forms; and to determine the limitations of this waste form.

2.0 Experimental Considerations

2.1 Vitreous Ceramics Preparation

The vitreous ceramics (VC) were batched and melted according to Pacific Northwest Laboratory (PNL) Procedure PSL-417-GBM ("Procedure for Glass Batching and Melting, Rev. 0"). For each VC, the chemical components to be varied were batched together as oxides and carbonates. Using an Angstrom grinding machine, each batch was mixed in a grinding cell for 5 min to achieve a homogeneous mixture.

About 500 g of each VC was melted in a platinum crucible under a lid (to reduce volatilization) using an electrically heated resistance furnace (Deltech DT-31). Furnace temperature was controlled by a Honeywell controller/programmer and monitored by one S-type thermocouple on the controller and a second, independent S-type thermocouple. The thermocouples were located in the middle of the furnace hot zone. Variation in temperature readout from the two thermocouples was $\pm$ 1.0°C with respect to the preset melting temperatures.

The VC was removed from the furnace after one hour of melting. A portion of the molten VC was poured onto a steel plate and quenched. The remainder was annealed for 2 h at 515° to 525°C. Samples (4 to 5 g) of selected glasses were sent for elemental analysis to compare the final compositions with the as-batched compositions.

2.2 Viscosity Measurements

Viscosity was measured by a rotating-spindle technique and evaluated using standard viscosity-measurement procedures GDL-VSC ("Viscosity Spindle Calibration, Rev. 0") and GDL-VIS ("Standard Viscosity Measurement, Rev. 0"). Each VC sample was heated to its approximate melting temperature (5 Pa·S) in a platinum crucible and maintained until thermal equilibrium is reached (approximately 30 minutes). A measurement was then taken at the melting temperature; subsequent measurements were taken about 50°C apart. To cover the range of viscosities in the operation of a melter (4 to 10 Pa·S), viscosity measurements are taken first at two lower temperatures (viscosity > 5 Pa·S) and then at two higher temperatures (below 4 Pa·S). To ensure the reproducibility of the measurement, two replicate viscosity measurements were made at the same nominal temperature as the initial measurement during the cycle, i.e., the viscosity was measured three times at each temperature. Usually eleven measurements were made for each VC (i.e., three measurements at initial melting temperature and eight duplicate measurements at four temperatures near the melting temperature). The melt viscosity was expected to be affected by volatilization and crystallization. Examination of viscosity changes at the initial melting temperature provided additional information on the volatilization and crystallization behavior of each formulated VC.

Temperatures at a viscosity of 10 Pa·S were obtained for each glass by fitting the raw viscosity data within the temperature region to the Arrhenius equation:

$$\ln(V) = A + B/T \quad (1)$$

where

A is a constant
B = the activation temperature (K)
T = temperature (K), and
V = viscosity in Pa·S.

The equipment was calibrated using National Institute of Standards and Technology (NIST) lead-silicate glass (NBS-711). Previous experience demonstrated that viscosity measurements of the same glass by different laboratories typically had good agreement. Also, overcheck measurements of viscosity were made by Corning, Inc. on glass samples provided by this laboratory.

2.3 Durability Tests

The chemical durability of a vitreous ceramic is a measure of its capability to resist corrosion when in contact with an aqueous solution or water vapor. The durability of the slags was measured by three tests: the toxicity characteristic leaching procedure (TCLP), modified product consistency test (PCT), and Argonne National Laboratory (ANL) vapor-hydration tests. The detailed test matrix for each slag is shown in Table 2-1.

Table 2.1. Vitreous Ceramic Test Matrix

VC (LVC-xx)	PCT	TCLP	Vapor Hydration	Viscosity	Flow Through	EDS
1	X	X				
2	X	X				
3	X	X				X
4	X	X				
5	X	X	X	X	X	
6	X	X	X	X	X	
7	X	X	X		X	
8	X	X	X		X	
9	X	X	X		X	
10	X	X	X		X	X
11	X	X			X	X
12	X	X			X	
13	X	X			X	
14	X		X		X	X
15	X		X		X	
16	X					
17	X					

2.3.1 Toxicity Characteristic Leaching Procedure Test

The U.S. Environmental Protection Agency (EPA) toxicity characteristic leaching procedure (TCLP) (EPA 1988) was used to determine if arsenic, barium, cadmium, chromium, lead, mercury, selenium, and silver leached. The leachate concentrations, obtained after 18 hours of reaction of vitreous ceramic powders at 22°C in a sodium acetate buffer solution, were measured. This test was used to satisfy EPA regulatory requirements for RCRA-controlled toxic metals and to compare the performance of the VC in the TCLP test to that of other waste forms.

2.3.2 Product Consistency Test

The product consistency test (PCT) is based on previous research (Jantzen 1992) and was adapted as PNL Procedure MCC-TP-19 ("Leaching Test Using PCT Test Method, Rev. 0"). The test was conducted using deionized water in Teflon™ containers at 90°C. New containers were baked at 200°C for one week to drive off residual fluorine and then washed thoroughly according to the PCT procedure. The VC was ground in a tungsten-carbide grinding cell and then sieved through +200 -100 mesh stainless-steel sieves to obtain particle sizes between 75 and 150 μm (equivalent spherical diameter). The large particles remaining on the top of the 100-mesh sieve were crushed repeatedly until all VC particles could pass through it. Using an ultrasonic cleaner, the crushed material was cleaned in deionized water and ethanol. It was then dried, weighed, and 4 g of glass was added to a 60 mL Teflon container filled with 40 mL of deionized water. The ratio of the surface area of VC to solution volume was taken as 2000/m. The Teflon container and its contents were placed for 7, 28, or 91 days in an oven that had been preheated to 90°C. After the tests were terminated, aliquots of the leachate were filtered through a 0.45-μm filter and analyzed by ICP/AES. The PCT was performed in duplicate.

Results are reported as normalized elemental-mass losses according to the following equation:

$$NL_i = \frac{C_i}{f_i \cdot \frac{S}{V}} \qquad (2)$$

where

NL_i = the normalized mass loss based on element i (g/m^2),
C_i = the analyzed concentration of element i in leachate (g/m^3),
f_i = mass fraction of element i in the vitreous ceramics (unitless), and
S/V = the ratio of glass surface are to solution volume (1/m), which is 2000/m here.

Nominal compositions are used for the normalized mass loss calculations.

2.3.3 Single-Pass Flow-Through Test

In this test, monolithic or powdered samples were exposed to controlled environmental conditions, including pH and temperature. A general schematic of the single-pass flow-through test equipment is shown in Figure 2.1. The test equipment used 13 holding reservoirs to evaluate the effect of pH on dissolution kinetics of various waste-form compositions. Twelve of the 13 holding reservoirs were 2000-ml vessels, into which a range of pH buffer solutions could be placed, allowing the evaluation of the effect of pH on a single waste-form composition. The single large holding reservoir (25-liter carboy) held a constant pH solution that was supplied to twelve independent cells/lines from which the dissolution kinetics of 12 varying waste-form compositions could be evaluated at a constant pH. The system also could have been set up to evaluate 24 varying compositions as a function of a constant pH (i.e., a single buffer solution placed in the twelve 2000-ml vessels as well as the 25-liter carboy). Nitrogen was used continuously as a cover gas for the buffer-solution reservoirs.

Once the test conditions (buffers, flow rates, temperature, etc.) were defined and verified through pretest procedures, a predetermined quantity of material (powder or monolith) was added to the solution in each preheated, 2-port sample vessel. The 2-port vessels were then sealed and flow of the buffer solution was initiated by activating the pump(s) and the cover gas source. The buffer composition was chosen to minimize compositional overlap between the buffer solution and the sample components. Nitrogen flowed into the 3-port vessels and aided in the transfer of buffer solution to and through the 2-port sample vessels into the sample collection vessels. Flow rates were varied depending on the durability of the sample, pH of the buffer solution, and the test temperature. The test conditions were controlled to keep the leachant undersaturated with respect to precipitation of secondary phases, but above elemental detection limits of the analytical equipment used.

Corrosion rates in the single-pass flow-through experiments were calculated for each pH value from the steady-state concentrations of component (i) measured in the effluent. The measured concentrations were converted to corrosion rate by the following equation:

$$R_{i,j} = \frac{Q_i C_{i,j}}{S_j f_i} \tag{3}$$

where

$R_{i,j}$ = corrosion rate for component i at time period j ($g/m^2/d$),
$C_{i,j}$ = blank corrected steady-state concentration of Si (g/m^3),
Q_i = flow rate at time period j (m^3/d),
f_i = mass fraction of component i in the sample, and
S_j = average total glass surface area over time period j-1 to j (m^2).

The test conditions for the VC were as follows:

- Test temperature: 90°C
- Sample size: approximately 1 g
- Sample type: powder between 75 and 150 μm
- Flow Rate: approximately 100 ml/d
- Buffer solution: deionized water.

Flow-through testing of the VC samples was underway as this report was compiled. Results of this test will be presented in a future report.

2.3.4 Vapor Hydration Test

The vapor hydration test (Bates 1982; Ebert 1991) was developed as an accelerated corrosion test to evaluate the long-term durability of glasses. This test was performed in saturated water vapor at various temperatures. Durability was measured as a function of the rate and amount of secondary alteration phase-formation on the surface of the material and the thickness of the altered surface layers surrounding the samples, as measured in cross-section. This information provided insight into the long-term durability of the material.

Monoliths were used in the vapor hydration tests. The sample preparation procedure involved cutting 10-mm-diameter cylinders from solidified VC casts. These cylinders were sectioned into 1-mm-thick circular disks which then had a small hole drilled into them to attach the support threads to the samples. Surfaces of the samples were next polished to a 600-grit finish and cleaned ultrasonically in a methanol bath. All samples were examined by optical microscopy before and after undergoing vapor hydration testing to detect and changes in the structure as a result of the test conditions.

Sample disks were suspended by Teflon threads or stainless-steel wire from a stainless-steel support rod. The entire sample-support-rod assembly was placed in a stainless-steel reaction vessel. A predetermined volume of water (0.25 mL for 150°C test) was added to each vessel; this amount was sufficient to saturate the vessel atmosphere with water vapor after heating to the appropriate experimental temperature, but was not sufficient to result in water refluxing between the samples and the fluid in the bottom of the vessel.

After adding the water, the vessels were hermetically sealed and inserted into a preheated oven controlled to 150 $\pm$ 2°C. The elevated temperatures were chosen to accelerate reactions between the condensed fluid and the samples.

After completion of the prescribed test interval, the sample vessels were removed from the oven, cooled in an ice bath, and opened. All sample disks were first examined visually and only one disk from each test was subjected to detailed scanning electron microscopy/energy-dispersive X-ray analysis (SEM/EDS). Surfaces of the altered samples were characterized with respect to the extent of alteration phase development.

2.4 Solution and Solid Analyses

2.4.1 Solution Analysis

Cations and radionuclides were analyzed with inductively coupled plasma mass spectrometry (ICP-MS) with an accuracy of ± 10% for major elements and ± 50% for radionuclides and minor elements. Anions were analyzed with ion chromatography with an accuracy of about 50%. The pH was measured with an combination electrode with an accuracy of ± 0.1 pH unit.

2.4.2 Fusion Method for Composition Analysis

The composition of selected VC after melting was determined through the fusion method. The portions of the solid sample were ground and dissolved in molten potassium hydroxide and sodium peroxide. Each flux solution was solidified, then dissolved in deionized water (DIW). The resulting solutions were then analyzed by ICP to identify the elements contained in the sample. Two different flux agents were used so that all major metal ions could be analyzed.

2.4.3 Solids Analyses

X-Ray Diffraction Analysis

X-ray powder diffraction (XRPD) analysis was performed using a Philips vertical goniometer incorporating a variable divergence slit, a fixed (0.2°) receiving slit, and a graphite diffracted beam monochromator. The X-ray source was a fixed-anode, long fine-focus Cu tube operated at 40 kV, 45 mA (1800 W). The 2-theta range studied was 5-75°, step-scanned at 0.05°/1.5sec.

Specimens for XRPD analysis were mounted in front-loading, cavity-type holders. Cavity dimensions were approximately 12mm diameter x 0.5 mm dp. (holding approximately 0.05 cm^3 or 0.13g of sample material). The sample holders were fabricated from off-axis single-crystal quartz (Gem Dugout, State College, PA) and produced low X-ray background.

Optical Microscopy Analysis

The samples were first cut into thin sections using a diamond saw. The thin sections were polished to 30 to 50 μm thick with 15- and 3-μm diamond paste before examination under an optical microscope to identify and quantify the crystalline phases present.

Scanning Electron Microscopy

Scanning electron microscopy was done using a Hitachi S-450 with a Tracor-Northern TN-2000 energy-dispersive X-ray analysis system (EDS) which uses a solid state Si(Li) spectrometer for qualitative chemical analysis of major elements. Cross-sectional SEM samples were prepared by resin impregnation and polishing cross-sections of cuts perpendicular to the original surface. Final polishing was done with 0.1-μm diamond paste to ensure smooth surfaces.

Transmission Electron Microscopy

Analytical transmission electron microscopy (TEM) was performed using both a JEOL JEM-200FX microscope with a Noran TN-5500 EDS system and a JEOL JEM-2010 microscope with an Oxford Link ISIS EDS system. Both microscopes were operated at 200KeV during analysis. Detailed TEM analyses included high-resolution electron microscopy (HRTEM), bright-field imaging and selected area diffraction (SAD) were conducted.

Quantitative EDS analyses were performed using Noran's Semi-Quantitative (software package for) Metallurgical Thin Films (SQMTF). The K-factors used were well calibrated in the laboratory from simple minerals and 202U glass samples. However, the software could only handle nine elements and light elements (e.g. oxygen, boron) were undetectable with the TN5500 system. Final results were calculated based on the stoichiometry of the oxides.

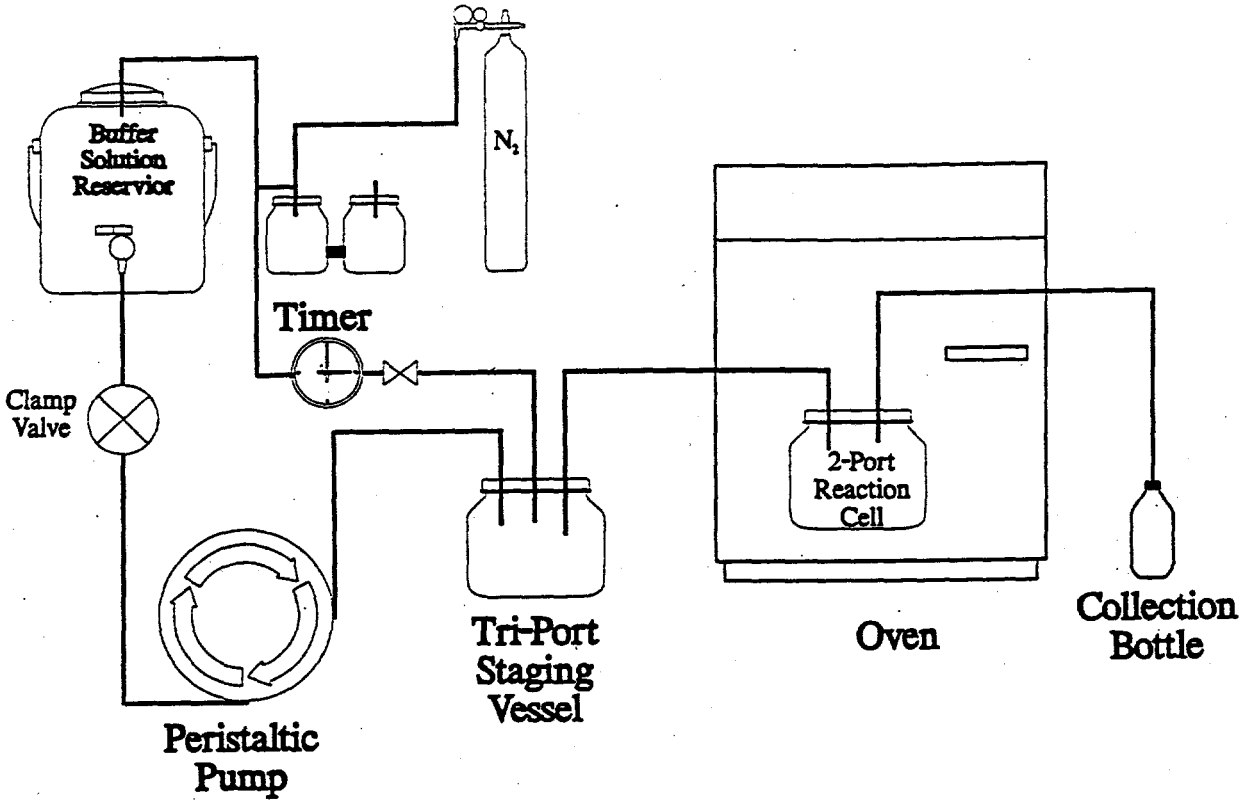

Figure 2.1. Single-Pass Flow Through Test Apparatus

3.0 Results and Discussion

3.1 Vitreous Ceramics for High Sodium Hanford Site Low-Level Wastes

3.1.1 Approach

Vitreous ceramics (VC) are composed of metal oxide crystals embedded in a silicate glassy matrix. The overall chemical durability is determined by the least durable part of the VC, i.e., by crystalline phases, if they are more soluble in water and less stable than glass under test conditions, or by the glassy matrix if the crystals are more stable and less soluble.

In our previous approach for immobilizing high metal and low alkali waste streams (Feng 1994a; 1994b; 1994c), the success of VC was due to several factors. Low aqueous solubility crystalline phases (such as spinel, zirconolite, and perovskite) form and are thermodymanically more stable than glass. These phases have high contents of oxides of Fe, Cr, Ni, Zr, and Ti and usually do not incorporate network-forming elements such as Si and Al. Since SiO_2 and Al_2O_3 are not incorporated from the selected crystal structure their concentration is respectivelly high in the glassy matrix. Alkalis are usually concentrated in the glassy matrix, but the total alkali content in the wastes and additives is so small that it does notsignificantly decrease the chemical durability of the glassy matrix. Therefore, the VC waste form is very resistant to corrosion, even under extreme testing conditions such as those of vapor hydration tests (Wronkiewicz 1995).

To apply VC to the remediation of high sodium Hanford Site tank waste, the sodium has to be immobilized in the waste form. Our approach is to develop alkali-binding crystals in VC. The aqueous solubility of the alkali-binding crystals in VC can be either very low (which is the preferred case) or high. The overall durability of the VC depends on the relative durability of the alkali-binding crystalline phases and the vitreous (glassy) matrix and the spacial distribution of the crystals in the vitreous matrix. If the crystalline phases are more durable than the vitreous matrix, the overall durability is determined by the durability of the vitreous matrix. If the crystalline phases are less durable than the vitreous matrix, their overall durability is determined by the spacial distribution of these crystals in the VC. Crystal phases determine durability if they are major phases of the VC and are interconnected into a continuous matrix; the vitreous matrix determines the overall durability if the crystals are very fine and are uniformly dispersed in a more durable vitreous matrix.

The low-solubility, alkali-binding crystalline phases include two types: phases that do not incorporate SiO_2 and/or Al_2O_3, but bind alkalis; and phases that incorporate both Si/Al and alkalis. The former includes $NaZr_2(PO_4)_3$ (NZP), sodium-titanium-phosphate (NTP), alkali-containing perovskite, and other phosphate compounds that have low solubility in water. Use of alkalis by these crystals will reduce the alkali content in the residual glass matrix. The latter phases are crystalline compounds that must use more alkali molecules per SiO_2 and Al_2O_3 in the crystal than in the overall composition to enhance the chemical durability of the residual glassy matrix. Nepheline and acmite are examples of the second type of low-solubility crystals under investigation.

To date, VC waste forms have not been demonstrated for immobilizing waste streams with high alkali content, although glass waste forms (Hrma 1994, Varma 1988) and the crystalline waste form NZP (Scheetz 1985) have been studied. Efforts at Pacific Northwest Laboratory (PNL) are extending the success of VC waste forms to waste streams that have relatively high alkali contents. The PNL approach includes developing alkali-binding and low-solubility crystalline phases in a glass matrix; developing isolated alkali-binding fine crystals, which can be water soluble, dispersed in a durable glass matrix; and controlling the VC glass matrix composition by selective crystallization so the residual glassy matrix has an optimized balance of alkalis and network forming oxides of SiO_2 and Al_2O_3. The purpose of this research is twofold: to develop acceptable VC waste forms in which alkaline wastes can be effectively incorporated with high loading: and to understand the advantages and limitations of VC in stabilizing various wastes.

To facilitate the application of VC waste forms to treat actual wastes, PNL's investigation used simulated Hanford Site low-level waste (LLW) containing 84 wt% Na_2O; the alkali contents in the waste forms investigated were up to 28.5 wt% of Na_2O.

3.1.2 Formulation and Melting

The VC samples, LVC-1, -2, -3, -4, and -11, were made from mixtures of reagent-grade powdered chemicals. Table 3.1 shows the composition of the VC samples, which are combinations of glass-making additives and simulated nominal Hanford Site LLW. The Hanford Site LLW contains 84.4 wt% Na_2O. High Na content limits waste loading. The highest waste loading of this study was 34 wt% for LVC-1, and the lowest waste loading was 15 wt% for LVC-11. Part of the additives represent Hanford soil composition. The waste loading is up to 80%, if Hanford soil is considered.

Batched materials of about 400 g were mixed in an agate disc mill for about 6 min and were then melted for 1 h at a specific temperature (Table 3.2) in a platinum crucible. The melt was cooled by quenching the outside of the crucible in a room-temperature water bath. The quenched VC was then milled in a tungsten carbide disk mill for 3 min, producing a fine powder. The VC was next remelted in a platinum crucible at melting temperature for another 60 min. Half of the melt was quenched in air, and the other half was heat-treated to nucleate and develop crystalline phases. Those samples subjected to heat treatment were labeled HT. The temperatures for melting and heat treatment are shown in Table 3.2. All VC samples were annealed at 520°C for 2 h and then allowed to cool to room temperature inside the annealing oven.

The VC samples were then analyzed to determine the consistency between targeted batch compositions and the melted compositions (Table 3.1). Special attention was given to the Na content, since sodium oxide is easily volatilized at the melting temperatures, which ranged from 1200 to 1515°C. The VC samples were dissolved through K- and Na-fusion. The solution analysis was performed using inductively coupled plasma atomic emission spectrometry (ICP-AES). The results reported in Table 3.1 are averages from Na- and K-fusions. The differences between the target and analyzed compositions are very small, i.e., within the analytical error ($< 10\%$). LVC-11 had the highest silica and iron oxide contents and the lowest Na content. Loss of elements due to volatilization for LVC-11 was expected to be smaller than any of the other VC samples, therefore, LVC-11 was not analyzed. All of the target compositions were used to calculate normalized element releases from these VC samples.

Table 3.1. Target (a) and Analyzed (b) Compositions (wt%) of Alkali-Binding Vitreous Ceramics

	LVC-1		LVC-2		LVC-3		LVC-4		LVC-11
	Target	Anal.	Target	Anal.	Target	Anal.	Target	Anal.	Target
SiO_2	19.22	17.22	48.60	45.74	38.66	36.32	28.64	25.88	50.96
Al_2O_3	3.50	3.23	9.35	8.91	32.80	30.96	5.59	5.30	0.95
Fe_2O_3									33.40
Na_2O	28.49	27.79	24.08	24.64	19.14	19.91	24.41	24.38	12.46
CaO	2.74	2.68	0.00	0.09	0.00	0.11	4.47	4.32	0.00
P_2O_5	27.13	25.11	14.75	15.46	0.00	1.23	15.28	15.45	0.00
TiO_2					5.97	5.66	18.43	17.00	
ZrO_2	15.88	17.35	0.00	0.03	0.00	0.02	0.00	0.03	0.00
Others	3.04	3.10	3.22	3.33	3.43	3.56	3.18	3.40	2.24
Total	100.0	96.5	100.00	98.2	100.0	97.8	100.0	95.7	100.0

(a) Target = Batched Composition.
(b) Anal. = Analyzed Composition.

Waste SiO_2: 0.03 Na_2O: 84.42 CaO: 0.01 Al_2O_3: 6.19 Others: 9.35 Total: 100.0

Others Bi_2O_3: 0.63 Cl: 4.20 Cr_2O_3: 1.61 F: 9.63 Fe_2O_3: 0.16 K_2O: 14.74 MnO: 0.32 Nd_2O_3: 0.54 P_2O_5: 53.57 SO_3: 14.39 ZrO_2: 0.20 Total: 100.0

3.1.3 Characterization of As-Melted Vitreous Ceramics

As-melted VC samples were examined using XRD, SEM/EDS, and TEM/EDS. The unaltered VC waste form is composed of both crystalline and glassy phases. The texture of the VC can best be described as porphyritic, with relatively coarse-grained crystalline phenocrysts suspended in a glassy matrix. The distribution of crystalline phases was generally nonuniform. These characterizations are to verify the actual formation of the targeted crystals in VC.

Sample LVC-1

This VC composition was intended to form alkali-binding NZP (sodium-zirconium-phosphate) crystals which have low water solubility. XRD results showed approximately 35 vol% crystallinity in both quenched and heat-treated samples, and only about 2 vol% was NZP. The primary crystalline phases identified by XRD were Na_3PO_4 (19 vol%) and baddeleyite (14 vol%).

Table 3.2. Melting and Heat Treatment Conditions of Alkali-Binding Vitreous Ceramics

Sample	Melting Temperature (°C)	Heat Treatment (°C)	Crystallinity (vol%)	Color
LVC-1Q	1350		35	Aqua and cream
LVC-1HT	1350	950° for 24 h	35	Light aqua and cream
LVC-2Q	1400		15	Dark green
LVC-2HT	1400	950° for 24 h	15	Cloudy, light green
LVC-3Q	1515		0	Green
LVC-3HT	1515	900° for 45 h	100	Tan with blue flecks
LVC-4Q	1200		15	Aqua
LVC-4HT	1200	950° for 28 h	30	Tan
LVC-11Q	1350		0	Black
LVC-11HT	1350	850° for 24 h	100	Rust colored in parts, some metallic-looking

Sample LVC-2

This VC was designed to develop isolated fine sodium-phosphate crystals dispersed in a durable glass matrix. The XRD data showed the formation of Na_3PO_4 crystals in both quenched and heat-treated samples. The volume fraction of the crystals was about 15% for both quenched and heat-treated samples. LVC-2-HT was apple-green in color and was homogeneous in texture and morphology under optical microscopy. Examination of LVC-2-HT using TEM showed a microstructure of spherical particles (about 1000nm) uniformly dispersed in the glassy matrix (Figure 3.1a [Figure 3.1b an the enlarged view of Figure 3.1a]). The matrix was completely amorphous with a composition rich in Si and Al. A typical EDS spectrum is displayed in Figure 3.2a. The spherical particles are Na_3PO_4 (Figure 3.2b). EDS results and electron diffraction patterns (Figure 3.2c) indicated that these particles were mainly crystalline Na_3PO_4. It was very interesting to find that the quenched sample, LVC-2Q, (Figure 3.3) showed the same morphology as the heat-treated sample, LVC-2HT, except that the crystal size was about 7 times smaller (150nm in LVC-2Q vs. 1000nm in LVC-2HT). The total volume of crystallinity, 15%, was the same for both LVC-2Q and LVC-2HT. This means the heat treatment combined small crystals into large crystals. The impact of these results on the durability and processibility of the waste form will be discussed later.

Sample LVC-3

This VC was produced to develop nepheline ($NaAlSiO_4$) crystals that bind sodium. The batch composition ratio of Na:Al:Si was 1.00:1.04:1.04, as shown in Table 3.1, with TiO_2 added as a nucleation agent. The XRD data suggestes that crystals were not present in the quenched sample, while the heat-treated sample was 100% crystalline nepheline. Under optical microscopy, LVC-3-HT showed two distinct gray and brown regions. These two regions were very similar in terms of morphology and composition under TEM (Figure 3.4). EDS and electron diffraction analyses indicated the needle-like crystals were rutile, and the major matrix phase was nepheline.

The diffraction patterns for individual phases are shown in Figure 3.5. The brown region had a composition ratio of Na:Al:Si = 1.00:1.14:1.18, while the gray region had a ratio of 1.00:1.35:1.73. The crystals in the brown region were closest to the theoretical ratio of nepheline.

Sample LVC-4

The intent for LVC-4 was to develop alkali-binding crystals of perovskite types such as $(Ca_{1-x}Na_x)(Ti_{1-x}Nd_x)O_3$. The XRD data indicated 15 vol% crystallinity in the quenched sample and about 30 vol% of crystals in the heat-treated LVC-4-HT. Crystals in the quenched sample were 90% Na_3PO_4 and 10% $NaCaPO_4$. In LVC-4-HT, 55% of the crystals were Na_3PO_4, 35% rutile, and 5% $NaCaPO_4$. Insufficient Nd in the formulation probably caused the absence of perovskite-type crystals, and P was unable to function like Nd. Optical observations of the cross-section of the melt revealed a homogeneous microstructure consisting of needle-like rutile and a glassy matrix (Figure 3.6).

Morphologically, rutile crystals are classified into two varieties, very long needle-like ($> 100\mu m$ prolonging along C-axis), and short cylinder-like (approximately $20\mu m$). The EDS and selected area diffraction (SAD) analyses did not reveal any difference in composition or structure between these two morphologically different rutile crystals. It is possible the micrographs show the same type of crystals with different orientations. The total volume fraction of rutile identified with an optical microscope was about 35%.

Under TEM, two distinct regions were observed. One was a P-Na and P-Ca-Na rich crystalline region (Figure 3.7a); the other was a Si-Al-Ti-Na glassy region (Figure 3-7b). The differences between the sodium-phosphate crystalline region in LVC-4-HT and that in LVC-2-HT occurred because the P-Na crystals in LVC-2-HT were isolated spheres, while the crystals in LVC-4-HT were connected throughout of the matrix, as shown in Figure 3.6, which had an important impact on the durability differences between the two samples.

Sample LVC-11

This melt was designed to form acmite, $NaFe(III)Si_2O_6$. The XRD data showed that the quenched sample was 100% glassy, and the heat-treated sample was 100% crystalline. Ninety-nine volume percent of the crystals in LVC-11-HT were acmite, and the remaining 1 vol% was hematite. The SEM micrograph in Figure 3.8a shows the morphology of acmite; the EDS spectrum (Figure 3.8b) shows the composition (light area of Figure 3.8a). The TEM micrograph of Figure 3.9 shows both glassy and crystalline regions in the LVC-11HT sample.

Acmite belongs to the clinopyroxene family (or monoclinic chain silicates) and is often refered to as aegirine. The crystals usually occur as slender prisms with steep terminations. Chemical compositions analyzed (Table 3.3) were in support of the results of SAD identifications, indicating these crystals are almost pure aegirine. Morphologically different glasses were found, as shown in Figures 3.9 and 3.10. The uniform glass was dominant and occupied 80 vol% of the total glasses. Chemically, these two types of glasses had major differences in SiO_2 and Fe_2O_3 contents, as shown in Table 3.4. In acmite crystals, Fe-rich phases occur as tiny inclusions, as shown in Figure 3.11. The Fe-rich phases were identified by the ring-pattern of SAD and EDS composition as hematite, Fe_2O_3. Obviously, these hematite crystals were formed from the reaction of reactants during acmite-phase crystallization.

Heat Treatment Effect on Crystallinity

Upon heat treatment, the samples usually underwent a noticeable color change and became more opaque, as shown in Table 3.2. The XRD data showed a large increase in the volume fraction of crystallinity after heat treatment, except for LVC-1 and LVC-2 where change did not occur (Table 3.2). However, the crystal size in LVC-2HT increased by 7 times after heat treatment.

3.1.4 Waste Form Chemical Durability

The analysis of the Toxicity Characteristics Leach Procedure (TCLP) leachate indicated that all the VC samples passed the U.S. Environmental Protection Agency (EPA) TCLP limit for hazardous elements concentrations of Ag, As, Ba, Cd, Cr, Hg, Pb, and Se in the TCLP leachates. While an EPA limit is unavailable for Ni, all the VC samples passed the more restrictive land-disposal limit of 0.32 ppm as shown in Table 3.5.

The 7-day PCT results are tabulated in Table 3.6, while the longer duration PCT and vapor hydration test data are tabulated in Appendix B. The sodium release rate for the high-level nuclear waste reference glass (EA glass [DOE 1982]) was 6.4 g/m^2 in the 7-day PCT (see Appendix C). The 7-day PCT results in Table 3.6 suggest that LVC-2, LVC-3, and LVC-11 were much more durable than the EA glass, while the durabilities of LVC-1 and LVC-4 were much less.

Table 3.3. EDS Chemical Compositions (wt%) of Aegirine in LVC-11HT

Sample #	3-100	3-101*	3-112	3-113	2-306*	2-305
SiO_2	50.61	48.62	50.52	48.29	46.25	50.71
Fe_2O_3	35.72	40.61	34.89	38.90	41.33	35.51
Na_2O	13.41	10.62	12.65	12.14	12.42	13.12
CaO	0.25	0.15	0.53	0.31	--	--
Cr_2O_3	0.00	0.00	0.24	0.29	--	--
K_2O	0.00	0.00	0.09	0.07	0.00	0.06
P_2O_3	0.00	--	0.62	0.00	0.00	0.00
MgO	0.00	--	0.46	0.00	--	--
Al_2O_3	0.00	0.00	0.00	0.00	0.00	0.60

* These analyses covered the areas which enclosed Fe_2O_3 inclusions.

Table 3.4. EDS Chemical Compositions (wt%) of Glasses in LVC-11HT

Sample #	3-104*	3-106*	2-312**	3-102**	3-111**
SiO_2	42.25	43.74	61.62	63.25	59.40
Fe_2O_3	26.75	32.38	15.38	13.91	13.56
Na_2O	15.07	15.56	16.20	13.52	16.55
CaO	6.92	4.25	--	0.16	0.26
Cr_2O_3	0.37	0.79	--	0.20	0.00
K_2O	0.41	0.12	1.48	1.22	1.48
P_2O_3	6.20	0.61	1.79	1.61	2.70
MgO	--	0.61	--	--	0.72
Al_2O_3	2.04	1.94	3.53	6.12	5.30

* Spherical glasses.
** Uniform glasses.

LVC-2 had a crystal content of about 15 vol%, which was mainly Na_3PO_4 crystals in the form of spheres isolated in a durable glassy matrix, as shown in Figures 3.2 and 3.3. Although the Na_3PO_4 was very soluble in water, the glassy matrix was enriched in SiO_2 and Al_2O_3 (over 90 wt% of SiO_2 plus Al_2O_3) and depleted in alkalis (less than 2 wt%), as shown in Table 3.7 (for LVC-2Q), and hence, was very durable. The durable glassy matrix limited the access of water to the Na_3PO_4 crystals, resulting in the overall durability of LVC-2. This was similar to the liquid-liquid or glass-in-amorphous phase separations observed in borosilicate glasses (Peeler). The normalized 7-day Na release from LVC-2HT was 0.504 g/m^2, which was a factor of 13 times smaller than the 6.4 g/m^2 of the EA glass. Note that LVC-2HT had an alkali content of 25 wt%, while the EA glass had an alkali content of 21 wt%. The longer duration of PCT results are shown in Figure 3.12 and Figure 3.13 for LVC-2Q and LVC-2HT. The 7-day PCT durability was similar for LVC-2Q and LVC-2HT in terms of Na releases. in PCTs. However, the 91-day PCT durability for LVC-2HT was much better than that of LVC-2Q. The heat-treated LVC-2HT had a sodium release of 0.95 g/m^2 while LVC-2Q had a release of 2.01 g/m^2. The better durability of heat-treated sample LVC-2HT may be due to larger separation of the Na_3PO_4 crystals, because the crystals of Na_3PO_4 were 7 times larger than those in LVC-2Q, while the total volume of crystallinity of both samples was the same. It could also be due to the lower Na_2O content in the glassy matrix of LVC-2HT, due to better extraction of Na_2O from glassy matrix during the long heat-treatment process as shown in Table 3.7.

The 7-day PCT pH of LVC-2HT was 10.77, much lower than the pH of 11.55 for the quenched sample. The pH difference between LVC-2HT and LVC-2Q was maintained through 91-day PCTs. The 91-day PCT pH of LVC-2HT was 11.25, while it was 12.09 for LVC-2Q. The lower pH in LVC-2HT may have been responsible for the lower Si release (0.14 and 0.24 g/m^2 in 7- and 91-day PCTs) compared to the quenched LVC-2Q sample (0.19 and 0.49 g/m^2,respectively).

The above durability results were obtained through PCT, which required a water-washing process to get rid of the fine particulates that were present in the powders of vitreous ceramics before the particles were used for PCTs. This may have caused some concern regarding the vitreous ceramic samples that contain water soluble phases, such as Na_3PO_4, because the water-washing step could have selectively removed the water-soluble phases, leaving phases that were less water soluble. Therefore, results from such a test may not represent the actual durability of the waste form. To address these concerns, samples of LVC-2Q and LVC-2HT were washed only with acetone to remove the fine particulates, as required by a PCT, but not to dissolve Na_3PO_4 crystals. The acetone-washed powder samples were subjected to the same PCT; the results of which are summarized in Appendix C. The new data show that LVC-2HT had a pH of 11.01, Na release of 0.33 g/m^2, and Si release of 0.02 g/m^2 in 7-day PCTs, while LVC-2Q had a pH of 10.81, Na release of 0.82 g/m^2, and Si release of 0.16 g/m^2. The 7-day PCT results from the acetone-washed vitreous-ceramic particles were consistent with the 91-day PCT results (of the regular PCT tests) in that LVC-2HT was more durable than LVC-2Q.

Table 3.5. Leachate Concentrations from TCLP Tests

	Element (μg/mL)								
Vitreous Ceramic	As	Ba	Cd	Cr	Pb	Hg	Se	Ag	Ni
LVC-1	<0.001	<.01	<.01	1.55	<.08	<0.001	<0.001	<.01	<.02
LVC-2	<0.001	<.01	<.01	<.02	<.08	<0.001	<0.001	<.01	<.02
LVC-3	<0.001	<.01	<.01	0.8	<.08	<0.001	<0.001	<.01	<.02
LVC-4	<0.001	<.01	<.01	<.02	<.08	<0.001	<0.001	<.01	<.02
LVC-5	<0.001	0.21	<.01	<.02	<.08	<0.001	<0.001	<.01	<.02
LVC-6	0.034	0.05	<.01	2.28	<.08	<0.001	<0.001	<.01	<.02
LVC-7	0.0050	1.31	<.01	<.02	<.08	<0.001	0.013	<.01	0.38
LVC-8	<0.001	<.01	<.01	<.02	<.08	<0.001	<0.001	<.01	<.02
LVC-9	<0.001	<.01	<.01	<.02	<.08	<0.001	<0.001	<.01	<.02
LVC-10HT	<0.001	<.01	<.01	<.02	<.08	<0.001	0.003	<.01	<.02
LVC-12	<0.001	<.01	<.01	<.02	<.08	<0.001	<0.001	<.01	<.02
LVC-13	<0.001	<.01	<.01	<.02	<.08	<0.001	<0.001	<.01	<.02
LVC-14		.24	<0.01	<.02	<.08			<.01	<.02
LVC-15		.10	<0.01	<.02	<.08			<.01	<.02
Regulatory Level	5	100	1	5	5	0.2	1	5	
Land Disposal Limit			0.006	5.2	0.51			0.072	0.32

Table 3.6. Normalized Elemental Releases (g/m^2) from 7-Day PCT of Alkali-Binding Vitreous Ceramics

	Element	Oxide (wt%)	Sample C NL(g/m^2)	Sample D NL(g/m^2)	Average	pH
LVC-1Q	Na	28.49	36.59	38.02	37.31	11.44
	Si	19.22	0.23	0.20	0.21	
	Cr	0.05	16.17	16.71	16.44	
	Nd	0.02	0	0	0	
LVC-1HT	Na	28.49	31.04	29.89	30.46	11.38
	Si	19.22	0.25	0.25	0.25	
	Cr	0.05	16.39	16.22	16.30	
	Nd	0.02	15.77	21.56	18.67	
LVC-2Q	Na	24.08	0.53	0.57	0.55	11.55
	Si	48.60	0.15	0.23	0.19	
	Cr	0.05	0.40	0.13	0.26	
	Nd	0.02	0.77	0.07	0.42	
LVC-2HT	Na	24.08	0.53	0.50	0.52	10.77
	Si	48.60	0.15	0.14	0.14	
	Cr	0.05	0.40	0.40	0.40	
	Nd	0.02	0.77	0.91	0.84	

Table 3.6 Normalized Elemental Releases (g/m^2) from 7-Day PCT of Alkali-Binding Vitreous Ceramics, Continued

	Element	Oxide (wt%)	Sample C NL(g/m^2)	Sample D NL(g/m^2)	Average	pH
LVC-3Q	Na	19.14	0.39	0.40	0.39	11.12
	Si	38.66	0.19	0.20	.020	
	Cr	0.06	0.08	0.08	0.08	
	Nd	0.02	0	0	0	
LVC-3HT	Na	19.14	1.04	1.05	1.04	9.28
	Si	38.66	0.05	0.05	0.05	
	Cr	0.06	2.82	2.85	2.83	
	Nd	0.02	0.69	0.00	0.35	
LVC-4Q	Na	24.38	16.88	18.16	17.52	12.38
	Si	28.64	2.00	2.06	2.03	
	Cr	0.05	9.78	10.13	9.96	
	Nd	0.02	2.4	0.00	1.12	
LVC-4HT	Na	24.38	19.08	16.59	17.83	12.05
	Si	28.64	0.10	0.81	0.46	
	Cr	0.05	479.5	13.26	246.4	
	Nd	0.02	17.19	36.92	27.05	

Table 3.6. Normalized Elemental Releases (g/m^2) from 7-Day PCT of Alkali-Binding Vitreous Ceramics, Continued

	Element	Oxide (wt%)	Sample C NL(g/m^2)	Sample D NL(g/m^2)	Average	pH
LVC-11Q	Na	12.46	1.08	1.11	1.09	10.70
	Si	50.96	0.45	0.46	0.46	
	Cr	0.04	0.00	0.00	0.00	
	Nd	0.01	0.00	0.00	0.00	
LVC-11HT	Na	12.46	1.16	1.16	1.16	11.26
	Si	50.96	0.34	0.34	0.34	
	Cr	0.04	0.00	0.00	0.00	
	Nd	0.01	0.24	0.19	0.22	

Table 3.7. Glassy Matrix Composition (wt%) of LVC-2Q and LVC-2HT Analyzed by TEM EDS

	LVC-2Q				LVC-2HT		
	A	B	C	Average	A	B	Average
SiO_2	77.79	77.24	79.18	78.07	79.05	79.12	79.09
Al_2O_3	14.20	15.04	13.83	14.36	12.56	12.25	12.41
P_2O_5	6.19	6.09	5.13	17.41	7.26	7.06	7.18
Na_2O	1.82	1.14	1.76	1.57	0.80	1.39	1.10
K_2O	0.00	0.35	0.09	0.15	0.11	0.17	0.14
FeO	0.00	0.14	0.00	0.05	0.22	0.00	0.11
MgO	0.00	0.00	0.00	0.00	0.00	0.00	0.00

The above results indicated that LVC-2Q was already 8 times more durable than the EA glass and that the LVC-2HT can be 19 times more durable than the EA glass (by comparison of 7-day PCT results of EA glass with those of acetone-washed vitreous ceramic samples of LVC-2). In actual large-scale production of waste forms, the molten vitreous ceramics can be poured into large monolith blocks where the waste form is not quenched (as in LVC-2Q) and the product will be more like LVC-2HT, depending on the size of the monolith produced. The larger the block is, and the longer it stays in the pouring chamber, the more durable the product will be. Therefore, devitrification of VC will not be the concern as it would be in a glass waste form production process. The results from LVC-2Q and LVC-2HT confirmed the approach of developing a durable waste form through isolating water-soluble crystals in a durable glassy matrix.

The nepheline crystals were successfully developed in LVC-3HT; the 7-day PCT results suggested that the nepheline-containing LVC-3HT had a sodium release of 1.05 g/m^2, a factor of 2.6 higher than 0.40 g/m^2 for LVC-3Q, the counterpart homogeneous glass. The 7-day leachate pH of LVC-3HT was 9.28, almost 2 units lower than the pH 11.12 of LVC-3Q. This lower pH lead to a low Si release of 0.05 g/m^2, a factor of 4.3 lower than 0.20 g/m^2 for LVC-3Q. The longer term durability is shown in Figures 3.14 (LVC-3Q) and 3.15 (LVC-3HT). These results indicated that the corrosion rate of LVC-3Q accelerated after 28 days of PCT, while the corrosion rate for LVC-3HT was very stable. In 91-day PCT, LVC-3HT had a Na release of 1.35 and a Si release of 0.04 g/m^2, while LVC-3Q had a Na release of 1.82 and a Si release of 0.645 g/m^2. This means that vitreous ceramic LVC-3HT had better long-term durability than the corresponding glass LVC-3Q, although both had exactly the same compositions (in fact, they were formed from the same melt: the glass resulted from quenching the melt and the vitreous ceramic was formed through additional heat treatment). This was a good demonstration that crystalline nepheline is thermodynamically more stable and more corrosion-resistant than the corresponding glass. Vapor-hydration testing of the nepheline-containing vitreous ceramics will be discussed in the next section; however, nepheline was found to be very durable and stable even under vapor-hydration testing conditions.

Acmite formed in LVC-11HT, and the 7-day PCT results show that the acmite-containing VC was slightly less durable than the corresponding glass melt of LVC-11Q. The PCT leachate pH was 11.26 for LVC-11HT, much higher than 10.78 of the corresponding glass sample, LVC-11Q. The Si, Cr, and Nd releases were similar for both LVC-11Q and LVC-11HT. The acmite-containing VC, LVC-11HT, was slightly less durable than the nepheline-containing LVC-3HT. However, the low alkali-loading and the higher PCT leachate pH of the acmite-containing VC made it less useful than the nepheline-containing VC for treating high-alkali wastes. The longer duration tests of LVC-11Q and LVC-11HT have not been performed yet.

The high sodium release rates from both LVC-1Q and LVC-1HT indicated that the high sodium and low silica contents weakened the structure of the waste form. The longer duration durability, presented in Figures 3.16 and 3.17, showed that the total structure of the waste form was corroded and the elemental concentration reached a maximum that did not change with test duration. The failure to produce a sufficient amount of NZP crystals made LVC-1HT similar to LVC-1Q in durability. The optimized conditions for NZP synthesis will be further investigated.

The failure to produce perovskite types of crystals in LVC-4HT resulted in the formation of a large amount of soluble Na_3PO_4 crystals. Although the sodium content of LVC-4HT was similar to that of LVC-2HT, the silica and alumina contents in LVC-4HT were too low to form a continous durable glass matrix to isolate the soluble Na_3PO_4 phase. On the other hand, the soluble phases of Na-P and

Na-Ca-P were so abundant that they formed a interconnected matrix, which severly deteriorated the durablility of LVC-4HT. The longer duration durability for LVC-4Q and LVC-4HT (Appendix C) showed the same situation as in LVC-1: the waste form was essentially totally dissolved in 7-day PCTs and therefore the longer duration durability was the same as those of 7 day PCT for both LVC-4Q and LVC-4HT.

3.1.5 Summary

The work described above extended the success of VC waste forms to treat wastes with both high metal and high alkali contents. This work included two approaches: developing high-durability alkali-binding crystals in a durable glassy matrix and developing water-soluble crystals in a durable and continuous glassy matrix.

The development of low-solubility alkali-binding crystalline phases included: (1) phases free of SiO_2 and Al_2O_3 that bind alkalis such as NZP, NTP, alkali-containing perovskite, and other phosphate compounds that have low solubility in water (this development is ongoing, and the melting conditions for these types of crystals must be optimized); and (2) phases incorporating Si, Al, and alkalis such as nepheline and acmite. Nepheline and acmite were successfully developed. Nepheline is more promising than acmite because of its high alkali-loading and low-leachate pH. The longer durability of nepheline-containing vitreous ceramics was much better than the corresponding glass with the same chemical compositions.

The development of durable vitreous ceramics that consist of isolated water-soluble alkali-binding crystals must satisfy the following conditions: (1) the alkali-binding crystals have to be isolated in the waste form; (2) the glassy matrix has to be enriched in network-forming elements such as SiO_2 and Al_2O_3 and be low in alkalis; and (3) the glassy matrix has to be continuous. These conditions were successfully met in this project.

LVC-2Q/LVC-2HT showed a microstructure consisting of round particles (about 1000nm) dispersed uniformly in the glassy matrix. The fine particles were crystalline Na_3PO_4, and the glassy phase was enriched in SiO_2 and Al_2O_3. Although the Na_3PO_4 was soluble in water, the durable glassy phase limited the access of water to Na_3PO_4, and the overall durability of this VC was very good. The normalized Na release from LVC-2Q was 0.50 g/m^2 in a 7-day PCT, which was a factor of 13 times smaller than the 6.4 g/m^2 for the 7-day PCT of the high-level EA glass. The LVC-2Q had morphology similar to the LVC-2HT, but the size of the Na_3PO_4 crystalline phases was only about 150nm and the longer term chemical durability was not as good as LVC-2HT. This was probably due to the shorter separation between Na_3PO_4 crystals in LVC-2Q and less complete extraction of alkalis from glassy matrix due to lack of heat treatment. The LVC-2 samples had a sodium-loading of 24 wt% with good chemical durability. The heat-treated sample, LVC-2HT, further reduced the sodium release. Therefore, these types of waste forms can withstand a large variation in cooling rates during actual production, which provides more flexibility in terms of the product shape and production rate.

These results are significant based on the following: (1) the range of waste streams that can be treated with VC waste forms will be expanded to include those with high alkali contents, especially those with high metal contents; (2) the DOE vitrification technology can be applied to a wider range of DOE waste streams; and (3) higher waste-loading, smaller final-waste volume, more flexible waste-form productions, and larger remediation cost-savings may be realized.

3.2 Nepheline Formation in Vitreous Ceramics

In the previous section, we described the formation of nepheline crystals in vitreous ceramics that enhanced chemical durability, especially in terms of long-term durability. How the crystalline formation changes with the variation in batching compositions and which part of the vitreous ceramics, nepheline crystals or glassy matrix, controls the overall durability of the waste form are not well understood. The work described in this section is intended to provide some understanding of these conditions, which will help in the optimization of waste forms for the actual remediation efforts using vitreous ceramics.

3.2.1 Nepheline Formation Condition and Starting Compositions

Four melts of vitreous ceramics were conducted to produce nepheline crystals (LVC-3HT, LVC-10HT, LVC-12HT, and LVC-13HT). During the production of these vitreous ceramics, a part of each melt was quenched to produce the corresponding glass waste form, LVC-3Q, LVC-10Q, LVC-12Q, and LVC-13Q, so that a comparison could be made between nepheline-containing vitreous ceramics and glasses with exactly the same chemical compositions. The melting conditions for these melts are shown in Table 3.8. The batch compositions are shown in Table 3.9. In LVC-3 and LVC-12, TiO_2 was added as the nucleation agent for nepheline formation. It was later found that the nepheline crystals can be formed under these melting conditions without the addition of TiO_2, as shown in LVC-10 and LVC-13. The formula of nepheline is $NaAlSiO_4$, which corresponds to a theoretical ratio of Na_2O:Al_2O_3:SiO_2 as 1.0:1.0:2.0. To incorporate sodium in the nepheline structure completely, slightly more SiO_2 and Al_2O_3 were added for some of the melts, as shown by the mole ratios in Table 3.9. The corresponding Na_2O:Al_2O_3:SiO_2 ratios were 1.00:1.00:2.00 for LVC-12; 1.00:1.04:2.08 for LVC-3; 1.00:1.00:2.32 for LVC-13; and 1.00:1.17:2.53 for LVC-10. LVC-10 and LVC-13 had substantially higher SiO_2 and Al_2O_3.

3.2.2 Solid Phase Characterization

LVC-12

LVC-12 was formulated with exactly the same ratio of Na_2O:Al_2O_3:SiO_2 as found in a perfect nepheline crystal. LVC-12Q was completely amorphous and LVC-12HT was completely crystalline, with up to 98% of nepheline according to XRD analyses. Under the optical microscope, as shown in Figure 3.18, LVC-12HT consisted of 5- to 10-μm particles. These were nepheline, rutile, and glass as shown by the TEM micrograph in Figure 3.19. The dominant phase was nepheline. Rutile crystals and glassy spheres were scattered randomly in a nepheline matrix. Two morphologically different rutile phases are found: a large pillar form (2- to 10-μm in size) and very tiny crystallites (100 nm long), as seen in Figure 3.20.

Table 3.8. Melting and Heat Treatment Conditions For Nepheline Formation

Sample	Melting Temperature (°C)	Heat Treatment (°C)	Crystallinity	Color
LVC-3Q	1515		0	Green
LVC-3HT	1515	900° for 45 h	100	Pale green opaque
LVC-10Q	1600		0	Green
LVC-10HT	1600	850° for 2 h then 1050° for 4 hr	100	Pale green opaque
LVC-12Q	1600		0	Green
LVC-12HT	1600		0	pale green opaque
LVC-13Q	1600		0	Green
LVC-13HT	1600	850° for 4 h then 1050° for 2 hr	100	pale green opaque

The glassy phases also have two morphologically different forms, as shown in Figure 3.19: large and small glassy inclusions in nepheline matrix. Large glassy inclusions (3-to 6-μm in size and preferentially thinned by ion milling) usually grew at junctions of nepheline grain boundaries. Small glass inclusions were also enclosed in the inner zones of nepheline crystals.

The chemical compositions of both nepheline crystals and glassy phases analyzed with TEM EDS are shown in Tables 3.10 and 3.11. The average compositions of the five EDS analysis shown in Table 3.10 were SiO_2 44.1, Al_2O_3 34.3, and Na_2O 21.0 wt% These compositions were very similar to the perfect nepheline crystals of SiO_2 42.3, Al_2O_3 35.9, and Na_2O 21.8 wt%. This composition and SAD pattern shown in Figure 3.19b positively identify the matrix of LVC-12HT as nepheline. Two groups of glassy compositions can be recognized in Table 3.11: Group A was highly enriched in Na and relatively lower in Si and Al compared to Group B. However, Group B was much more common than the Group A composition. The high-sodium glassy phase may have an important effect on the overall durability of LVC-12HT. Because these glassy phases were tiny and embedded in nepheline crystals, the errors associated with the EDS composition analysis may have been large.

LVC-13

LVC-13 was formulated with slightly more SiO_2 than the perfect nepheline crystal; the Na_2O:Al_2O_3:SiO_2 ratio was 1.0:1.0:2.32. LVC-13Q was completely amorphous and LVC-13HT was completely crystalline, as indicated by XRD analysis. LVC-13HT was similar to LVC-12HT in microstructure except that no TiO_2 was added as an nucleation agent. Only two phases were found in LVC-13HT: nepheline and glass inclusions, as shown by Figure 3.21. Nepheline crystals occurred as isogranular structures. The glassy phases, like LVC-12HT, had two morphologically different types: large (2- to 6-μm in size) and small ($<$1-μm) inclusions. These glassy inclusions were distributed randomly in the nepheline matrices. Some large inclusions may have also occurred at junctions of nepheline grain boundaries (Figure 3.22).

Chemical compositions of nepheline crystals analyzed by TEM EDS are shown in Table 3.12. Compared to LVC-12HT, nepheline in LVC-13HT had a higher Si/Al ratio (Table 3-12), which was consistent with the higher SiO_2 content in the batching composition. Extensive EDS analyses on these glassy inclusions were done to examine chemical composition variation of the glasses, as shown in Table 3.13. Two groups of glasses were found: Group A was high in P and low in Na, and Group B was high in Si and low in P. One obvious feature of these glassy inclusions was the low content of sodium as compared to the nepheline matrix of LVC-13HT and to the glassy phases in LVC-12HT. Figure 3.23 shows the two kinds of morphologically different glassy inclusions: large and small particles. The numbers in Figure 3.23 correspond to the analytical IDs of Table 3.13. These low sodium-containingg glassy phases may have had a large impact on the overall durability of LVC-13HT, which will be discussed in later sections.

Table 3.9. Batch Compositions of Nepheline-Vitreous Ceramics (wt% and Molar Ratios)

	LVC-3	LVC-10	LVC-12	LVC-13	Nepheline	LVC-3	LVC-10	LVC-12	LVC-13	Nepheline
Chemical	Oxide (wt%)	Oxide (wt%)	Oxide (wt%)	Oxide (wt%)	Oxide (wt%)	Oxide mole	Oxide mole	Oxide mole	Oxide mole	Oxide mole
SiO_2	38.66	44.79	38.77	44.89	42.30	2.084	2.529	2.000	2.316	2.000
Al_2O_3	32.80	35.00	32.89	32.89	35.88	1.042	1.165	1.000	1.000	1.000
Fe_2O_3	0.01		0.00	0.00						
Na_2O	19.14	18.27	20.00	20.00	21.82	1.000	1.000	1.000	1.000	1.000
K_2O	0.51	0.33	0.33	0.33						
TiO_2	5.97	0.00	6.12	0.00						
Cr_2O_3	0.06	0.04	0.04	0.04						
CuO	0.00		0.00	0.00						
MnO	0.01	0.01	0.01	0.01						
SO_3	0.49	0.32	0.32	0.32						
ZrO_2	0.01	0.01	0.00	0.00						
P_2O_3	1.84	1.18	1.19	1.19						
F	0.33	0.21	0.21	0.21						
Cl	0.14	0.09	0.09	0.09						
Bi_2O_3	0.01	0.01	0.01	0.01						
Nd_2O_3	0.02	0.01	0.01	0.01						
total	100.0	100.0	100.0	100.0	100.0	4.1	4.7	4.0	4.3	4.0

Table 3.10. Chemical Composition of Nepheline in LVC-12HT by EDS

SAMPLE #	3-2	3-3	3-4	3-5	3-6
SiO_2	44.58	44.42	43.76	44.45	43.46
Al_2O_3	34.13	35.13	34.13	33.74	34.30
Na_2O	20.87	20.02	21.41	21.13	21.60
Fe_2O_3	0.06	0.09	0.10	0.00	0.00
CaO	0.14	0.00	0.08	0.00	0.08
Cr_2O_3	0.00	0.00	0.05	0.19	0.08
K_2O	0.21	0.33	0.46	0.47	0.47
Cation					
Si	1.049	1.042	1.036	1.050	1.022
Al	0.945	0.969	0.950	0.937	0.990
Na	0.951	0.909	0.981	0.965	0.956
Fe	0.001	0.001	0.001	0.000	0.000
Ca	0.003	0.000	0.002	0.000	0.002
Cr	--	0.000	0.001	0.003	0.002
K	0.006	0.010	0.014	0.014	0.014

Table 3.11. Chemical Compositions of Glasses (wt%) in LVC-12HT by EDS

SAMPLE #	3-7*	3-10*	3-8	3-11	3-12	3-13	3-14	3-15	AVERAGE
SiO_2	27.07	29.56	37.72	39.00	41.07	40.08	35.18	38.83	36.11
Al_2O_3	21.06	23.89	29.71	30.84	33.86	33.89	28.79	31.05	29.14
P_2O_5	1.42	0.97	0.82	3.04	4.07	6.94	6.92	1.71	3.24
Na_2O	45.16	42.29	27.28	17.75	16.47	14.57	19.14	19.27	25.24
CaO	0.93	0.68	0.50	1.88	1.90	1.74	1.11	0.34	1.14
TiO_2	3.58	1.76	3.30	6.60	1.33	1.35	2.04	6.77	3.34
Cr_2O_3	0.11	0.23	0.22	0.21	0.25	0.33	1.36	0.20	0.36
Fe_2O_3	0.67	0.61	0.47	0.69	1.05	1.11	5.10	1.26	1.37
K_2O	--	--	--	--	--	--	0.36	0.38	0.37

* The glasses are quite different from most glasses in composition, with higher sodium.

LVC-3

LVC-3 was formulated with compositions that very similar to a pure nepheline; the ratios of Na_2O:Al_2O_3:SiO_2 were 1.00:1.04:2.08. TiO_2 was also added as a nucleation agent. The solid characteristics of the as-melted LVC-3 were briefly described above. XRD and TEM identified three types of phases, nepheline, rutile, and glassy inclusions. The optical micrograph of LVC-3 is shown in Figure 3.24; nepheline crystals were gray and brown in color, although they had similar chemical compositions, as discussed above. The TEM micrograph of Fig. 3.25 shows that the residual glassy phases are found as inclusions in the nepheline matrix.

The chemical compositions of the nepheline phases and glassy phases are shown in Tables 3.14 and 3.15, respectively.

LVC-10

LVC-10 was the only formulation among the nepheline formulations of LVC-3, LVC-10, LVC-12, and LVC-13, which that had an excess of both SiO_2 and Al_2O_3 in comparison with a pure nepheline crystal. The ratios of Na_2O:Al_2O_3:SiO_2 of LVC-10 were 1.00:1.17:2.53, as shown in Table 3-9. Visual inspection and XRD analysis indicated that LVC-10Q was completely amorphous. LVC-10HT was the only one among the nepheline formulations, which had a crystallinity of 75 vol.%, according to XRD analysis. This was consistent with the formulation presented in Table 3.9. Among the crystals, XRD identified 90% of them as nepheline.

Table 3.12. Chemical Compositions of Nepheline in LVC-13HT by EDS

SAMPLE #	3-20	3-30	3-37		3-20	3-30	3-37
SiO_2	47.10	46.43	46.25	Si^{4+}	1.109	1.092	1.087
Al_2O_3	30.80	31.92	32.36	Al^{3+}	0.853	0.884	0.895
Na_2O	21.63	21.14	20.93	Na^{+}	0.985	0.963	0.952
Fe_2O_3	0.11	0.00	0.09	Fe^{3+}	0.002	0.000	0.001
CaO	0.00	0.00	0.00	Ca^{2+}	0.000	0.000	0.000
Cr_2O_3	0.11	0.00	0.00	Cr^{3+}	0.002	0.000	0.000
K_2O	0.26	0.51	0.37	K^{+}	0.008	0.015	0.011

Table 3.13. Chemical Compositions of Glass Phases (wt%) in LVC-13HT by EDS

	3-21	3-22	3-23	3-24	3-28	3-29	3-34	3-26*	3-27	3-31	3-32	3-36
SiO_2	53.55	51.04	53.64	56.27	58.54	52.49	59.26	10.83	48.47	23.45	40.23	40.48
Al_2O_3	38.36	27.57	31.99	37.00	33.52	35.52	34.53	21.56	33.82	26.00	21.88	28.45
P_2O_3	1.15	4.30	1.32	0.67	3.49	0.31	1.65	60.99	11.56	42.80	29.92	22.00
Na_2O	6.06	12.55	11.12	5.39	3.74	10.93	2.59	3.93	5.40	4.80	4.70	8.25
CaO	0.00	0.31	0.10	0.00	0.32	0.12	0.26	1.00	0.29	1.15	0.93	0.17
Cl	--	0.68	0.15	0.11	0.00	0.08	0.00	0.24	0.00	0.13	0.19	0.15
$Cr2O_3$	0.29	1.33	0.35	0.00	0.18	0.21	0.37	1.30	0.18	0.98	0.66	0.21
Fe_2O_3	0.16	2.21	1.23	0.21	0.00	0.34	1.33	0.15	0.00	0.23	1.48	0.14
K_2O	0.42	0.00	0.20	0.34	0.20	0.00	0.00	0.00	0.28	0.46#	0.00	0.17

Table 3.14. Chemical Compositions (wt%) of Nepheline from Gray Particles and Brown Matrix in LVC-3

Oxides	Brown matrix	Gray particles
SiO_2	42.91	48.84
Na_2O	18.77	14.58
Al_2O_3	35.14	32.42
P_2O_5	0.87	1.33
K_2O	0.43	0.70
CaO	0.00	0.04
TiO_2	1.88	2.03
MgO	0.00	0.06

Table 3.15. Compositions of Two Glass Regions in LVC-3HT

Oxide	Gray*	Brown**
SiO_2	53.12	55.18
FeO	0.08	0.16
Na_2O	2.72	1.96
CaO	0.00	0.06
Al_2O_3	38.27	36.23
P_2O_5	1.75	3.28
TiO_2	.50	.61

* Average of 7 EDS samples.
** Average of 12 EDS samples.

The fluidal structure of the LVC-10HT specimen could be recognized through visual inspection of the specimen and was confirmed by the optical micrograph shown in Figure 3.26. Under TEM, nepheline was the dominant phase, occurring as microtwins as shown in Figure 3.27a. The chemical composition analyzed by TEM EDS are shown in Table 3.16. It was noted that the measured sodium value was between 0.85 to 0.97, slightly lower than the theoritical vale of 1.0. The rosette-like crystals in Figure 3.26b are spinel as confirmed with TEM analysis; these spinel phases were very small, only 0.1 to 0.5 micron across, as shown in Figure 3.27b. The EDS analysis shown in Table 3.17 indicated that the spinel can be expressed as $(Mg,Cr(+2), Zn)(Cr(+3), Al)_2O_4$.

There were two types of glassy phases in LVC-10HT: inclusions from fluidal microstructure in the nepheline matrix (Figure 3.27c) which also corresponded to the fluidal structure observed under optical microscope, as shown in Figure 3.26, and a residue glassy phase which filled the gap in the nepheline matrix, as shown in Figure 3.27d. The glasses in fluidal structure were dominant; their compositions were enriched with SiO_2 and Al_2O_3, but depleted in alkalis, as shown in Table 3.18. The remaining glassy phases were minor and rich in sulphur and molybdenum, but low in SiO_2, as shown in Table 3.18. This composition was typical of the left-over from the crystallization process in LVC-10HT. This residual glassy phase must not be durable, but it may not contribute to the overall durability of the waste form since it was a minor phase embedded in a durable nepheline matrix, which will be discussed more below.

3.2.3 Chemical Durability

The chemical durability of the nepheline-vitreous ceramics was evaluated with PCT up to 91 days at 90°C; LVC-10HT was also tested in a vapor-hydration test for 28 days at 150°C. The detailed PCT results are shown in Appendix C and the selected major element releases in PCT are shown in Table 3.19.

Table 3.16. EDS Measurements (wt%) of Nepheline in LVC-10HT

Sample #	MNS36 (wt%)	2-53 (wt%)	2-53 (wt%)	2-52 (wt%)	2-51 (wt%)
	EDS/EMPA	EDS/AEM	EDS/AEM	EDS/AEM	EDS/AEM
SiO_2	47.56	48.91	47.07	46.98	47.33
Al_2O_3	33.06	31.75	30.49	30.66	31.13
Na_2O	18.53	18.91	21.43	21.14	20.53
P_2O_5	0.75	0.32	0.62	0.72	0.44
K_2O	0.29	0.11	0.11	0.34	0.38
formula					
Si	1.10	11.13	1.11	1.10	1.11
Al	0.90	0.90	0.84	0.85	0.86
Na	0.83	0.85	0.97	0.96	0.93
P	0.02	0.01	0.01	0.01	0.01
K	0.00	0.00	0.00	0.01	0.01
Method	ZAF	K_{Na}=2.89	K_{Na}=3.42	K_{Na}=3.42	K_{Na}=3.42

Table 3.17. Selected Chemical Compositions (wt%) for Spinel in LVC-10HT

Sample #	2-58 (wt%)	2-57 (wt%)	2-56 (wt%)	2-01 (wt%)
MgO	14.39	12.89	11.40	13.55
Cr_2O_3	46.84	55.15	51.10	53.72
Al_2O_3	27.75	21.96	24.78	24.94
FeO	1.55	1.26	1.28	1.07
ZnO	2.80	2.18	1.96	2.24
NiO	0.53	0.51	0.26	0.44
SiO_2	4.06	3.14	6.70	1.83
Na_2O	2.07	2.92	2.53	2.20

Table 3.18. EDS Compositions (wt%) of Glassy Phases in LVC-10HT

Fluidal Structures					Residual Type
Sample	4-119	4-110	4-111	4-113	27.19
SiO_2	59.40	63.04	59.90	61.89	6.71
FeO	0.07	0.01	1.12	0.22	6.02
Na_2O	1.88	1.10	1.33	2.71	0.55
NiO	--	---	--	--	20.65
SO_3	--	--	--	--	--
MgO	0.00	0.01	0.00	0.05	16.56
Al_2O_3	38.32	34.41	37.00	34.71	--
CaO	0.11	0.01	0.00	0.05	--
K_2O	0.22	0.11	0.00	0.46	--
P_2O_5	--	1.33	0.64	0.00	--
SrO	0.00	0.00	0.00	--	--
Cr_2O_3	--	--	--	--	2.40
MoO_3	--	--	--		19.92

Table 3.19. Major Elemental Releases (g/m^2) of Nepheline Vitreous Ceramics in PCTs

ID	7-day				28-day				91-day			
	Na	Si	Al	pH	Na	Si	Al	pH	Na	Si	Al	pH
LVC-12Q	0.328	0.190	0.196	10.80								
LVC-12HT	0.623	0.063	0.157	9.43								
LVC-3Q	0.393	0.196	0.204	11.12	0.483	0.204	0.211	11.27	1.821	0.635	0.652	11.20
LVC-3HT	1.044	0.046	0.101	9.28	1.197	0.040	0.090	9.16	1.347	0.039	0.091	9.40
LVC-13Q	0.305	0.168	0.171	10.75								
LVC-13HT	0.406	0.036	0.065	9.07								
LVC-10Q	0.282	0.152	0.142	10.63.	0.372	0.174	0.161	10.88	0.454	0.180	0.166	10.97
LVC-10HT	0.222	0.155	0.151	9.89	0.263	0.176	0.175	10.17	0.285	0.179	0.177	10.04

3.3 Comparison Between Nepheline-Vitreous Ceramics and Glasses with Same Chemical Compositions

The durability of the waste forms is mainly discussed in terms of the most leachable element, Na. This is a most conservative approch since all the other hazardous elements and radionuclides have release rates often smaller or at least equivalent to the most leachable element, Na. The 7-day PCT durability comparison (Table 3.19) between the nepheline-vitreous ceramics (LVC-XXHT) and the corresponding glass samples (LVC-XXQ) showed that only the nepheline vitreous ceramics of LVC-10HT were more durable than the corresponding glass, LVC-10Q, in terms of sodium release and that the opposite was true for all the other formulations. The longer-term durability is shown in Figures 3.14 and 3.15 for LVC-3 and in Figures 3.28a and 3.28b for LVC-10. By comparing the glassy phase compositions in nepheline-vitreous ceramics (Tables 3.11, 3.13, and 3.15) with the corresponding glass compositions (Table 3.9, assuming LVC-12Q, LVC-13Q, and LVC-3Q had the same compositions as the batch compositions), it can be seen that some of the glassy phase compositions in the VCs have lower SiO_2 and Al_2O_3, but more alkalis and P_2O_5 than the corresponding quenched-glass samples, i.e., these glassy phases in VC were less durable than the corresponding glasses. These less-durable glassy phases in VC determine overall waste-form durability, especially during short-term tests. However, the total fraction of the glassy phase in these VCs (LVC-3HT, LVC-12HT, and LVC-13HT) was very limited because the XRD data indicated up to 99% crystallinities in these VCs and the longer term durability would be controlled by the nepheline phases when the accessable glassy phases were consumed. This was the case for LVC-3HT, where the 91-day durability of LVC-3HT was better than that of LVC-3Q, although the 7-day PCT results indicated the opposite durability order. Unfortunately, only 7-day PCTs have been performed for LVC-12 and LVC-13. In the case of LVC-12, the fluidal structure glassy phase (the majority) of LVC-10HT had chemical compositions (Table 3.18) more durable than the glass composition of LVC-10Q (Table 3.9, assuming the glass had the batch composition). The lower sodium releases, from 7 to 91 days in LVC-10HT than those in LVC-10Q, suggested that both of the glassy phases and the nepheline phase of LVC-10HT were more durable than the corresponding glass, LVC-10Q.

It is usually true that a higher sodium release results in higher solution pH. However, the leachate pHs from both short: 7-day to long: 91-day tests showed substantially higher solution pHs in glasses than in corresponding nepheline-vitreous ceramics (Table 3.19), regardless of the sodium releases. The SO_3 was uniformly distributed in the glass waste forms (LVC-XXQ) and was released as the glass matrix corroded. The SO_3 in nepheline-vitreous ceramics (LVC-XXHT) was highly concentrated in the less durable glassy phase, as shown in Table 3.18, where SO_3 was concentrated up to 20.65 wt%, and this SO_3 was quickly released into the leachate. This explaines why the SO_3 releases were 2 to 40 times higher in the leachates of nepheline-vitreous ceramics than in those of glasses, as shown in Table 3.20.

Table 3.20. SO_3 Concentrations (mg/L) Measured in PCTs

ID	Days		
	7	28	91
LVC-12Q			
LVC-12HT			
LVC-3Q		0.070	0.200
LVC-3HT		2.727	2.894
LVC-13Q			
LVC-13HT			
LVC-10Q	0.082	0.045	0.066
LVC-10HT	0.246	0.160	0.178

This higher concentration of SO_3 from the nepheline-vitreous ceramics buffered the leachates at lower pHs (Table 3.20). In the case of LVC-3 formulation, a difference in SO_3 concentrations between VC and glass were the least, but the lower sodium released from LVC-10HT (lower than those released from LVC-10Q) also favored the lower pHs of the leachates. The solution pH had a direct effect on SiO_2 concentration, that is, the higher the solution pH, the higher the silica concentration. However, SiO_2 concentration is not a good indicator of waste-form durability evaluation.

The above data suggested that nepheline formation enhanced or weakened waste form durability. The longer durability seems to favor the nepheline-vitreous ceramics. The leachate pHs were always lower with nepheline-vitreous ceramics than the pH of the corresponding glass. Low solution pH was usually associated with lower waste corrosion rates in glass(Feng 1993). Although the beneficial effects of low pH associated with vitreous ceramics are not obvious with the available data presented here.

3.3.1 Comparison Among the Nepheline Formulations

As discussed above, in nepheline formulations, the order of SiO_2 and Al_2O_3 in excess of their stoichiometric values was LVC-10 > LVC-13 > LVC-12 = LVC-3 (Table 3.9). The 7-day PCT durability order for glasses was LVC-10Q > LVC-13Q > LVC-12Q > LVC-3Q (Table 3.19), which was consistent with the chemical composition expected from the batch compositions listed in Table 3.9. The chemical durability order for the nepheline-vitreous ceramics was LVC-10HT > LVC-13HT > LVC-12HT > LVC-3HT (Table 3.19), which was the same as the order among the glasses. If all of the nepheline-vitreous ceramics were made of the same nepheline compounds which control waste-form durability, similar chemical durability is expected for all of the nepheline formulations.

The observed differences among these nepheline formulations suggested the following: (1) nepheline compounds can be different and have different chemical durabilities; and (2) nepheline crystals may or may not control the overall durability of the waste forms. The average EDS-analyzed compositions of the nepheline crystals and the residual glass phases in the nepheline-vitreous ceramics are summarized in Table 3.21. The nepheline compositions in all of these vitreous ceramics had some degree of variation and the relationship between these variations; the chemical durabilities of the corresponding vitreous ceramics was not obvious. However, the residual glass phase compositions showed a clear order of durability that was consistent with the observed durability order of these VCs. This suggested that the residual glass phase controlled the overal durability of the nepheline-vitreous ceramics. This may further suggest that the pure nepheline crystals may be more durable or as durable as LVC-10HT. It was noted that the durability of LVC-10HT had a sodium release of 0.222 g/m^2, which was a factor of 30 better than EA glass durability. More importantly, the reaction rate did not increase much with reaction duration. The reaction rate of LVC-10HT between 7 and 91 days is 7.5×10^{-4} $g/m^2/d$, while the reaction rate of the corresponding glass, LVC-10Q, was 20.5×10^{-4} $g/m^2/d$ during the same test period.

This meant that the reaction rate of a nepheline-vitreous ceramics was about 3 times slower. This difference was expected to be even larger at longer reaction times, because themodynamically nepheline may be much more stable than its glass counterpart. Also, the difference was expected to be larger with less-durable compositions, such as LVC-3, where the instability of the glass showed earlier. The reaction rate rate of LVC-3HT between 7- and 91-day PCTs was 36.1×10^{-4} $g/m^2/d$, while the reaction rate of the corresponding glass, LVC-3Q, was 0.017 $g/m^2/d$ during the same test period. This reaction rate difference was about 5 times that of the LVC-3 composition.

By comparing LVC-3 with LVC-12, the effects of the heat-treatment temperature and duration on the formation of nepheline, and possibly the effects of melting temperature, can be seen. LVC-3 and LVC-12 had the same batch composition as shown in Table 3.9. LVC-3 was melted at 1515°C and was heat-treated at 900°C for 45 h to form LVC-3HT, while LVC-12 was melted at 1600°C and was heat-treated at 1050°C for 2h and at 850°C for 4h to form LVC-12HT. The glasses, LVC-3Q and LVC-12Q, had similar 7-day PCT durability as shown in Table 3.19 and suggested that the different melting temperature did not influence the product durability. However, the 7-day PCT sodium release of LVC-12HT was 0.623 g/m^2, which was 68% less than the sodium release of LVC-3HT; this suggested that the heat-treatment condition had large effects on product durability.

The difference in LVC-12 and LVC-13 was that LVC-12 had 6.12% TiO_2 as a nucleation agent for the formation of nepheline and LVC-13 had no TiO_2, but 6.12% more SiO_2. Both VCs formed almost 100% nepheline crystals, which suggested that the nucleation agent was not necessary for the formation of nepheline in vitreous ceramics. LVC-12Q and LVC-13Q had similar 7-day PCT durability, while the LVC-13HT was about 40% more durable than LVC-12HT. This suggested that the replacement of SiO_2 by TiO_2 had no significant influence on glass durability, the effect on nepheline-vitreous ceramic durability is significant. Excess SiO_2 in LVC-13HT stabilized the residual glassy phase and enhanced the chemical durability, while the TiO_2 in LVC-12HT formed only separate rutile crystals which the presence of TiO_2 did not benefit the glassy phase durability.

Table 3.21. Average EDS Compositions of the Nepheline Phases and the Glass Phases (wt%)

	LVC-3	LVC-12	LVC-13	LVC-10	Nepheline	LVC-3	LVC-12	LVC-13	LVC-10
Chemical	Nepheline Wt %	Nepheline Wt%	Nepheline Wt %	Nepheline Wt %	Wt%	Glass Wt %	Glass Wt%	Glass Wt %	Glass Wt %
SiO_2	45.880	44.134	46.593	47.24	42.300		36.110	45.688	61.060
Al_2O_3	33.780	34.3	31.693	31.34	35.880		29.140	30.850	36.110
Fe_2O_3		0.05	0.067				1.370	0.623	0.355
Na_2O	16.680	21.006	21.230	20.41	21.820		25.240	6.620	1.755
K_2O		0.388	0.380	0.28			0.370	0.173	0.083
TiO_2	1.955						3.340		
Cr_2O_3		0.064					0.360	0.505	
CuO									
MnO									
SO_3									
ZrO_2									
P_2O_5	1.100			0.633			3.240	15.010	0.608
F	0.565								
Cl								0.144	
Bi_2O_3									
Nd_2O_3									
CaO		0.060					1.140	0.388	
Total	100.0	100.0	100.0	99.9	100.0	0.0	99.2	100.0	100.0

3.3.2 Chemical Durability of LVC-10HT Under Vapor Hydration Test Conditions

LVC-10HT was the only nepheline-vitreous ceramic tested with the vapor-hydration test at 150°C for 28 days. This was an accelerated durability test condition which may provide information about the long-term durability of nepheline vitreous ceramics. After the samples were removed from the test vessel, both samples appeared slightly swollen and slightly discolored. The SEM micrograph (Figure 3.29a) shows ditching and pitting on the surface of LVC-10HT; a cross-section of this sample showed no layer formation on the surface of the sample (Figure 29b), which may indicate good long-term chemical durability of this nepheline-vitreous ceramic. More detailed analysis of these samples using TEM is in progress.

3.3.3 Summary

Nepheline vitreous ceramics were successfuly formed in a temperature range between 1500° and 1600°C, followed by heat treatment between 850° to 1050°C for 6 to 45 hours. The melting temperature was not critical for the formation of nepheline as long as the maretial had completely melted and had sufficient fluidity. However, the different heat-treatment schedules affected the product durability. For a six-hour heat-treatment at 850° or 1050°C, time was sufficient for nepheline formation and also produced more durable nepheline-vitreous ceramics, although no shorter heat treatment time has been tested. The nucleating agent seemed to be unnecessary for the formation of nepheline the in vitreous ceramics tested; the preferred approach was to replace nucleation agent with excess SiO_2 to enhance product durability. This enhancement in durability was achieved mainly through increasing the content of SiO_2 in residual glasses. The residual glass phases in vitreous ceramics seemed to control the overall waste-form durability. The nepheline-vitreous ceramics were usually more durable than the corresponding glasses with the same chemical composition, especially in the longer duration tests. The reaction acceleration with nepheline-vitreous ceramics was much slower than the corresponding glasses, probably due to the fact that nepheline crystals are thermodynamically more stable than were the glasses with the same chemical compositions. The nepheline-vitreous ceramics also had lower leachate pHs, which was believed to benefit the long-term durability of waste forms. Nepheline-vitreous ceramics can be used to immobilize high-alkali wastes with alkali contents up to 21 wt%.

3.4 Cesium-Containing Vitreous Ceramics

Many waste streams contain ^{137}Cs, which presents a potential internal radiological hazard if ingested or inhaled, as well as an external hazard to the entire body. Knowledge from the above study on nepheline-vitreous ceramics can be used, since the cation Cs can potentially occupy the same lattice position as sodium in Na_3PO_4 in nepheline crystals.

3.4.1 Batch Composition and Melting Conditions

LVC-16 and LVC-17 were batched from reagent chemicals according to Table 3.22 with melting conditions as shown in Table 3.23. THe analyzed Cs in both LVC-16 and LVC-17 are almost the same as the batch composition, indicationg insignificant volitilization of Cs during melting. LVC-16 represented an effort to reproduce the type of structure developed in LVC-2, where isolated water-soluble Na_3PO_4 particles were dispersed uniformly in a durable silicate glassy matrix and the overall durability of LVC-2 was acceptable. Replacing sodium with cesium required the addition of lithium oxide to lower the viscosity. LVC-17 was an effort to produce nepheline-like structure.

Table 3.22. Batch and Analyzed Chemical Compositions of Cs-Containing Vitreous Ceramics (wt%)

	LVC-16Q Batch	LVC-16HT Analyzed	LVC-17Q Batch	LVC-17HT Analyzed
SiO_2	34.42	30.43	38.46	34.99
Al_2O_3	9.39	7.16	16.12	15.42
Cs_2O_3	35	35.1	35.42	41.38
P_2O_3	16.19	16.21	0	0
Li_2O	5	6.1	10	8.95

Table 3.23. Melting Conditions for Cs-Containing Melts

Sample	Melting (C and h)	Heat Treatment (C and h)	Description	Crystals
LVC-16Q	1540C, 1 h		white, crystalline	pollucite, Li_3PO_4,
LVC-16HT	1540C, 1 h	950C, 24 hr	white, crystalline	pollucite, Li_3PO_4, $CsAlSi_5O_{12}$/ $Cs_4Al_4Si_{20}O_{48}$
LVC-17Q	1530C, 1 h		white, crystalline	pollucite, $CsAlSiO_4$
LVC-17HT	1530C, 1 h	900C, 24 h	white, crystalline	pollucite, $CsAlSiO_4$

3.4.2 Solid Phases and Chemical Durability

The solid-phase characterization is still underway; only XRD data were available at the time this report was written. The following information is from semi-quantitative XRD analysis. LVC-16Q had about 15 vol% of crystallinity. These crystals are 85 wt% of pollucite, $CsAlSi_2O_6$, and 15 wt% of Li_3PO_4. The heat-treated sample of LVC-16HT showed 60 vol% of crystallinity. Among these crystals, 40% was pollucite, 15% of crystals with formulation of $CsAlSi_5O_{12}/Cs_4Al_4Si_{20}O_{48}$, 10% was Li_3PO_4, and the rest 35% were peaks which have not been identified yet. It was obvious that the Li_3PO_4 was more stable than Cs_3PO_4, and Cs_2O was more stable with the formation of pollucite and similar Cs-Al-Si structures. LVC-17Q already showed 50 vol% crystallinity, among which 90% was $CsAlSiO_4$ and 10% was pollucite. LVC-17HT was completely crystalline according to XRD; these crystals consist of 70% $CsAlSiO_4$ and 30% pollucite.

The PCT durability for LVC-16 is shown in Figures 3.30a and 3.30b and in Appendix C. The Cs releases from LVC-16HT were consistently lower than LVC-16Q by 3.4 times at 7-day PCT to 5.8 times at 28-day PCTs, suggesting the longer time durability of LVC-16HT was much better than LVC-16Q. The Cs release of LVC-16HT, 0.834 g/m^2 at 7-day PCT, was a factor of 8 better than EA glass. It was also interesting to note that the leachate pHs of LVC-16Q, 7.37 at 7-day and 7.25 at 28-day PCTs, were much lower than those of LVC-16HT, 9.79 at 7-day and 10.01 at 28-day. This is attributed to the P_2O_5 release of LVC-16Q, which was a factor of 3 to 4 times faster than that of LVC-16HT, and the high concentration of phosphorus that buffered the leachates of LVC-16Q at lower pHs.

The PCT durability for LVC-17 is shown in Figures 3.31a and 3.31b and in Appendix C. The Cs releases from LVC-17HT were consistently lower than LVC-17Q by 1.6 times at 7-day PCT to 15.5 times at 28-day PCTs, suggesting the longer time durability of LVC-17HT is much better than that of LVC-16Q. The Cs release rate of LVC-17HT, 0.004 g/m^2/day between 7- and 28-day PCTs, was a factor of 250 better than the 1.0g/m^2/d requirement for high-level nuclear-waste glasses. The solution pHs for both LVC-17Q and LVC-17HT were similar. These results suggest that the crystalline $CsAlSiO_4$ and polucite were much more durable and insoluble than were the corresponding glass compositions.

The Cs releases for LVC-16HT at 7- and 28-day PCTs and LVC-17HT at 7- and 28-day PCTs were 0.83, 0.86, 0.74, and 0.83, respectively, and these values are similar. This may suggest that the durabilities among pollucite crystals ($CaAlSi_2O_6$) and various Cs-Al-Si crystals, such as $CsAlSi_5O_{12}$ and $CsAlSiO_4$, are similar. The similarity between 7- and 28-day results further suggested that the long-term durabilities of these crystals may be very good since the dissolution of these crystals were controlled mainly by reaction affinity that is a function of the activities of the constituents in solution (Lasaga 1984). The 7-day PCT dissolved sufficient amounts of the constituents into the solution and sufficiently lowered the reaction affinity for these crystals. The pollucite and Cs-Al-Si crystals in these vitreous ceramics were stable and there were no tendencies to form other types of crystals that would decrease reaction affinity in solution. The long-term durability of these vitreous ceramics may be very good. The Cs releases for LVC-16Q at 7- and 28-day PCTs and LVC-17Q at 7- and 28-day PCTs were 2.82, 5.02, 1.16, and 12.76, respectively. These values varied greatly, especially between 7- and 28-day results. This may suggest that the corresponding glass waste form for immobilizing Cs was not as durable as was the vitreous ceramic waste form; and that the long-term durability was much worse than the corresponding vitreous ceramic waste forms, because a factor of 10 increase in

normalized Cs release was already observed between the 21-day period of 7- and 28-day PCTs. The degree of solution saturation in the leachates of these glasses affected reaction affinity, but the possible formation of more stable precipitates and crystals than glasses will decrease solution saturation and increase reaction affinity (Bourcier 1990).

3.4.3 Summary

Vitreous ceramics with Cs_2O loading up to 35.4 wt% were developed. These waste forms contain pollucite ($CaAlSi_2O_6$), and various Cs-Al-Si crystals, such as $CsAlSi_5O_{12}$ and $CsAlSiO_4$; the data suggested that these crystals had similar stability and water solubility. The corrosion rates of these vitreous ceramics were up to 15 times lower than the corresponding glass waste form of the same chemical compositions and were a factor of 8 better than EA glass. The similarity in normalized release between short and long PCTs suggested that the long-term durabilities of these vitreous ceramics were very good. This is probably due to the reaction affinity, which is quite low throughout test duration. This low reaction affinity can be maintained because of the thermodynamic stability of the pollucite crystals and other Cs-Al-Si compounds. The longer-term durability of the corresponding glasses was expected to be much worse due to the possible precipitation and formation of more stable crystalline phases.

3.5 Vitreous Ceramics for K-25 Pond Sludge, Oak Ridge National Laboratory

The K-25 pond sludge at Oak Ridge contains EPA-listed F006 waste and radionuclides such as U, Tc, and Cs (Bostick 1994). A simulated K-25 pond sludge composition, shown in Table 3.24, was used in this study. The waste loading of K-25 sludge cannot usually exceed 30% in a glass waste form to meet a 0.32 ppm land disposal restriction (LDR) limit on Ni release in an EPA TCLP test. This project initiated the treatment of this waste using vitreous ceramics (VC). By selectively crystallizing the melts, spinel types of crystals will immobilize Ni and other hazardous elements.

Table 3.24. K-25 Pond Sludge, ORNL Soil, and Nominal Compositions of LVC-5 and LVC-6 (wt%)

	ORNL Soil	K-25 Waste	LVC-5 100% W	LVC-6 90W+10S
SiO_2	76.68	17.97	17.97	23.84
Al_2O_3	15.22	13.38	13.38	13.56
Fe_2O_3	5.70	19.22	19.22	17.87
CaO	0.07	16.62	16.62	14.97
Na_2O	0.04	1.75	1.75	1.58
K_2O	0.81	4.08	4.08	3.75
MgO	0.49	3.11	3.11	2.85
TiO_2	0.67	1.63	1.63	1.53
Ag_2O				0.00
BaO				0.00
Ce_2O_3		0.44	0.44	0.40
Cr_2O_3	0.01	0.33	0.33	0.30
CuO		0.27	0.27	0.24
MnO	0.06	0.89	0.89	0.81
N_2O_5				0.00
NaF				0.00
PbO		0.02	0.02	0.02
SO_3		0.64	0.64	0.58
ZnO		0.10	0.10	0.09
ZrO_2				0.00
P_2O_5	0.16	16.69	16.69	15.04
As_2O_3		0.03	0.03	0.03
NiO	0.01	2.72	2.72	2.45
F		0.03	0.03	0.03
Cl		0.07	0.07	0.06
B_2O_3	0.04			
CdO				
Sb_2O_3				
Cs_2O				
HgO				
SrO				
CaF_2				
	99.96	99.99	99.99	99.98

3.5.1 Formulation and Melting

Two melts were prepared for this study as shown in Table 3.24. Oak Ridge National Laboratory (ORNL) soil was used as a component to minimize additives, reduce waste volume, and reduce cost. The chemical composition of ORNL soil is shown in Table 3.24. By examining the composition of the K-25 pond sludge composition, it was observed that the sludge itself contains the essential elements for the formation of spinels and other durable crystals to stabilize this waste. Therefore, one melt, LVC-5, was prepared using 100% K-25 pond sludge, which generated the maximum waste loading and another melt, LVC-6, was formulated using 90 wt% of K-25 pond sludge and 10% of ORNL soil. LVC-5 was melted at 1425°C and heat-treated at 1000°C for 24 h to facilitate formation of the beneficial crystals. A black, hard, and dense vitreous-ceramic waste form was obtained. LVC-6 was melted at 1400°C and heat-treated at 1000°C for 16 h. A similar black, hard, and dense vitreous-ceramic waste form was obtained.

3.5.2 Solids Characterization

LVC-5

Under the optical microscope, the microstructure along the cross-section of the melt was homogeneous except for a little fluctuation in the volume fraction of an opaque phase and the transparent phase (Figure 3.32). The opaque phase accounted for about 45% of the total volume. XRD analysis indicated 100% crystallinity of the samples. The major phase identified by XRD lines are spinel (50%) (matching trevorite, $NiFe_2O_4$, very well), Ca_3PO_4 phase (35%), and leucite, $KAlSi_2O_6$ (15%). TEM showed the same three groups of major crystals: spinel (opaque, and Ni- and Fe-rich), Ca-P phase, and aluminosilicates (K-rich and Ca-rich). The aluminosilicates include hedenbergite, $CaFeSi_2O_6$, (a pyroxene-structure type); orthoclase, $KAlSi_3O_8$, and plagioclase, $CaAl_2Si_2O_8$ (both had the potassium-feldspar structure). In Figure 3.33, phase a, b, c, d, e are pyroxene, orthoclase, Ca-P phase, spinel, and plagioclase, respectively. The typical chemical compositions analyzed by EDS are shown in Table 3.25. The diffraction patterns for individual phases are shown in Figure 3.34. Figures 3.35a and 3.35b show the results of X-ray mapping and backscattered electron imaging on a sample from the top of the melt (Figure 3.35a) and a sample from the center of the melt (Figure 3.35b). Different morphology of the phases was evident.

The morphological features of the spinel phase were different from the top to the bottom of the melt. At the top of the melt (Figure 3.35a), the spinel phase occurred as dendritric crystals, indicating that these crystals form at a high quenching rate. At the center of the melt (Figure 3.35b), spinel crystallized as large (up to 50 microns), single octahedrons, indicating a slow cooling. The chemical composition in Table 3.25 and diffraction pattern in Figure 3.34 match trevorite. It contained 14.07% NiO. Some of the spinel also contained about 0.5% Cr_2O_3. The formula of the phase can be written as $(Fe^{+2},Ni,Mg,Mn,Ca)(Fe^{+3},Al,Cr,Ti)_2O_4$. This structure was responsible for the observed lower release of Ni and Cr.

Table 3.25. Representative Compositions (wt%) of Major Phases in LVC-5

Oxides	Spinel	K-Feldspar	Plagioclase	Ca-P phase #1	Ca-P phase #2	hedenber-gite	leucite
SiO_2	0.23	56.44	42.84	0.02	49.86	35.70	53.50
Al_2O_3	5.16	20.12	17.61	0.04	--	13.33	21.46
CaO	0.40	3.99	17.34	53.01	--	26.38	0.57
Na_2O	--	2.52	--	0.04	1.07	--	0.82
K_2O	0.29	11.38	1.52	0.45	0.39	--	20.93
MgO	4.58	0.74	2.58	1.84	1.33	3.95	--
TiO_2	2.00	1.69	6.23	0.52	--	7.06	--
FeO	70.20*	2.14	11.40	--	0.53	12.88	1.01
MnO	3.06	P_2O_5, 0.98	--	P_2O_5, 44.1	P_2O_5, 43.86	--	P_2O_5, 0.56
Cr_2O_3	--	--	--	--	Ce_2O_3, 2.96	--	Ce_2O_3, 0.53
NiO	14.07	--	0.48	--	--	0.69	--

*Assuming all iron is ferrous.

The chemical compositions in Table 3.25 have ratios of CaO to P_2O_5 close to $Ca_3(PO_4)_2$ with 3.04:1.00 for Ca-P[1] and 2.90:1.00 for Ca-P[2]. The X-ray mapping in Figures 3.35a and 3.35b shows clearly that most of the elements P and Ca were concentrated in $Ca_3(PO_4)_2$ phases. These figures also show the morphology of these Ca-P phases. It is interesting to note that Ca-P[2] had a Ce_2O_3 content of 2.96% (Table 3.25).

Hedenbergite crystals coexist alternatively with potassium feldspar crystals as laminae. The simplified formula of potassium feldspar is (K, Ca, Na, Mg)Al(Si,Al,Ti,P,Fe)$_3O_8$. Potassium feldspar is important because Cs^+ may concentrate into this phase. The actual formula for $Ca_3(PO_4)_2$ can be written as (Ca,Mg,K,Na)$_3$(P,Si,Al,Ti)$_2O_8$. Ce_2O_3 was detected in $Ca_3(PO_4)_2$ phases up to 3 wt%. Potassium feldspar minerals often contain Pb in pegmatites. Leucite, a member of feldspathoid group, is a very important phase of the sample. Chemically, it is quite pure. This phase can also be an important host for Cs^+. These Al-silicate phases contributed to the superior chemical durability observed in PCT and TCLP tests, and will be discussed below.

LVC-6

LVC-6 is similar to LVC-5 in microstructure and phase constituents. The formulation difference was that the K-25 pond sludge-loading for LVC-6 was 90% (plus 10% ORNL soil), while 100% K-25 pond sludge was used for LVC-5. Based on TEM observation, the major phases were trevorite (spinel-type), aluminosilicates, and $Ca_3(PO_4)_2$ phases in LVC-6. The relative abundances of these phases were 35% spinels, 35% aluminosilicates, and 30% $Ca_3(PO_4)_2$. The aluminosilicates also included K-feldspar, plagioclase, and hedenbergite. The relationship between those phases is shown in Figure 3.36. The glassy matrix was minor. The EDS compositions are shown in Table 3.26.

As in LVC-5, up to 11.81 wt% of NiO and 1.41% Cr_2O_3 were found in spinel phases. With Ni, Mn, Mg, and Fe^{+2} occupying octahedral sites, and Cr, Ti, Al, and Fe^{+3} in tetrahedral sites, a very complicated solid-solution series with the inverse spinel-type structures was formed.

Short, cylinder-like $Ca_3(PO_4)_2$ crystals array as lamellae in potassium-feldspar matrices. EDS indicated that the $Ca_3(PO_4)_2$ phases contained up to 3.18 wt% Ce_2O_3 (Table 3.26). The formula of this phase can also be written as (Ca,Ce,Mg,Na,K,Fe)$_3$[(P,Si,Al,Ti)O_4]$_2$. Rare-earth elements preferably partition into the $Ca_3(PO_4)_2$ structure, supported by basic crystallochemical roles. Ce^{3+} + (Na,K) = $2Ca^{+2}$; or a Ce atom replaces a Ca atom, while a Si atom substitutes for a P atom, to keep charge balance. This phase also provides potential sites to host arsenic, lead, and other hazardous elements.

Pyroxene-type phases present in LVC-5 were not found in LVC-6. The chemical compositions of potassium feldspar, higher in Ca and Na, were quite different from those in LVC-5 as indicated by their formula, (K,Ca,Na,Fe)(Si,Al,Ti)$_4O_8$. This phase actually may have been sanidine or orthoclase that belong to the feldspar group in structure. Usually, sanidine is characteristic of rocks that were cooled quickly from initial high eruption temperature. Orthoclase forms in moderately cooled rocks.

Table 3.26. Representative Compositions (wt%) of Major Phases in LVC-6

Oxides	Spinel #1	Spinel #2	K-feldspar #1	K-feldspar #2	Ca-P phase #1	Ca-P phase #2	hedenbergite #1	hedenbergite #2	plagioclase
SiO_2	0.47	0.68	58.93	57.86	--	0.42	33.26	30.90	53.80
Al_2O_3	5.16	6.71	19.79	19.56	--	--	14.15	12.81	115.38
CaO	2.91	0.93	3.86	4.29	47.26	48.57	27.65	29.07	13.51
Na_2O	--	--	2.35	1.56	1.18	0.24	--	--	--
K_2O	--	--	10.58	11.90	--	--	--	0.18	5.04
MgO	2.54	4.21	--	0.43	2.82	1.89	3.97	4.02	0.75
TiO_2	3.84	2.10	1.95	1.95	--	--	5.55	5.79	2.39
FeO	73.33*	68.95*	1.79	2.06	0.44	1.12	14.62	15.98	8.16
MnO	3.37	3.19	P_2O_5, 0.76	0.40	P_2O_5,44.93	P_2O_5, 44.57	0.41	0.63	0.35
Cr2O3	0.71	1.41	--	--	Ce_2O_3, 2.89	Ce_2O_3, 3.18	--	--	--
NiO	7.66	11.81	--	--	--	--	0.39	0.56	--

* Assuming all iron as ferrous.

3.5.3 Waste-Form Durability

The chemical durabilities of LVC-5 and LVC-6 were evaluated with TCLP, PCT, and vapor-hydration test procedures.

The TCLP results in Table 3.5 show that both LVC-5 and LVC-6 passed the EPA TCLP requirements for hazardous concentrations. In fact, most of the concentrations in the TCLP leachate were below the detection limits of ICP-AES and atomic-absorption techniques. Even more impressive was that the Ni concentrations detected in both LVC-5 and LVC-6 leachates were below the 0.02 ppm detection limits, which are at least a factor of 16 below the land disposal limit of 0.32 ppm on Ni concentration.

The PCT elemental releases for LVC-5 and LVC-6 are shown in Figures 3.37 and 3.38 and in Appendix C. The normalized release of 0.38 g/m^2 for Na was a factor of 18 lower than that of high-level EA glass. LVC-6, at 90 wt% loading of K-25 pond sludge and 10 wt% Oak Ridge soil, showed a PCT Na release of 0.16 g/m^2, which was 42 times lower than that of EA glass. Both LVC-5 and LVC-6 showed little change in normalized releases throughout the 91-day test duration, an indication of good long-term durability. The leachate pH for LVC-5 was essentially constant at pH 10, up to 91 days, and LVC-6 showed an even lower pH of about 9.0 thoughout the test duration.

After reacting LVC-5 and LVC-6 in saturated vapor at 150°C for 28 days, the samples looked almost the same as the fresh samples before the testing, except for a slight discoloration. These reacted samples were then further characterized with an electron microscope. This examination, discussed below, indicated very little corrosion to the waste form even after such severe vapor-hydration test conditions.

Reacted LVC-5

The reacted LVC-5 surface was homogeneously covered by a thin, "webby" alteration layer as shown by the SEM micrographs of Figure 3.39. This alteration layer was not extensive since most of the surface was not covered yet. A cross-section of the reacted LVC-5 was prepared in epoxy resin to assess the reacted layer thickness.

The thickness was difficult to assess since the layer thickness was not uniform throughout the sample surface. Some surface areas of crystals showed essentially no layer. The layer thickness can usually be enlarged during sample preparation cutting and polishing. A cross-section sample, shown in Figure 3.40, shows where a layer thickness of 0.0 to 0.5 microns may be possible. The preliminary analysis of the layer composition showed the enrichment of K, Ca, Al and Si. This webby layer may be the smectite-illite as these two phases are common alteration products of feldspar and proxene found in natural thermodynamic systems.

Reacted LVC-6

The reacted LVC-6 surface was also covered by a thin, "webby" alteration layer as shown in Figure 3.41. It seems that the glassy phases, Ca-P phases, and alumonosilicate phases corroded preferentially over the spinel phases, since an individual spinel crystal protruded from the surface (Figure 3.42). The sample cross-section (Figure 3.43) of LVC-6 showed the corroded surface structure

with spinel phases and needles of the P-Ca phase remaining on the surface. The alteration layer had a thickness of 0.0 to 0.5 microns, and had a composition similar to that found on LVC-5, discussed above. The extent of the alteration observed on both LVC-5 and LVC-6 was much less than that found on typical high-level nuclear-waste glasses under similar test conditions.

3.5.4 Summary

The VC sample, LVC-5, was formulated of nearly 100% ORNL K-25 pond sludge. Its heat treatment resulted in the targeted crystal formation of spinels (including trevorite and chromite, hosts for Ni and Cr), potassium feldspar (host for Cs^+), and Ca-P phases (host for Ce, a surrogate for U and Pu). LVC-5 was tested using PCT, EPA TCLP test, and the vapor-hydration test at 150°C for 28 days. The results show a normalized PCT release of 0.38 g/m^2 for Na, which was a factor of 18 lower than that of high-level environmental assessment glass. The hazardous element releases in an EPA TCLP test were at least 476 times lower than the EPA limits. More significantly, the Ni concentration in the TCLP leachate was less than 0.02 ppm (detection limit of ICP-AES), which was at least 16 times lower than the 0.32-ppm LDR limit. The vapor-hydration test sample showed almost no alteration by visual inspection; a thin, "webby" clay layer was found under SEM. This extent of alteration of LVC-5 was much less than the alteration found on typical high-level waste glasses. An improved formulation and melting of another VC sample, LVC-6, at 90 wt% loading of K-25 pond sludge and 10 wt% ORNL soil, showed a PCT Na release of 0.16 g/m^2, which was 42 times lower than that of EA glass. The TCLP concentration of LVC-6 was at least 2000 times lower than EPA limits. The vapor-hydration test again showed minimum corrosion to LVC-6. These data suggest that K-25 pond sludge can be immobilized with up to 100% waste-loading, using vitreous ceramics. The vitreous-ceramic waste-form was more durable than typical HLW glasses and could be processed at temperatures of about 1425°C.

3.6 Vitreous Ceramics for ICCP Calcined Waste

The liquid waste from nuclear fuel reprocessing has been calcined into solid granules and stored at the Idaho Chemical Processing Plant (ICPP) since 1963. Different types of calcines, fluorine/sodium blend, alumina, zirconia, and zirconia-sodium blend, have been produced (Vinjamuri 1994). Final disposal of the calcined waste requires further immobilization of the calcines into a more durable waste form. A preliminary effort to develop vitreous ceramics for the immobilization of the calcined wastes was included in this project which were focused on two calcined wastes: alumina (Run 1027) and zirconia (Run 80) calcines, as shown in Table 3.27. The zirconia-calcine (Run 80) contained 22.8% ZrO_2 and 34.1% of CaF_2. The alumina-calcine (Run 1027) contained up to 92.1% Al_2O_3.

Table 3.27. Compositions of ICPP Calcine and Associated Vitreous Ceramics (Batch)

	INEL Soil	Run-80 Calcine	Run-1027 Calcine	LVC-7 75Zr25S	LVC-8 60Al25S 15MgO	LVC-9 40Al50S 10Mg	LVC-14 10S+30Al 58Zr+2Fe	LVC-15 10S+25Al +10Ti 53Zr+2Fe
SiO_2	66.70			16.68	16.68	33.35	6.67	6.67
Al_2O_3	12.10	14.40	92.10	13.83	58.29	42.89	37.19	31.87
Fe_2O_3	5.40	0.20	0.20	1.50	1.47	2.78	2.72	2.70
CaO	8.40	25.90	5.70	21.53	5.52	6.48	17.57	15.99
Na_2O	1.20	0.30	0.40	0.53	0.54	0.76	0.41	0.38
K_2O	2.50	0.05	0.30	0.66	0.81	1.37	0.37	0.35
MgO	2.40			0.60	15.60	11.20	0.24	0.24
TiO_2	0.70			0.18	0.18	0.35	0.07	10.07
Ag_2O				0.00	0.00	0.00	0.00	0.00
BaO	0.10			0.03	0.03	0.05	0.01	0.01
Ce_2O_3		0.10	0.05	0.08	0.03	0.02	0.07	0.07
Cr_2O_3		0.70	0.20	0.53	0.12	0.08	0.47	0.42
CuO				0.00	0.00	0.00	0.00	0.00
MnO	0.10	0.05	0.05	0.06	0.06	0.07	0.05	0.05
NaF				0.00	0.00	0.00	0.00	0.00
PbO				0.00	0.00	0.00	0.00	0.00
SO_3	0.00	0.00	0.00	0.00	0.00	0.00	0.00	0.00
ZnO				0.00	0.00	0.00	0.00	0.00
ZrO_2		22.80	0.20	17.10	0.12	0.08	13.28	12.13
P_2O_5				0.00	0.00	0.00	0.00	0.00
As_2O_3				0.00	0.00	0.00	0.00	0.00
NiO		0.10	0.10	0.08	0.06	0.04	0.09	0.08
F	0.00	0.00	0.00	0.00	0.00	0.00	0.00	0.00
Cl	0.00	0.00	0.00	0.00	0.00	0.00	0.00	0.00
B_2O_3		0.30	0.40	0.23	0.24	0.16	0.29	0.26
CdO		0.05	0.05	0.04	0.03	0.02	0.04	0.04
Sb_2O_3	0.10			0.03	0.03	0.05	0.01	0.01
Cs_2O		0.30	0.05	0.23	0.03	0.02	0.19	0.17
HgO		0.05	0.05	0.04	0.03	0.02	0.04	0.04
SrO		0.80	0.05	0.60	0.03	0.02	0.48	0.44
CaF_2		34.10	0.40	25.58	0.24	0.16	19.90	18.17
	99.70	100.20	100.30	100.08	100.11	99.97	100.18	100.15

3.6.1 Formulation and Melting

Five vitreous-ceramic melts were performed: LVC-7, LVC-8, LVC-9, LVC-14, and LVC-15. The overall objective of these formulations was to produce waste forms with maximum waste-loading, good durability, and acceptable processibility.

Soil from the Idaho National Engineering Laboratory (INEL) was used as an additive to reduce cost, but the high waste-loading focused on calcined wastes since high loading of contaminated INEL soil is easy to achieve. There were some concerns regarding the feasibility of mixing different calcined wastes because of the quantities available and because the formulations were developed based on single-calcine waste and based on the blending of both calcine wastes. LVC-7 was formulated with 75 wt% zirconia-calcine plus 25% INEL soil. LVC-8 consisted of 60% alumina-calcine, 25% INEL soil, and 15% MgO. LVC-9 was made with 40% alumina-calcine, 50% INEL soil, and 10% MgO. LVC-14 was formulated with 30% alumina-calcine, 58% zirconia-calcine, 10% INEL soil, and 2% Fe_2O_3. LVC-15 was prepared with 25% alumina-calcine, 53% zirconia-calcine, 10% INEL soil, 10% TiO_2, and 2% Fe_2O_3. The calcined waste-loading order was LVC-14 (88%) > LVC-15 (78%) > LVC-7 (75%) > LVC-8 (60%) > LVC-9 (40%). If contaminated INEL soil was also counted as waste, the waste loadings were 100, 98, 90, 88, and 85 for LVC-7, LVC-14, LVC-9, LVC-15, and LVC-8, respectively. The melting conditions are shown in Table 3.28.

Table 3.28. Melting Conditions of Vitreous Ceramics for ICPP Calcines

Samples	Melt Temp. (°C)	Heat Treatment	Description
LVC-7	1375	960 for 7 h	dark grey with tan streaks
LVC-8	1600, sintered	None	grey-green
LVC-9	1600	1150 for 5 h	grey opaque, glassy
LVC-14	1500	1100 for 24 h	light brown, crystalline
LVC-15	1450	1050 for 24 h	light brown, crystalline

The high CaF_2 content in LVC-7 made the melt very fluid at 1375°C; the sample was dark gray with tan streaks. The high alumina content in LVC-8 allowed it to only sinter, not melt, at 1600°C. The sintered product was hard with a gray-green color. LVC-9 was melted at 1600°C; the end-product was hard and glassy with a gray, opaque color. LVC-14 was melted at 1500°C and resulted in a crystalline vitreous ceramic with a light-brown color. LVC-15 was melted at 1450°C; the product had the same morphology as LVC-14. These VC were characterized with optical microscopy prior to the durability tests.

3.6.2 Characterization of the As-Melted Vitreous Ceramics

LVC-7

XRD data indicated that the sample was completely crystallized with 55% fluorite $(CaF)_2$, 25% baddeleyite (ZrO_2), and 20% anorthite ($CaAl_2Si_2O_8$). The X-ray mapping and back-scattered image in Figure 3.44 shows the relationship between these phases. The large gray grains are fluorite, the small bright spots are baddeleyite, and the dark matrix is rich in Si and Al.

TEM confirmed four major phases: fluorite, baddeleyite, anorthite, and Si-Al-Ca-F glass (shown in Figure 3.45). Fluorite crystals occurred as spheres, 5 to 10 microns in size. Fluorite crystals were very easily thinned under ion milling and observed as holes. The baddeleyite crystals were small spherical particles or aggregates 0.5 to 1 micron in size and were scattered in the waste form. Anorthite occurred as big crystals with clear bend contours. Microtwin structure in anothite was very common along {010}. Glass phases occurred as lamellae or fillings among crystalline phases. A spinel phase, expressed as $(Fe^{+2},Mg,Ca)(Cr,Al,Fe^{+3},Ti)_2O_4$ was also identified to be less than 1 vol%. The representative compositions of these phases are summarized in Table 3.29.

LVC-8

XRD data suggested 60 vol% crystallinity; the only best match through XRD was spinel $MgAl_2O_4$. SEM confirmed that there were only two phases in the sample, spinel and glass matrix, as shown by Figure 3.46.

LVC-9

XRD data showed 40 vol% crystallinity. The crystals were spinel. Optical examination showed different morphologies at the top and the bottom of the melt. The top part of the sample consisted of spinel with a perfect octahedral structure in a glassy matrix (Figure 3.47). The bottom part (Figure 3.48) is composed of dendritrically-crystallized spinel phases in a glassy matrix. The TEM examination showed that the spinel was pure $MgAl_2O_4$ (SAD in Figure 3.47). $MgAl_2O_4$ was reported to be a stable ceramic material under various irradiation conditions.

LVC-14

XRD identified 75 vol% crystallinity in LVC-14. These crystals were 55% fluorite (CaF_2); 15% baddeleyite (ZrO_2); and 30% hibonite ($CaAl_{12}O_9$). Under the optical microscope, LVC-14 consisted of predominantly needle-like crystals, up to 0.8-mm long (Figure 3.49). This needle phase was confirmed to be hibonite by TEM study. Morphologically, the matrix may have consisted of three phases: small brown particles (baddeleyite), spherical transparent crystals (fluorite), and irregularly shaped transparent glasses.

Table 3.29. Representative Compositions (wt%) of Major Phases in LVC-7

Oxides	chromite	anorthite (1)	anorthite (2)	baddeleyite	glass**
SiO_2	--	44.37	43.42	1.30	25.66
Al_2O_3	4.77	34.48	33.57	2.67	11.42
CaO	1.03	20.23	21.64	0.65	35.94
Na_2O	--	0.24	0.83	--	0.97
K_2O	ZrO_2, 0.76	--	--	ZrO_2, 94.17	5.01
MgO	--	--	--	0.52	3.12
TiO_2	1.92	--	--	0.23	0.90
FeO	54.93*	0.67	0.55	0.46	3.74
MnO	0.75	--	--	--	--
Cr_2O_3	32.63	--	--	--	--
NiO	1.32	--	--	--	--
ZrO_2	--	--	--	--	2.40
F	--	--	--	--	10.84

* Assuming all iron as ferrous.

** More oxides with 1 wt% in concentrations: Mgo, SrO, K_2O, MnO, and TiO_2.

The high resolution TEM image for hibonite is shown in Figure 3.50; the arrow indicates the sharp interface between the hibonite crystal and glassy matrix. The electron diffraction pattern for hibonite was characteristic of {00l}-type spots (l=1,2,3,. . .). Hibonite was the magnetoplumbite structure-type with space group P63/mmc. This structure-type ($AM_{12}O_{19}$) was a major constituent phase in tailored ceramics.

The structure was based on principles of crystallographic close-packing where 38 anions and 2 A-cations made up the close-packed sequence of ten oxygen layers parallel to {0001} in the unit cell. The 24 small cations, M, consisted of 18 in octahedral coordination and 6 in tetrahedral coordination (five different M-sites). The compositions from naturally occurring magnetoplumbite-type phases are very complicated. As usual, large A-site cations included Ca, Sr, Pb, RE (Rare Earth Element), K, Na, Ba, and actinides. Small B-site cations were Al, Mn, Ti, Zr, Cr, Fe^{3+}, and V. Compositions of hibonite in LVC-14 were fairly simple as compared to naturally occurring phases (Table 3.30). A typical formula of hibonite in LVC-14HT is:

$$(Ca_{1.38}Sr_{0.02})_{1.40}(Al_{10.49}Fe^{3+}_{0.65}Zr_{0.27}Cr^{3+}_{0.14}Si_{0.06}Ti_{0.01})_{11.62}O_{19}.$$

The sum of A-site cations was usually more than 1.0 as required for a magnetoplumbite-type structure and the excess of A-site cations was often observed in naturally occurring minerals. One possibility was that more than two A-site cations may occupy anion sites to form the close-packing sequences.

The typical composition for the glassy phases in LVC-14 was present as: SiO_2 29.96, CaO 23.90,Fe_2O_3 2.26, ZrO_2, 1.21, Al_2O_3 29.38, Na_2O 4.48; P_2O_5 2.25, SrO 0.72, K_2O,1.04, and F 4.80 (wt%). Other existing elements in glasses were Ni, Cs, Mn, Mg, and Cr (less than 0.5 wt%). The estimated contents of fluorine ranged from 3 to 5 wt%. Table 3.31 lists chemical data for glassy phases in LVC-14; fluorine data is not included. The glasses present in LVC-14HT were high in Ca but very low in Na.

LVC-15

LVC-15 is very complicated, both in chemical and textural aspects. Optical microscope observations indicated that the bottom part of LVC-15 may consist of the following phases: brown particle aggregates, spherical transparent crystals (fluorite) with irregular glassy matrices, and large cylindrical crystals as indicated by the arrow in Figure 3.51b. The bulk sample of LVC-15 was characteristic of giant crystalline needles (Figure 3.51a).

Figure 3.52 shows five major constituent phases in LVC-15: corundum (α-Al_2O_3) as a big chunk (referred to be as CR), spherical fluorite (CaF_2), zirconolite ($CaZrTi_2O)_7$ as crystalline aggregates, indicated by the arrow; rutile (TiO_2), and glassy phases as matrices. Additional small crystallites occurred in the glassy matrices which may be armalcolite, $FeTi_2O_5$. Baddeleyite crystals are rarely seen in this sample. XRD analysis confirmed the crystal identity. The total crystallinity identified by XRD was 75 vol%. The relative wt% of these crystals was fluorite, 50%, zirconolite 25%, corundum 10%, and 15% others (includes baddeleyite, rutile, and armalcolite).

Table 3.30 The Chemical Composition of Hibonite in LVC-14*

oxide	3-43	3-44	3-46	3-52	cation #	3-43	3-44	3-46	3-52
SiO_2	0.54	0.72	0.34	0.28	Si^{4+}	0.064	0.083	0.042	0.035
Al_2O_3	74.86	78.13	79.14	74.05	Al^{3+}	10.487	10.766	10.910	10.437
ZrO_2	4.62	0.48	1.71	4.72	Zr^{4+}	0.269	0.029	0.096	0.276
Na_2O	0.00	0.75	0.75	0.32	Na^{+}	0.000	0.170	0.170	0.074
CaO	10.79	10.05	9.77	11.03	Ca^{2+}	1.377	1.261	1.225	1.415
SrO	0.26	0.60	0.76	0.42	Sr^{2+}	0.019	0.042	0.051	0.029
Cr_2O_3	1.54	0.18	0.22	1.02	Cr^{3+}	0.144	0.016	0.019	0.096
Fe_2O_3	7.30	8.71	7.21	8.16	Fe^{3+}	0.653	0.766	0.634	0.732
TiO_2	0.09	0.38	0.09	0.00	Ti^{4+}	0.006	0.032	0.010	0.000

Hibonite crystals were very common as big chunks or small crystals in the glassy matrix. The hibonite crystals with perfect crystallographic forms coexisted with zirconolite crystals. Part of the hibonite crystal was examined by HRTEM. The zone axis was vertical to the C-axis, featured by 00l-type diffraction spots. The disordering of layers in hibonite was evident.

Armalcolite crystals may be abundant, as shown by Figure 51. These crystals occurred in the glassy matrix. An unidentified phase was revealed, as shown by Figure 52. This phase was consistent with the formula $Ca(Ti,Al,Fe)_2O_8$, but matches no known phase in Powder Diffraction File 1989. In the bottom part of the sample of LVC-15, some hibonite crystals had very interesting microstructures as revealed by Figure 3.53. Many precipitates occurred as inclusions in the hibonite crystalline matrix and produced moiré fringes. Extensive EDS analyses on these inclusions did not detect any perceivable deviation from hibonite. The HRTEM image (Figure 3.54) of these inclusions and the hibonite matrix showed that the atomic lattices continued to go through in the moiré fringe area. The chemical compositions of hibonite in LVC-15HT usually deviated from the formula $CaAl_{12}O_{19}$.

Table 3.32 gives chemical compositions of hibonite in LVC-15. Al_2O_3 ranges from 68 to 75 wt%; TiO_2 6.5-11.5 wt%; CaO 5.3-9.0 wt%; Fe_2O_3 6.3-8.0 wt%. The chemical formula is based on a typical composition of hibonite (3-86) given as:

$$(Ca_{1.03}Sr_{0.05})_{1.08}(Al_{10.28}Fe^{3+}_{0.60}Ti_{0.57}Zr_{0.15}Mg_{0.08}Cr^{3+}_{0.04})_{11.73}O_{19}.$$

Table 3.31. Compositions of Glassy Phases in LVC-14
(3-5 wt% Fluorine is not Included in all Analysis)

	3-41	3-45	3-48(1)	3-49	10-20*	10-21	10-22
SiO_2	25.59	28.99	14.28	26.67	33.64	24.14	31.30
Al_2O_3	30.89	30.26	19.84	28.74	32.96	26.86	33.55
P_2O_5	1.69	2.29	5.21	3.16	2.34	1.81	2.70
Na_2O	4.63	4.29	0.97	2.37	3.76	1.37	3.13
CaO	29.19	28.03	37.31	27.53	21.09	32.65	21.44
ZrO_2	1.73	1.25	8.61	2.54	0.76	1.18	0.78
SrO	1.49	1.17	1.33	1.09	1.20	0.55	1.16
Fe_2O_3	4.16	2.63	11.42	7.21	3.22	7.83	4.77
K_2O	0.63	1.08	0.931	0.69	1.03	1.99(2)	1.20

(1) Data from the glassy phase with spherical morphology.
(2) Contains 1.51 wt% CoO. Cr, Ti, and Mg exist in less than 0.5 wt%.
* 10-20, 10-21, and 10-22 were analyzed by JEM2010 electron microscope.

Table 3.32. The Chemical Compositions of Hibonite in LVC-15

Oxide	3-81#	3-82	3-84	3-86	3-87	3-121	3-122	3-123	10-30	3-206*
Al_2O_3	75.82	73.77	68.20	74.20	70.28	74.71	73.26	75.66	70.74	71.39
ZrO_2	0.00	2.81	2.92	2.64	4.66	0.00	3.24	0.00	3.26	0.49
TiO_2	7.64	6.58	8.55	6.44	7.55	8.49	7.23	6.54	10.23	11.17
CaO	7.95	8.49	9.68	8.16	8.20	7.74	8.23	8.75	5.33	7.21
SrO	0.45	0.65	0.71	0.74	0.62	1.04	0.29	0.96	0.12	0.69
Cr_2O_3	0.00	0.63	0.92	0.49	1.31	0.00	0.89	0.36	2.20	0.09
MgO	1.14	0.74	0.84	0.47	0.00	1.21	0.46	0.66	0.18	1.20
Fe_2O_3	6.99	6.33	8.19	6.85	7.38	6.80	6.41	7.05	7.93	7.21

From 3-18 to 3-123, analyses were made on JEM2000FX on LVC-15HT/B. 10-030 was analyzed at JEM2010 on LVC-15HT/B.
* 3-206 is from LVC-15HT/A on which HRTEM imaging was done.

Table 3.33. Chemical Compositions for Other Phases in LVC-15

Phase	$FeTi_2O_5$	$FeTi_2O_5$	uniden.	uniden.	corundum	corundum
oxide	3-61	3-63	3-67	3-68	3-204	3-205
Al_2O_3	5.83	4.88	15.03	11.79	93.91	94.84
ZrO_2	6.11	3.48	3.04	2.64	0.00	0.66
TiO_2	62.53	66.64	51.47	53.83	1.00	0.41
CaO	0.90	0.30	14.77	15.14	0.55	0.18
SrO	0.00	0.00	0.45	0.46	0.36	0.27
Na_2O	0.99	0.64	0.34	0.37	MgO 0.87	0.00
SiO_2	0.00	0.19	1.35	1.66	Cr_2O_3 0.11	0.00
FeO	22.66	23.54	13.55	14.10	3.21*	3.64*

* As Fe_2O_3.

The simplified formula is $(Ca,Sr)(Al,Fe,Ti,Mg,Cr)_{12}O_{19}$. Compared to hibonite in LVC-14, the TiO_2 content was greater in LVC-15HT. Magnetoplumbite-type provided appropriate sites for Cs, Sr, RE, Ni, as well as Pu in tailored ceramics.

The large crystalline needles which are easily recognized from Figure 3.51a were identified by EDS/AEM as corundum, α-Al_2O_3. Al_2O_3 crystals in LVC-15HT/A was around 95 wt%. The others are Fe_2O_3 and TiO_2, since Fe^{3+} and Ti^{4+} can substitute for Al^{3+} as a solid-solution. Fe_2O_3 was higher than TiO_2 because hematite is isostructural to corundum. The chemical compositions of corundum are shown in Table 3.33.

Zirconolite is a major phase in LVC-15HT as well as in Synroc and the tailored ceramics. $CaZr_xTi_{3-x}O_7$ ($0.8 < x < 1.37$) and nominally $CaZrTi_2O_7$ is used as a generic term. Chemical compositions for zirconolite in LVC-15 are given in Table 3.34. In zirconolite, ZrO_2 ranges from 38 to 45 wt%; TiO_2 36-42 wt%; and CaO 13.3-14.1 wt%. A typical chemical formula is:

$$(Ca_{0.87}Fe^{2+}_{0.12}Sr_{0.01})_{1.00}\ (Ti_{1.61}Zr_{1.29}Al_{0.13})_{3.03}O_7.$$

The simplified formula is $(Ca,Fe,Sr)(Ti,Zr,Al)_3O_7$. The Ti/Zr ratio ranged from 1.25 to 1.68. The compositional variety exhibited by naturally occurring examples of the zirconolite family confirmed that zirconolite can accommodate up to 27 wt% UO_2, 22 wt% ThO_2, 29 wt% RE oxides, and 1 wt% SrO. This remarkable flexibility is due to the five distinct cation sites in the zirconolite structure which allow a wide variety of cations of different size and charge to be accommodated. This is very similar to magnetoplumbite-type structure and $AM_{21}O_{38}$-crichtonite type for accommodating HLW elements.

Armalcolite in LVC-15HT is very close to pseudobrookite ($FeTi_2O_5$) in composition (Table 3.33). ZrO_2 is high in this phase because of the substitution pair of Zr-Ti. The calculated formula is:

$$(Fe_{0.74}Na_{0.05}Ca_{0.01}Mg_{0.02}Al_{0.18})_{1.00}(Ti_{1.87}Zr_{0.06}Si_{0.01}Al_{0.04})_{1.98}O_{5.00}$$

which can be simplified as $(Fe,Mg,Al,\ldots)(Ti,Zr,Al)_2O_5$. This phase also frequently appears in tailored ceramics. The chemical composition of an unidentified phase was also included in Table 3.33.

The glass compositions for LVC-15HT are given in Table 3.35. All of these analyses exclude the data for fluorine. According to EDS analyses, fluorine content changes a lot from point to point. The typical composition, including fluorine, is given by: SiO_2 27.54, CaO 24.86, Fe_2O_3 2.23, ZrO_2 1.35, Al_2O_3 27.45, K_2O 0.93, Na_2O 3.22, SrO 1.22, TiO_2 6.07, and F 5.13 (wt%).

3.6.3 Chemical Durability

The chemical durability of these ICPP waste-loaded vitreous ceramics was evaluated with EPA TCLP tests, PCT, and vapor-hydration tests.

The 7-day PCT sodium releases (Appendix C and Figures 3.55 to 3.59) suggested that the alumina-calcine wastes can be made into durable waste forms at both 60 (LVC-8) and 40% (LVC-9) calcine waste-loadings. The 7-day PCT durabilities of LVC-8 and LVC-9 were a factor of 10 and 30 times better than the EA glass, respectively. The main concern with alumina-calcine was the melting temperature, since both LVC-8 and LVC-9 required a melting temperature of 1600°C or higher. The zirconia-calcine was made into LVC-7 with 75% waste loading. The 7-day PCT durability was also acceptable at 1.3 g/m^2, which was a factor of 5 more durable than EA glass. However, it was obvious that the waste-loading, waste-form

Table 3.34. Chemical Compositions of Zirconolite from LVC-15

Oxide	3-63	3-70	3-71	3-203	3-207	3-208	3-84**
Al_2O_3	1.89	1.65	1.27	2.70	1.28	2.27	1.35
ZrO_2	45.13	40.89	41.24	38.11	42.63	38.41	44.10
TiO_2	36.43	40.33	40.32	41.75	38.78	41.61	37.59
CaO	13.85	13.82	13.75	14.13	13.35	13.95	13.75
SrO	0.19	0.23	0.51	0.00	0.35	0.68	0.48
Na_2O	--	0.84	0.47	0.00	MgO 0.39	--	--
SiO_2	--	--	--	0.43	Cr* 0.39	Cr 0.15	0.00
FeO	2.51	2.24	2.44	2.87	2.95	2.93	2.65

* Cr is referred to be as Cr_2O_3.
** 3-84 is from LVC-15HT/B and others from LVC-15HT/A.

Table 3.35. The Chemical Compositions of Glass in LVC-15HT

Oxide	3-60*	3-66*	3-202*	10-40*	10-41*	10-42*	3-80	3-83	3-120
Al_2O_3	31.07	30.02	28.96	30.43	25.98	19.30	32.21	29.92	49.71
ZrO_2	1.66	1.24	1.42	0.53	0.43	0.97	2.58	1.83	0.79
TiO_2	3.03	3.19	6.40	8.01	8.62	14.14	3.50	4.13	7.36
CaO	23.62	26.56	26.22	18.90	22.19	28.50	16.42	24.09	13.03
SrO	1.20	1.26	1.28	1.41	1.60	0.43	1.18	0.71	1.10
MgO	--	--	--	0.03	0.05	0.36	--	--	--
K_2O	1.14	0.93	1.00	1.27	2.71	1.53	0.87	0.62	0.78
Na_2O	3.39	3.37	3.34	2.60	1.51	1.17	2.44	4.04	1.73
Fe_2O_3	1.50	1.20	2.34	3.03	3.21	8.47	0.99	1.55	6.20
SiO_2	33.39	32.23	29.04	33.52	34.54	19.49#	39.80	33.11	19.30

* Analyses made on LVC-15HT/A. Other three analyses from LVC-15HT/B.
# Contains 5.64 wt% other oxides: Cs_2O 1.50, CoO 3.46, and P_2O_5 1.13.

durability, and melting temperature were all improved by blending alumina-calcine and zirconia-calcine together. LVC-14 had a calcine loading of 88%, which was higher than either LVC-7 or LVC-8, or LVC-9; had a 7-day PCT durability more than 6 times better than EA glass; and had an acceptable melting temperature of 1500°C. LVC-15 had a calcine loading of 78%; had a PCT durability 8 times better than EA glass; and had a melting temperature of 1450°C. The longer duration (up to 91-day) PCT durability results are shown in Figures 3.55 to 3.59, which are consistent with the 7-day results discussed above. The leachate pHs for all the tests were below 10.0.

The TCLP concentrations were shown in Table 3.5. All these vitreous ceramics passed the EPA limits on concentrations of hazardous elements of As, Ba, Cd, Cr, Pb, Hg, Se, and Ag. All the vitreous ceramics also passed the more restrictive land disposal limits, except that the 0.38 ppm of Ni in LVC-7 was slightly over the Ni limit of 0.32 ppm.

After reacting samples of LVC-7, LVC-8, LVC-9, LVC-14, and LVC-15 at 90°C in saturated water vapor, the samples were examined for surface alterations. The thickness of the alteration layer is an indicator of the extent of waste form corrosion. The following are the results of our observations of the vapor-reacted samples.

LVC-7

The bulk sample of LVC-7 was composed of fluorite (CaF_2), baddeyelite (ZrO_2), plagioclase ($CaAl_2Si_2O_8$), and glass matrix. The original surface of this sample was not smooth. Under SEM, the uneven original surface was covered a thin crust, which was bent and folded (Figure 3.60). The crust was only several microns thick. Cross-sectional SEM studies revealed that the glass matrix was preferentially corroded and the crystals were exposed (Figure 3.61). The chemical composition of the surface layer was very similar to the glass matrix, supporting the argument of preferential corrosion of the glassy phase.

LVC-8

Originally LVC-8 was only composed of two phases, spinel [$(Mg,Fe)Al_2O_4$], and glass matrix. Under SEM, the glassy matrix was preferentially corroded and spinel crystals seemed to protrude in some areas (Figure 3.46). The surface layer is 1-μm thick, on average, as shown by the cross-sectional SEM (Figure 3.46). The surface layer consisted of small spinel particles and the matrix. The matrix of the layer was composed of Ca, Al, and Si, if the peaks of spinel were removed. The matrix of the layer may be smectite.

LVC-9

Originally LVC-9 consisted of two phases, spinel [$(Mg,Fe)Al_2O_4$] and glass matrix. The surface of the sample was corroded and covered with a continuous fine, flake-like layer (Figure 3.62). This layer did not fully cover the surface, since the crystals can be seen clearly under these flakes. The morphology of the surface was very similar to that of smectite. The thickness of the surface layer is less than 0.8 μm (Figure 3.63). The composition of the surface layer is almost the same as that of the unaltered glass, indicating the glass was corroded preferentially. Therefore, the glass was dissolved into solution and then precipitation from the solution formed the surface layer. Smectite (the composition is between nontronite and montmorillonite) was the dominant clay in the surface layer.

Table 3.36. Chemical Compositions of partheite on the surface of LVC-14

	partheite	gismondine	#1	#2	#3
sample#	ref.1	ref.2	4-103	4-104	4-105
SiO_2	40.24	36.26	42.02	39.20	42.98
Al_2O_3	31.99	27.22	37.78	35.50	34.85
CaO	16.38	14.51	19.05	22.20	19.67
Na_2O	0.32	0.24	0.00	0.04	0.49
K_2O	0.23	0.77	0.35	0.69	0.52
SrO	--	0.24	0.79	1.01	1.29
FeO	--	--	0.00	0.36	0.21
MgO	--	--	0.00	0.00	0.00
H_2O	10.83	20.76	--	--	--

LVC-14

LVC-14 originally consisted of four phases, hibonite ($Ca(Al,Fe,Zr,Cr)_{12}O_{19}$), baddeyelite ($ZrO_2$), fluorite ($CaF_2$), and the glass matrix. Under SEM, a precipitated phase developed on the sample surface (Figures 3.64a and 3.64b). The precipitated phases were composed of many small crystals which inter-grew with each other forming elliptical spheres 50- to 80-μm in size (Figure 3.64b). The quantitative chemical compositions for the precipitated phases (#1, #2, and #3) are compared with reference compositions of partheite and gismondine in Table 3.36.

Chemically, the precipitated phases on the surface of LVC-14 were close to the compositions of partheite and gismondine. Both phases were zeolite. Partheite conformed to the formula,

$$(Ca_{7.14}Na_{0.26}K_{0.12})(Al_{15.41}Si_{16.63}O_{64}) + 16.00\ H_2O.$$

The simplified formula is $Ca_8(Si_{16}Al_{16}O_{64}) + 16\ H_2O$. Gismondine has a formula of $Ca_4(Al_8Si_8O_{32}) + 16\ H_2O$. It is difficult to distingush these two zeolite phases based on chemical data only. Partheite may be a polymorph of gismondine if the water content is neglected.

Electron diffraction patterns (in Figure 3.64c) indicated that the precipitated phases most possibly were partheite. Only two natural occurrences were revealed in the world: monoclinic, C2/c, cell parameter, a = 21.59; b = 8.78; c = 9.31(Å), and =91°28'. Based on a 64-oxygen equivalent basis, a typical formula is given by:

$$(Ca_{7.60}Sr_{0.17}K_{0.17})_{7.94}(Si_{15.65}Al_{16.56})_{32.21}O_{64},$$

which is simplified as $Ca_8Si_{16}Al_{16}O_{64}$. H_2O cannot be directly measured by EDS/AEM.

The cross-section of LVC-14 showed a complicated surface-layer structure. Besides the precipitated surface layer, there is also an in-situ altered surface layer (labeled as "preferably leached glass" in Figure 3.65). The preferable corrosion of the glass and fluorite was very evident: fluorite crystals dissolved and became small in size. Dissolution along the cleavages within a fluorite crystal was also

evident. The surrounding glass of the fluorite crystals cracked and must have been hydrated. When CaF_2 dissolved in water, the following reaction may have occurred: $CaF_2 + 2H_2O = Ca(OH)_2 + 2HF$. The reaction resulted in an alkaline environment because HF is a weak acid, the release of HF can attack the glass structure and thus increase the rate of corrosion of the glass. The $Ca(OH)_2$ can be also mixed with the clay matrix in the surface layer which results in a high CaO content in the layer. However, it is very interesting to note that hibonite and baddeyelite were not corroded and the altered zone of the glass and fluorite ended in front of the giant hibonite needles. The hibonite needles formed a three-dimensional network which effectively prevented the bulk sample from a further attack by water. This hibonite structure formed an internal barrier, which may have important effects on the long-term durability of LVC-14.

LVC-15

The unreacted LVC-15 sample contains five major phases, such as fluorite (CaF_2), baddeyelite (ZrO_2), zirconolite ($CaZrTi_2O_7$), corundum (Al_2O_3), and glass. Under SEM, a precipitated phase similar to that found on the surface of LVC-14 was formed. The precipitated Si-Al-Ca phase on the surface of LVC-15 was the same as that of LVC-14, identified as partheite. The chemical information is listed in Table 3.37.

The calculated formula on a 64-oxygen basis is:

$$Ca_{7.78}Sr_{0.29}K_{0.62})_{8.69}(Si_{6.13}Al_{15.53}F\ e_{0.06})_{31.78}O_{64.00}.$$

The matrix was characterized by tiny particles (Figure 3.66a). The thickness of the surface alteration was thinner than that in LVC-14 (Figure 3.65). The precipitated phases were deposited on the original surface of the sample (Figure 3.66). The glass between corundum was preferentially corroded, forming the pits within the leach zone (Figure 3.67). Compared to the unaltered glass, the reacted glass on the top side was lower in Ca, indicating Ca is removable. Zirconolite, baddeyelite, and corundum were not altered during vapor-phase alteration, which form barriers from further corrosion.

3.6.4 Summary

ICPP calcined wastes were immobilized into vitreous ceramics. The waste loading was up to 100% if contaminated soil was used as a glass-forming additive. The highest calcine-loading achieved with alumina- and zirconia-calcines was 88%. By allowing the blending of alumina- and zirconia-calcines, increased calcine-loading, increased vitreous ceramic durability, and reduced melting temperature (to immobilize alumina-calcine) were achieved. These blended melts can be melted at below 1500°C.

All of these vitreous ceramics passed the EPA TCLP concentration tests on hazardous elements and the alumina- and zirconia-calcine blended vitreous ceramics also passed the more restrictive land disposal limits on hazardous elements. These vitreous ceramics are factors of 5 to 30 times more durable than the high-level EA glass when evaluated in a 7-day PCT. The leachate pHs of these vitreous ceramics were consistently lower than 10.

Table 3.37. Chemical Compositions of Partheite in LVC-15

phase	partheite	partheite
sample#	4-101	4-102
SiO_2	42.05	42.84
Al_2O_3	34.39	35.06
CaO	19.92	19.30
Na_2O	*	*
K_2O	1.62	1.28
SrO	1.91	1.33
FeO	0.10	0.19
H_2O	--	--

*Na_2O is not included in the analyses.

Even after corrosion in saturated water vapor at 150°C for 28 days, all of the vitreous-ceramics showed only minor alteration, characterized by the thin alteration layers. Two types of the surface layers were found on these altered vitreous ceramics. One layer formed in situ on the surface and grew into the inner zone of the sample. However, the crystalline phases, such as $Ca_3(PO_4)_2$, magnetite $[(Fe^{2+}Ni,Mn)Fe^{3+}{}_2O_4]$, hibonite $[Ca(Al,Fe,Zr,Cr)_{12}O_{19}]$, baddeyelite ($ZrO_2$), zirconolite ($CaZrTi_2O_7$), and corundum ($Al_2O_3$), were very durable and showed insignificant corrosion. The glass alteration usually ended in front of these crystals. More interesting is that durable hibonite in LVC-14 and corundum formed three-dimensional internal barriers within the waste form, which may provide excellent long-term durability to these waste forms. The silicate phases, such as feldspar ($KAlSi_3O_8$) and $CaAl_2Si_2O_8$, leucite ($KAlSiO_4$), and pyroxene ($CaFeSi_2O_6$) were less durable than the above crystals, but they were still more durable than most of the glasses. Another type of surface layer was the precipitated layer that formed through the solution deposition onto the original surface. The deposited materials in solution came from the preferential corrosion of the leached phases, such as Ca-high glass and fluorite. The hydroxylization of fluorite favors the corrosion of the glass. The common alteration products from these silicate phases were clay minerals, such as smectite-illite. Surface-precipitated phases developed well only on two samples, LVC-14 and LVC-15, and were identified as prehnite $[Ca_2Al_2Si_3O_{10}(OH)_2]$.

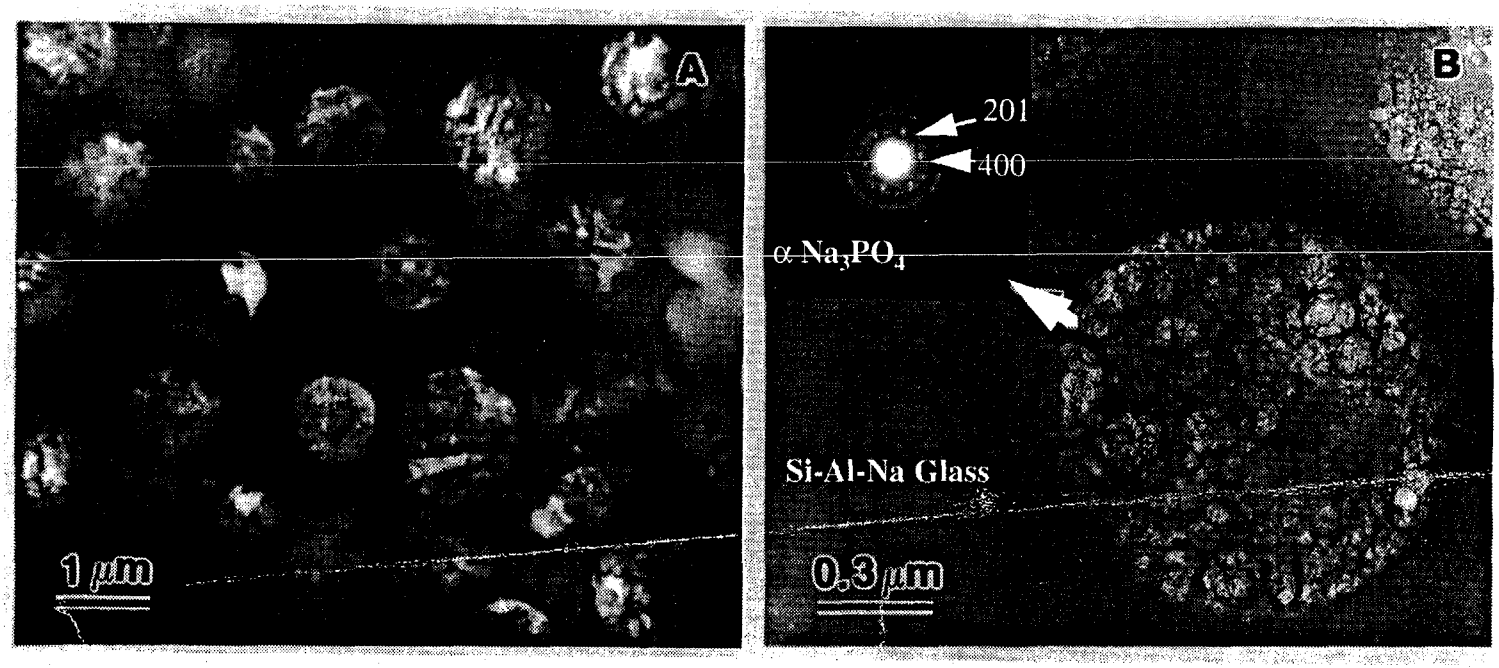

Figure 3.1. Bright Field Images of LVC-2HT. (a) Spherical Na_3PO_4 crystals in Si-AL rich glassy matrix, (b) An enlarged image of Figure 3-1a, and (c) Electron diffraction patterns of P-Na phase.

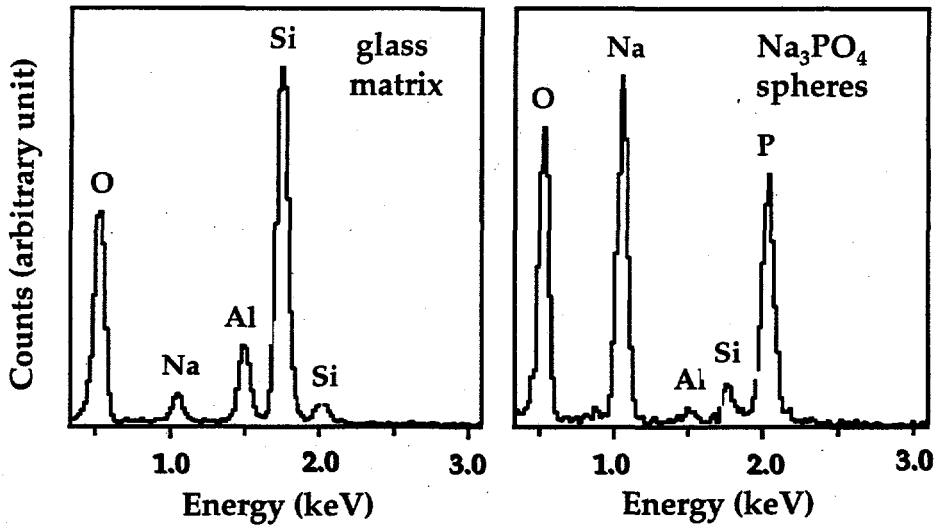

Figure 3.2. (a) EDS Spectrum for Si-Al Glassy Matrix of LVC-2HT.
(b) EDS Spectrum for Na-P Spheres of LVC-2HT.

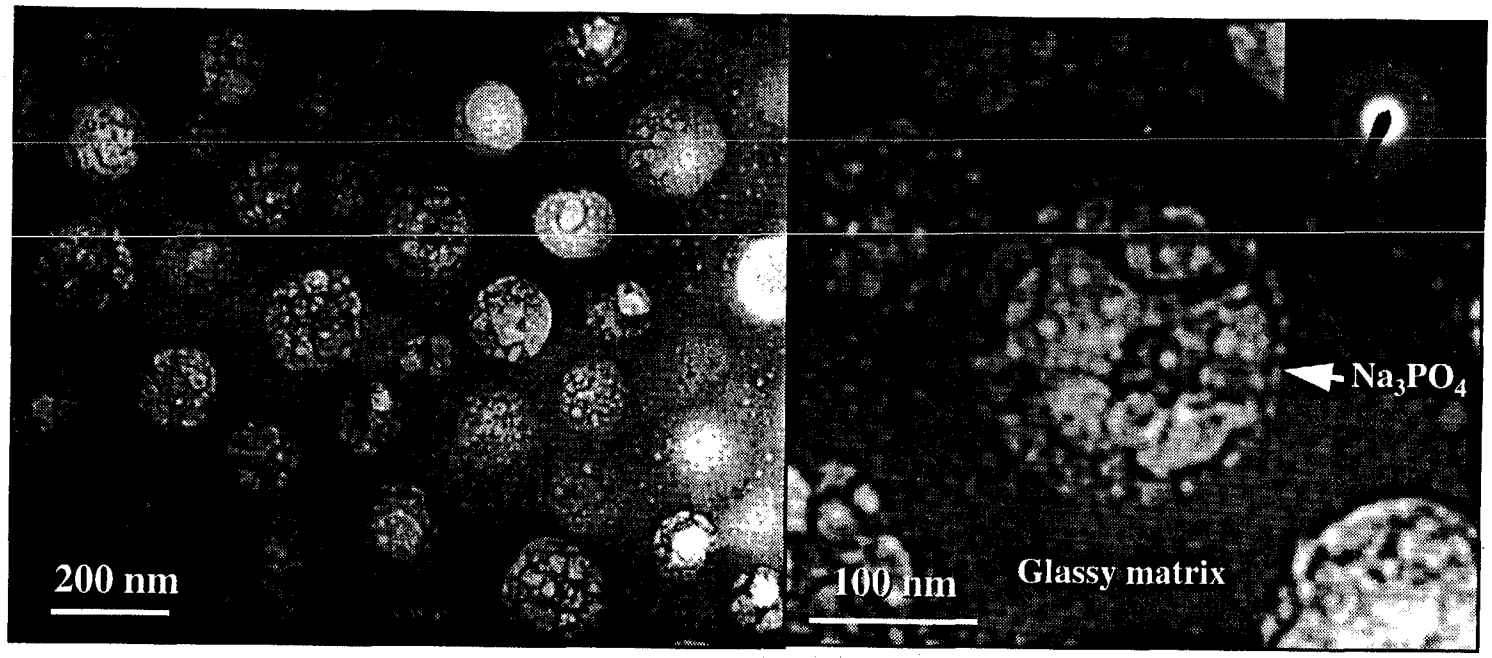

Figure 3.3. Bright Field Images of LVC-2Q: (Left) Spherical Na_3PO_4 Crystals of the Size 150 nm in a Si-Al Rich Glassy Matrix, (Right) and Enlarged View of the Spherical Na_3PO_4 and its Diffraction Pattern

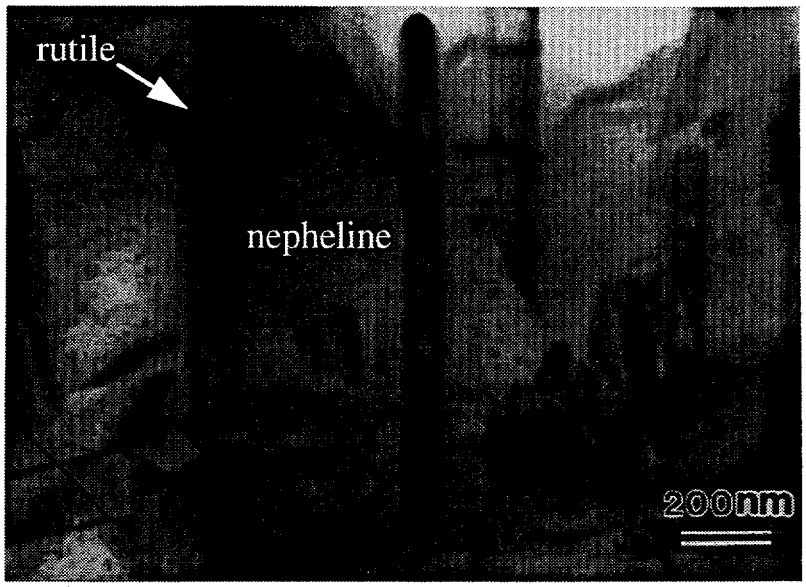

Figure 3.4. Bright Field Images of LVC-3HT the Gray Region and Brown Region

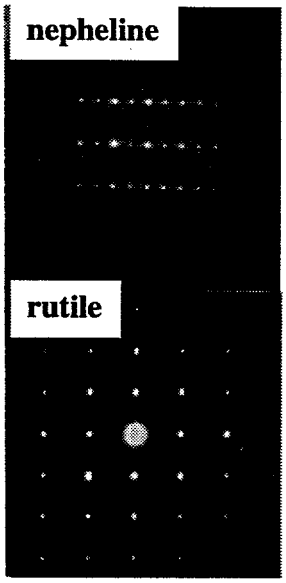

Figure 3.5. Selected Data on Diffraction Patterns for Different Regions of LVC-3HT, (a) Nepheline from a Brown Region, (b) Epheline from a gray spherical particle, (c) Rutile.

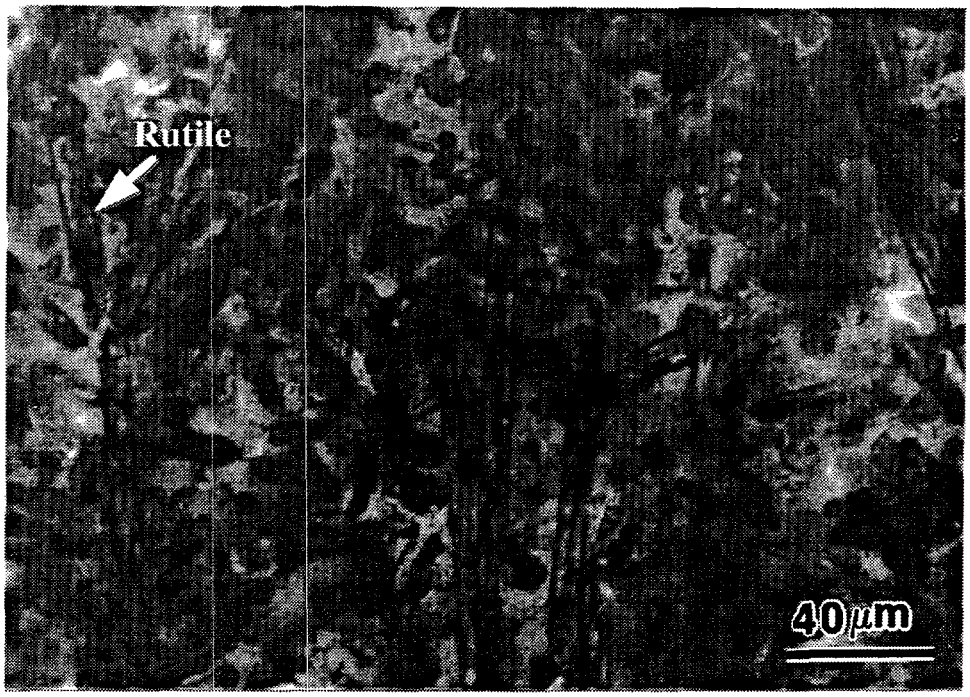

Figure 3.6. Optical Photo of LVC-4HT. Rutile is identified with a needle-like habit.

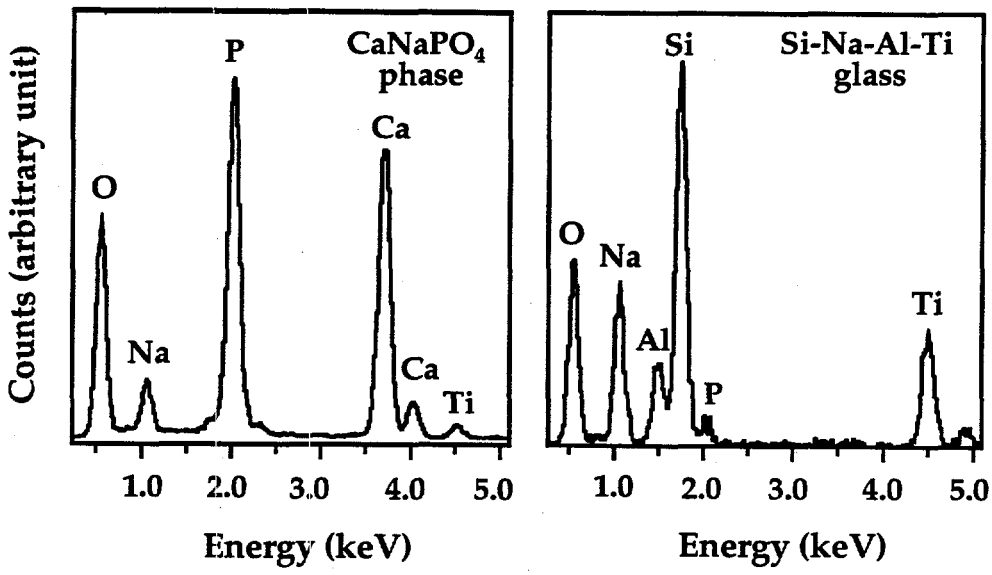

Figure 3.7. EDS Spectrums of LVC-4HT. (a) The P-Ca-Na crystalline phase, (b) The Si-Al-rich glassy matrix.

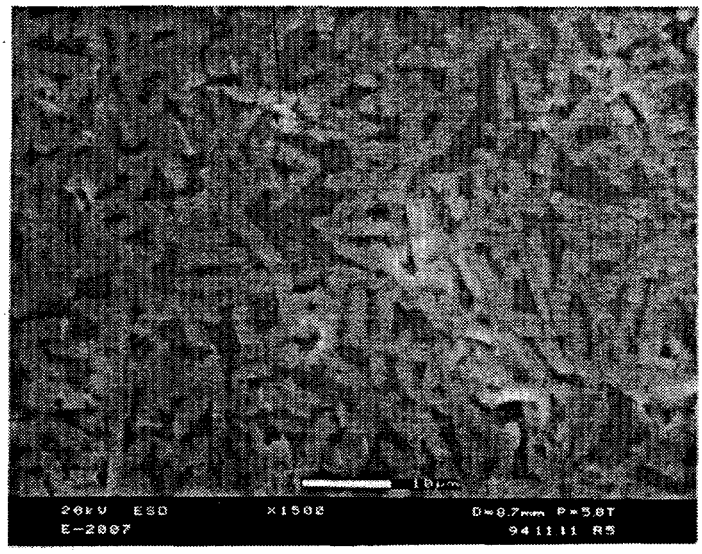

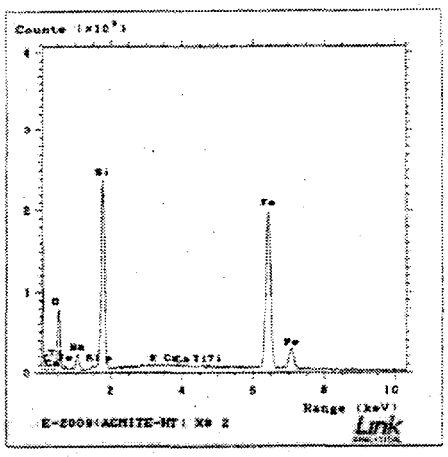

Figure 3.8. (a) SEM Micrograph of LVC-11HT, (b) EDS Composition of the Fe-Si Crystal (light areas in Figure 3.8a)

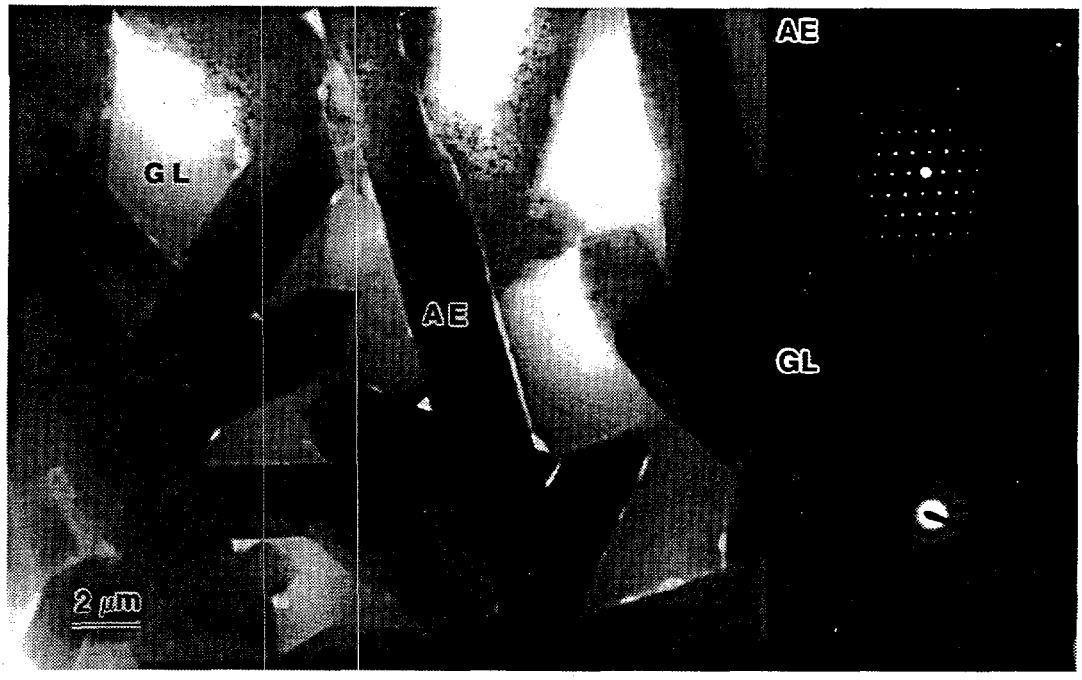

Figure 3.9. TEM Micrograph of LVC-11HT Showing Both Aegrine (i.e., acmite) and Glassy Matrix, with the Selected Area Diffraction Pattern of Glass (GL) and Aegrine (AE)

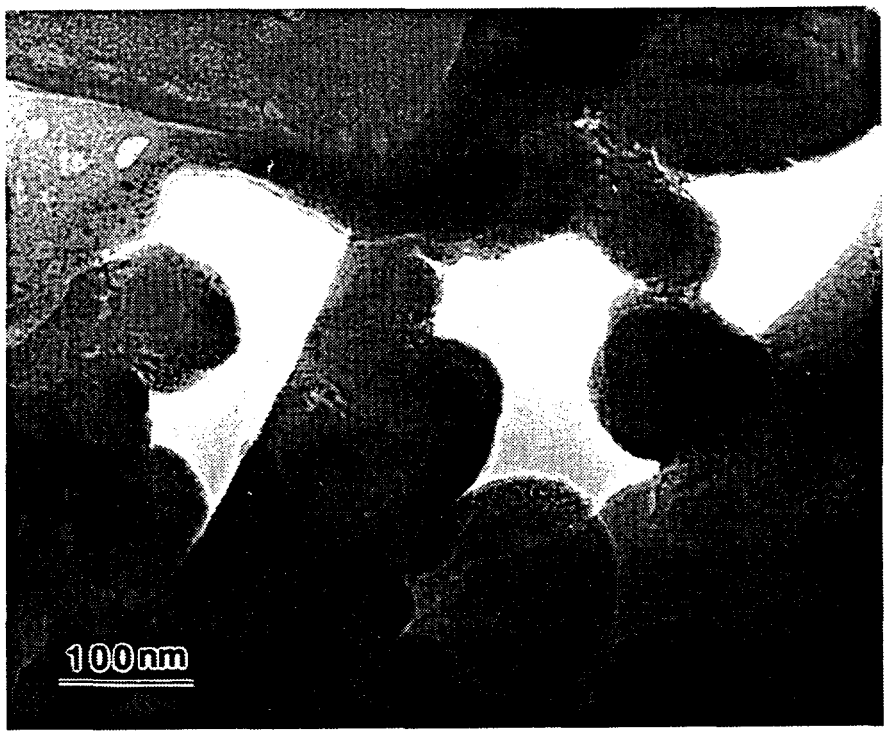

Figure 3.10. TEM Micrograph of LVC-11HT Showing Morphologically Different Glass Regions

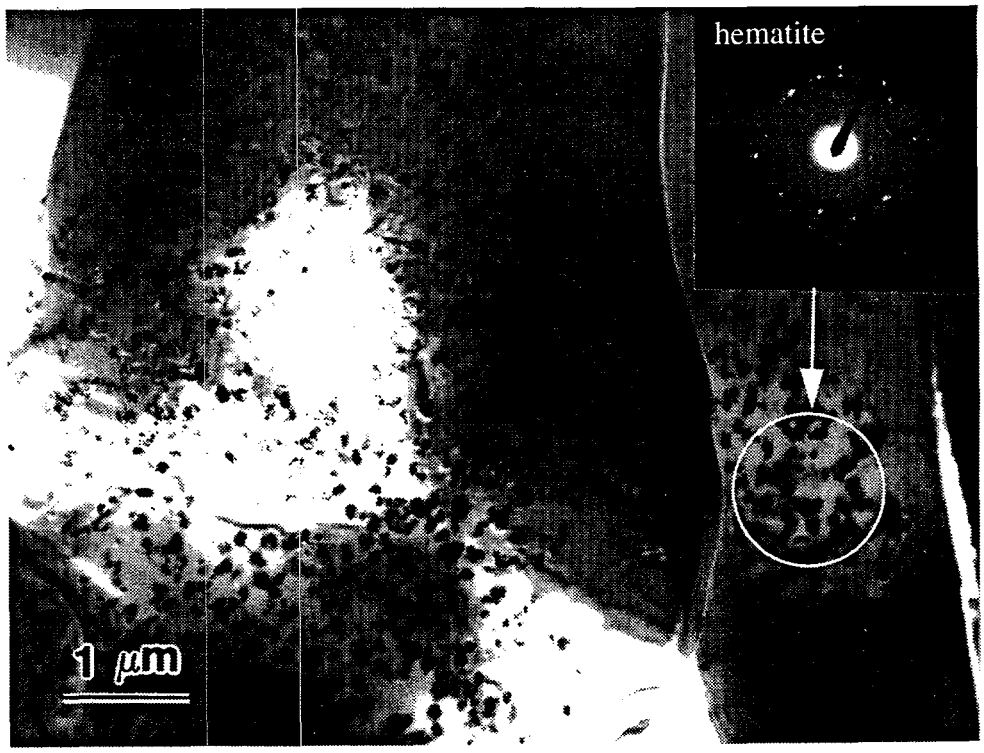

Figure 3.11. TEM Micrograph of LVC-11HT Showing the Inclusion of Hematite in Aegrine Crystals. The SAD pattern of hematite is shown in the upper right corner.

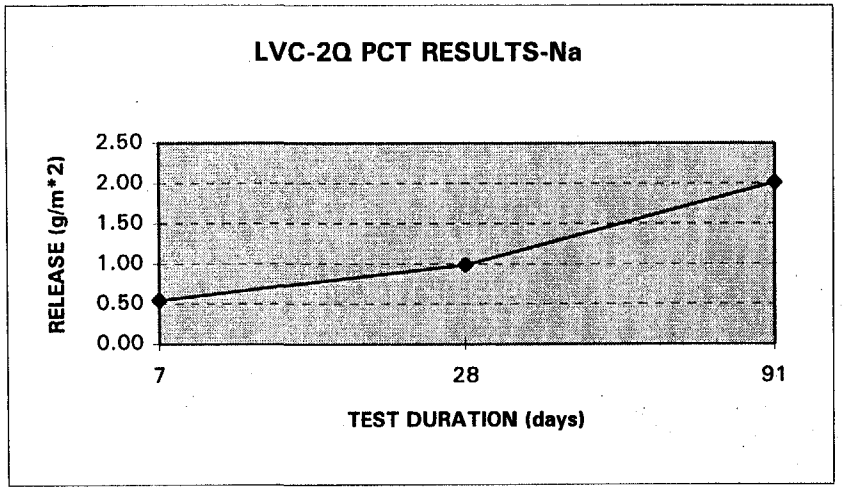

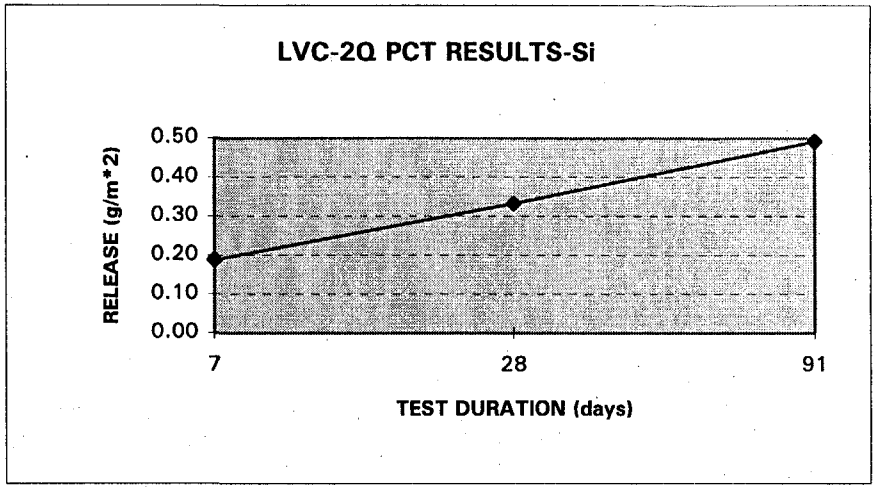

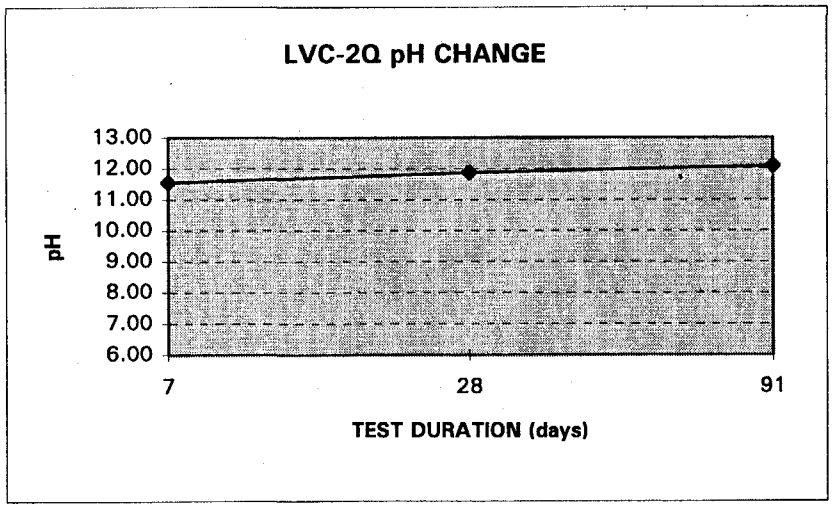

Figure 3.12. Elemental Releases and pH of LVC-2Q in PCT

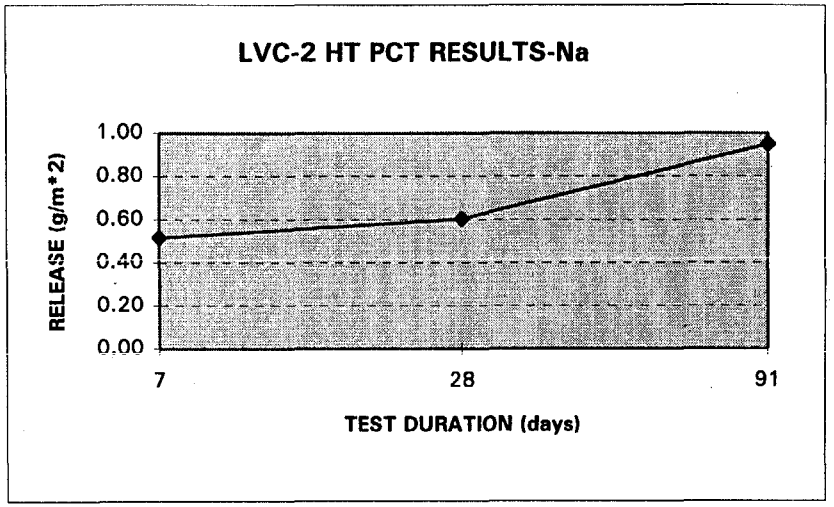

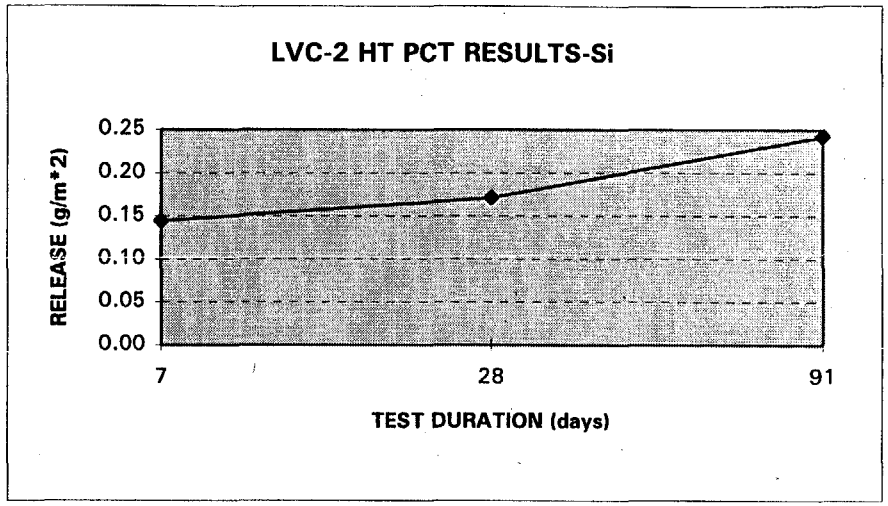

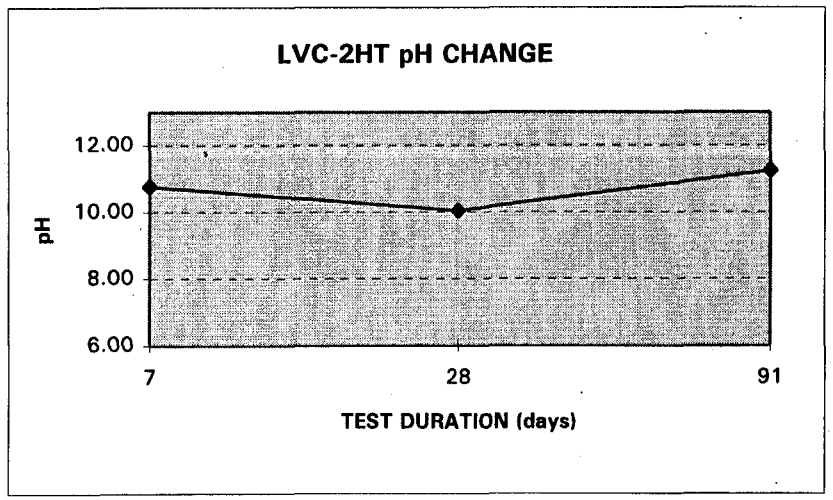

Figure 3.13. Elemental Releases and pH of LVC-2HT in PCT

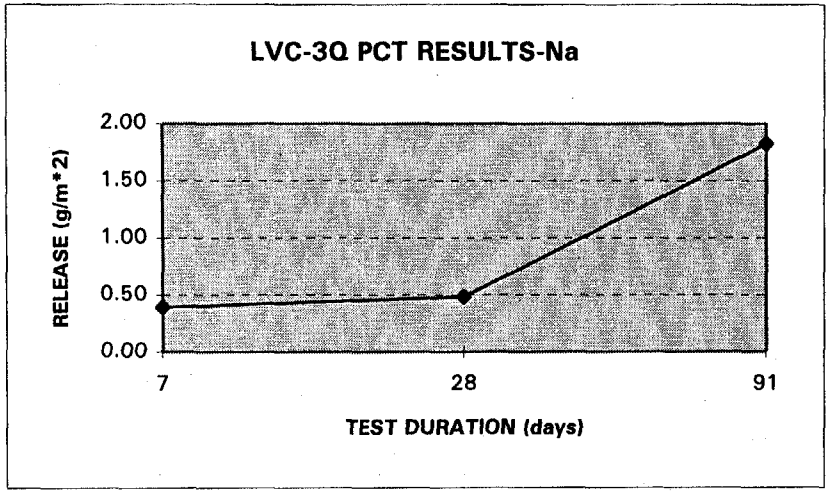

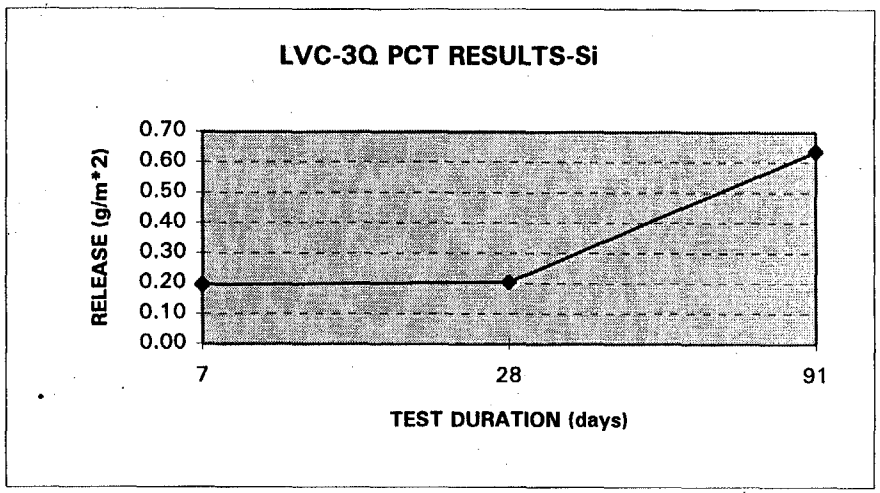

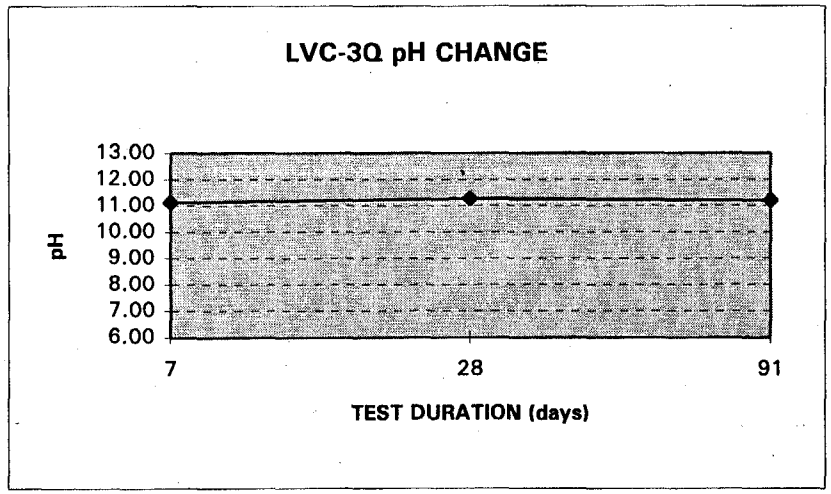

Figure 3.14. Elemental Releases and pH of LVC-3Q in PCT

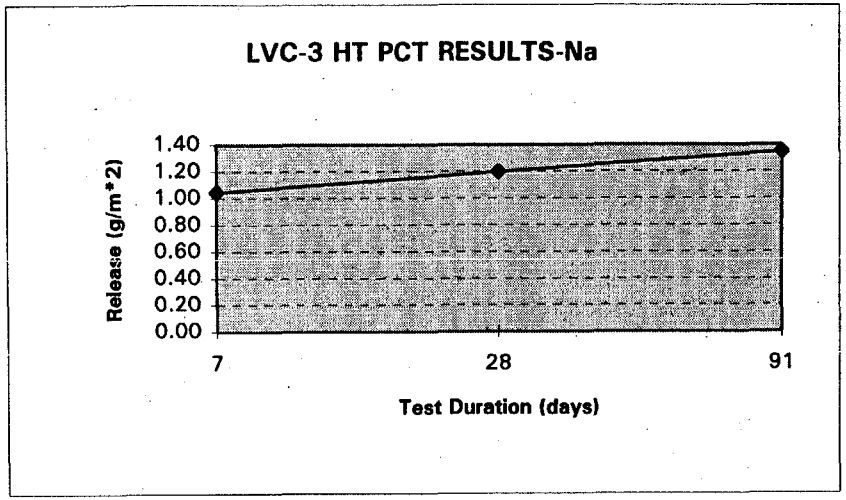

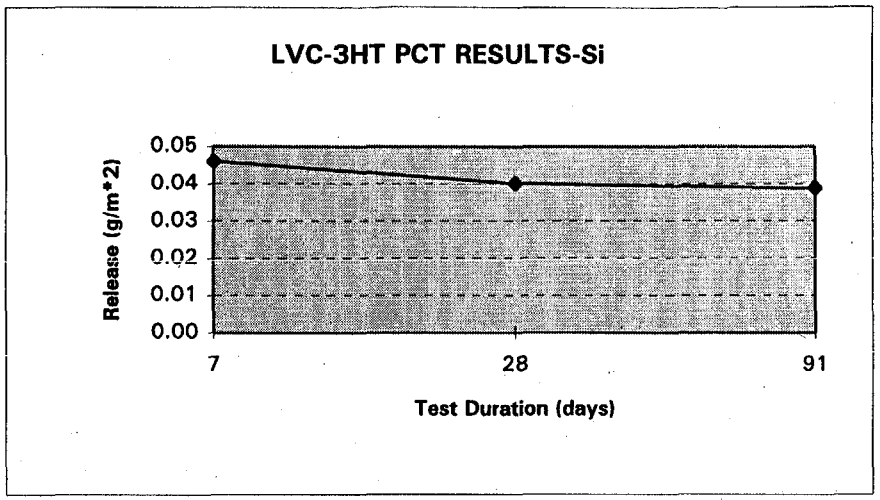

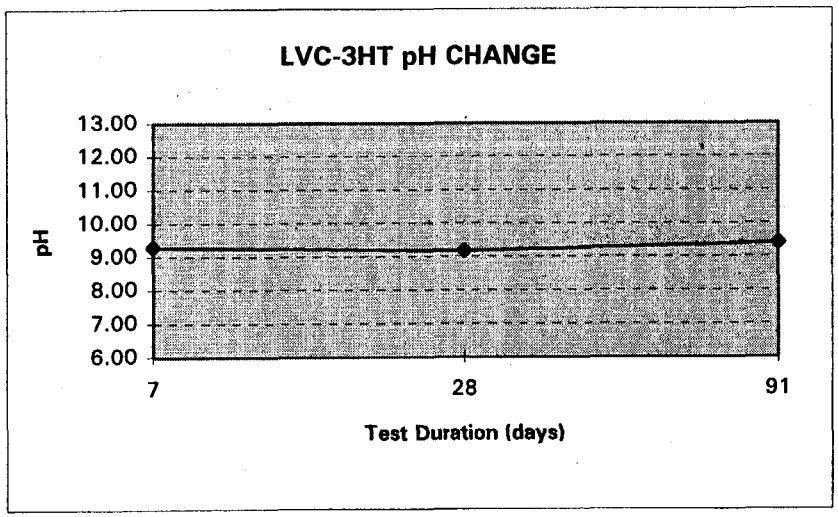

Figure 3.15. Elemental Releases and pH of LVC-3HT in PCT

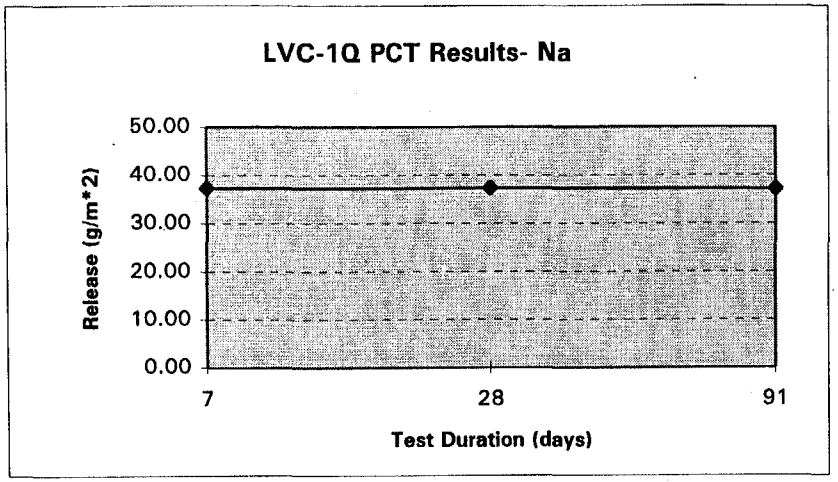

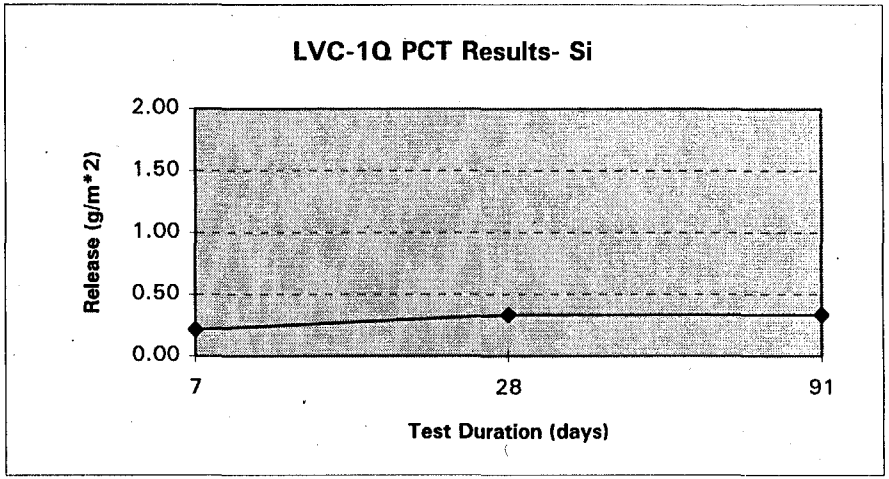

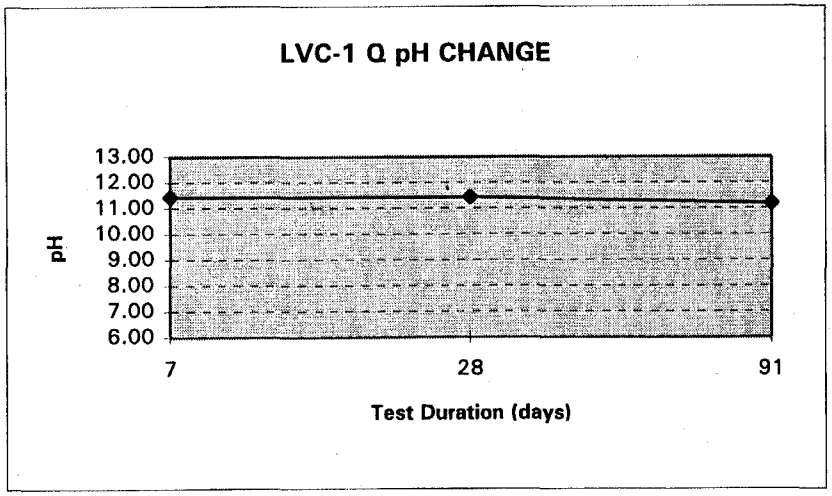

Figure 3.16. Elemental Releases and pH of LVC-1Q in PCT

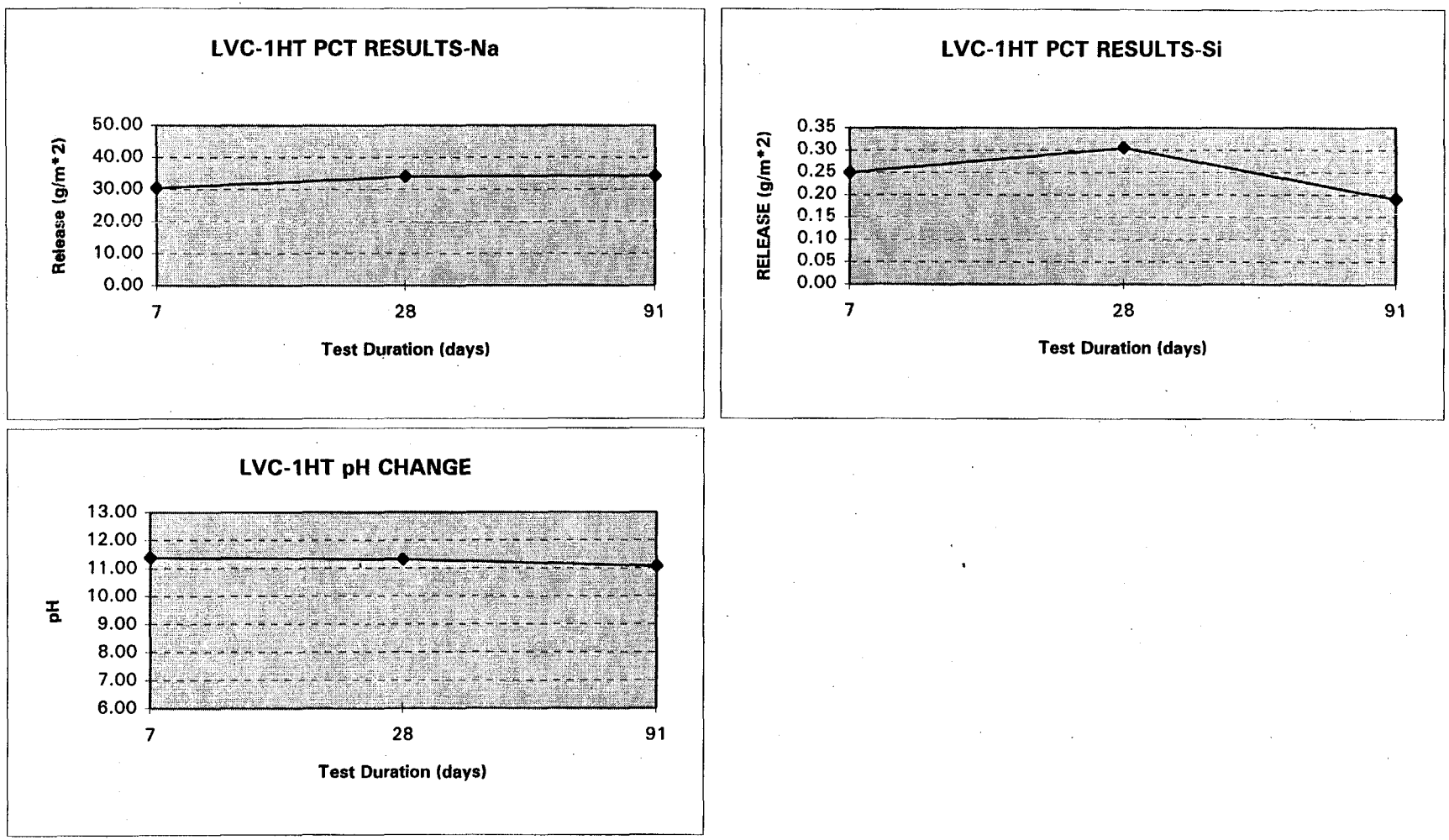

Figure 3.17. Elemental Releases and pH of LVC-1HT in PCT

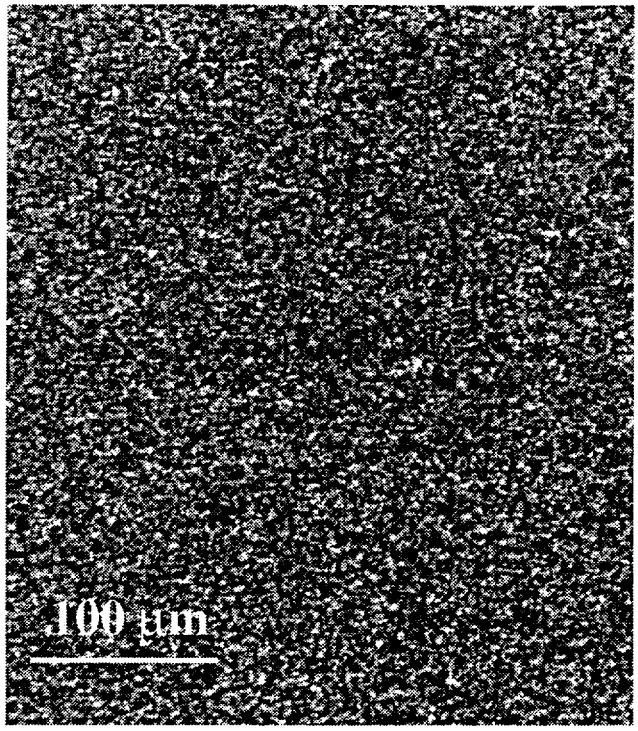

Figure 3.18. Optical Micrograph of LVC-12HT Shows 5 to 10 nm Particles

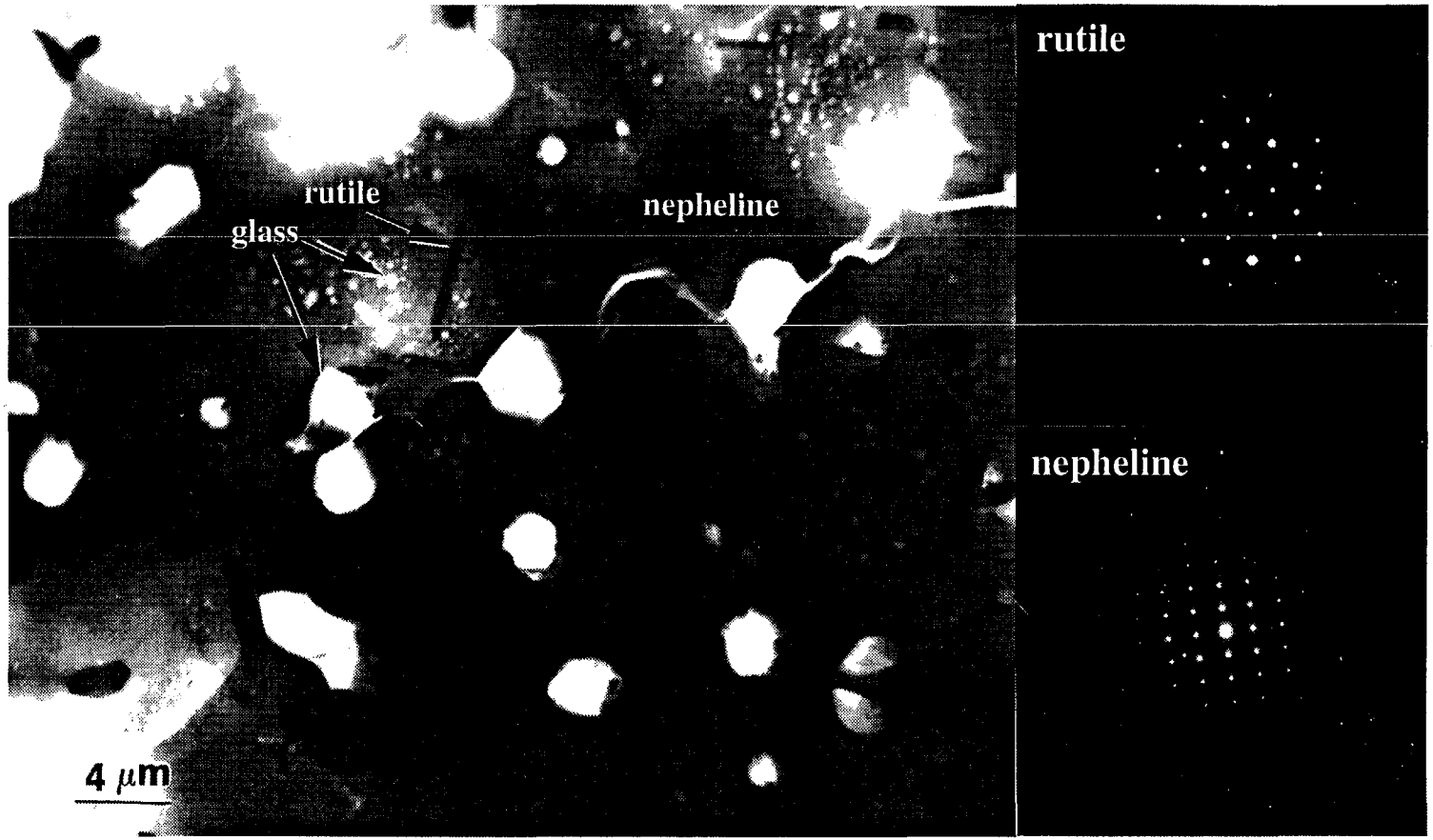

Figure 3.19. Bright Field TEM Image Shows Three Phases in LVC-12HT: Rutile, Glass, and Nepheline Matrices. The large spherical glassy regions were prefentially thinned by ion milling and small glassy particles are pointed out by the arrow. (a) SAD of rutile needles, (b) SAD of nepheline matrix.

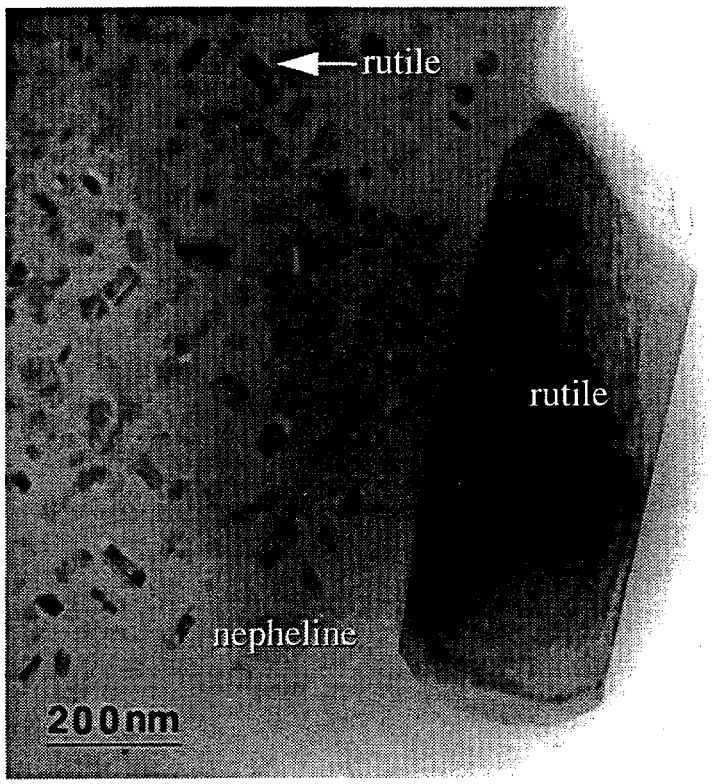

Figure 3.20. TEM Bright Field Image Shows Two Kinds of Morphologically Different Rutile Crystals in LVC-12HT

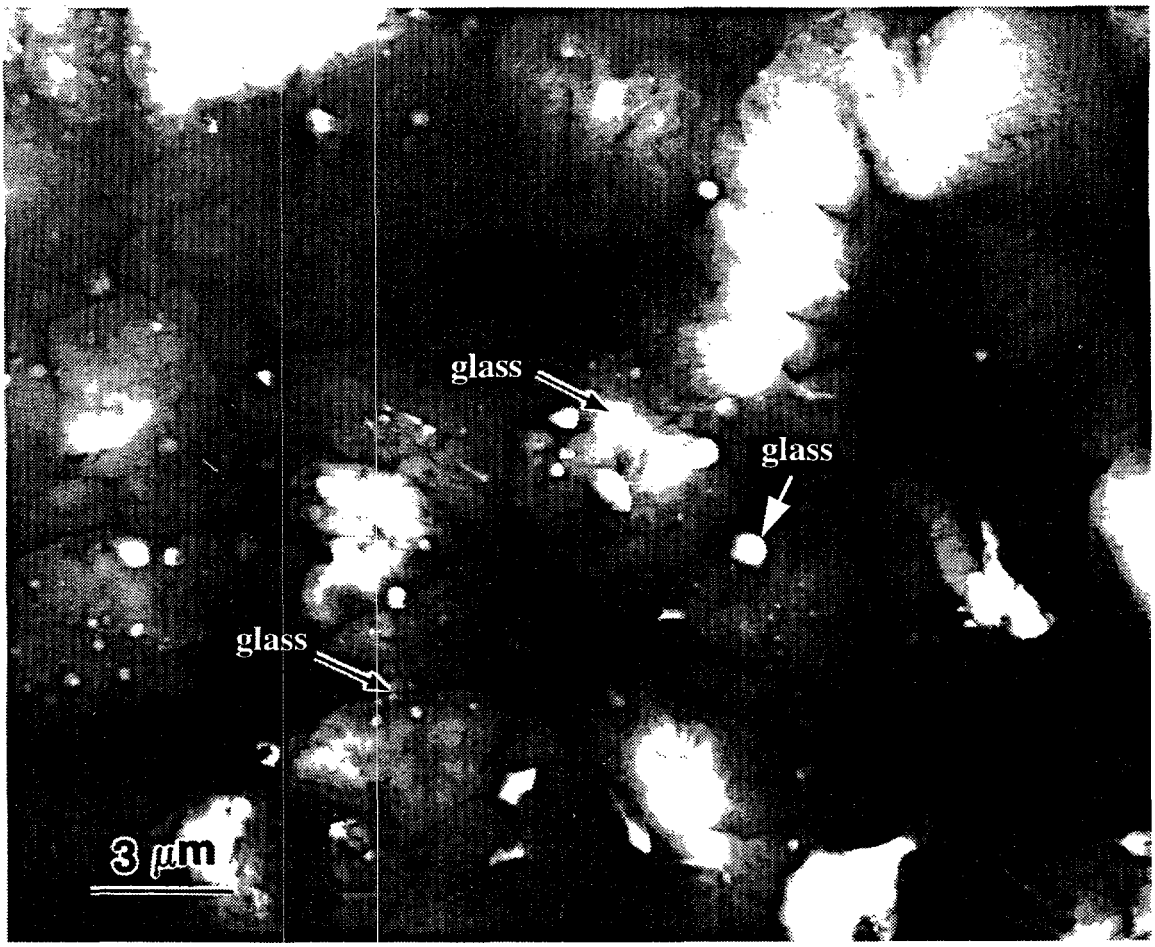

Figure 3.21. The TEM Bright Field Image of LVC-13HT. The glassy inclusions are indicated by arrows.

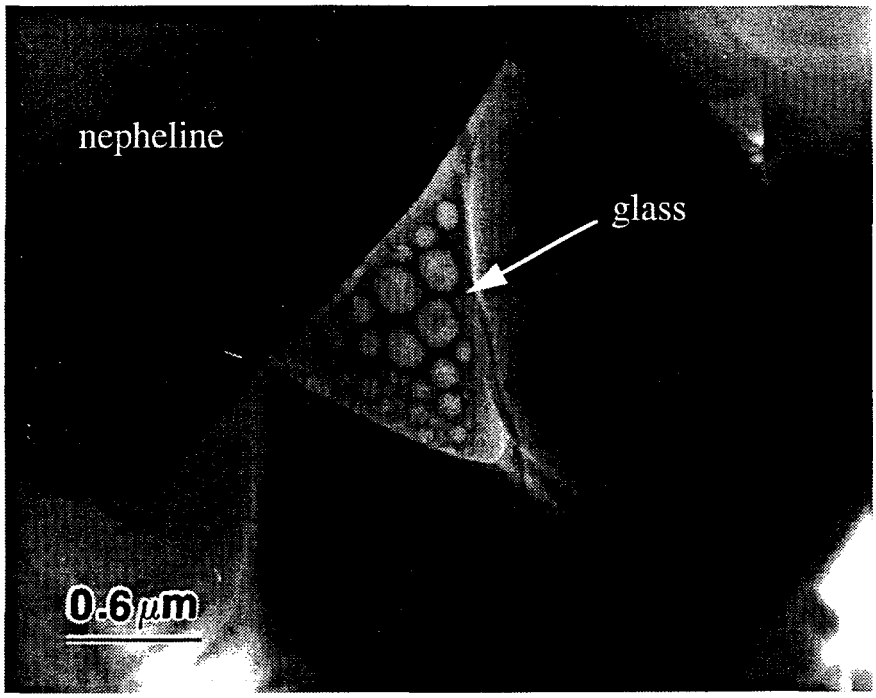

Figure 3.22. The TEM Bright Field Image of LVC-13HT Shows the Detailed Microstructure of a Glassy Inclusion in the Grain Boundaries of Nepheline Crystals

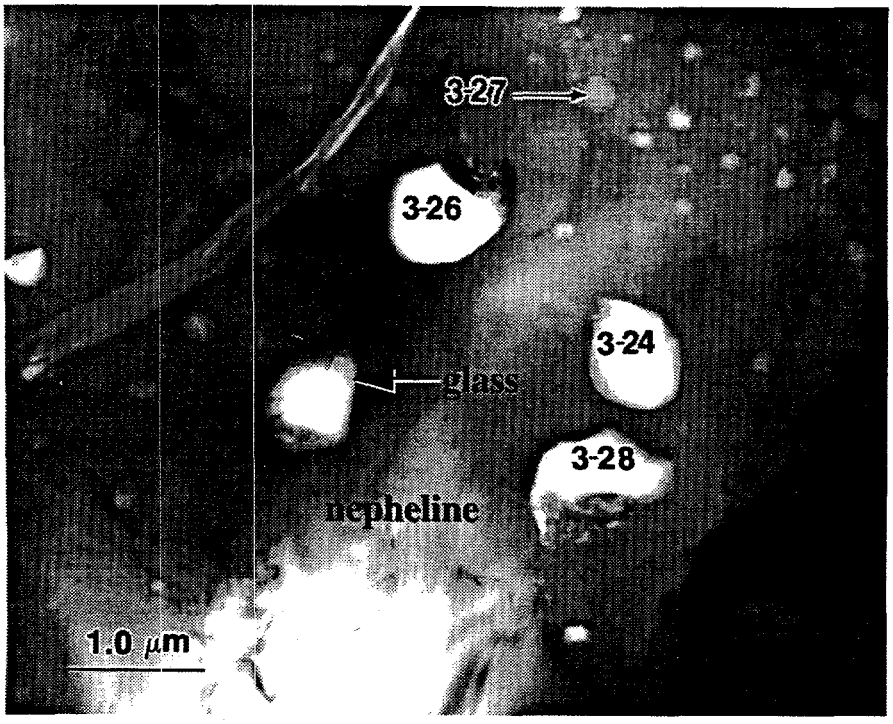

Figure 3.23. TEM Bright Field Image of LVC-13HT Shows Two Kinds of Morphologically Different Glassy Inclusions: Large and Small Glassy Particles. The numbers correspond to the analytical ID's in Table 3.13.

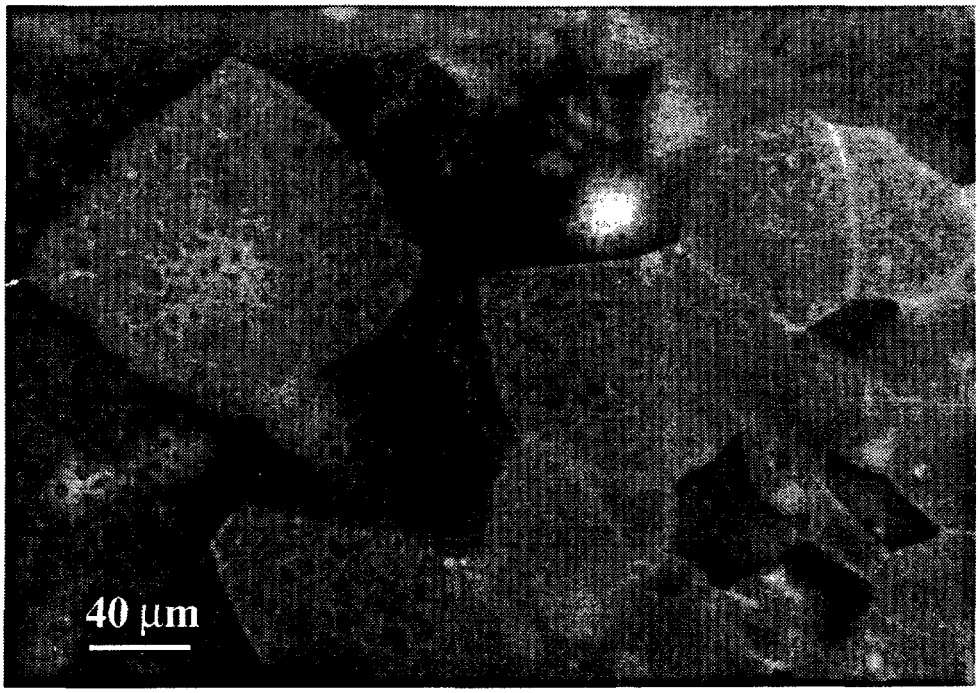

Figure 3.24. Optical Photo of the Microstructure of LVC-13HT

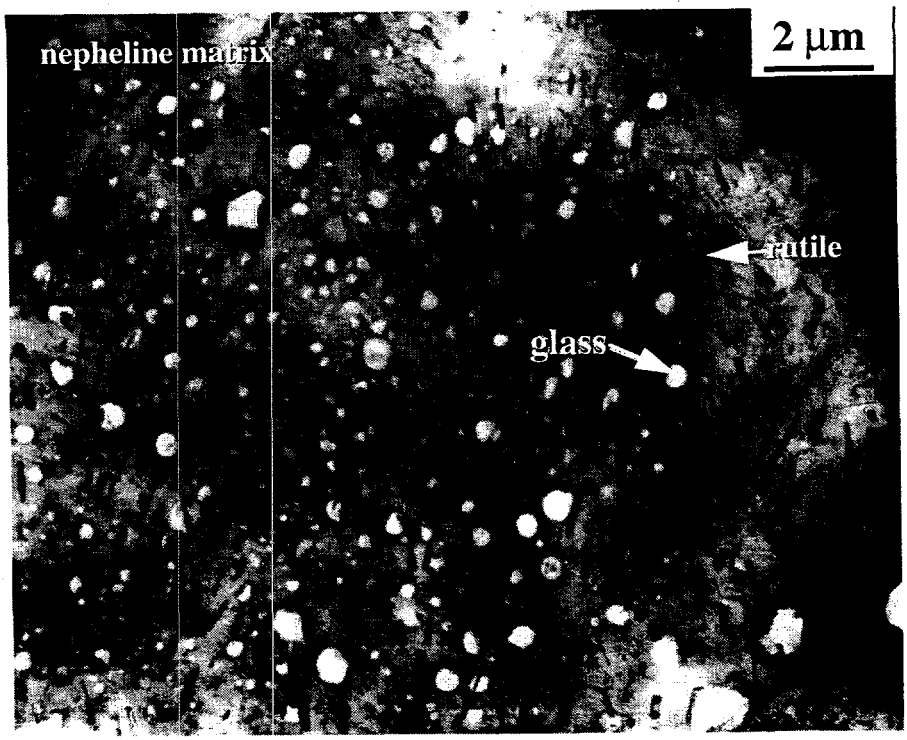

Figure 3.25. TEM of LVC-3HT Showing the Glassy Phase

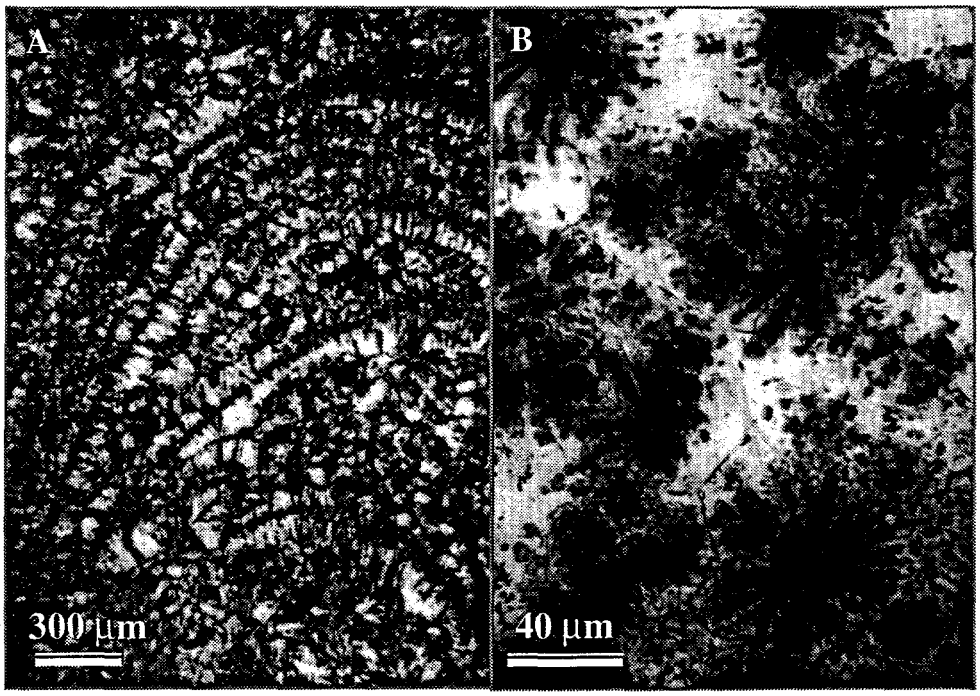

Figure 3.26. Optical Micrographs for LVC-10HT. (a) The glass regions in the nepheline matrix form a fluidal structure, (b) The spinel skeleton crystals occur as rosettes.

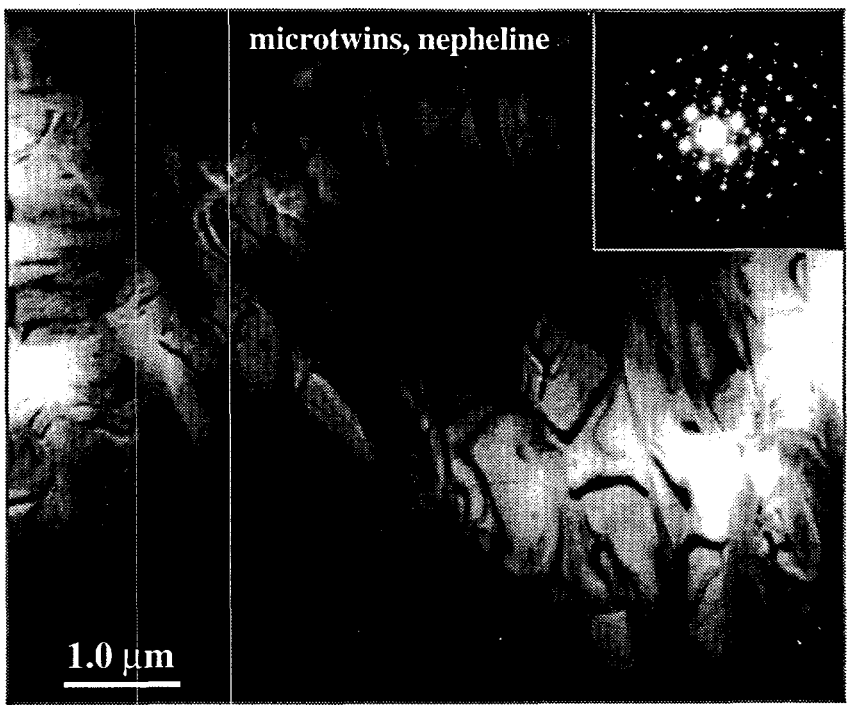

Figure 3.27a. TEM Micrograph Shows the Microtwin Structure of Nepheline in LVC-10HT and SAD of Nepheline

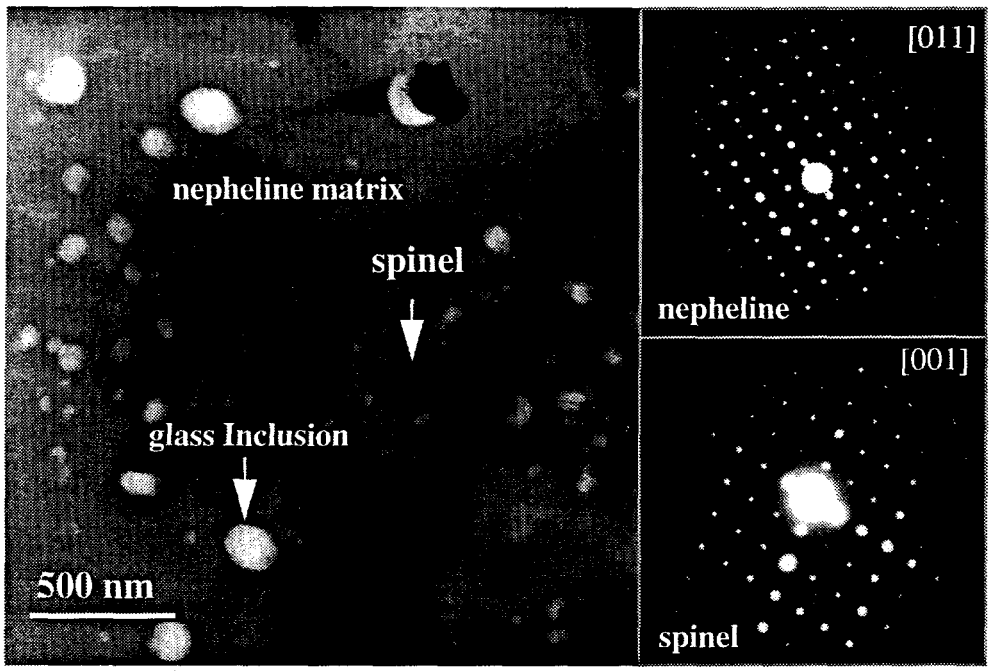

Figure 3.27b. Spinel Type Phases $(Mg,Cr^{2+},Zn)(Cr^{3+}, Al)_2O_4$, with Less than 5 Vol.%, are Identified as Small Inclusion in the Nepheline Matrix in LVC-10HT. The SAD of nepheline and spinel are also shown.

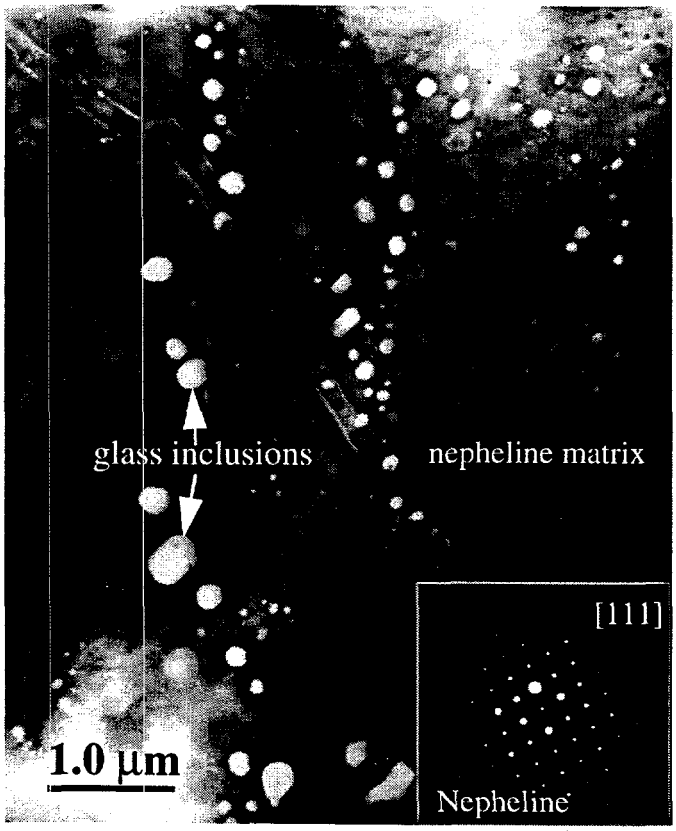

Figure 3.27c. Glass Inclusions Form a Fluidal Microstructure in the Nepheline Matrix in LVC-10HT

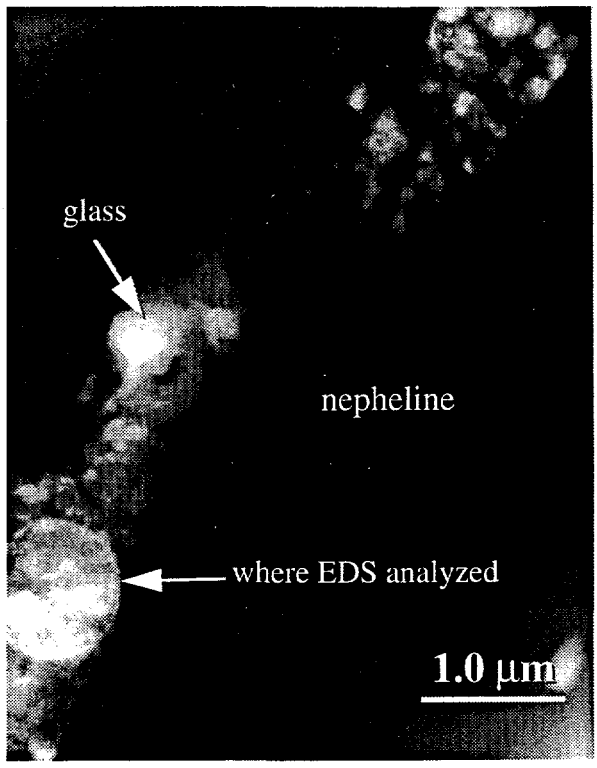

Figure 3.27d. Glassy Phases Seem to Fill the Gaps in the Nepheline Matrices in LVC-10HT

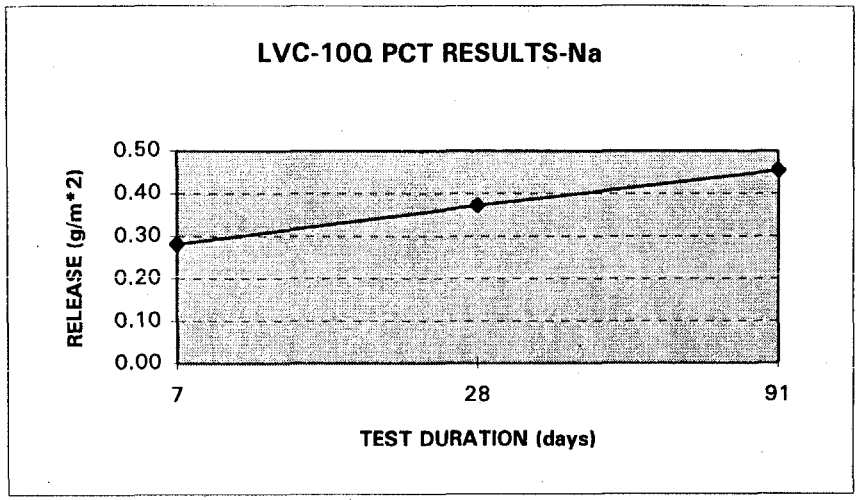

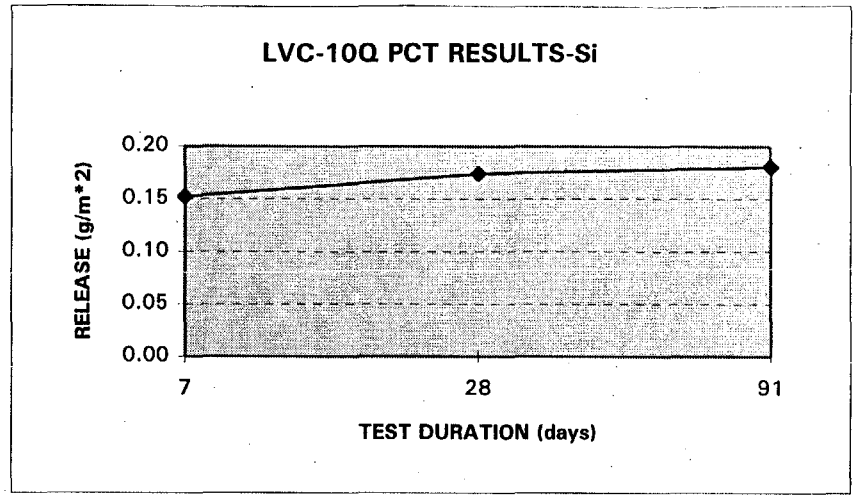

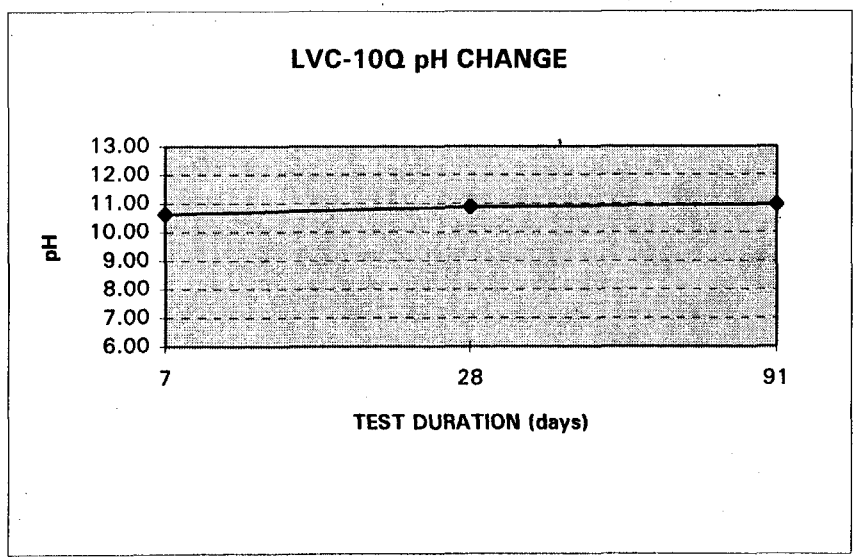

Figure 3.28a. PCT Elemental Releases (g/m^2) for LVC-10Q

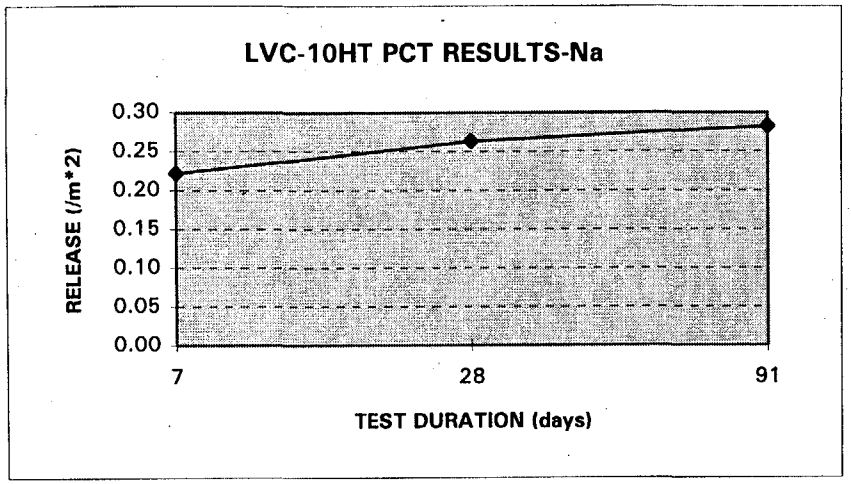

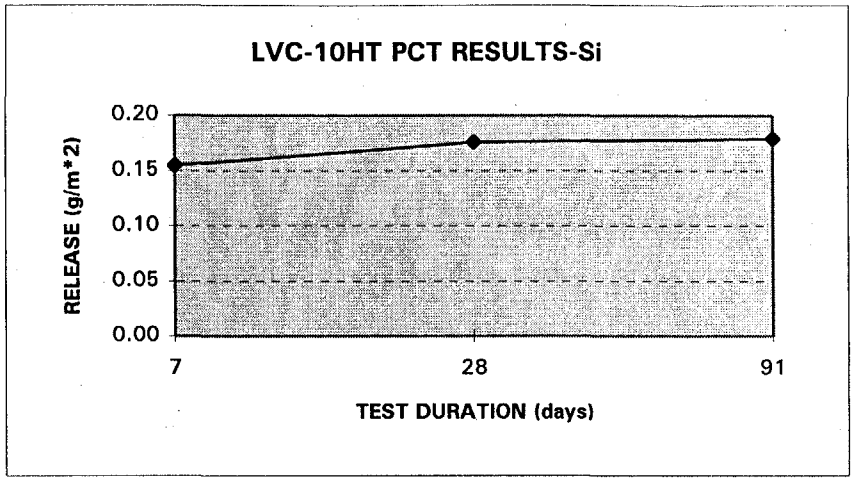

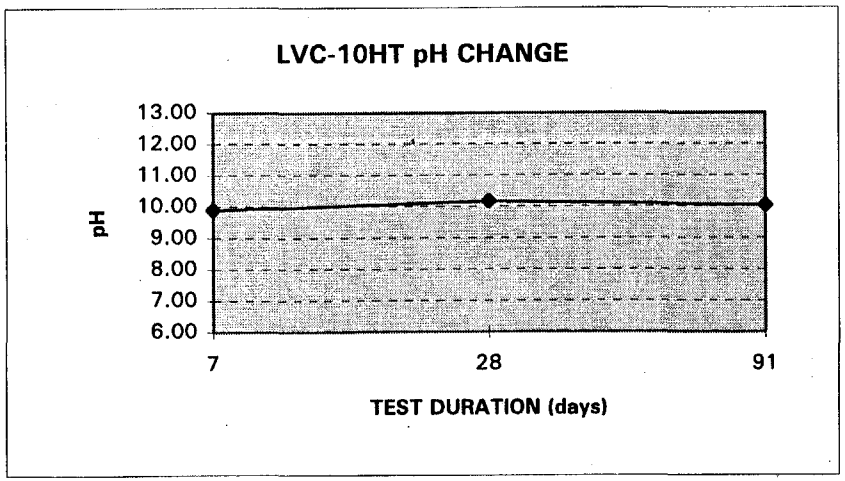

Figure 3.28b. PCT Elemental Releases (g/m^2) for LVC-10HT

Figure 3.29a. SEM Micrograph Shows Ditching Pitting After Vapor Hydration Tests of LVC-10HT

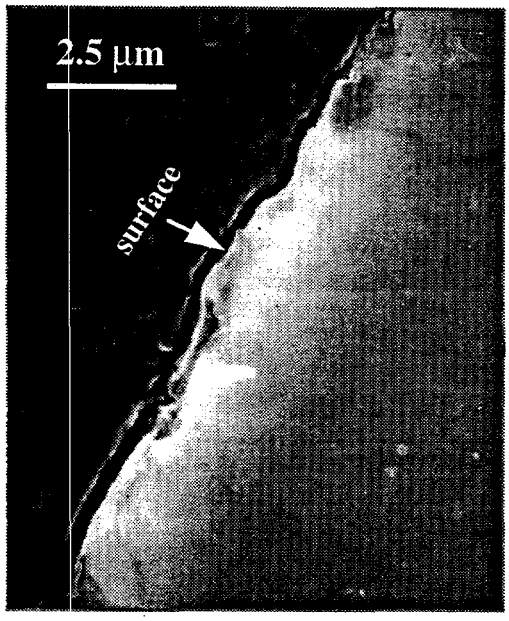

Figure 3.29b. SEM Shows no Layer was Formed on LVC-10HT After Vapor Hydration Tests

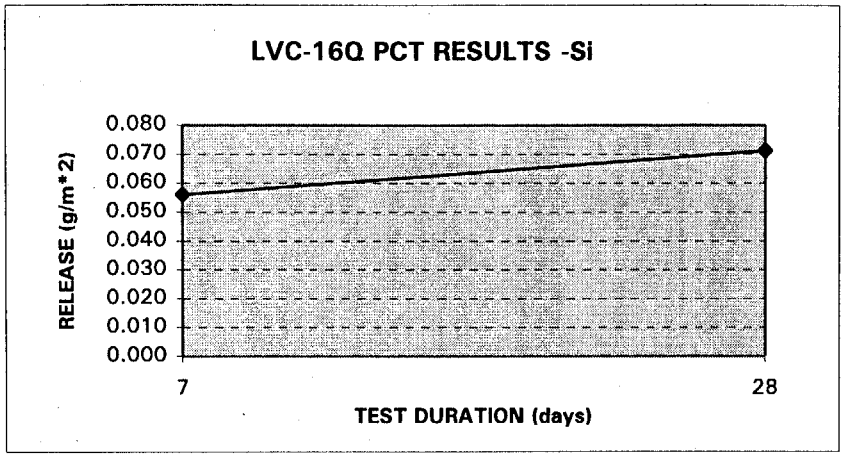

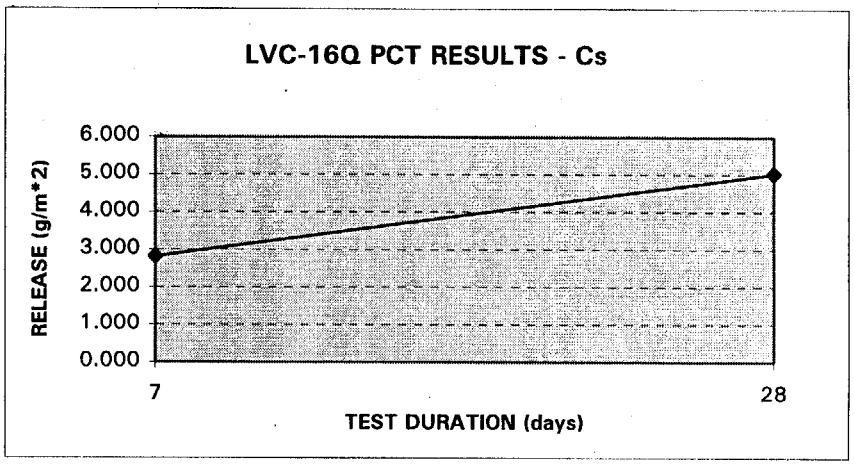

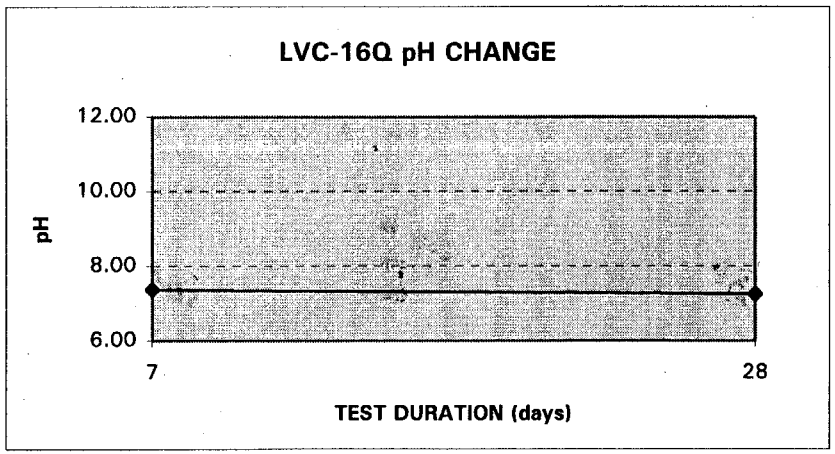

Figure 3.30a. Elemental Releases (g/m^2) of LVC-16Q from PCT

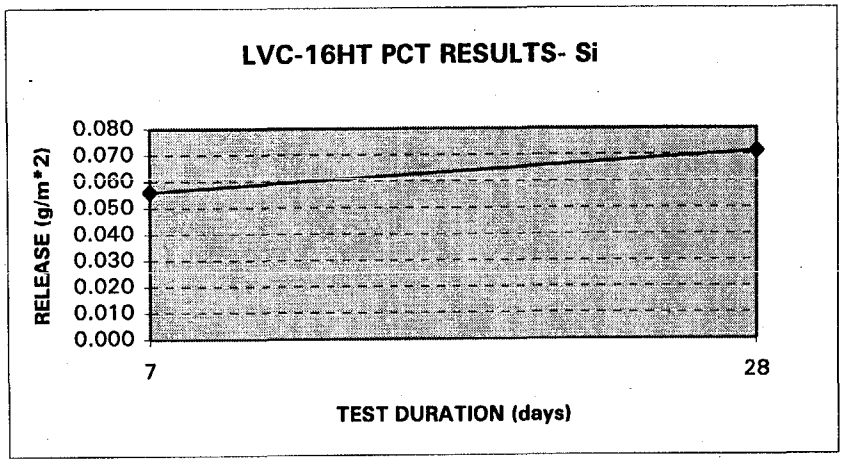

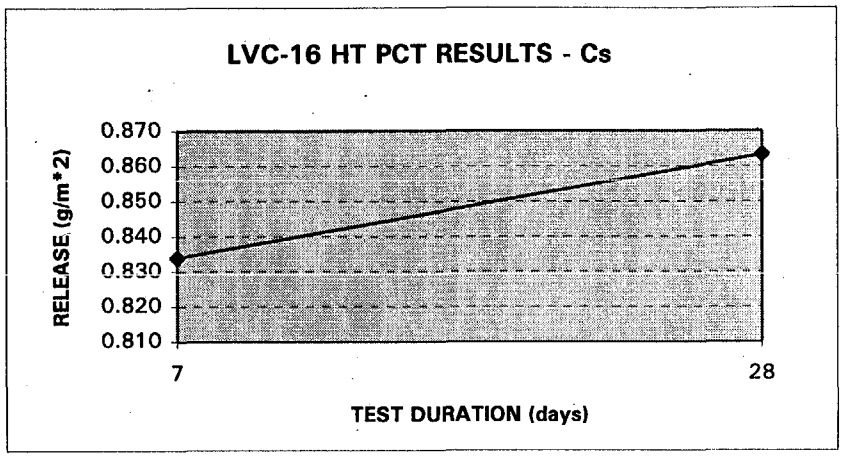

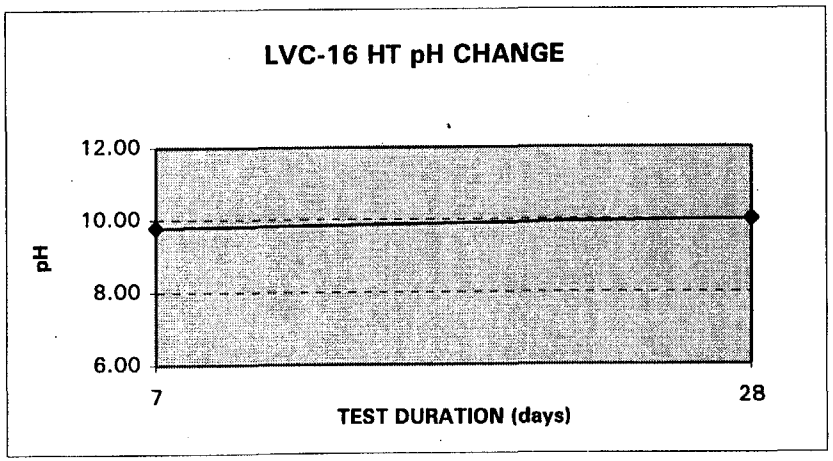

Figure 3.30b. Elemental Releases (g/m^2) of LVC-16HT from PCT

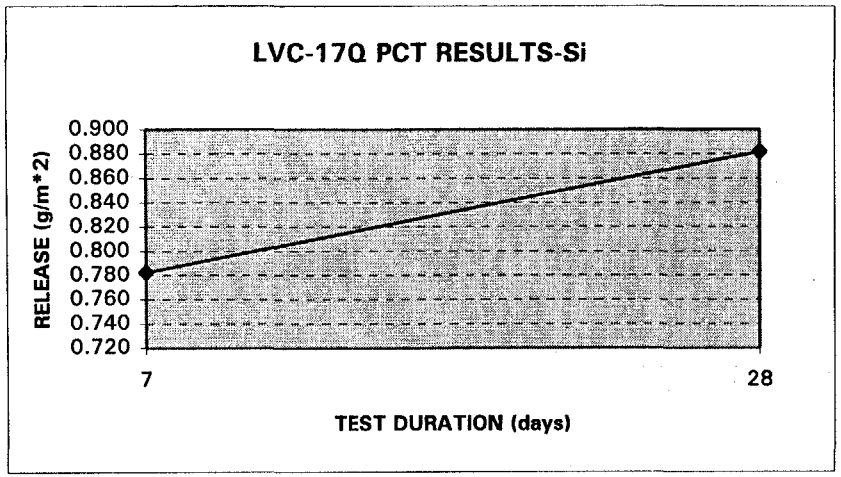

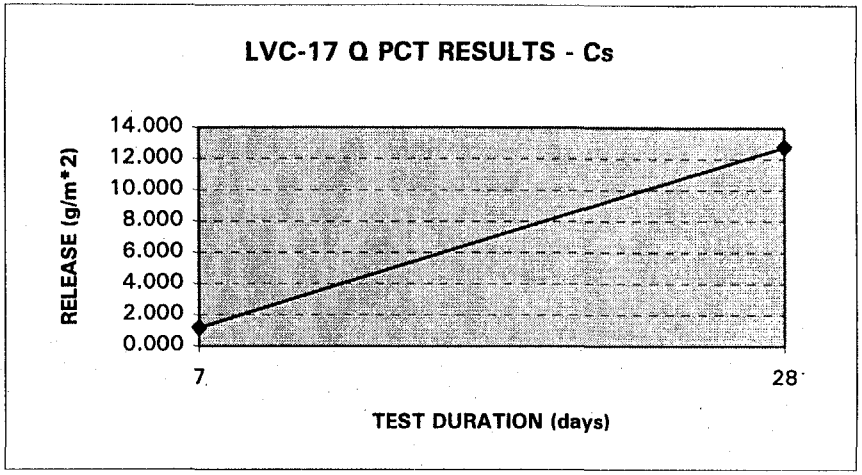

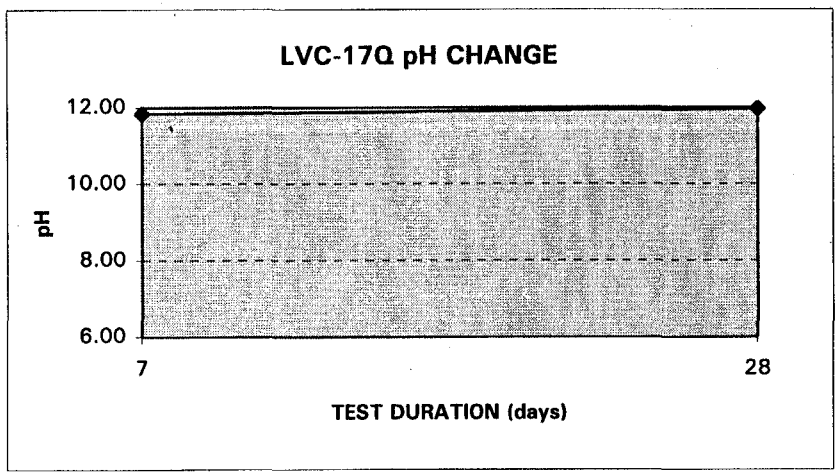

Figure 3.31a. Elemental Releases (g/m^2) of LVC-17Q from PCT

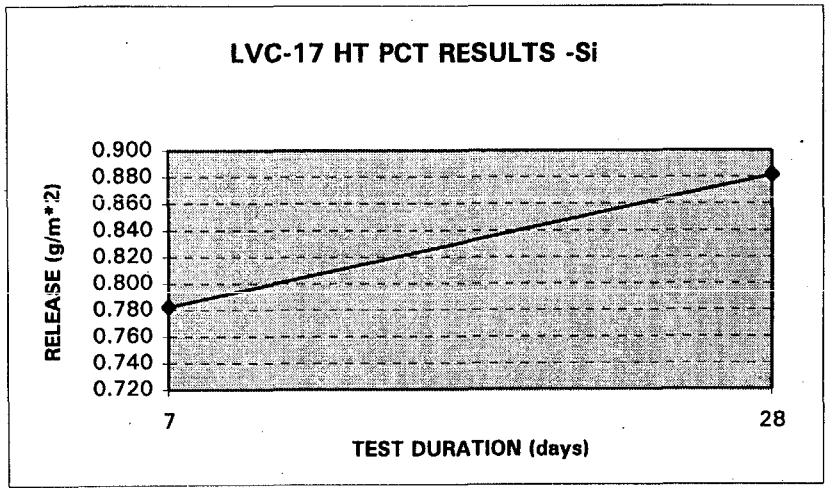

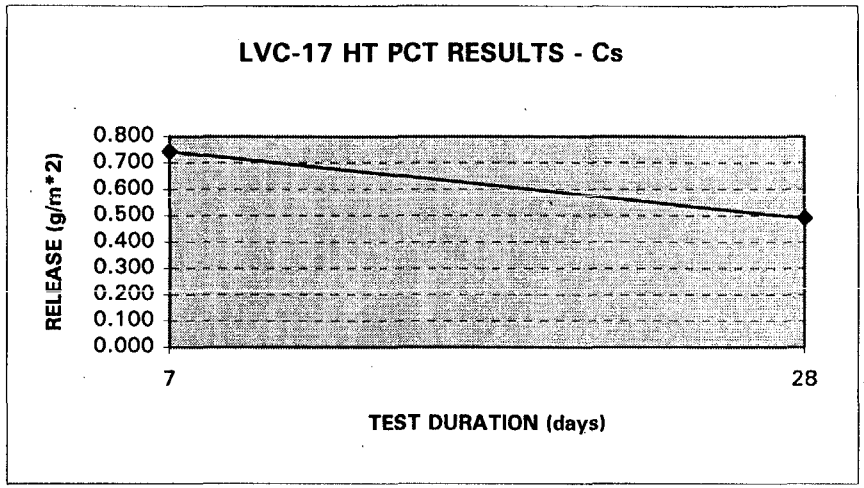

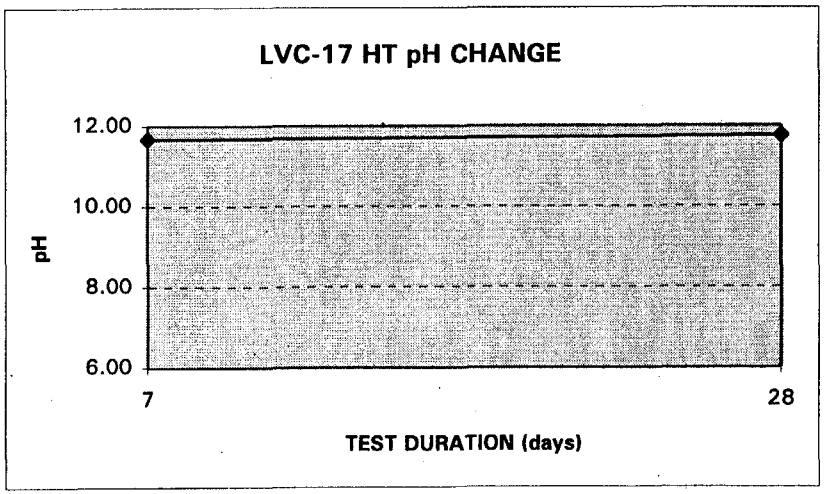

Figure 3.31b. Elemental Releases (g/m^2) of LVC-17HT from PCT

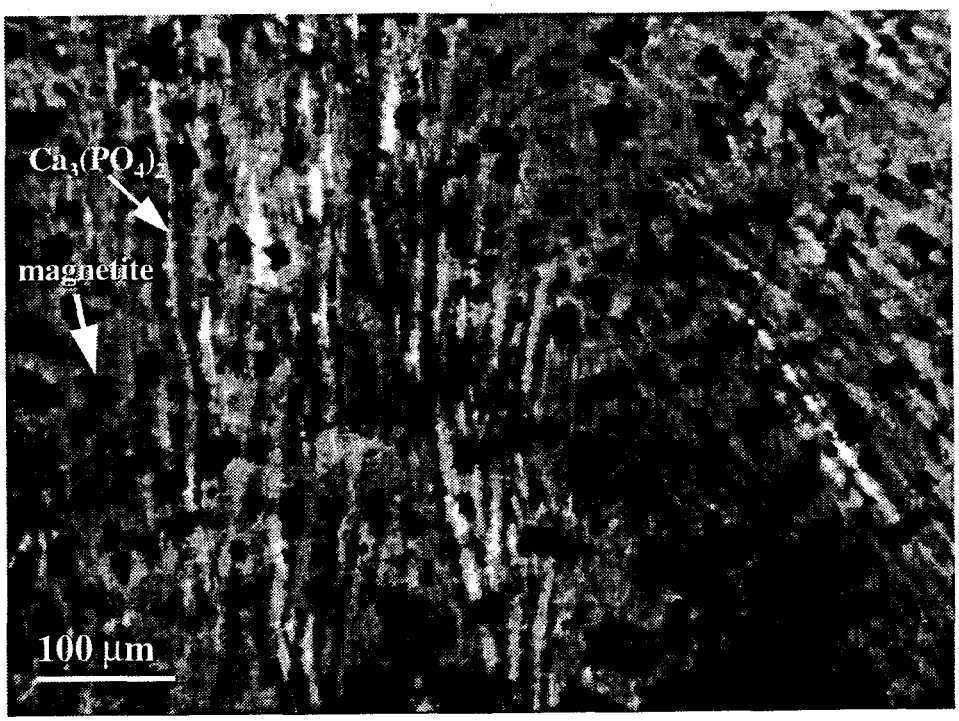

Figure 3.32. Optical Photos for the Microstructure of LVC-5.
(a) Opaque phase is spinel,
(b) Is the enlarged image of Figure 3.32a.

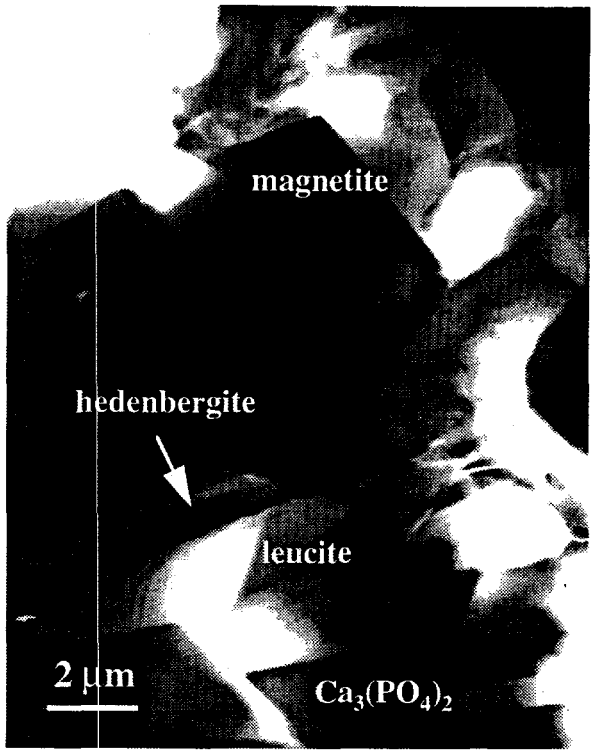

Figure 3.33. TEM Bright Field Images of LVC-5.
(a) Pyroxene, (b) Orthoclase,
(c) Ca_3PO_4, (d) Spinel, and
(e) Plagioclase.

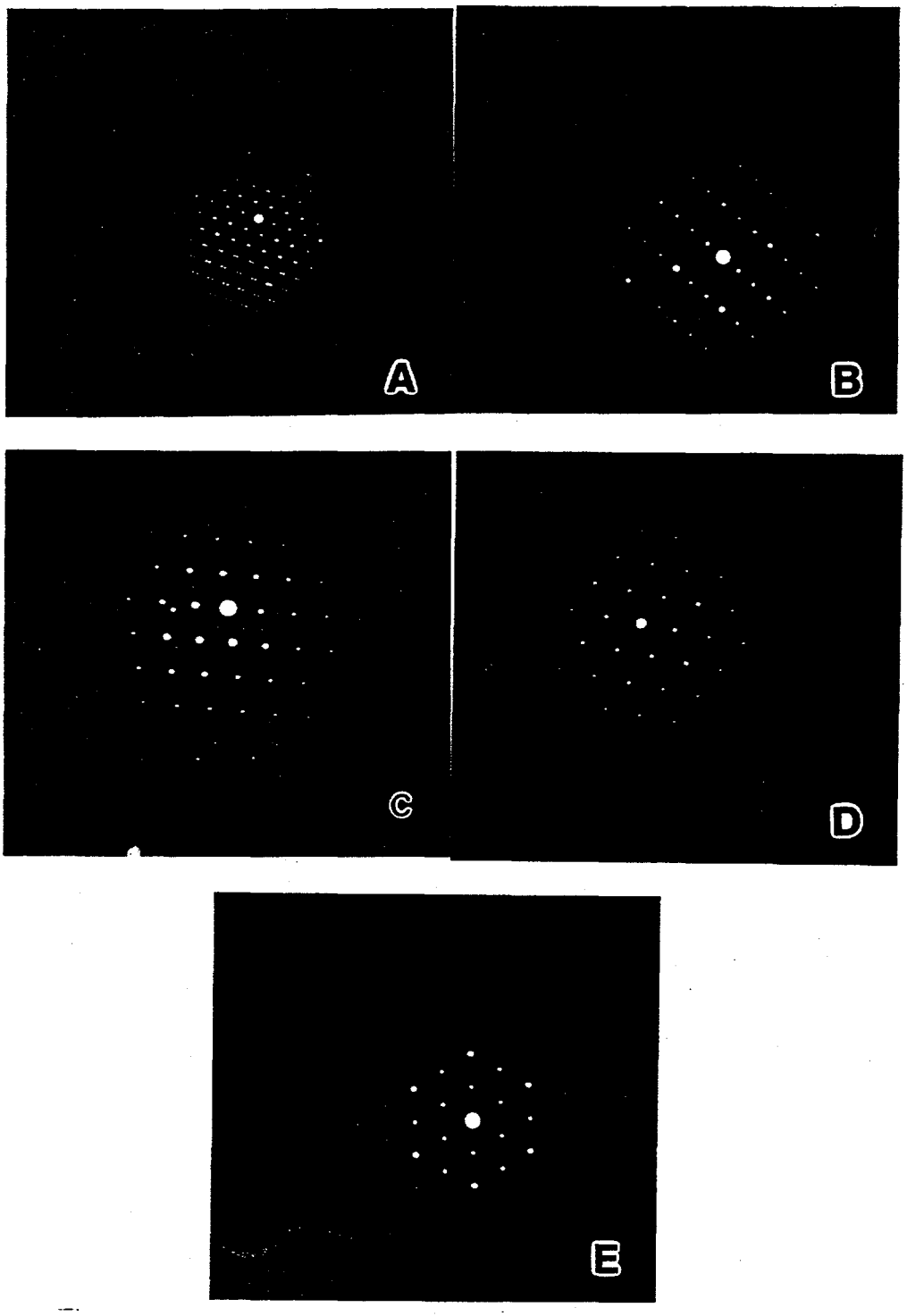

Figure 3.34. SAD Data of Individual Phases from LVC-5. (a) Ca-P phase, (b) Orthoclase, (c) Plagioclase, (d) Pyroxene, (e) Spinel.

Top

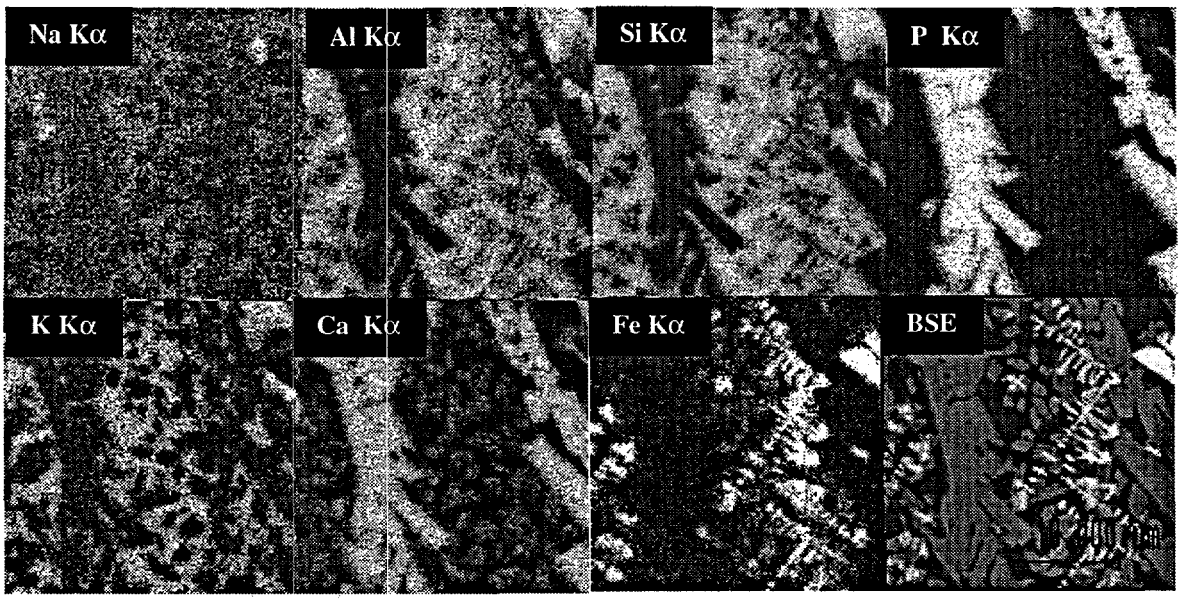

Bottom

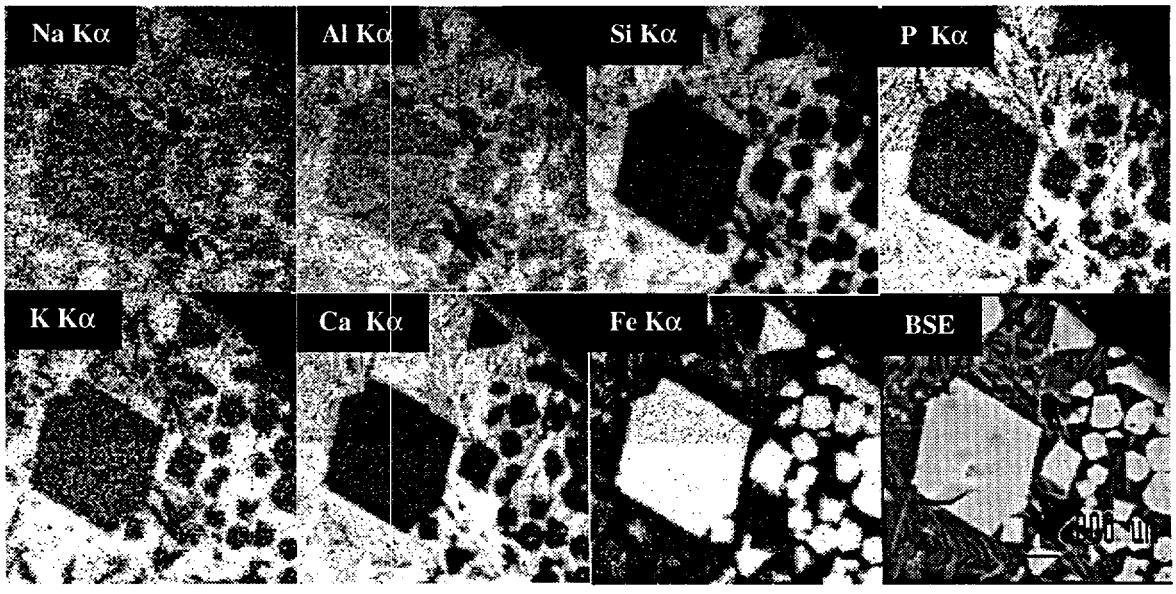

Figure 3.35. X-Ray Mapping and Backscattering Electron Imaging of a Sample from the Top and Bottom of the Melt of LVC-5

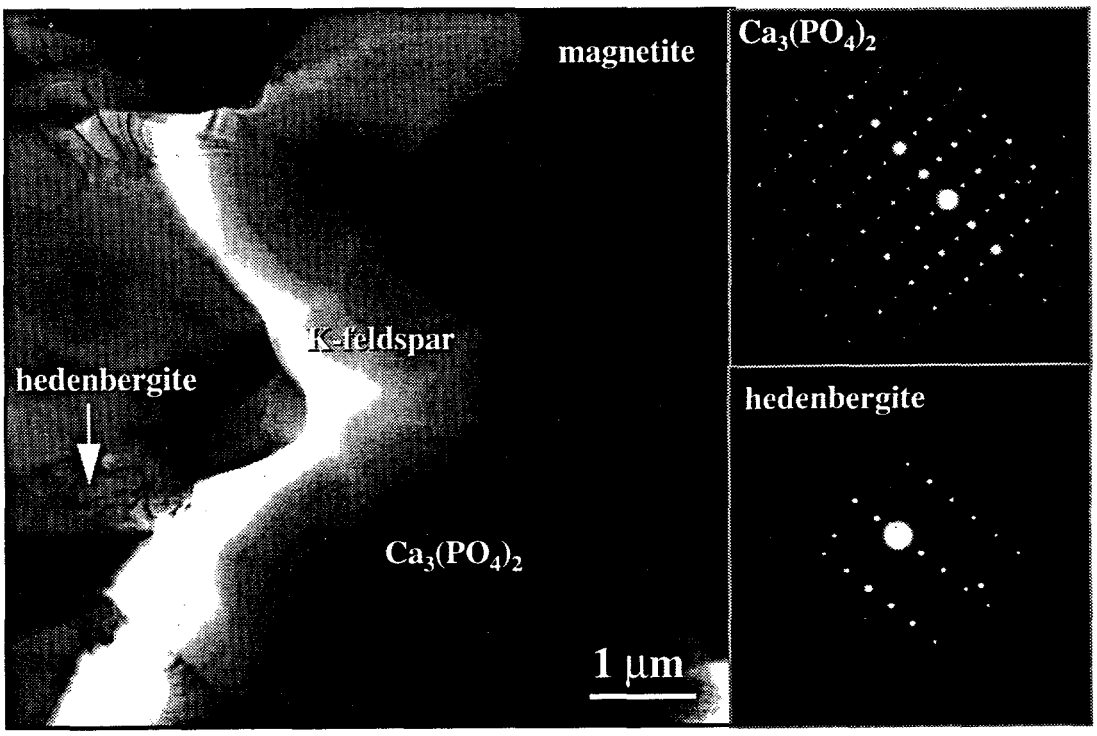

Figure 3.36. TEM Micrograph of (a) K-Feldspar, (b) Ca-P Phase, (c) Spinel, (d) Hedenbergite. The top-right insert is the SAD pattern from the Ca-P phase and the bottom-right insert is the SAD from hedenbergite.

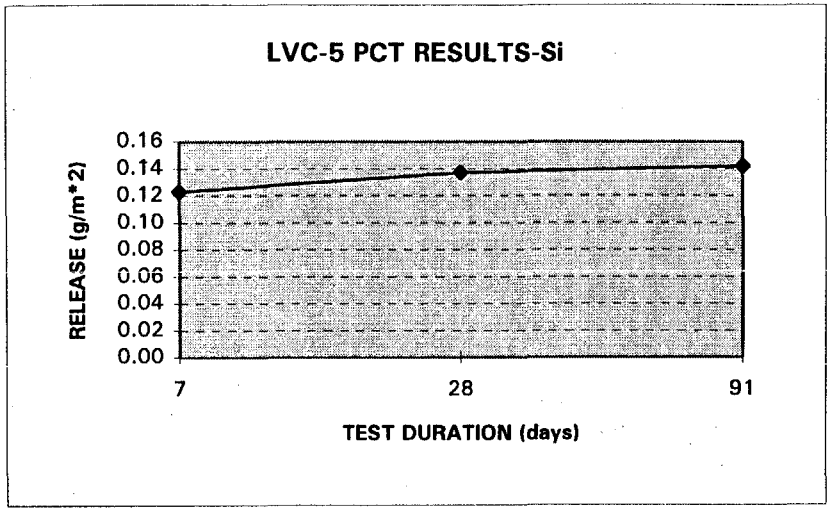

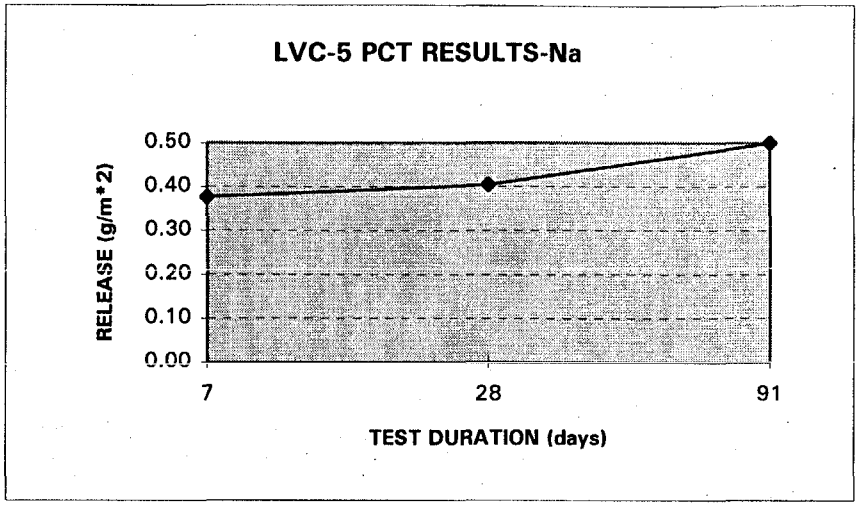

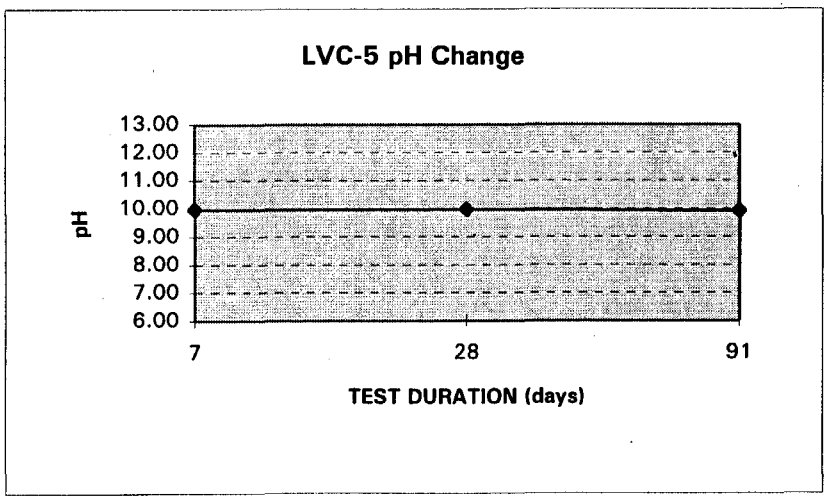

Figure 3.37. Elemental Releases (g/m^2) of LVC-5 from PCT

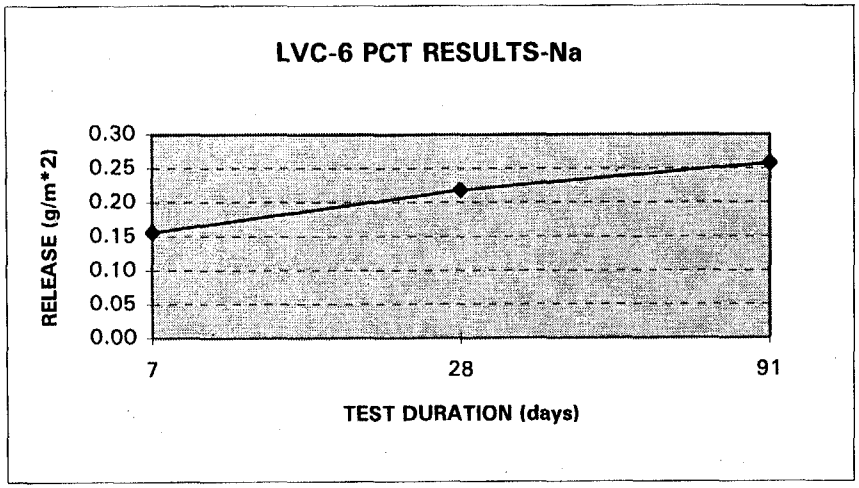

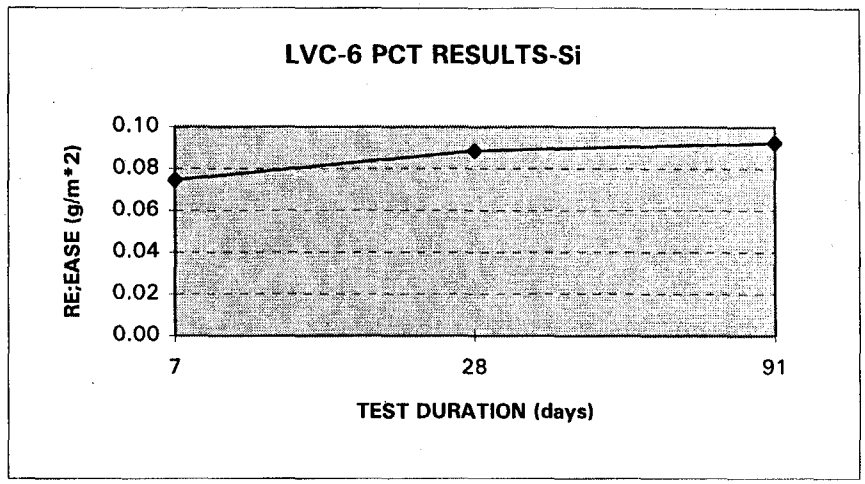

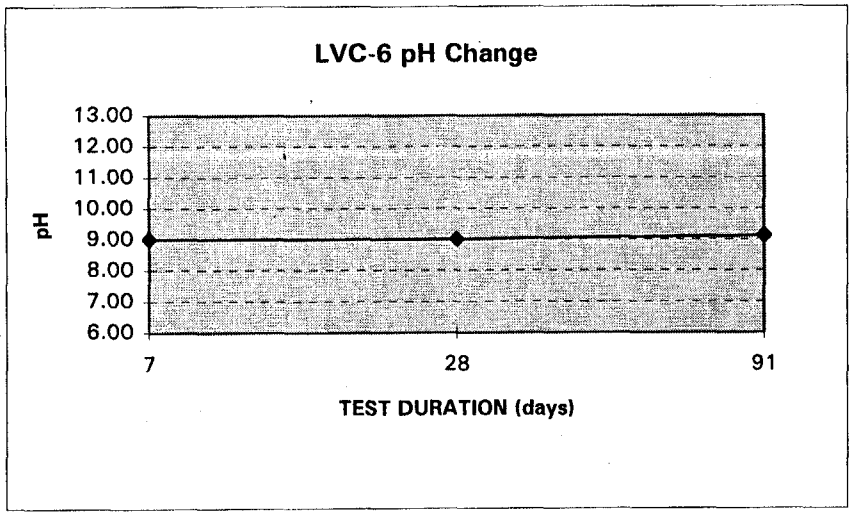

Figure 3.38. Elemental Releases (g/m^2) of LVC-6 from PCT

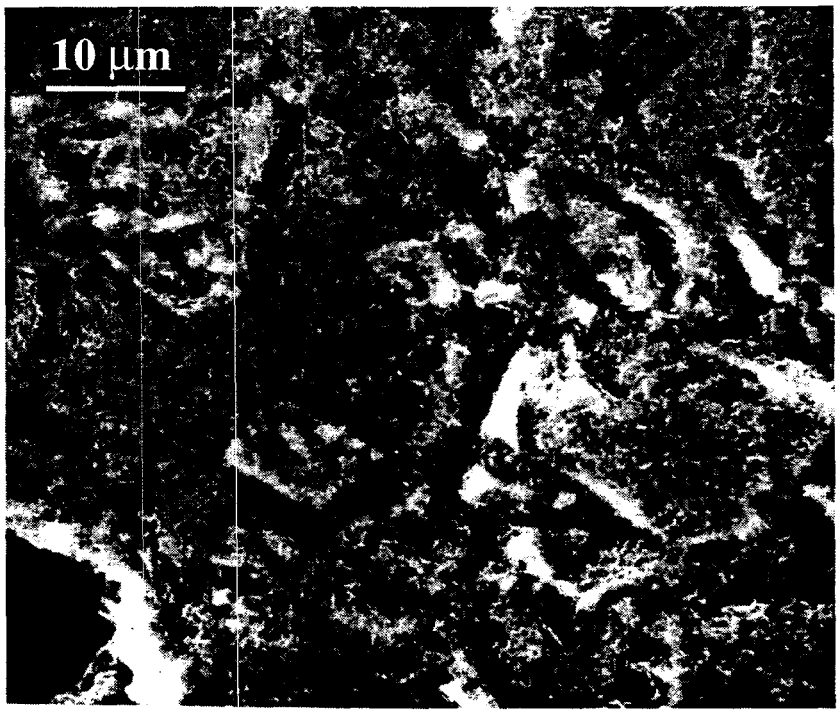

Figure 3.39. SEM Micrograph Showing a Thin "Webby" Clay Layer on the Surface of LVC-5 After Vapor Hydration Testing for 28 Days at 150°C

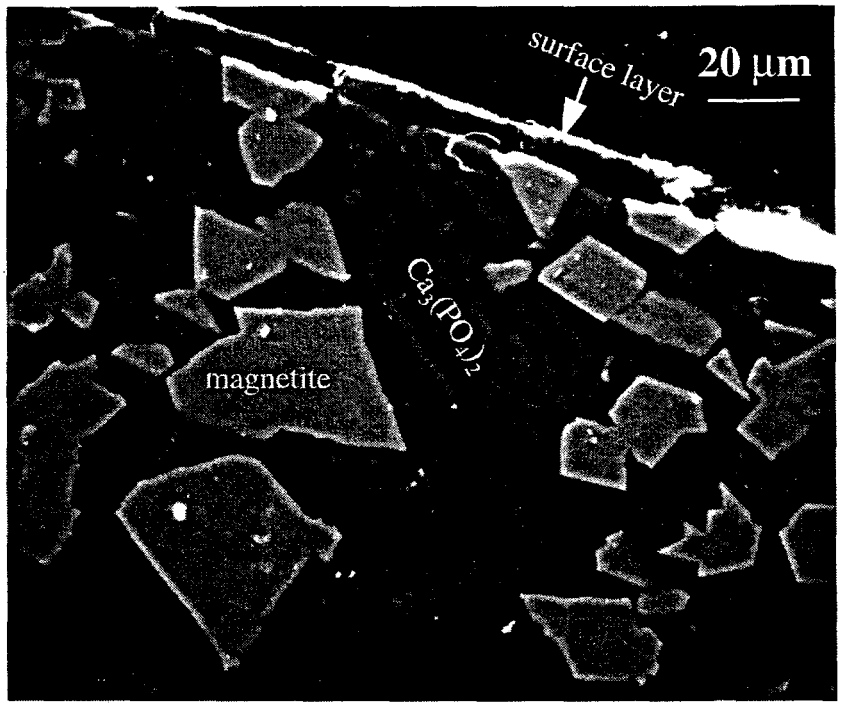

Figure 3.40. A Cross-Sectional SEM Micrograph Showing the Microstructure of the Surface Layer and the Unaltered Zone of LVC-5 After Vapor Hydration Testing.

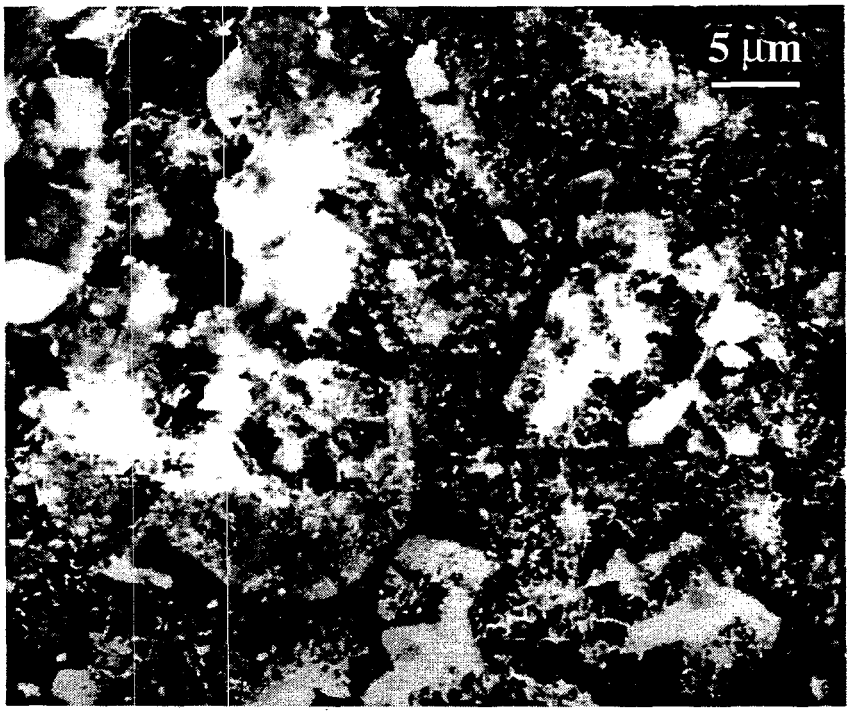

Figure 3.41. SEM Micrograph Showing That Reacted LVC-6 was Covered by a Thin "Webby" Layer of Alteration Products

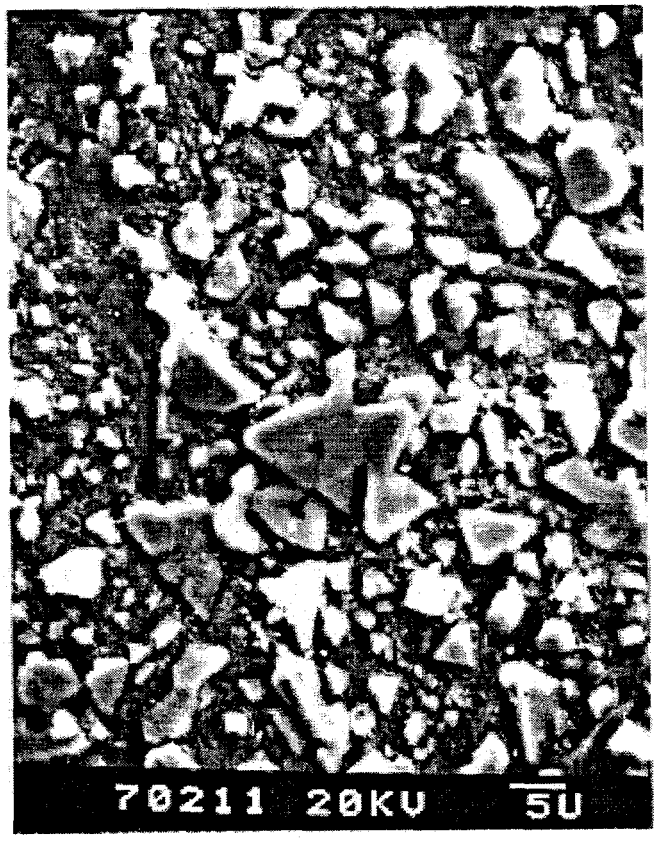

Figure 3.42. SEM Micrograph Showing the Corroded LVC-6 with the Spinel Phase Protruding from the Surface

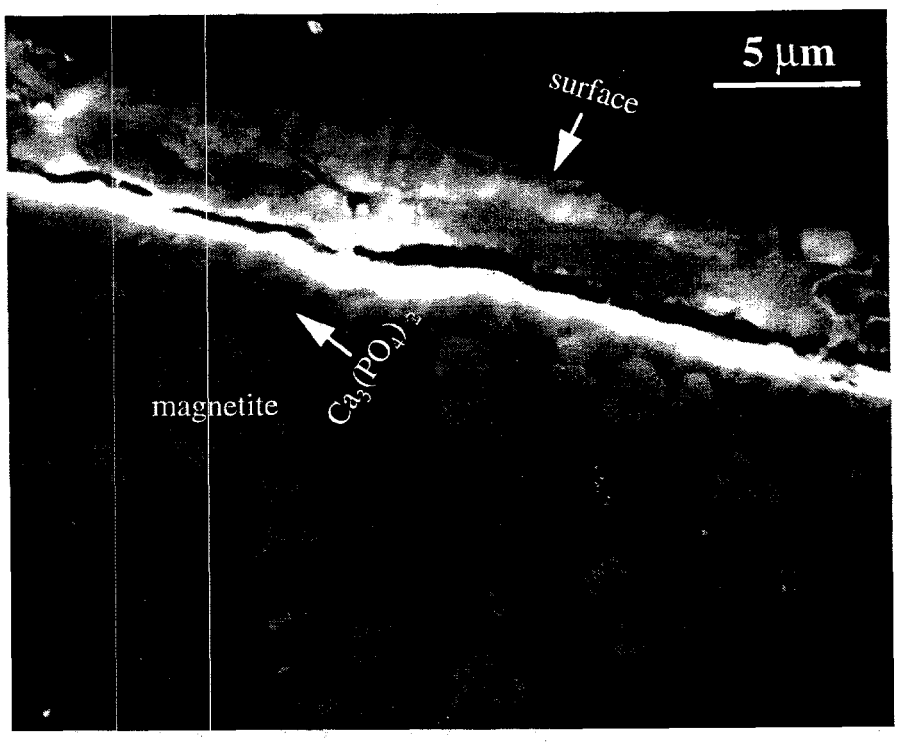

Figure 3.43. Cross-Sectional SEM Micrographs of LVC-6 After Vapor Hydration Testing, Showing the Protrusion of the Spinel Phase

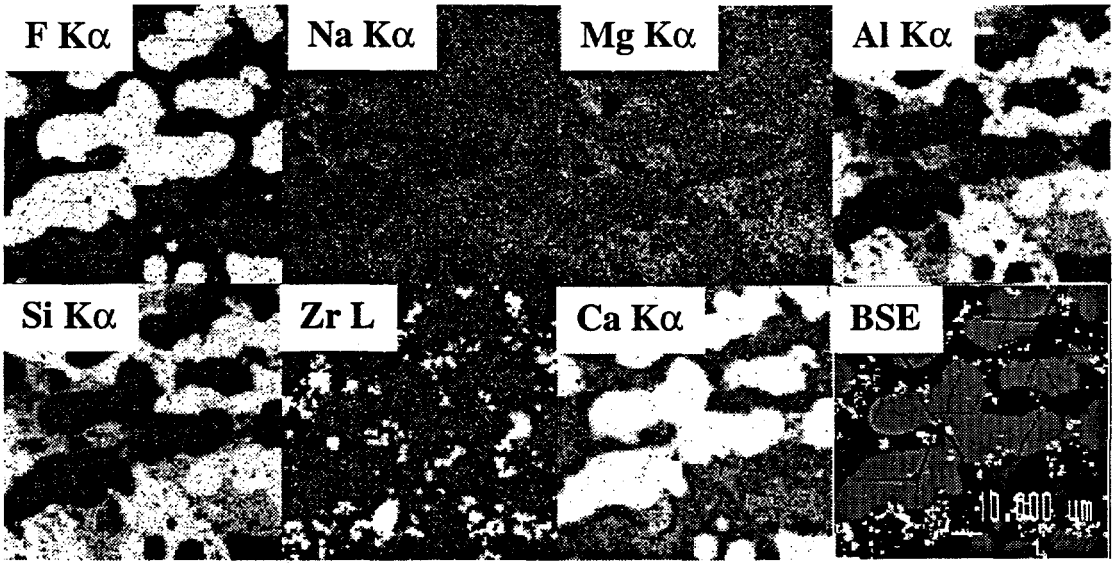

Figure 3.44. X-Ray Mapping and Backscattered Electron Image of LVC-7

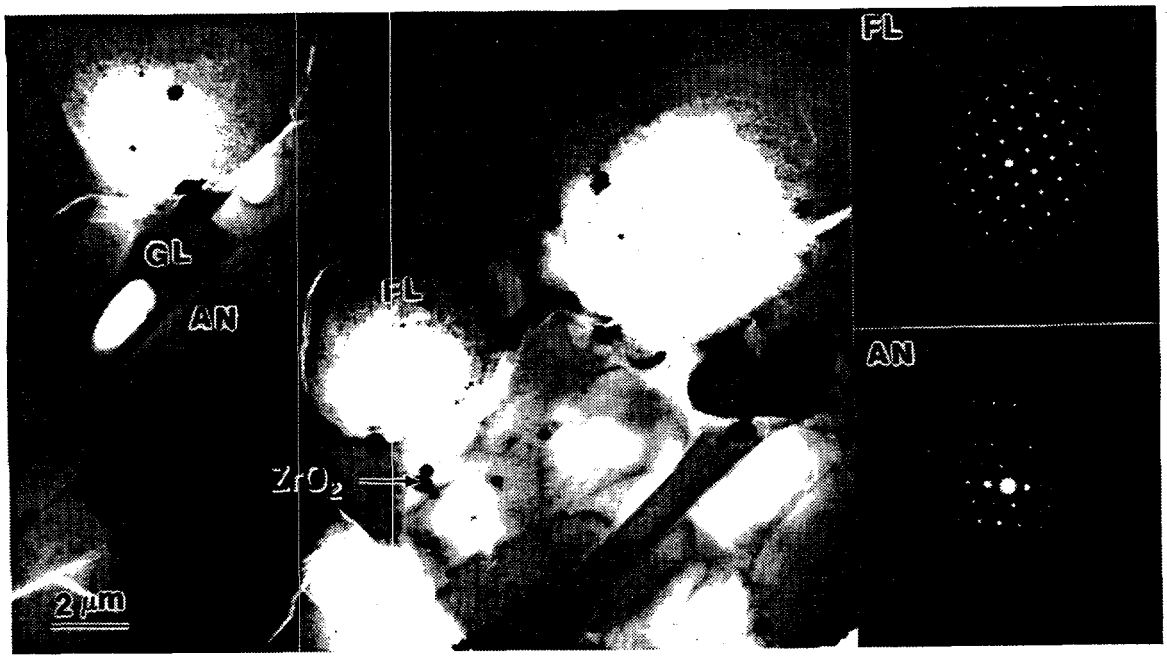

Figure 3.45. Typical Micrograph of LVC-7 Showing Four Major Phases: GL - Glassy Phase, An - Anorthite FL - Fluorite. The arrow points to baddeleyite.

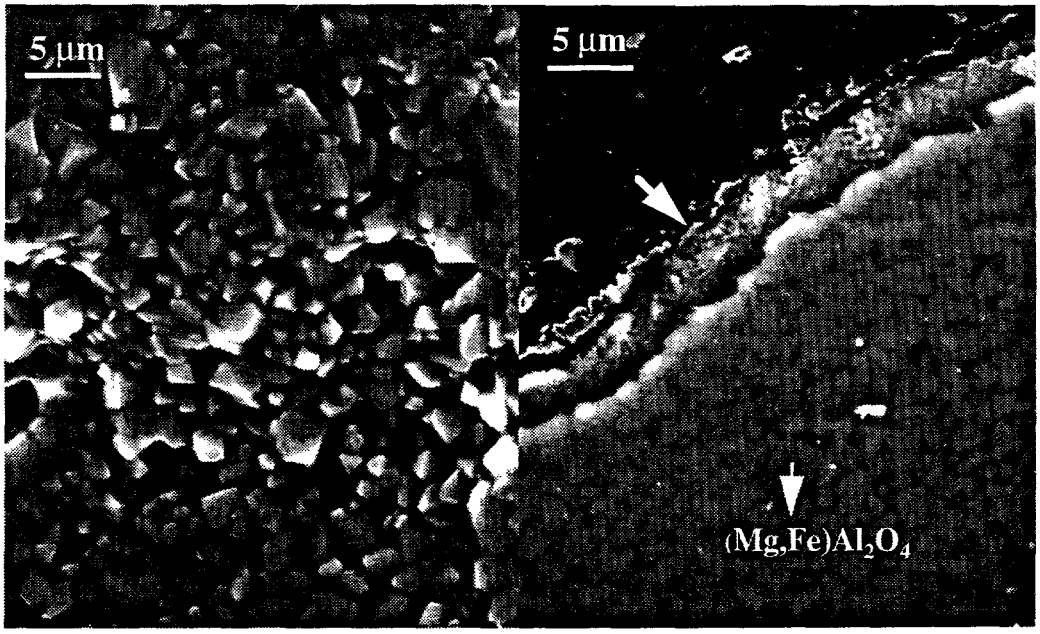

Figure 3.46. SEM of LVC-8. (a) Spinel suspended in a glassy matrix, (b) The cross-section of the altered surface layer.

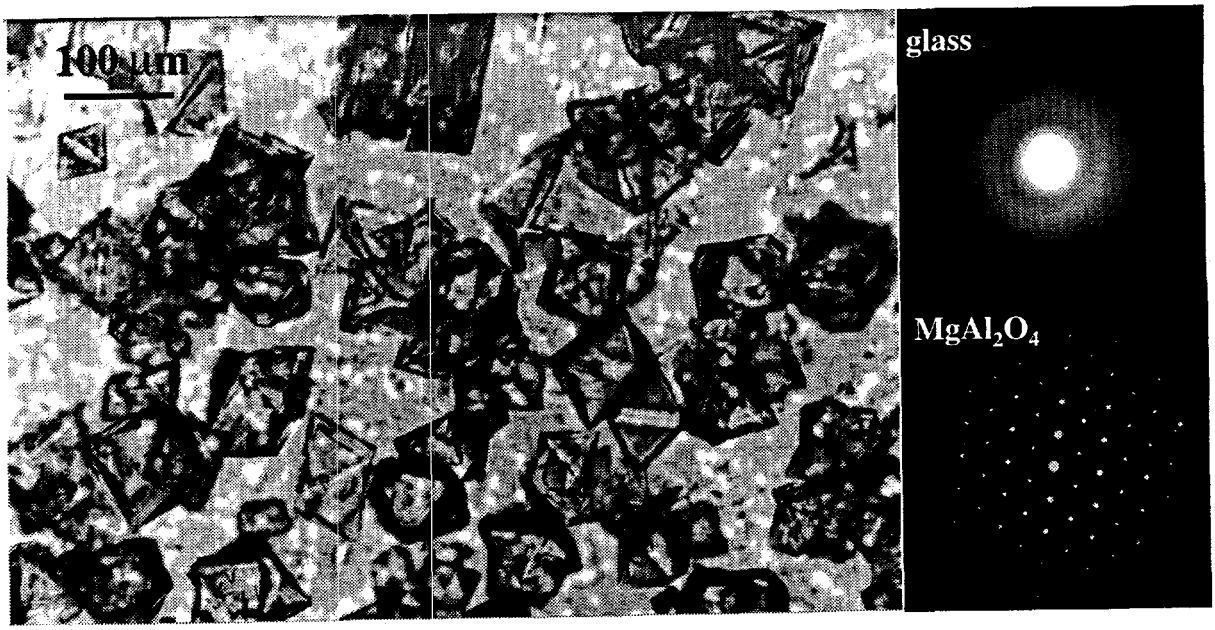

Figure 3.47. Optical Micrographs of the Top Part of the LVC-9 Sample. SAD of spinel is shown on the left and on the right is the glassy matrix SAD.

Figure 3.48. Optical Micrograph of the Bottom Part of LVC-9

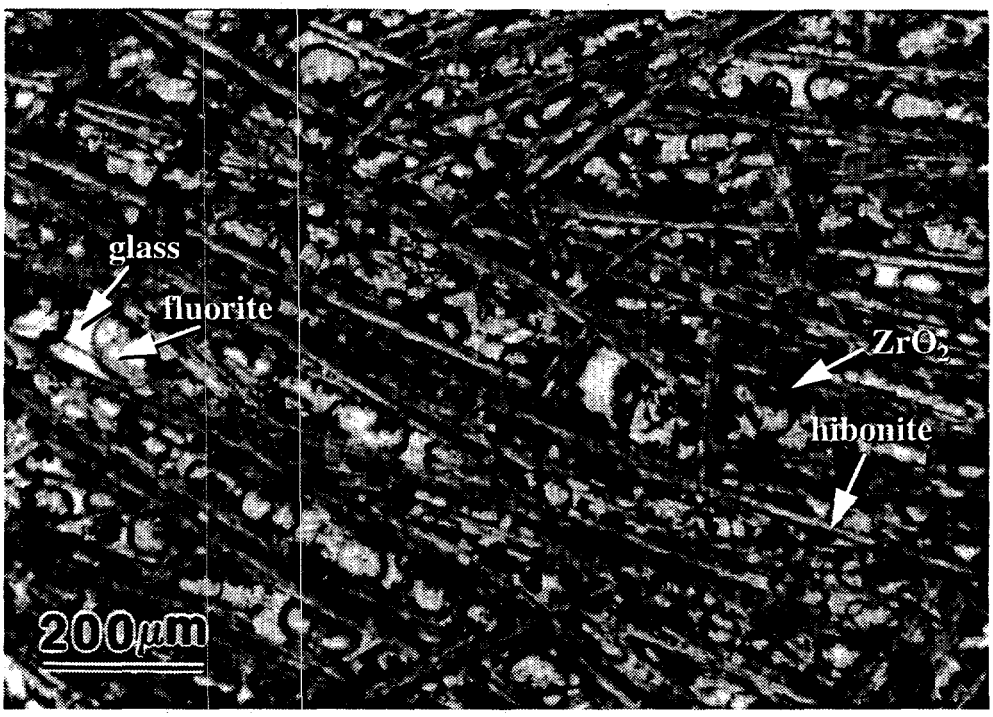

Figure 3.49. Optical Micrograph of LVC-14 Showing Needle Structures

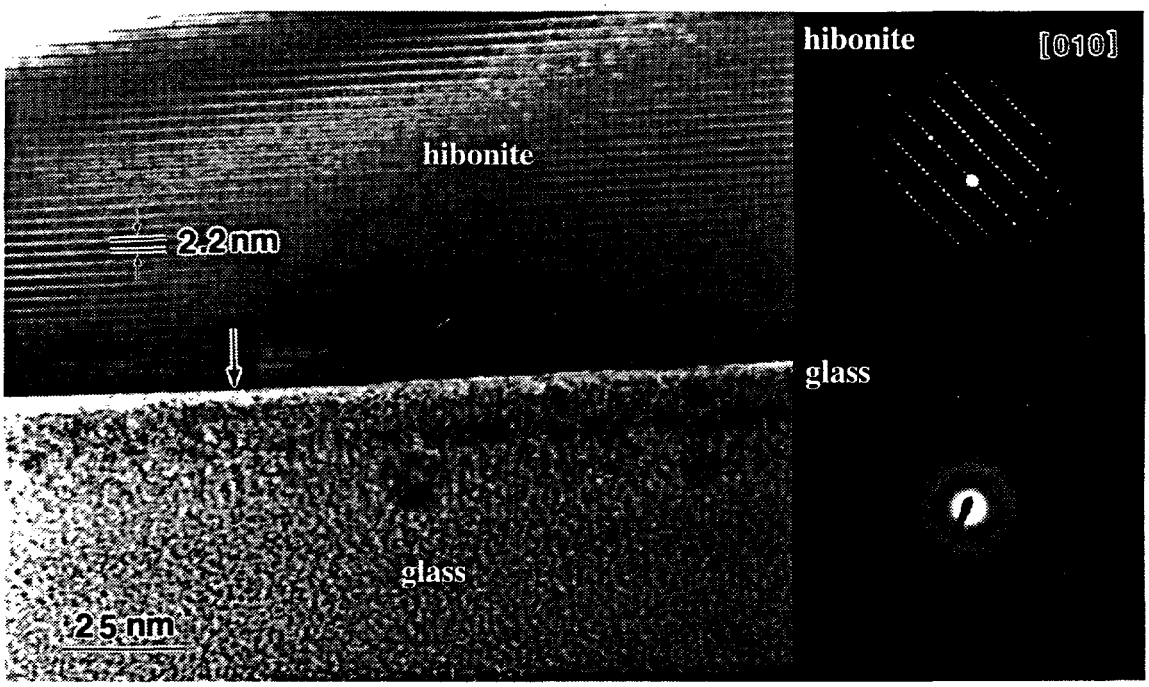

Figure 3.50. The HRTEM Image Showing Lattice Fringes of a Hibonite Crystal in LVC-14. The arrow indicates the interface of hibbonite and the glassy phase.

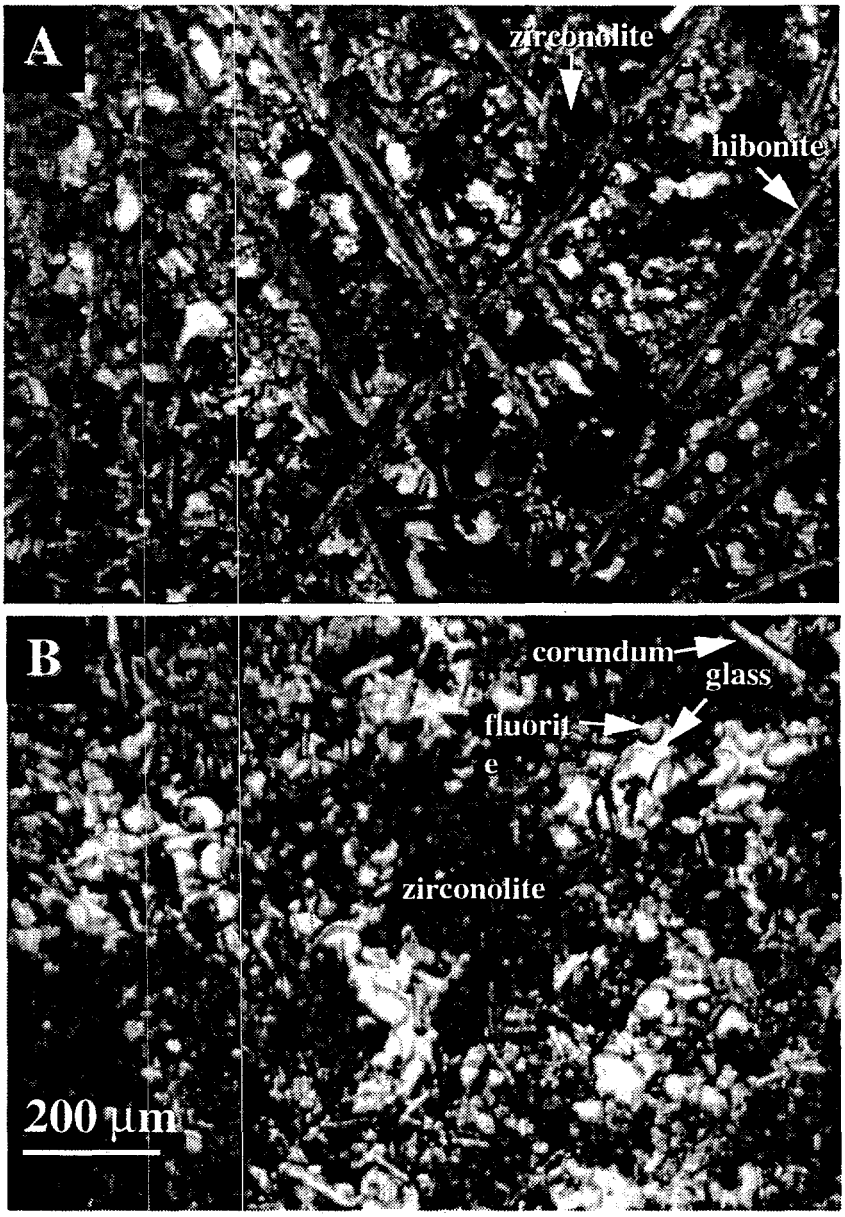

Figure 3.51. Optical Micrograph of LVC-15. (a) Bulk sample; (b) Bottom part of sample.

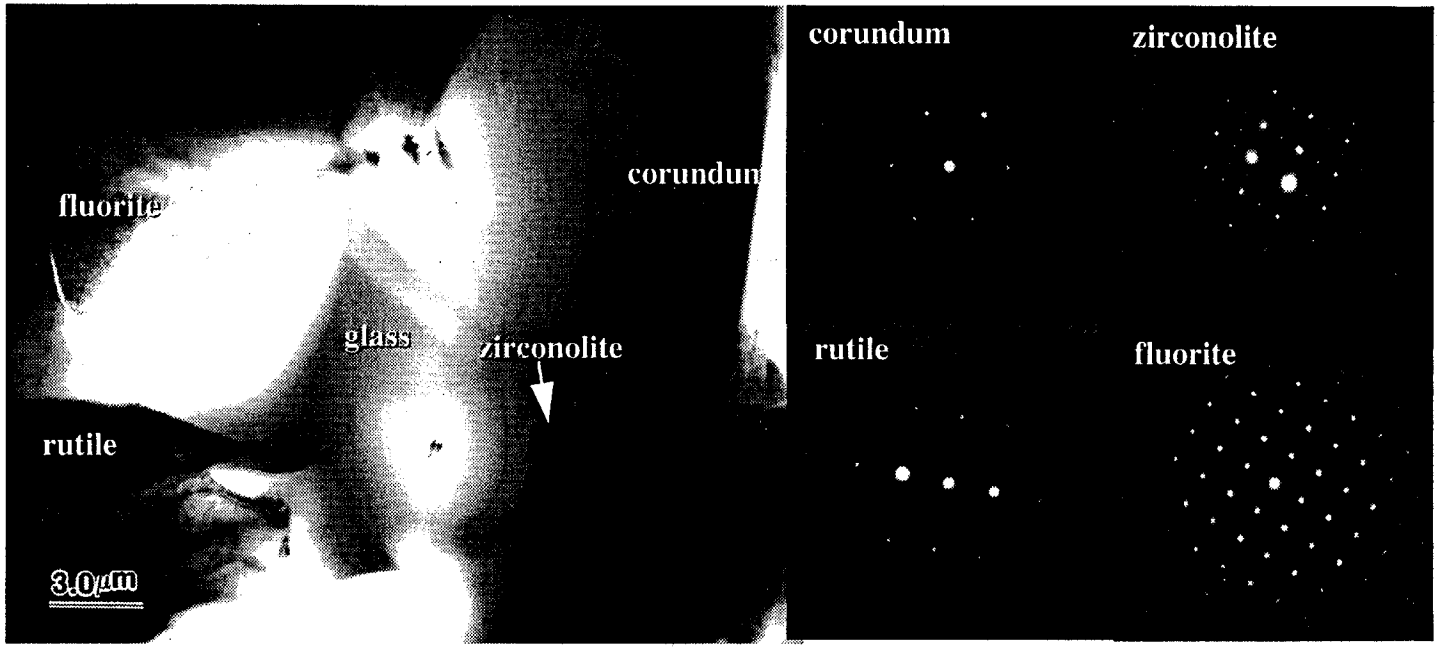

Figure 3.52. Bright Field Image of LVC-15, Showing Five Major Phases: Corrundum (CR), Rutile (Rt), Glass, Fluorite, and Zirconolite (indicated by the arrow).

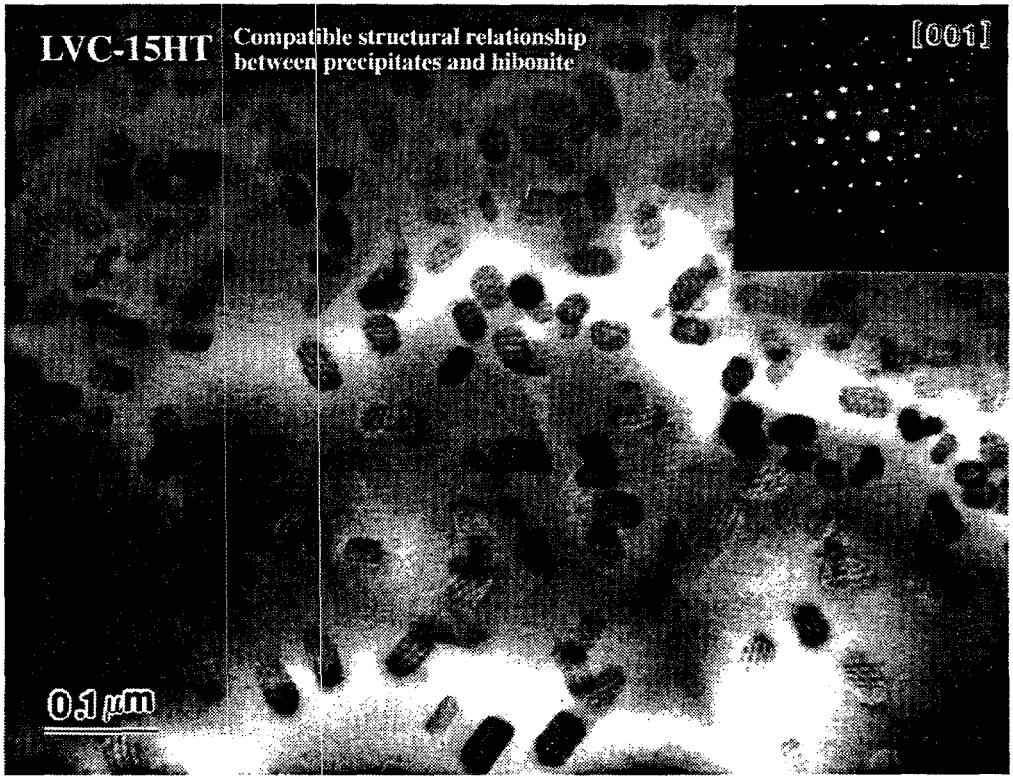

Figure 3.53. The Bright Field Image Shows Small Precipitates in the Hibonite Crystal

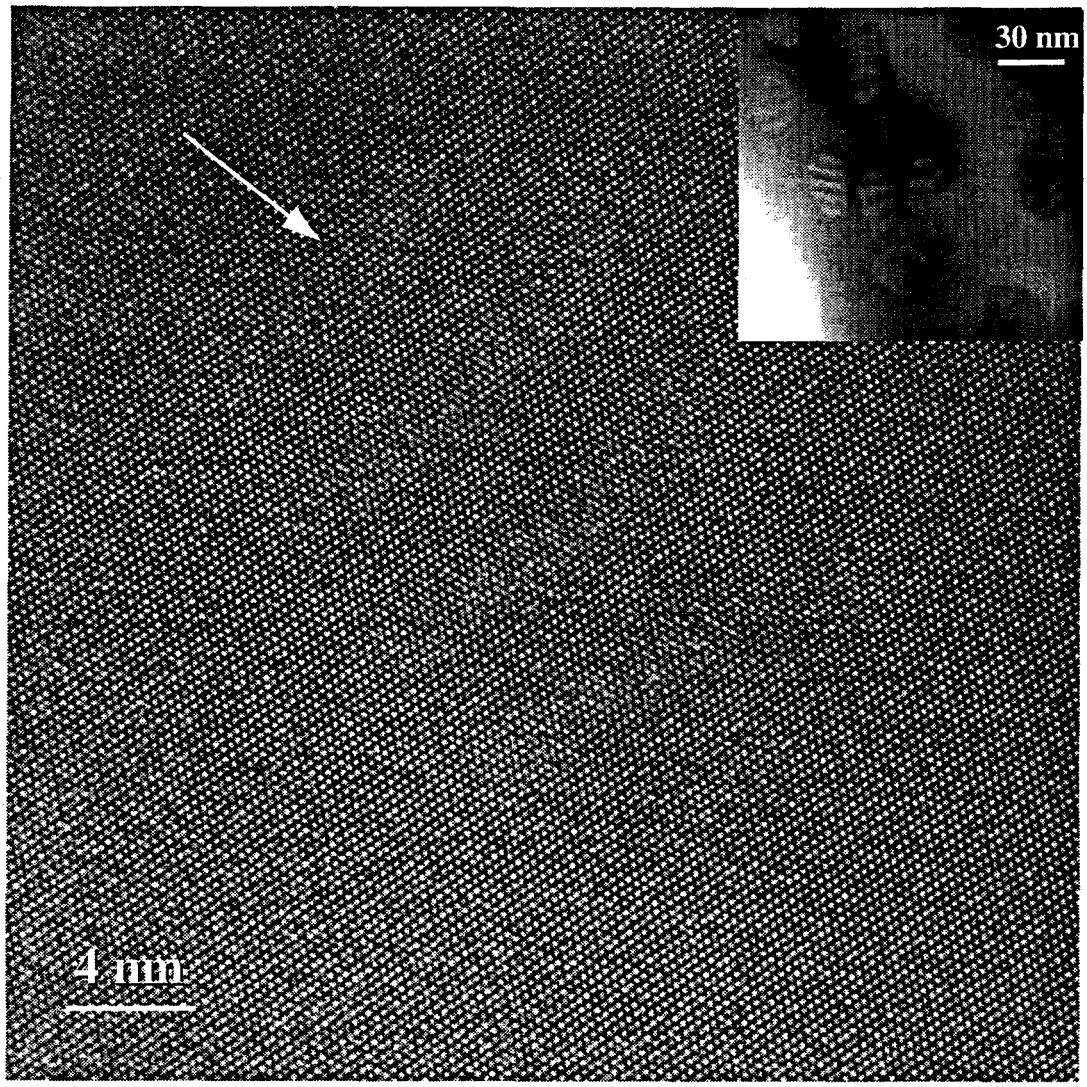

Figure 3.54. The HRTEM Image Showing the Fringes of a Precipitate Within a Hibonite Crystal

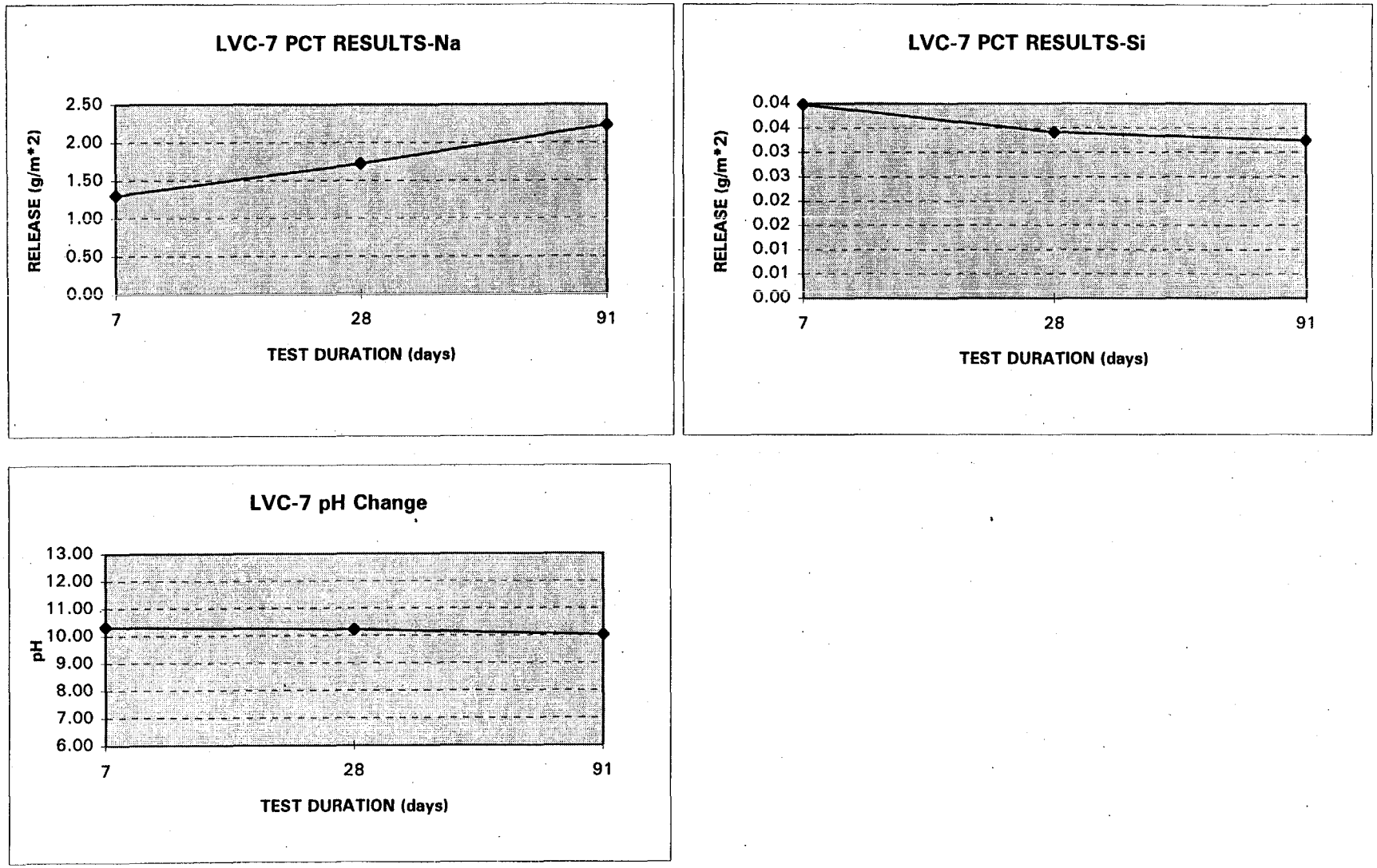

Figure 3.55. Elemental Releases (g/m^2) of LVC-7 from PCT

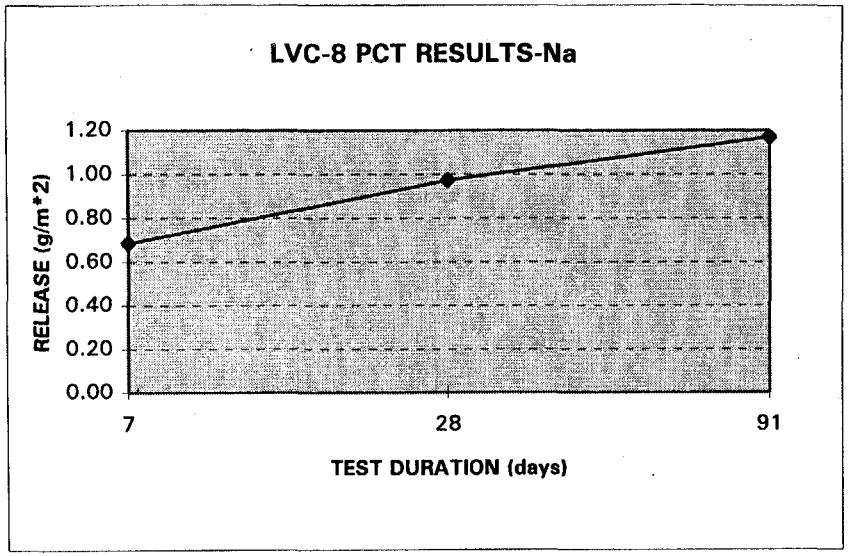

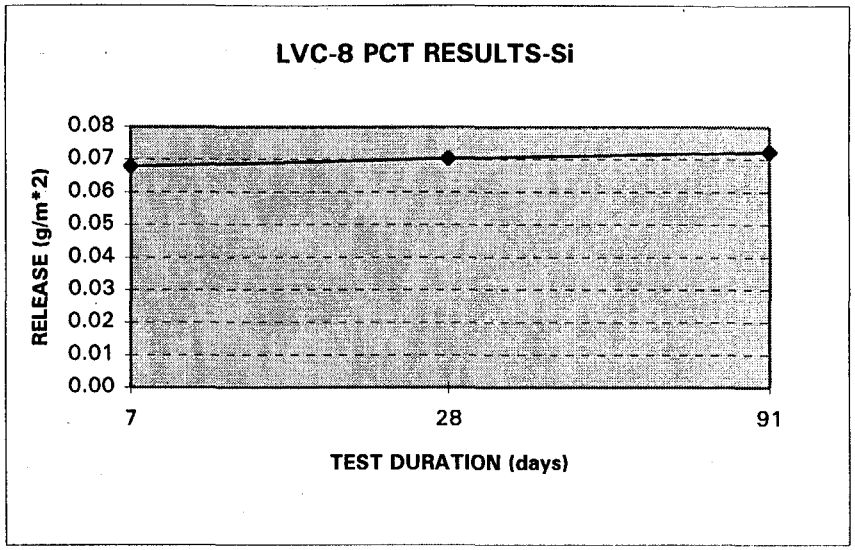

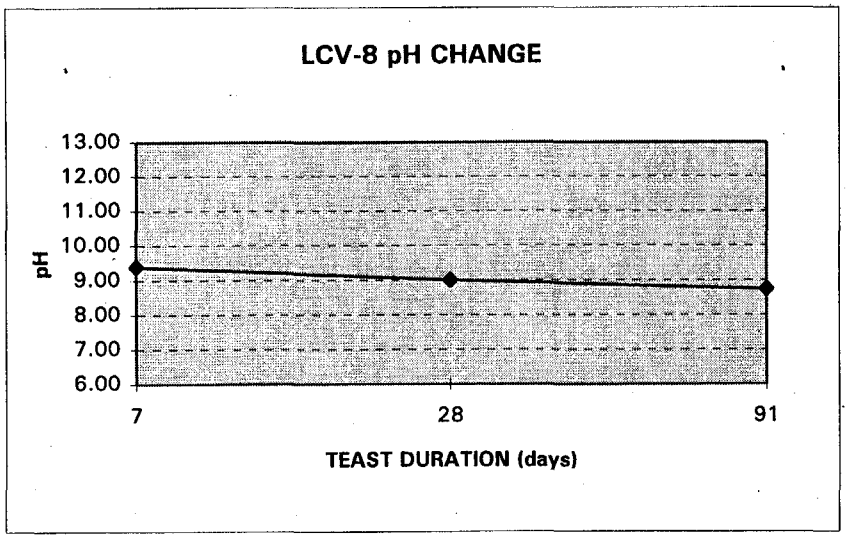

Figure 3.56. Elemental Releases (g/m^2) of LVC-8 from PCT

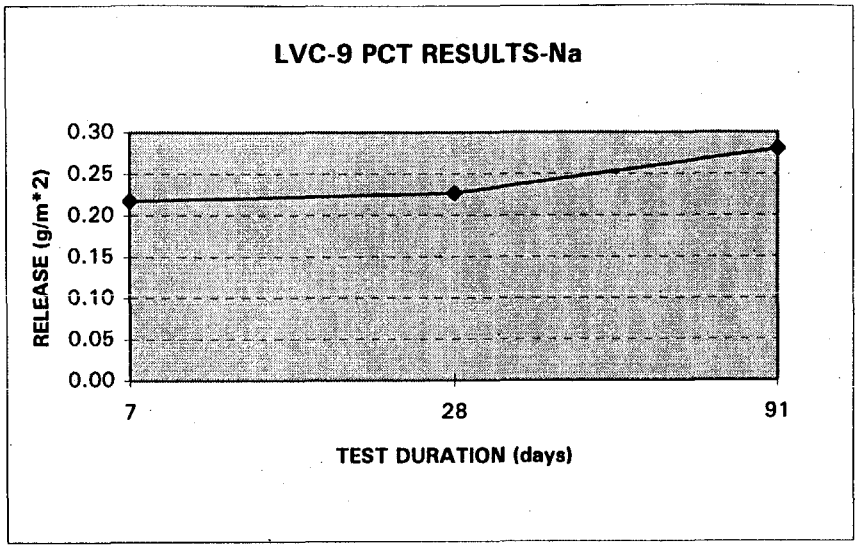

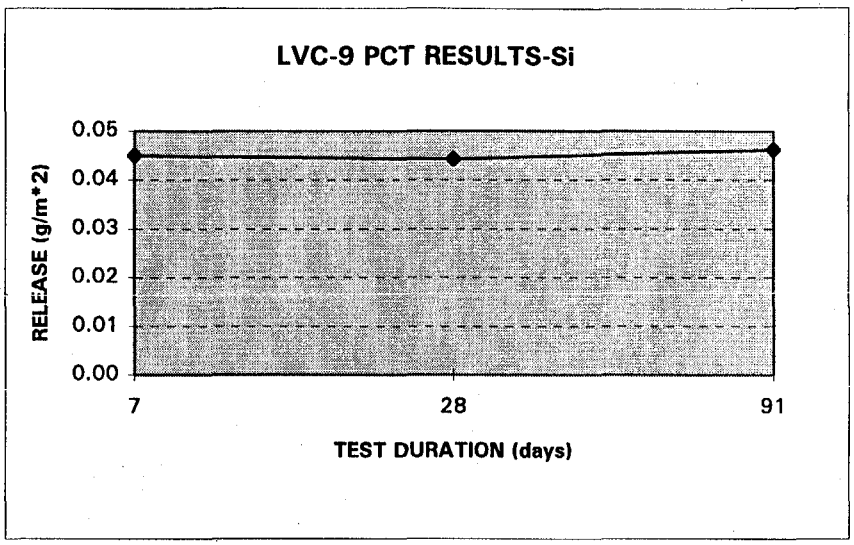

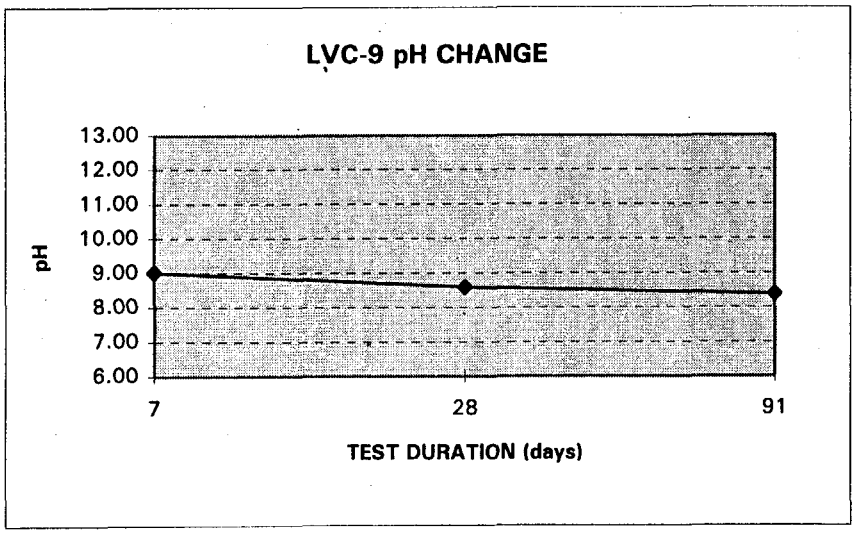

Figure 3.57. Elemental Releases (g/m^2) of LVC-9 from PCT

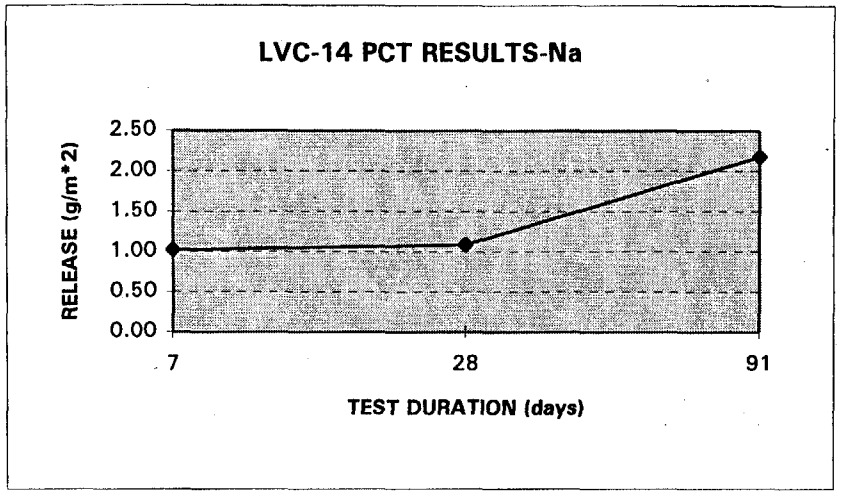

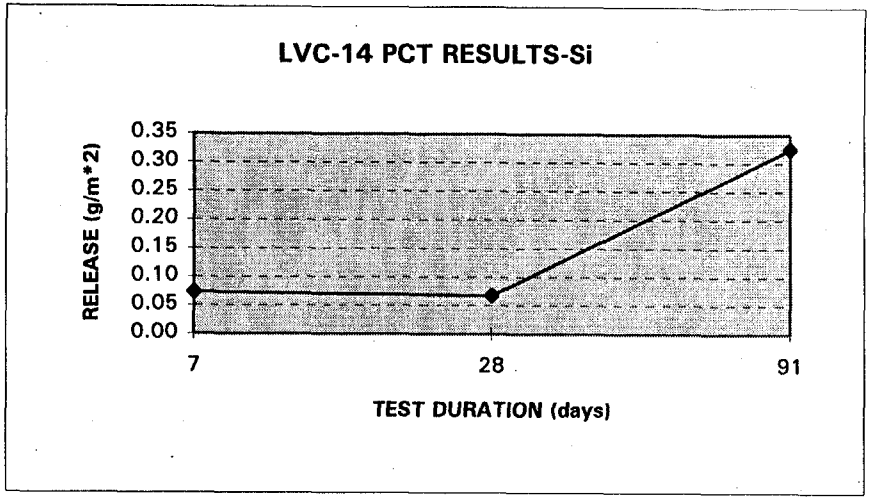

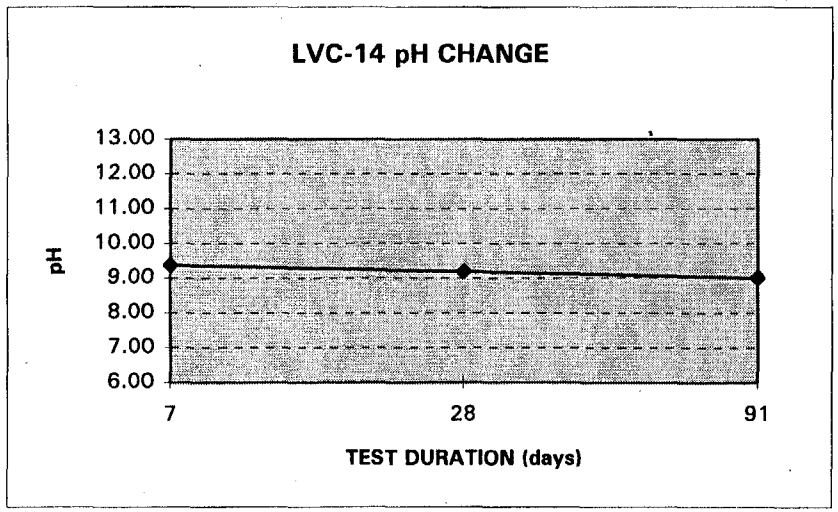

Figure 3.58. Elemental Releases (g/m^2) of LVC-14 from PCT

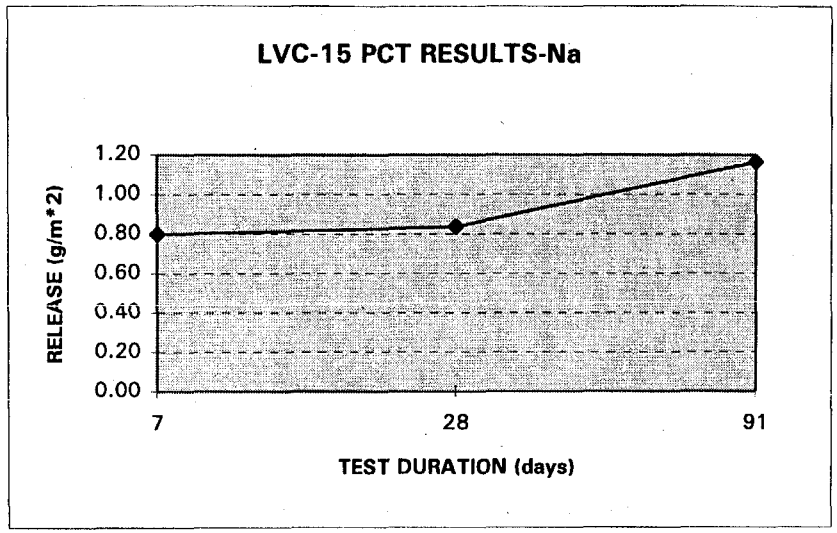

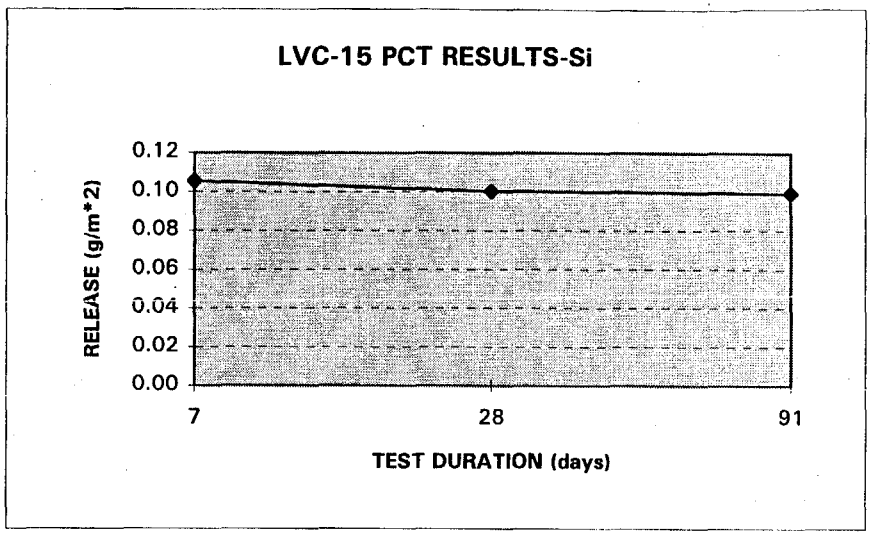

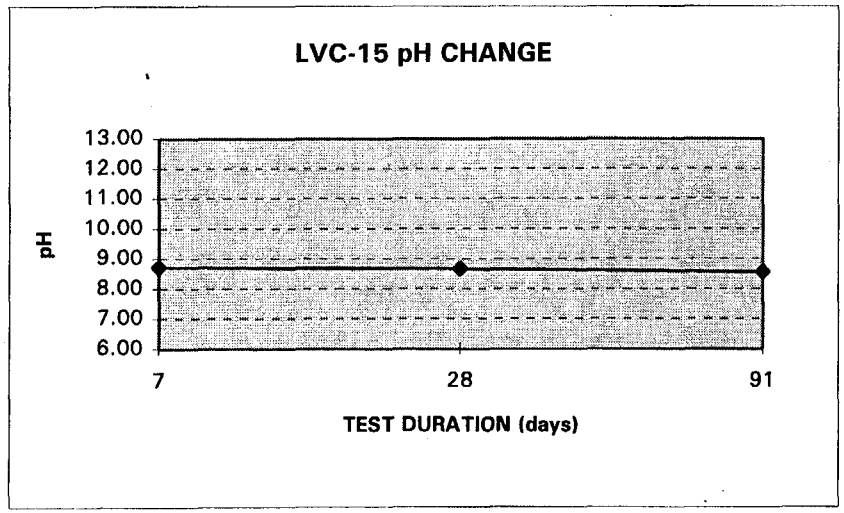

Figure 3.59. Elemental Releases (g/m^2) of LVC-15 from PCT

Figure 3.60. SEM Micrograph Shows a Thin Crust Developed on LVC-7 After Vapor Hydration Testing

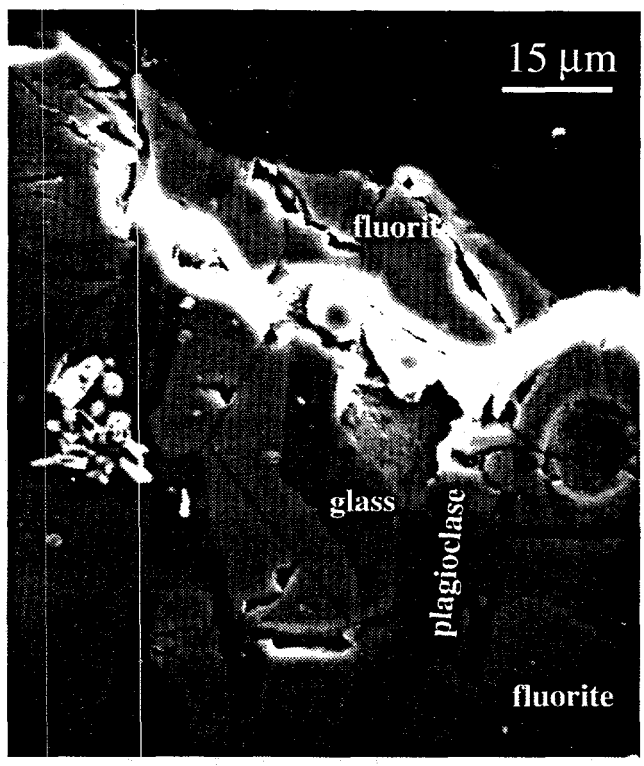

Figure 3.61. Cross-Sectional SEM Micrograph of LVC-7 After Vapor Hydration Testing

Figure 3.62. SEM Micrograph of LVC-9 After Vapor Hydration Testing

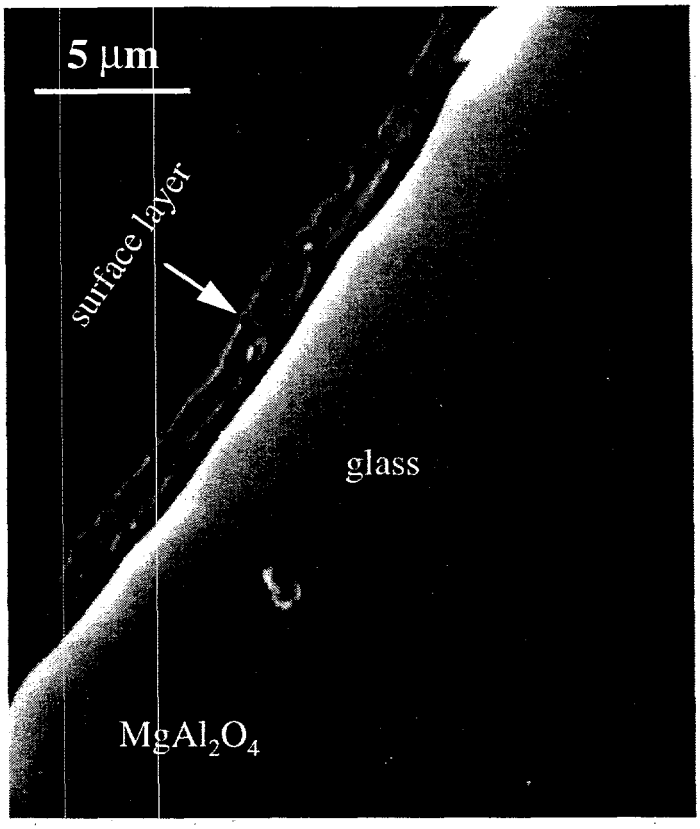

Figure 3.63. SEM Cross-Section of LVC-9 After Vapor Hydration Testing

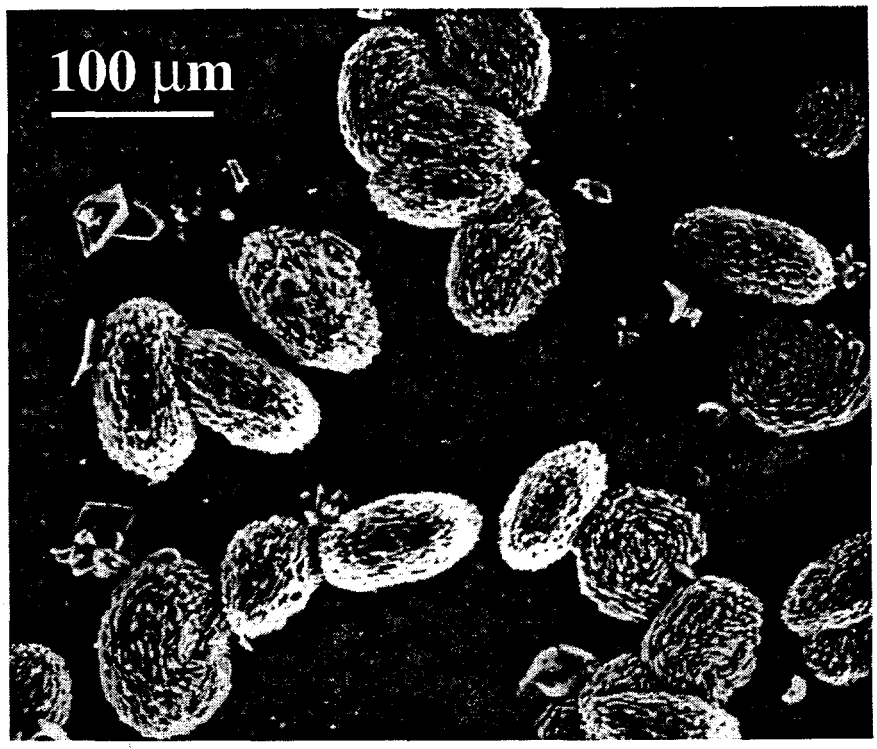

Figure 3.64a. SEM Micrograph of LVC-14 After Vapor Hydration Testing

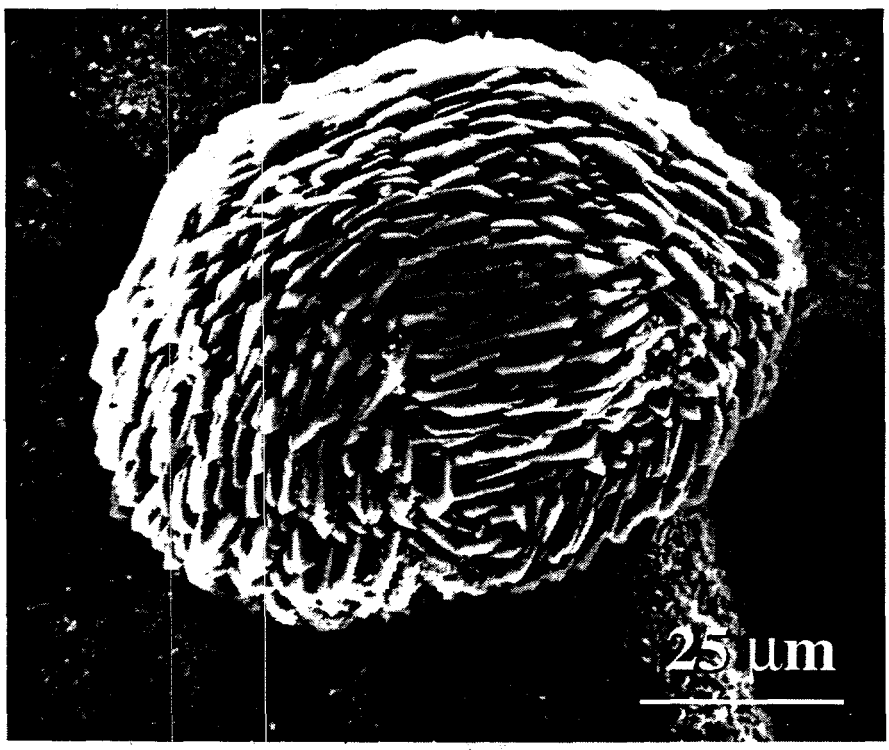

Figure 3.64b. An Enlarged View of (a) Showing the Partheite Phase

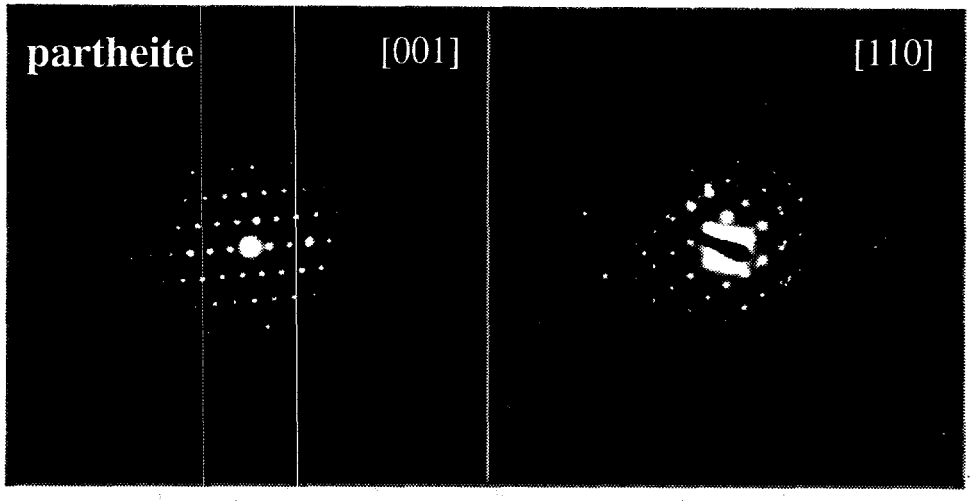

Figure 3.64c. SAD Patterns of the Partheite Phase

Figure 3.65. A Cross-Section SEM Micrograph Showing the Surface Layer Structure of LVC-14 After Vapor Hydration Testing

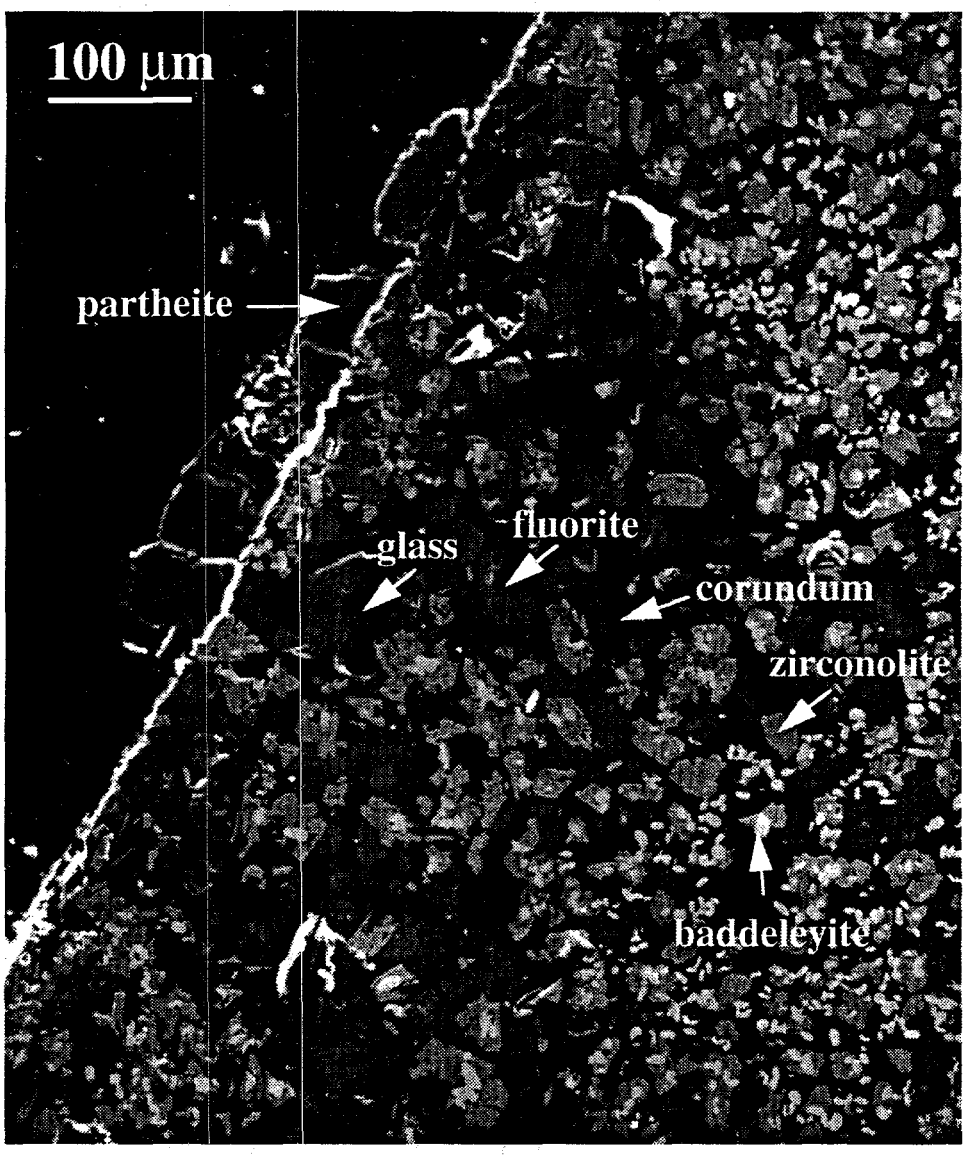

Figure 3.66. Cross-Section SEM Micrograph of LVC-15 After Vapor Hydration Testing

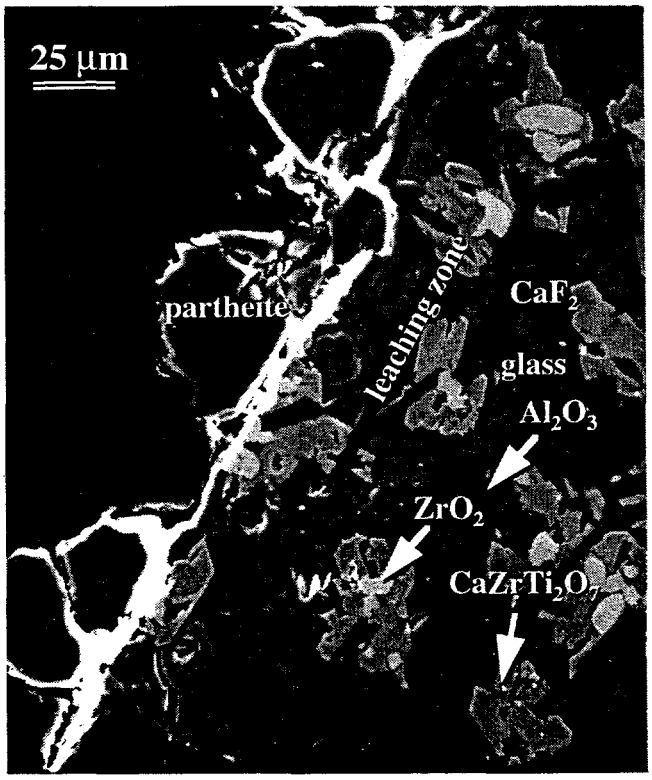

Figure 3.67. A Cross-Sectional SEM Micrograph of Reacted LVC-15

4.0 Relationship Between Vitreous Ceramics and Glasses

Vitreous ceramic waste forms are being developed to complement glass waste forms in implementing the Minimum Additive Waste Stabilization (MAWS) Program that supports the U.S. Department of Energy's (DOE) environmental restoration efforts. These vitreous ceramics are composed of various metal-oxide crystalline phases embedded in a silicate-glass phase. Glass is an amorphous solid. Both glass and vitreous ceramics are produced in vitrifiers. The main difference between these two materials is the presence of lack of crystals.

4.1 Devitrification in Glasses versus Controlled Crystallization in Vitreous Ceramics

The vitrification process uses high temperatures (typically between 1100° and 1800°C) to chemically incorporate wastes into a stable amorphous liquid. If this liquid is cooled to become a solid without crystallization, the unordered liquid freezes and becomes a glass waste form that is amorphous. Crystalline phases may be either thermodynamically unstable or kinetically unable to form due to the rapid cooling in the glass forming process.

When working with high-metal wastes, the low solubilities of metals in borosilicate glass, make the crystalline-phase formation both thermodynamically and kinetically favorable during the cool-down period. There are two possible scenarios: crystallization in a glass melt where sufficient fluxing elements exist, and controlled crystallization in a vitreous-ceramic melt where metal oxides are abundant and fluxes are deficient. The crystallization process in a glass melt can result in high viscosity, making glass flow out of melters difficult; precipitation of crystals, which can lead to clogging of the melter; formation of crystals that are very soluble in water, such as the lithium-phosphate phases observed in West Valley nuclear-waste glass (Buechele 1990); and enrichment of fluxes in the vitreous phase which can lead to decreased durability of glasses.

On the other hand, crystallization is a controlled and preferred process in vitreous ceramics. The high viscosity due to crystallization is much less of a concern due to the use of the plasma centrifugal furnace for the vitreous-ceramics production. The crystallization is controlled by the vitreous-ceramic formulations so that only stable and durable crystals are formed. The wastes treated with vitreous ceramics usually contain small amounts of fluxes and there is less concern of forming a soluble vitreous phase in the slags. By contrast, the crystallization process expels SiO_2 and Al_2O_3 from the crystalline phases, resulting in a SiO_2- and Al_2O_3- rich vitreous phase that is very durable. Another approach in vitreous ceramics is to form isolated aqueous-soluble crystals in a durable and continuous glassy matrix.

Therefore, crystallization in vitreous ceramics is a preferred process; in fact, heat treatment or the addition of nucleation agents promote controlled crystallization. Crystallization in commercial glass-making, or devitrification, is usually avoided. In waste glasses, devitrified product may be acceptable as long as the durability of the devitrified material is acceptable, but devitrified waste glasses are usually less durable than the crystal-free glasses.

4.2 The Relationship Between Vitreous Ceramics and Homogeneous Glasses

The relationship of the two distinct regions of composition, from a waste form-making point of view, is shown in Figure 4.1. Both regions have been identified as having the potential to yield environmentally sound final waste forms. Figure 4.1 shows that to form a durable and processible homogeneous glass, sufficient "structure-making" components, such as SiO_2, Al_2O_3, ZrO_2, have to be included to achieve good chemical durability. Sufficient "fluxes," such as alkalis and boron, have to be included to obtain a reasonable operating temperature, and "intermediates" or crystal-formers (such as iron, nickel, and chromium oxides) have to be limited to the solubility limits of these intermediates in glasses. For instance, the solubilities for Cr and Ni oxides are usually less than 2 and 4%. These requirements limit the homogeneous glass region in Figure 4.1.

Glass is more amenable to lower-temperature melters. A vitreous-ceramic waste form can accept more of the "structure-making" components than a glass can, because it usually melts at higher temperature. It can accept more intermediates than a glass can because it has no solubility limits, but it usually cannot accept as much flux as a glass. These properties determine the regions of vitreous ceramics in Figure 4.1.

Vitreous ceramics are usually processed at higher temperatures due to the low content of flux. However, the work discussed in Section 3.1 and 3.2 showed that vitreous ceramics can also be made with as much alkalis as a glass can accommodate, which means that the region identified in Figure 4.1 can be substantially enlarged to include more flux.

The vitreous ceramic region in Figure 4.1 is deficient in flux and rich in metal oxides, which favors crystallization and produces both durable vitreous and crystalline phases. The glass region in Figure 4.1 favors formation of amorphous solids and discourages crystalline phase formation.

Vitreous ceramics are good for waste streams with high metal content and with low flux (alkalis and boron) content, while homogenous glass waste forms are suitable for waste streams with low metal content and with sufficient flux content. Therefore, the vitreous-ceramic waste forms will encompass different compositions than that of homogenous glass waste forms. However, the regions indicated in Figure 4.1 may overlap, especially when, as shown in this report, vitreous ceramics can incorporate the same levels of alkali content as in glass.

4.3 Chemical Durability Differences

The durability of a glass is mainly determined by the relative amount of structure-making elements of SiO_2 and Al_2O_3 to the total alkalis. More silica and alumina and less alkalis are usually more durable. The durability of the glassy phases in vitreous ceramics is determined by the same factor as in glass, but the glassy phase can usually have much higher SiO_2 and Al_2O_3 and far less alkalis than normal glasses. The glassy phases in vitreous ceramics can usually be made more durable than normal glasses.

The crystal phases in vitreous ceramics, such as $Ca_3(PO_4)_2$, magnetite, $(Fe^{2+}Ni,Mn)Fe^{3+}{}_2O_4$, hibonite, $Ca(Al,Fe,Zr,Cr)_{12}O_{19}$, baddeyelite, ZrO_2, zirconolite, $CaZrTi_2O_7$, and corundum, Al_2O_3, are thermodynamically more stable than normal glasses and are also less soluble in water than glasses. Therefore, vitreous ceramics can be made very durable. This durability is better demonstrated in the longer-term tests or in vapor hydration tests.

4.4 Summary

Use of vitreous-ceramics waste forms allows MAWS technology to be applied to a much wider range of waste streams than those amenable to glass waste forms. Work in the MAWS Program has indicated that vitreous ceramics are good final waste forms because of their high chemical durability, especially the long-term durability (when properly formulated); its capability to incorporate large amounts of metal oxides; its capability to incorporate waste streams with low contents of flux components; its less stringent requirements on processing parameters, such as viscosities, compared to glass waste forms; and its production requires little or no purchased additives, which means greater waste volume reduction and treatment cost-savings. Because the high temperatures in the vitreous ceramic-making furnaces can destroy organic materials, this technology should be able to treat wastes containing large amounts of toxic organic contaminants.

The vitreous ceramics produced in through the MAWS Program represent a class of waste forms that contain significant amounts of both vitreous and crystalline phases. The crystalline phases may account for up to 99% of the total volume of waste forms with high metal-oxide loadings. Vitreous ceramics may be formulated in such a way that both crystalline and glass phases are very durable. Alternatively, vitreous ceramics can be made such that most of the hazardous and radioactive compounds are concentrated in crystalline phases. Vitreous-ceramic compositions developed through crucible melts were also produced in a Retech pilot-scale plasma centrifugal furnace at Ukiah, California, with up to 100% waste loadings (Feng 1994d). These successful campaigns demonstrate the processibility of vitreous ceramics.

Vitreous ceramics waste forms are being developed to complement, not to replace, glass waste forms in implementing the MAWS Program. Usage of both glass and vitreous ceramics waste forms will make vitrification technology applicable to the disposal of a much larger range of nuclear and mixed wastes.

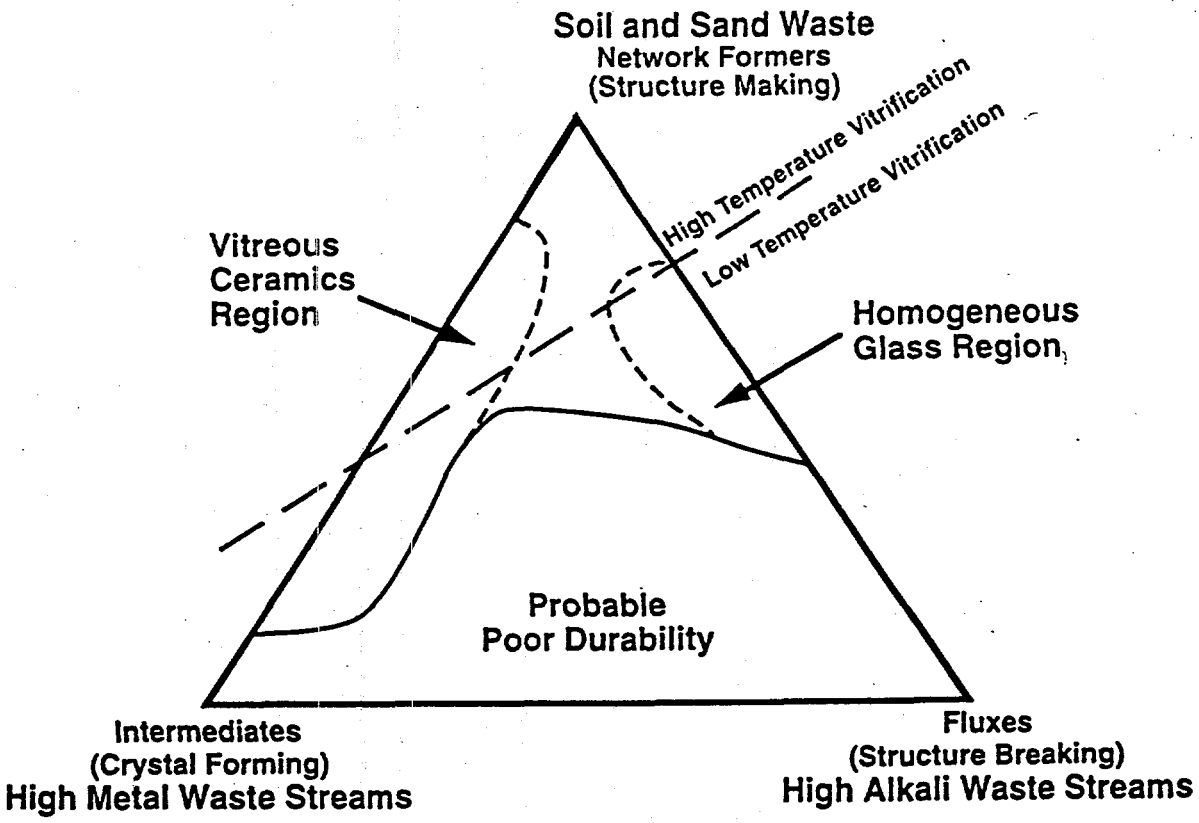

Figure 4.1. The Relationship Between Glass and Vitreous Ceramic Waste Forms

5.0 References

Bostick, W.D, D.P. Hoffmann, R.J. Stevenson, A.A. Richmond, and D. F. Bickford. 1994. "Surrogate Formulations for Thermal Treatment of Low-Level Mixed Wastes, Part IV: Wastewater Treatment Sludges." DOE/MWIP-18, Martin Marietta Energy Systems, Inc. Oak Ridge, Tennessee.

Bourcier, W.L., D.W. Peiffer, K.G. Knauss, K.D. McKeegan and D.K. Smith. 1990. "A Kinetic Model for Borosilicate Glass Dissolution Based on the Dissolution Affinity of a Surface Alteration Layer." Mat. Res. Soc. Symp. Pro. **176**:209-216.

Buechele, A.C., X. Feng, H. Gu, and I.L. Pegg. 1991. "Alteration of Microstructure of West Valley Glass by Heat Treatment," Mat. Res. Soc. Symp. Proc. **176**:393.

Feng, X., G. Ordaz, and P. Krumrine. 1994a. "Vitreous ceramics - A Complementary Waste Form to Homogenous Glass for the Implementation of MAWS in Treating DOE Low-Level/Mixed Wastes," Proc. Spectrum '94, Atlanta, Georgia, pp 1275-1285.

Feng, X. 1994b. "Development of Vitreous Ceramic as Final Waste Forms for Mixed Wastes," Proc. American Chemical Society Special Symposium, *Emerging Technologies in Hazardous Waste Management VI*, Atlanta, Georgia, pp 235-239.

Feng, X., D. J. Wronkiewicz, J. K. Bates, N. R. Brown, E. C. Buck, N. L. Dietz, M. Gong, and J. W. Emery. 1994c. *Vitreous Ceramic for Minimum Additive Waste Stabilization, Interim Program Report, May 1993 - February 1994*, ANL-94/24, Argonne National Laboratory, Argonne, Illinois.

Feng, X., D. J. Wronkiewicz, N. R. Brown, M. Gong, C. Whitworth, K. Filius, and D. Battleson. 1994d. "Comparison of Vitreous Ceramics Waste Forms Produced in Laboratory Crucibles and in a Pilot Scale Plasma Furnace," Proc. American Chemical Society Special Symposium, *Emerging Technologies in Hazardous Waste Management VI*, Atlanta, Georgia, pp 872-875. (1994).

Lasaga, J. 1984. Geophysical Res. 89:4009-40025.

Peeler, D.K., P.R. Hrma, "Predicting Liquid Immiscibility in Multicomponent Nuclear Waste Glasses", *Environmental and Waste Management Issues in the Ceramic Industry*, Ceramic Trans. **45**(1994).

Peng, I.L., "Development of the Minimum Additive Waste Stabilization (MAWS) Program for Fernald", Ceramic Trans. 39. 13(1994)

U.S. Department of Energy. 1994. "Minimum Additive Waste Stabilization (MAWS)." Office of Environmental Management, Office of Technology Development. DOE/EM-0124P,

Vinjamuri, K. 1994. "Soil Based Glass-Ceramic Waste Forms for Immobilization of the Fluorine/Sodium Calcined High-level Waste Stored at the Idaho Chemical Processing Plant." Proc. Spectrum '94, Atlanta, Georgia, pp 755-760.

Wronkiewicz, D. J. S.F. Wolf, E.C. Buck, T. DiSanto, M.T. Surchik, J.A. Fortner, N.L. Dietz, J.W. Richardson, X.Feng, M.Gong, and N.L. Brown. 1995. "Glass-Crystal Composites For Minimum Additive Waste Stabilization: Interim Progress Report, March 1994 -February 1995" Argonne National Laboratory Report ANL-95/xx, Argonne, Illinois.

Wronkiewicz, D. J., X. Feng, and N. R. Brown. 1994. "Radionuclide and Hazardous Element Retention in Vitreous Ceramics Waste Forms," Proc. American Chemical Society Special Symposium, *Emerging Technologies in Hazardous Waste Management VI*, September 19-21, 1994, Atlanta, Georgia, pp 645-648.

Appendix A: Nominal Compositions (wt%) of Vitreous Ceramics

		LVC-1	LVC-2	LVC-3	LVC-4	LVC-5	LVC-6	LVC-7	LVC-8	LVC-9	LVC-10	LVC-11	LVC-12	LVC-13	LVC-14	LVC-15	LVC-16	LVC-17
Chemical	Element	NOMINAL	NOMINAL	NOMINAL	NOMINAL	NOMINAL	NOMINAL	NOMINAL	NOMINAL	NOMINAL	NOMINAL	NOMINAL	NOMINAL	NOMINAL	NOMINAL	NOMINAL	NOMINAL	NOMINAL
		wt%	wt %	wt %	wt %	wt %	wt %	wt %	wt %	wt %	wt %	wt %	wt %	wt %	wt %	wt %	wt %	wt %
SiO2	Si	19.22	48.60	38.66	28.64	17.97	23.84	16.68	16.68	33.35	44.79	50.96	38.77	44.89	6.67	6.67	34.42	38.46
Al2O3	Al	3.50	9.35	32.80	5.59	13.38	13.56	13.83	58.29	42.89	35.00	0.95	32.89	32.89	37.19	31.87	9.39	16.12
Fe2O3	Fe	0.00	0.01	0.01	0.01	19.22	17.87	1.50	1.47	2.78	0.00	33.40	0.00	0.00	2.72	2.70	0.00	0.00
CaO	Ca	2.74	0.00	0.00	4.32	16.62	14.97	21.53	5.52	6.48	0.00	0.00	0.00	0.00	17.57	15.99	0.00	0.00
Na2O	Na	28.49	24.08	19.14	24.38	1.75	1.58	0.53	0.54	0.76	18.00	12.46	20.00	20.00	0.41	0.38	0.00	0.00
K2O	K	0.45	0.47	0.51	0.47	4.08	2.85	0.60	15.60	11.20	0.33	0.00	0.00	0.00	0.24	0.24	0.00	0.00
MgO	Mg	0.00	0.00	0.00	0.00	3.11	3.75	0.66	0.81	1.37	0.33	0.33	0.33	0.33	0.37	0.35	0.00	0.00
TiO2	Ti	0.00	0.00	5.97	18.43	1.63	1.53	0.18	0.18	0.35	0.00	0.00	6.12	0.00	0.07	10.07	0.00	0.00
BaO	Ba	0.00	0.00	0.00	0.00	0.00	0.00	0.03	0.03	0.05	0.00	0.00	0.00	0.00	0.01	0.01	0.00	0.00
Ce2O3	Ce	0.00	0.00	0.00	0.00	0.44	0.40	0.08	0.03	0.02	0.00	0.00	0.00	0.00	0.07	0.07	0.00	0.00
Cr2O3	Cr	0.05	0.05	0.06	0.05	0.33	0.30	0.53	0.12	0.08	0.04	0.04	0.04	0.04	0.47	0.42	0.00	0.00
CuO	Cu	0.00	0.00	0.00	0.00	0.27	0.24	0.00	0.00	0.00	0.00	0.00	0.00	0.00	0.00	0.00	0.00	0.00
MnO	Mn	0.01	0.01	0.01	0.01	0.89	0.81	0.06	0.06	0.07	0.01	0.01	0.01	0.01	0.05	0.05	0.00	0.00
PbO	Pb	0.00	0.00	0.00	0.00	0.02	0.02	0.00	0.00	0.00	0.00	0.00	0.00	0.00	0.00	0.00	0.00	0.00
SO3	S	0.44	0.46	0.49	0.46	0.64	0.58	0.00	0.00	0.00	0.32	0.32	0.32	0.32	0.00	0.00	0.00	0.00
ZnO	Zn	0.00	0.00	0.00	0.00	0.10	0.09	0.00	0.00	0.00	0.00	0.00	0.00	0.00	0.00	0.00	0.00	0.00
ZrO2	Zr	15.89	0.01	0.01	0.01	0.00	0.00	17.10	0.12	0.08	0.01	0.00	0.00	0.00	13.28	12.13	0.00	0.00
P2O3	P	28.76	16.47	1.84	16.98	16.69	15.04	0.00	0.00	0.00	1.18	1.20	1.19	1.19	0.00	0.00	16.19	0.00
As2O3	As	0.00	0.00	0.00	0.00	0.03	0.03	0.00	0.00	0.00	0.00	0.00	0.00	0.00	0.00	0.00	0.00	0.00
NiO	Ni	0.00	0.00	0.00	0.00	2.72	2.45	0.08	0.06	0.04	0.00	0.00	0.00	0.00	0.09	0.08	0.00	0.00
F	F	0.29	0.31	0.33	0.31	0.03	0.03	0.00	0.00	0.00	0.21	0.22	0.21	0.21	0.00	0.00	0.00	0.00
Cl	Cl	0.13	0.14	0.14	0.13	0.07	0.06	0.00	0.00	0.00	0.09	0.09	0.09	0.09	0.00	0.00	0.00	0.00
B2O3	B	0.00	0.00	0.00	0.00	0.00	0.00	0.23	0.24	0.16	0.00	0.00	0.00	0.00	0.29	0.26	0.00	0.00
CdO	Cd	0.00	0.00	0.00	0.00	0.00	0.00	0.04	0.03	0.02	0.00	0.00	0.00	0.00	0.04	0.04	0.00	0.00
Sb2O3	Sb	0.00	0.00	0.00	0.00	0.00	0.00	0.03	0.03	0.05	0.00	0.00	0.00	0.00	0.01	0.01	0.00	0.00
Cs2O	Cs	0.00	0.00	0.00	0.00	0.00	0.00	0.23	0.03	0.02	0.00	0.00	0.00	0.00	0.19	0.17	35.00	35.42
HgO	Hg	0.00	0.00	0.00	0.00	0.00	0.00	0.04	0.03	0.02	0.00	0.00	0.00	0.00	0.04	0.04	0.00	0.00
SrO	Sr	0.00	0.00	0.00	0.00	0.00	0.00	0.60	0.03	0.02	0.00	0.00	0.00	0.00	0.48	0.44	0.00	0.00
CaF2	Ca	0.00	0.00	0.00	0.00	0.00	0.00	25.58	0.24	0.16	0.00	0.00	0.00	0.00	19.90	18.17	0.00	0.00
Bi2O3		0.00	0.00	0.00	0.00	0.00	0.00	0.00	0.00	0.00	0.01	0.01	0.01	0.01	0.00	0.00	0.00	0.00
Nd2O3	Nd	0.02	0.02	0.02	0.02	0.00	0.00	0.00	0.00	0.00	0.01	0.01	0.01	0.01	0.00	0.00	0.00	0.00
Li2O	Li	0.00	0.00	0.00	0.00	0.00	0.00	0.00	0.00	0.00	0.00	0.00	0.00	0.00	0.00	0.00	5.00	10.00
	TOTAL	99.98	99.98	99.98	99.80	99.99	100.00	100.08	100.11	99.97	100.33	100.01	100.00	100.00	100.18	100.15	100.00	100.00

Appendix B: Analyzzed and Nominal Compositions (wt%) for Selected Vitreous Ceramics

		LVC-1		LVC-2		LVC-3		LVC-4		LVC-16 -	Q	HT	LVC-17 -	Q	HT
Chemical	Element	NOMINAL	ANALYZED	NOMINAL	ANALYZED	NOMINAL	ANALYZED	NOMINAL	ANALYZED	NOMINAL	ANALYZED	ANALYZED	NOMINAL	ANALYZED	ANALYZED
		wt %	wt%	wt %	wt%	wt %	wt%	wt %	wt%	wt %	wt%	wt%	wt %	wt%	wt%
SiO2	Si	19.22	17.07	48.60	44.93	38.66	35.84	28.64	25.62	34.42	35.39	30.43	38.46	36.05	34.99
Al2O3	Al	3.50	3.23	9.35	8.91	32.80	30.96	5.59	5.3	9.39	8.52	7.16	16.12	15.54	15.42
Fe2O3	Fe	0.00	0.07	0.01	0.06	0.01	0.07	0.01	0.06		0.26	0.27		0.26	0.24
CaO	Ca	2.74	2.68	0.00	0.09	0.00	0.11	4.32	4.32		0.03	0.03		0.03	0.03
Na2O	Na	28.49	27.79	24.08	24.64	19.14	19.91	24.38	24.38		0.36	0.41		0.45	0.56
K2O	K	0.45	2.71	0.47	2.99	0.51	3.37	0.47	2.65		0	0		0.01	0
MgO	Mg	0.00	0.02	0.00	0.01	0.00	0.02	0.00	0.13		0.91	0		1.18	1.21
TiO2	Ti	0.00	0.01	0.00	0	5.97	5.66	18.43	17		0.02	0.01		0.01	0.01
BaO	Ba	0.00	0.01	0.00	0	0.00	0	0.00	0		0.01	0.01		0.01	0.01
Ce2O3	Ce	0.00	0.06	0.00	0.08	0.00	0.03	0.00	0.07		0	0		0	0
Cr2O3	Cr	0.05	0.04	0.05	0.04	0.06	0.05	0.05	0.04		0.07	0.07		0.07	0.06
CuO	Cu	0.00	0	0.00	0	0.00	0	0.00	0		0	0		0	0
MnO	Mn	0.01	0.01	0.01	0.01	0.01	0	0.01	0		0.01	0.01		0.01	0.01
PbO	Pb	0.00	0	0.00	0	0.00	0	0.00	0		0	0		0	0
SO3	S	0.44	0.24	0.46	0.01	0.49	0	0.46	0.3		0.05	0.04		0.24	0.28
ZnO	Zn	0.00	0.25	0.00	0.3	0.00	0.3	0.00	0.34		0	0		0	0
ZrO2	Zr	15.89	17.35	0.01	0.03	0.01	0.02	0.01	0.03		0	0.00		0	0
P2O3	P	28.76	25.11	16.47	15.46	1.84	1.23	16.98	15.45	16.19	11.71	16.21		0	0
As2O3	As	0.00		0.00		0.00		0.00							
NiO	Ni	0.00	0.04	0.00	0.03	0.00	0.05	0.00	0.03		0.04	0.05		0.04	0.04
F	F	0.29		0.31		0.33		0.31							
Cl	Cl	0.13		0.14		0.14		0.13							
B2O3	B	0.00	0.06	0.00	0.04	0.00	0	0.00	0		0	0.04		0	0.04
CdO	Cd	0.00	0	0.00	0	0.00	0	0.00	0		0	0		0	0
Sb2O3	Sb	0.00		0.00		0.00		0.00							
Cs2O	Cs	0.00		0.00		0.00		0.00		35	36.9	35.1	35.42	38.83	41.38
HgO	Hg	0.00		0.00		0.00		0.00							
SrO	Sr	0.00	0.01	0.00	0	0.00	0	0.00	0		0	0		0	0
CaF2	Ca	0.00		0.00		0.00		0.00							
Bi2O3											0	0		0	0
Nd2O3	Nd	0.02	0.08	0.02	0.1	0.02	0.1	0.02	0.11		0.05	0.04		0.07	0.06
Li2O	Li									5	4.17	6.1	10	9.37	8.95
	TOTAL	99.98	96.84	99.98	97.73	99.98	97.72	99.80	95.83	100.00	98.50	95.98	100.00	102.17	103.29

Appendix C: Elemental Releases in PCT Tests

EA Glass (CVS2-101)				Sample C		Sample D		
Chemical	Element	Oxide						
		Wt %	ug/ml	NL (g/m^2)	ug/ml	NL (g/m^2)	Ave	pH
SiO2	Si	48.95		1.80		1.84	1.82	11.91
Al2O3	Al	3.67						11.94
Fe2O3	Fe	8.97						
CaO	Ca	1.13						11.93
Na2O	Na	16.71		6.39		6.39	6.39	
K2O	K	0.04						
MgO	Mg	1.66						
TiO2	Ti	0.71						
BaO	Ba							
Ce2O3	Ce							
Cr2O3	Cr							
CuO	Cu							
MnO	Mn	1.34						
PbO	Pb							
SO3	S							
ZnO	Zn							
ZrO2	Zr	0.41						
P2O5	P							
As2O3	As							
NiO	Ni	0.61						
F	F							
Cl	Cl							
B2O3	B	11.12		8.64		8.64	8.64	
CdO	Cd							
Sb2O3	Sb							
Cs2O	Cs							
HgO	Hg							
SrO	Sr							
CaF2	Ca							
Nd2O3	Nd							
La2O3	La	0.41						

LVC-1			7 DAY						28 DAY						91 DAY					
Chemical	Element	Oxide	Sample C		Sample D				Sample C		Sample D				Sample C		Sample D			
		Wt %	ug/ml	NL (g/m^2)	ug/ml	NL (g/m^2)	Ave	pH	ug/ml	NL (g/m^2)	ug/ml	NL (g/m^2)	Ave	pH	ug/ml	NL (g/m^2)	ug/ml	NL (g/m^2)	Ave	pH
SiO2	Si	19.22	40.71	0.23	36.13	0.20	0.21	11.43	58.86	0.33	60.75	0.34	0.33	11.43	53.09	0.30	66.70	0.37	0.33	11.18
Al2O3	Al	3.50	0.00	0.000	50.74	1.370	0.68	11.44	26.69	0.720	36.50	0.985	0.85	11.44	12.01	0.324	18.20	0.491	0.41	11.19
Fe2O3	Fe	0.00	0.00	0.000	1.65	24.250	12.13		2.70	39.682	0.00	0.000	19.84		0.00	0.000	0.00	0.000	0.00	
CaO	Ca	2.74	1.06	0.014	0.00	0.000	0.01	11.44	0.00	0.000	0.00	0.000	0.00	11.44	0.00	0.000	0.00	0.000	0.00	11.19
Na2O	Na	28.49	15469.78	36.593	16074.84	38.024	37.31		15759.86	37.279	15806.72	37.390	37.33		15583.88	36.863	15891.2	37.590	37.23	
K2O	K	0.45	0.00	0.000	0.00	0.000	0.00		0	0.000	58.11	7.811	3.91		82.41	11.077	159.67	21.462	16.27	
MgO	Mg	0.00	0.00		0.00				0		0				0		0			
TiO2	Ti	0.00							0.53		0.32				0.35		0			
BaO	Ba	0.00	0.00		0.00				0		0				0		0			
Ce2O3	Ce	0.00							0		0				0		0			
Cr2O3	Cr	0.05	10.83	16.170	11.19	16.707	16.44		11.6	17.320	12.01	17.932	17.63		11.97	17.872	12.57	18.768	18.32	
CuO	Cu	0.00	0.00		0.00				0		0				0		0			
MnO	Mn	0.01	0.00	0.000	0.00	0.000	0.00		0	0.000	0	0.000	0.00		0	0.000	0	0.000	0.00	
PbO	Pb	0.00	0.00		0.00				0		0				0		0			
SO3	S	0.44		0.000		0.000	0.00		89.61	25.575	93.13	26.579	26.08		90.85	25.929	93.16	26.588		
ZnO	Zn	0.00	1.53		1.42				0		0				0		0			
ZrO2	Zr	15.89	0.00	0.000	0.00	0.000	0.00		3.19	0.014	0	0.000	0.01		0	0.000	0	0.000	0.00	
P2O3	P	28.76	8121.63	32.356	8487.67	33.814	33.09		8714.69	34.718	8910.8	35.499	35.11		8848.24	35.250	9103.98	36.269	35.76	
As2O3	As	0.00																		
NiO	Ni	0.00	0.00		0.00				0		0				0		0			
F	F	0.29																		
Cl	Cl	0.13																		
B2O3	B	0.00	0.00		0.00				2.13		0				0		0			
CdO	Cd	0.00	0.00		0.00				0		0				0		0			
Sb2O3	Sb	0.00																		
Cs2O	Cs	0.00																		
HgO	Hg	0.00																		
SrO	Sr	0.00	0.00		0.00				0		0				0		0			
CaF2	Ca	0.00																		
Nd2O3	Nd	0.02	0.00	0.000	0.00	0.000	0.00		0	0.000	2.08	7.389	3.69		2.76	9.805	4.83	17.159	13.48	

LVC-1 H.T.			7 DAY						28 DAY						91 DAY					
Chemical	Element	Oxide	Sample C		Sample D				Sample C		Sample D				Sample C		Sample D			
		Wt %	ug/ml	NL (g/m^2)	ug/ml	NL (g/m^2)	Ave	pH	ug/ml	NL (g/m^2)	ug/ml	NL (g/m^2)	Ave	pH	ug/ml	NL (g/m^2)	ug/ml	NL (g/m^2)	Ave	pH
SiO2	Si	19.22	44.51	0.25	45.46	0.25	0.25	11.37	58.60	0.33	51.22	0.28	0.31	11.33	37.57	0.21	30.87	0.17	0.19	11.07
Al2O3	Al	3.50	6.99	0.189	9.16	0.247	0.22	11.38	82.50	2.227	84.13	2.271	2.25	11.29	2.79	0.075	18.17	0.490	0.28	11.08
Fe2O3	Fe	0.00	0.00	0.000	0.99	14.550	7.28		0.66	9.700	0.00	0.000	4.85		0.00	0.000	0.00	0.000	0.00	
CaO	Ca	2.74	1.44	0.018	4.93	0.063	0.04	11.38	0.00	0.000	0.00	0.000	0.00	11.31	0.00	0.000	0.00	0.000	0.00	11.08
Na2O	Na	28.49	13124.19	31.044	12634.08	29.885	30.46		14586.21	34.503	14185.29	33.554	34.03		14389.77	34.038	14550.57	34.418	34.23	
K2O	K	0.45	91.63	12.316	145.03	19.494	15.91		0	0.000	160.3	21.546	10.77		0	0.000	0	0.000	0.00	
MgO	Mg	0.00	0.00		0.00				0		0				0		0			
TiO2	Ti	0.00							0		0				0		0			
BaO	Ba	0.00	0.00		0.00				0		0		0.00		0		0			
Ce2O3	Ce	0.00	0.00		4.26				0		0				0		0			
Cr2O3	Cr	0.05	10.98	16.394	10.86	16.215	16.30		11.86	17.708	12.35	18.439	18.07		11.76	17.559	11.9	17.768	17.66	
CuO	Cu	0.00	0.00		0.00				0		0				0		0			
MnO	Mn	0.01	0.00	0.000	0.00	0.000	0.00		0	0.000	0	0.000	0.00		0	0.000	0	0.000	0.00	
PbO	Pb	0.00	0.00		0.00				0		0				0		0			
SO3	S	0.44		0.000		0.000	0.00		86.85	24.787	86.36	24.647			85.77	24.479	86.74	24.756	24.62	
ZnO	Zn	0.00	1.60		2.08				0		0				0		0			
ZrO2	Zr	15.89	0.00	0.000	0.00	0.000	0.00		0	0.000	1.76	0.007	0.00		0	0.000	0	0.000	0.00	
P2O5	P	28.76	7269.91	28.962	7044.19	28.063	28.51		8289.89	33.026	8306.59	33.092	33.06		8084.63	32.208	8197.75	32.659	32.43	
As2O3	As	0.00																		
NiO	Ni	0.00	0.00		0.00				0		0				0		0			
F	F	0.29																		
Cl	Cl	0.13																		
B2O3	B	0.00	0.00		0.00				1.15		1.15				1.11		1.54			
CdO	Cd	0.00	0.00		0.00				0		0				0		0			
Sb2O3	Sb	0.00																		
Ce2O	Ce	0.00																		
HgO	Hg	0.00																		
SrO	Sr	0.00	0.00		0.00				0		0				0		0			
CaF2	Ca	0.00																		
Nd2O3	Nd	0.02	4.44	15.774	6.07	21.564	18.67		0	0.000	5.14	18.260	9.13		0	0.000	0	0.000	0.00	

LVC-2Q			7 DAY						28 DAYS						91 DAYS					
Chemical	Element	Oxide	Sample C		Sample D				Sample C		Sample D				Sample C		Sample D			
		Wt %	ug/ml	NL (g/m^2)	ug/ml	NL (g/m^2)	Ave	pH	ug/ml	NL (g/m^2)	ug/ml	NL (g/m^2)	Ave	pH	ug/ml	NL (g/m^2)	ug/ml	NL (g/m^2)	Ave	pH
SiO2	Si	48.60	66.44	0.15	104.48	0.23	0.19	11.55	151.40	0.33		0.00	0.17	11.88	222.53	0.49	224.87	0.49	0.49	12.09
Al2O3	Al	9.35	16.07	0.162	22.59	0.228	0.20	11.55	32.08	0.324		0.000	0.16	11.86	47.58	0.481	47.61	0.481	0.48	12.08
Fe2O3	Fe	0.01	0.21	2.914	0.08	1.110	2.01		0.10	1.388		0.000	0.69		0.17	2.359	0.18	2.498	2.43	
CaO	Ca	0.00	0.25		0.27		0.00	11.55	0.12					11.87	0.00		0.00			12.09
Na2O	Na	24.08	188.61	0.528	202.02	0.565	0.55		352.49	0.986		0.000	0.99		703.99	1.970	731.71	2.048	2.01	
K2O	K	0.47	1.28	0.162	0.00	0.000	0.08		2.48	0.315		0.000	0.31		11.1	1.409	6.31	0.801	1.10	
MgO	Mg	0.00	0.10		0.00				0.07						0		0			
TiO2	Ti	0.00	0.03						0.02						0.04		0.04			
BeO	Be	0.00	0.00		0.00				0						0		0			
Ce2O3	Ce	0.00	0.00		0.00				0.05						0.22		0			
Cr2O3	Cr	0.05	0.28	0.395	0.09	0.127	0.26		0.13	0.183		0.000	0.09		0.2	0.282	0.19	0.268	0.27	
CuO	Cu	0.00	0.01		0.00				0						0		0			
MnO	Mn	0.01	0.07	0.439	0.00	0.000	0.22		0.01	0.063		0.000	0.06		0.03	0.188	0.02	0.125	0.16	
PbO	Pb	0.00	0.00		0.00				0						0		0			
SO3	S	0.46							0.3	0.081		0.000	0.08		0.44	0.119	0.44	0.119	0.12	
ZnO	Zn	0.00	0.02		0.00				0						0.08		0.08			
ZrO2	Zr	0.01	0.02	0.210	0.00	0.000	0.10		0.05	0.524		0.000	0.52		0.11	1.154	0.1	1.049	1.10	
P2O3	P	16.47	77.59	0.540	22.43	0.156	0.35		34.67	0.241		0.000	0.24		51.55	0.358	53.37	0.371	0.36	
As2O3	As	0.00																	0.00	
NiO	Ni	0.00	0.02		0.00				0.02						0		0			
F	F	0.31																		
Cl	Cl	0.14																		
B2O3	B	0.00	0.21		0.30				0.3						0.08		0.35			
CdO	Cd	0.00	0.00		0.00				0						0		0			
Sb2O3	Sb	0.00																		
Cs2O	Cs	0.00																		
HgO	Hg	0.00																		
SrO	Sr	0.00	0.00		0.00				0						0		0			
CeF2	Ce	0.00																		
Nd2O3	Nd	0.02	0.23	0.771	0.02	0.067	0.42		0.14	0.470		0.000	0.47		0.39	1.308	0.26	0.872	1.09	

Appendix C: Elemental Releases in PCT Tests

LVC-2 H.T.			7 DAY						28 DAYS						91 DAYS					
Chemical	Element	Oxide	Sample C		Sample D				Sample C		Sample D				Sample C		Sample D			
		Wt %	ug/ml	L (g/m^2	ug/ml	L (g/m^2	Ave	pH	ug/ml	L (g/m^2	ug/ml	L (g/m^2	Ave	pH	ug/ml	L (g/m^2	ug/ml	L (g/m^2	Ave	pH
SiO2	Si	48.60	66.44	0.15	65.03	0.14	0.14	10.76	77.13	0.17	78.43	0.17	0.17	9.90	107.70	0.24	112.68	0.25	0.24	11.24
Al2O3	Al	9.35	16.07	0.162	15.57	0.157	0.16	10.77	17.76	0.179	18.18	0.184	0.18	10.17	23.33	0.236	24.61	0.249	0.24	11.26
Fe2O3	Fe	0.01	0.21	2.914	0.20	2.775	2.84		0.23	3.191	0.24	3.330	3.26		0.25	3.469	0.35	4.856	4.16	
CaO	Ca	0.00	0.25		0.29			10.77	0.23		0.26			10.04	0.00		0.00			11.25
Na2O	Na	24.08	188.61	0.528	180.23	0.504	0.52		214.07	0.599	217.07	0.608	0.60		328.86	0.920	349.04	0.977	0.95	
K2O	K	0.47	1.28	0.162	2.74	0.348	0.26		1.97	0.250	1.73	0.220	0.23		0	0.000	0.07	0.009	0.00	
MgO	Mg	0.00	0.10		0.14				0.1		0.09				0		0			
TiO2	Ti	0.00							0.03		0.03				0.03		0.04			
BaO	Ba	0.00	0.00		0.00				0		0				0		0			
Ce2O3	Ce	0.00	0.00		0.07				0.04		0.04				0		0			
Cr2O3	Cr	0.05	0.28	0.395	0.28	0.395	0.39		0.31	0.437	0.31	0.437	0.44		0.35	0.493	0.44	0.620	0.56	
CuO	Cu	0.00	0.01		0.01				0		0				0		0			
MnO	Mn	0.01	0.07	0.439	0.07	0.439	0.44		0.07	0.439	0.07	0.439	0.44		0.08	0.501	0.09	0.564	0.53	
PbO	Pb	0.00	0.00		0.00				0		0				0		0			
SO3	S	0.46		0.000		0.000			0.7	0.189	0.69	0.186	0.19		0.88	0.237	0.98	0.264	0.25	
ZnO	Zn	0.00	0.02		0.03				0.02		0.01				0		0			
ZrO2	Zr	0.01	0.02	0.210	0.00	0.000	0.10		0.03	0.315	0.01	0.105	0.21		0	0.000	0	0.000	0.00	
P2O5	P	16.47	77.59	0.540	74.64	0.519	0.53		73.57	0.512	73.59	0.512	0.51		90.94	0.632	96.63	0.672	0.65	
As2O3	As	0.00																	0.00	
NiO	Ni	0.00	0.02		0.03				0.03		0.03				0		0.09			
F	F	0.31																		
Cl	Cl	0.14																		
B2O3	B	0.00	0.21		0.17				0.17		0.19				0.18		0.24			
CdO	Cd	0.00	0.00		0.00				0		0				0		0.07			
Sb2O3	Sb	0.00																		
Cs2O	Cs	0.00																		
HgO	Hg	0.00																		
SrO	Sr	0.00	0.00		0.00				0		0				0		0			
CaF2	Ca	0.00																		
Nd2O3	Nd	0.02	0.23	0.771	0.27	0.906	0.84		0.25	0.839	0.24	0.805	0.82		0.21	0.704	0.19	0.637	0.67	

Appendix C: Elemental Releases in PCT Tests

7 DAY PCT	ACETONE WASH		LVC-2Q						LVC-2HT					
Chemical	Element	Oxide	Sample C		Sample D				Sample C		Sample D			
		Wt %	ug/ml	L (g/m^2	ug/ml	L (g/m^2	Ave	pH	ug/ml	L (g/m^2	ug/ml	L (g/m^2	Ave	pH
SiO2	Si	48.60	70.63	0.16	74.41	0.16	0.16	10.78	8.72	0.02	8.27	0.02	0.02	11.24
Al2O3	Al	9.35	15.97	0.161	16.50	0.167	0.16	10.84	3.87	0.039	3.49	0.035	0.04	11.20
Fe2O3	Fe	0.01	0.17	2.345	0.20	2.761	2.55		0.07	0.916	0.07	0.902	0.91	
CaO	Ca	0.00	0.18		0.12			10.81	0.04		0.05			11.22
Na2O	Na	24.08	271.89	0.761	315.511	0.883	0.82		129.81	0.363	106.619	0.298	0.33	
K2O	K	0.47	1.824	0.231	2.03	0.258	0.24		1.336	0.170	1.261	0.160	0.16	
MgO	Mg	0.00	0.069		0.074				0.064		0.062			
TiO2	Ti	0.00	0.035		0.041				0.014		0.012			
BaO	Ba	0.00	0.003		0.003				0.002		0.002			
Ce2O3	Ce	0.00	0.04		0.045				0.036		0.034			
Cr2O3	Cr	0.05	0.246	0.347	0.283	0.399	0.37		0.151	0.213	0.128	0.180	0.20	
CuO	Cu	0.00	0.033		0.049				0.01		0.009			
MnO	Mn	0.01	0.009	0.056	0.012	0.075	0.07		0.025	0.157	0.022	0.138	0.15	
PbO	Pb	0.00	0		0				0.033		0.027			
SO3	S	0.46	2.388		2.985		0.00		0.917		0.748		0.00	
ZnO	Zn	0.00	0.179		0.412				0		0			
ZrO2	Zr	0.01	0.009	0.094	0.01	0.105	0.10		0.009	0.094	0.006	0.063	0.08	
P2O3	P	16.47	104.043	0.724	122.833	0.854	0.79		64.57	0.449	52.627	0.366	0.41	
As2O3	As	0.00					0.00						0.00	
NiO	Ni	0.00	0.024		0.03				0.016		0.009			
F	F	0.31												
Cl	Cl	0.14												
B2O3	B	0.00	0.05		0.045				0.01		0.009			
CdO	Cd	0.00	0.002		0.003				0.004		0.003			
Sb2O3	Sb	0.00												
Cs2O	Cs	0.00												
HgO	Hg	0.00												
SrO	Sr	0.00	0.002		0.002				0.001		0.001			
CaF2	Ca	0.00												
Nd2O3	Nd	0.02	0.024	0.080	0.03	0.101	0.09		0.101	0.339	0.093	0.312	0.33	

LVC-3Q			7 DAY						28 DAY						91 DAY					
Chemical	Element	Oxide	Sample C		Sample D				Sample C		Sample D				Sample C		Sample D			
		Wt %	ug/ml	L (g/m^2	ug/ml	L (g/m^2	Ave	pH	ug/ml	L (g/m^2	ug/ml	L (g/m^2	Ave	pH	ug/ml	L (g/m^2	ug/ml	L (g/m^2	Ave	pH
SiO2	Si	38.66	69.87	0.193	71.67	0.198	0.196	11.11	74.32	0.205	73.48	0.203	0.204	11.26	381:51	1.054	78.22	0.216	0.635	11.15
Al2O3	Al	32.80	70	0.202	71.94	0.207	0.204	11.13	73.42	0.211	72.87	0.210	0.211	11.28	375.69	1.082	76.95	0.222	0.652	11.25
Fe2O3	Fe	0.01	0.03	0.391	0.04	0.521	0.456		0.04	0.521	0.04	0.521	0.521		0.22	2.866	0.04	0.521	1.693	
CaO	Ca	0.00	0.22		0.26			11.12	0.16		0.23			11.27	0.8		0.16			11.20
Na2O	Na	19.14	109.41	0.385	113.91	0.401	0.393		138.05	0.486	136.52	0.481	0.483		859.09	3.025	175.13	0.617	1.821	
K2O	K	0.51	0	0.000	0	0.000	0.000		2.69	0.320	0.01	0.001	0.161		9.58	1.141	2.13	0.254	0.698	
MgO	Mg	0.00	0		0				0.08		0				0		0			
TiO2	Ti	5.97		0.000		0.000	0.000		5.18	0.362	5.49	0.384	0.373		29.87	2.089	5.4	0.378	1.233	
BaO	Ba	0.00	0		0				0.01		0				0.02		0			
Ce2O3	Ce	0.00	0		0				0.05		0.04				0		0			
Cr2O3	Cr	0.06	0.06	0.079	0.06	0.079	0.079		0.07	0.093	0.08	0.106	0.099		0.39	0.516	0.08	0.106	0.311	
CuO	Cu	0.00	0		0				0		0				0		0			
MnO	Mn	0.01	0	0.000	0	0.000	0.000		0.01	0.059	0	0.000	0.029		0.02	0.118	0	0.000	0.059	
PbO	Pb	0.00	0		0				0		0				0		0			
SO3	S	0.49		0.000		0.000			0.27	0.068	0.28	0.071	0.070		1.31	0.331	0.27	0.068	0.200	
ZnO	Zn	0.00	0		0.01		0.000		0		0				0		0			
ZrO2	Zr	0.01	0.02	0.197	0.02	0.197	0.197		0.02	0.197	0.02	0.197	0.197		0.13	1.280	0.02	0.197	0.738	
P2O3	P	1.84	2.08	0.130	2.18	0.136	0.133		2.27	0.142	2.4	0.150	0.146		11.56	0.721	2.35	0.147	0.434	
As2O3	As	0.00																		
NiO	Ni	0.00	0		0				0.04		0.04				0.18		0.04			
F	F	0.33																		
Cl	Cl	0.14																		
B2O3	B	0.00	0.03		0.04		0.000		0.06		0.04				0.22		0.05			
CdO	Cd	0.00	0		0				0		0				0		0			
Sb2O3	Sb	0.00																		
Cs2O	Cs	0.00																		
HgO	Hg	0.00																		
SrO	Sr	0.00	0		0				0.01		0				0		0			
CaF2	Ca	0.00																		
Nd2O3	Nd	0.02	0	0.000	0	0.000	0.000		0.1	0.315	0.09	0.283	0.299		0.43	1.354	0.09	0.283	0.819	

LVC-3 H.T.			7 DAY						28 DAY						91 DAY					
Chemical	Element	Oxide	Sample C		Sample D				Sample C		Sample D				Sample C		Sample D			
		Wt %	ug/ml	L (g/m^2	ug/ml	L (g/m^2	Ave	pH	ug/ml	L (g/m^2	ug/ml	L (g/m^2	Ave	pH	ug/ml	L (g/m^2	ug/ml	L (g/m^2	Ave	pH
SiO2	Si	38.66	16.52	0.046	16.81	0.046	0.046	9.27	14.43	0.040	14.58	0.040	0.040	9.14	14.01	0.039		0.000	0.039	9.4
Al2O3	Al	32.80	35.01	0.101	35.45	0.102	0.101	9.28	31.12	0.090	31.44	0.091	0.090	9.18	31.6	0.091		0.000	0.091	
Fe2O3	Fe	0.01	0.01	0.130	0.01	0.130	0.130		0.01	0.130	0.01	0.130	0.130		0.01	0.130		0.000	0.130	
CaO	Ca	0.00	0.31		0.29			9.28	0.19		0.15			9.16	0					9.40
Na2O	Na	19.14	295.04	1.039	297.83	1.049	1.044		337.39	1.188	342.78	1.207	1.197		382.52	1.347		0.000	1.347	
K2O	K	0.51	2.81	0.335	2.73	0.325	0.330		1.31	0.156	1.2	0.143	0.150		0	0.000		0.000		
MgO	Mg	0.00	0.22		0.22				0.19		0.2				0.08					
TiO2	Ti	5.97		0.000		0.000			0.15	0.010	0.14	0.010			0.06	0.004		0.000	0.004	
BaO	Ba	0.00	0		0				0		0				0					
Ce2O3	Ce	0.00	0.09		0.08				0		0				0					
Cr2O3	Cr	0.06	2.13	2.819	2.15	2.845	2.832		2.09	2.766	2.13	2.819	2.792		2.24	2.964		0.000	2.964	
CuO	Cu	0.00	0.01		0.01				0		0				0					
MnO	Mn	0.01	0	0.000	0	0.000	0.000		0	0.000	0	0.000	0.000		0	0.000		0.000		
PbO	Pb	0.00	0		0				0		0				0					
SO3	S	0.49		0.000		0.000			10.88	2.752	10.68	2.702	2.727		11.44	2.894			2.894	
ZnO	Zn	0.00	0.02		0.02				0		0				0					
ZrO2	Zr	0.01	0.04	0.394	0.05	0.492	0.443		0.02	0.197	0.02	0.197	0.197		0	0.000		0.000	0.000	
P2O5	P	1.84	130.26	8.122	130.98	8.167	8.145		150.14	9.362	153.68	9.582	9.472		170.86	10.654		0.000	10.654	
As2O3	As	0.00																		
NiO	Ni	0.00	0.03		0.02				0		0.02				0					
F	F	0.33																		
Cl	Cl	0.14																		
B2O3	B	0.00	35.01		35.45				0.2		0.2				0.21					
CdO	Cd	0.00	0		0				0		0				0.01					
Sb2O3	Sb	0.00																		
Cs2O	Cs	0.00																		
HgO	Hg	0.00																		
SrO	Sr	0.00	0		0				0		0				0					
CaF2	Ca	0.00																		
Nd2O3	Nd	0.02	0.22	0.693		0.000	0.346		0.09	0.283	0.09	0.283	0.283		0.02	0.063		0.000	0.063	

LVC-4 Q			7 DAY						28 DAY						91 DAY					
Chemical	Element	Oxide	Sample C		Sample D				Sample C		Sample D				Sample C		Sample D			
		Wt %	ug/ml	L (g/m^2	ug/ml	L (g/m^2	Ave	pH	ug/ml	L (g/m^2	ug/ml	L (g/m^2	Ave	pH	ug/ml	L (g/m^2	ug/ml	L (g/m^2	Ave	pH
SiO2	Si	28.64	535.38	1.997	551.24	2.056	2.027	12.39	601.75	2.245	600.18	2.239	2.242	12.32	900.1	3.358	432.03	1.612	2.485	12.14
Al2O3	Al	5.59	18.93	0.320	20.54	0.347	0.334	12.36	2.77	0.047	2.15	0.036	0.042	12.32	11.98	0.202	11.75	0.199	0.201	12.09
Fe2O3	Fe	0.01	0	0.000	0	0.000	0.000		0	0.000	0.11	1.545	0.773		0	0.000	0.12	1.686	0.843	
CaO	Ca	4.32	0.4	0.003	1.48	0.012	0.008	12.38	0	0.000	0	0.000	0.000	12.32	0	0.000	0	0.000	0.000	12.12
Na2O	Na	24.38	6107.04	16.881	6569.22	18.159	17.520		6639.03	18.352	6658.21	18.405	18.378		6971.97	19.272	7172.7	19.827	19.549	
K2O	K	0.47	17	2.184	0	0.000	1.092		26.42	3.395	27.29	3.507	3.451		32.12	4.127	35.05	4.504	4.316	
MgO	Mg	0.00	0		0				0		0				0		0			
TiO2	Ti	18.43		0.000		0.000			0.07	0.002	0	0.000	0.001		0.09	0.002	0.31	0.007	0.005	
BaO	Ba	0.00	0		0				0		0				0		0			
Ce2O3	Ce	0.00	0		0				0		0				0		0			
Cr2O3	Cr	0.05	6.85	9.777	7.1	10.134	9.956		7.44	10.619	7.46	10.648	10.634		7.68	10.962	7.99	11.404	11.183	
CuO	Cu	0.00	0		0				0		0				0		0			
MnO	Mn	0.01	0	0.000	0	0.000	0.000		0	0.000	0	0.000	0.000		0	0.000	0	0.000	0.000	
PbO	Pb	0.00	0		0				0		0				0		0			
SO3	S	0.46		0.000		0.000	0.000		68.33	18.643	68.83	18.779	18.711		70.58	19.257	72.87	19.882	19.569	
ZnO	Zn	0.00	0.21		1.29				0		0				0.28		0.3			
ZrO2	Zr	0.01	0	0.000	0	0.000	0.000		0	0.000	0.58	6.159	3.080		0	0.000	0	0.000	0.000	
P2O3	P	16.98	2395	16.157	2525.6	17.038	16.597		2660.96	17.951	2671.22	18.020	17.985		2740.81	18.489	2837.64	19.143	18.816	
As2O3	As	0.00																		
NiO	Ni	0.00	0		0				0		0				0		0			
F	F	0.31																		
Cl	Cl	0.13																		
B2O3	B	0.00	0.75		0				0.54		0.7				0.67		0.78			
CdO	Cd	0.00	0		0				0		0				0		0			
Sb2O3	Sb	0.00																		
Cs2O	Cs	0.00																		
HgO	Hg	0.00																		
SrO	Sr	0.00	0		0				0		0				0		0			
CaF2	Ca	0.00																		
Nd2O3	Nd	0.02	0.66	2.241	0	0.000	1.121		0.96	3.260	0.98	3.328	3.294		1.06	3.600	1.08	3.668	3.634	

Appendix C: Elemental Releases in PCT Tests

LVC-4 H.T.			7 DAY						28 DAY						91 DAY					
Chemical	Element	Oxide	Sample C		Sample D				Sample C		Sample D				Sample C		Sample D			
		Wt %	ug/ml	L (g/m^2	ug/ml	L (g/m^2	Ave	pH	ug/ml	L (g/m^2	ug/ml	L (g/m^2	Ave	pH	ug/ml	L (g/m^2	ug/ml	L (g/m^2	Ave	pH
SiO2	Si	28.64	26.88	0.100	218.25	0.814	0.457	12.04	10.06	0.038	199.07	0.743	0.390	12.04	690.04	2.574	0.01	0.000	1.287	11.79
Al2O3	Al	5.59	12.14	0.205	26.44	0.447	0.326	12.05	0.1	0.002	0.83	0.014	0.008	12.05	18.23	0.308	8.99	0.152	0.230	11.81
Fe2O3	Fe	0.01	0.81	11.380	1.13	15.876	13.628		0.01	0.140	0.11	1.545	0.843		0	0.000	0	0.000	0.000	
CaO	Ca	4.32	2.28	0.018	4.15	0.034	0.026	12.05	0	0.000	0	0.000	0.000	12.05	0	0.000	0	0.000	0.000	11.80
Na2O	Na	24.38	6901.48	19.077	5999.79	16.585	17.831		335.29	0.927	6678.27	18.460	9.693		7421.95	20.516	7176.59	19.838	20.177	
K2O	K	0.47	210.05	26.990	315.98	40.602	33.796		0.48	0.062	27.23	3.499	1.780		0	0.000	0	0.000	0.000	
MgO	Mg	0.00	0		9.85				0		0				0		0			
TiO2	Ti	18.43		0.000		0.000			0	0.000	0	0.000	0.000		0	0.000	0	0.000	0.000	
BaO	Ba	0.00	0		0.33				0		0				0		0			
Ce2O3	Ce	0.00	0		8.15				0		0				0		0			
Cr2O3	Cr	0.05	335.93	479.486	9.29	13.260	246.373		0.45	0.642	9.19	13.117	6.880		9.81	14.002	9.41	13.431	13.717	
CuO	Cu	0.00	0		1.03				0		0				0		0			
MnO	Mn	0.01	0	0.000	0	0.000	0.000		0	0.000	0	0.000	0.000		0	0.000	0	0.000	0.000	
PbO	Pb	0.00	0		0				0		0				0		0			
SO3	S	0.46		0.000		0.000			4.02	1.097	80.98	22.094	11.596		83.83	22.872	82.04	22.383	22.628	
ZnO	Zn	0.00	2.36		2.03				0.06		0				0		0			
ZrO2	Zr	0.01	0	0.000	0	0.000	0.000		0	0.000	0	0.000	0.000		0	0.000	0	0.000	0.000	
P2O5	P	16.98	2687.72	18.131	2831.47	19.101	18.616		152.07	1.026	3064.65	20.674	10.850		3170.68	21.389	3136.73	21.160	21.275	
As2O3	As	0.00																		
NiO	Ni	0.00	0		0				0		0				0		0			
F	F	0.31																		
Cl	Cl	0.13																		
B2O3	B	0.00	0		1.29				0.15		3.42				3.04		3.48			
CdO	Cd	0.00	0		0				0		0				0		0			
Sb2O3	Sb	0.00																		
Cs2O	Cs	0.00																		
HgO	Hg	0.00																		
SrO	Sr	0.00	0		0				0		0				0		0			
CaF2	Ca	0.00																		
Nd2O3	Nd	0.02	5.06	17.185	10.87	36.917	27.051		0.03	0.102	1.08	3.668	1.885		0	0.000	0	0.000	0.000	

LVC-5			7 DAY						28 DAY						91 DAY					
Chemical	Element	Oxide	Sample C		Sample D				Sample C		Sample D				Sample C		Sample D			
		Wt%	ug/ml	NL (g/m^	ug/ml	NL (g/m^	Ave	pH	ug/ml	NL (g/m^	ug/ml	NL (g/m^	Ave	pH	ug/ml	NL (g/m^	ug/ml	NL (g/m^	Ave	pH
SiO2	Si	17.97	20.53	0.122	20.8	0.124	0.123	9.91	23.38	0.139	22.67	0.135	0.137	9.95	23.94	0.142	23.77	0.141	0.142	9.92
Al2O3	Al	13.38	11.07	0.078	11.16	0.079	0.078	10.02	12.63	0.089	12.19	0.086	0.088	9.98	13.01	0.092	12.92	0.091	0.092	9.92
Fe2O3	Fe	19.22	0.02	0.000	0.03	0.000	0.000		0.03	0.000	0.01	0.000	0.000		0.01	0.000	0.01	0.000	0.000	
CaO	Ca	16.62	1.02	0.002	1.01	0.002	0.002	9.965	0.59	0.001	0.54	0.001	0.001	9.965	0.51	0.001	0.53	0.001	0.001	9.92
Na2O	Na	1.75	9.62	0.370	9.93	0.382	0.376		10.8	0.416	10.2	0.393	0.404		12.85	0.495	13.09	0.504	0.499	
K2O	K	4.08	24.42	0.360	25.03	0.369	0.365		29.96	0.442	28.87	0.426	0.434		32.33	0.477	32.77	0.484	0.481	
MgO	Mg	3.11	0	0.000	0	0.000	0.000		0.08	0.002	0.07	0.002	0.002		0	0.000	0	0.000	0.000	
TiO2	Ti	1.63	0	0.000	0	0.000	0.000			0.000		0.000	0.000		0	0.000	0	0.000	0.000	
BaO	Ba	0	0		0				0		0				0		0			
Ce2O3	Ce	0.44	0	0.000	0	0.000	0.000		0.06	0.008	0.07	0.009	0.009		0	0.000	0	0.000	0.000	
Cr2O3	Cr	0.33	0	0.000	0	0.000	0.000		0	0.000	0	0.000	0.000		0	0.000	0	0.000	0.000	
CuO	Cu	0.27	0.02	0.005	0.02	0.005	0.005		0.03	0.007	0.02	0.005	0.006		0.01	0.002	0.01	0.002	0.002	
MnO	Mn	0.89	0	0.000	0	0.000	0.000		0	0.000	0	0.000	0.000		0	0.000	0	0.000	0.000	
PbO	Pb	0.02	0	0.000	0	0.000	0.000		0	0.000	0	0.000	0.000		0	0.000	0	0.000	0.000	
SO3	S	0.64	0.36	0.070	0.36	0.070	0.070		0.51	0.099	0.29	0.057	0.078		0.46	0.090	0.52	0.101	0.096	
ZnO	Zn	0.1	0	0.000	0	0.000	0.000		0	0.000	0	0.000	0.000		0	0.000	0	0.000	0.000	
ZrO2	Zr	0	0		0				0		0				0		0			
P2O5	P	16.69	0.19	0.001	0.2	0.001	0.001		0.82	0.006	0.74	0.005	0.005		0.87	0.006	0.89	0.006	0.006	
As2O3	As	0.03																		
NiO	Ni	2.72	0	0.000	0	0.000	0.000		0	0.000	0	0.000	0.000		0	0.000	0	0.000	0.000	
F	F	0.03																		
Cl	Cl	0.07																		
B2O3	B	0	0.07		0.08				0.08		0.06				0.05		0.06			
CdO	Cd	0	0.01		0				0		0				0		0			
Sb2O3	Sb	0																		
Cs2O	Cs	0																		
HgO	Hg	0																		
SrO	Sr	0													0		0			
CaF2	Ca	0																		
	total	99.99																		

LVC-6			7 DAY						28 DAY						91 DAY					
Chemical	Element	Oxide	Sample C		Sample D				Sample C		Sample D				Sample C		Sample D			
		Wt%	ug/ml	NL (g/m^	ug/ml	NL (g/m^	Ave	pH	ug/ml	NL (g/m^	ug/ml	NL (g/m^	Ave	pH	ug/ml	NL (g/m^	ug/ml	NL (g/m^	Ave	pH
SiO2	Si	23.84	16.89	0.076	16.44	0.074	0.075	9.05	19.81	0.089	19.67	0.088	0.088	9.06	21.19	0.095	20.03	0.090	0.092	9.17
Al2O3	Al	13.56	6.68	0.047	6.37	0.044	0.045	8.98	7.21	0.050	7.1	0.049	0.050	9.00	7.48	0.052	7.06	0.049	0.051	9.06
Fe2O3	Fe	17.87	0	0.000	0	0.000	0.000		0	0.000	0	0.000	0.000		0.01	0.000	0.01	0.000	0.000	
CaO	Ca	14.97	2.02	0.005	2.5	0.006	0.005	9.015	1.21	0.003	1.1	0.003	0.003	9.02	0.91	0.002	1.39	0.003	0.003	9.12
Na2O	Na	1.58	3.54	0.151	3.78	0.161	0.156		5.03	0.215	5.2	0.222	0.218		6.11	0.261	5.98	0.255	0.258	
MgO	Mg	2.85	0.19	0.004	0.24	0.005	0.005		0.22	0.005	0.22	0.005	0.005		0.13	0.003	0.16	0.003	0.003	
K2O	K	3.75	8.55	0.189	9.58	0.212	0.200		15.96	0.353	16.26	0.359	0.356		18.59	0.411	18.24	0.403	0.407	
TiO2	Ti	1.53	0	0.000	0	0.000	0.000			0.000		0.000	0.000		0	0.000	0	0.000	0.000	
BaO	Ba	0	0		0				0		0				0		0		0.000	
Ce2O3	Ce	0.4	0	0.000	0	0.000	0.000		0.07	0.010	0.06	0.009	0.010		0	0.000	0	0.000	0.000	
Cr2O3	Cr	0.3	0	0.000	0	0.000	0.000		0	0.000	0	0.000	0.000		0	0.000	0	0.000	0.000	
CuO	Cu	0.24	0	0.000	0	0.000	0.000		0.01	0.003	0.02	0.005	0.004		0	0.000	0	0.000	0.000	
MnO	Mn	0.81	0	0.000	0	0.000	0.000		0	0.000	0	0.000	0.000		0	0.000	0	0.000	0.000	
PbO	Pb	0.02	0	0.000	0	0.000	0.000		0	0.000	0	0.000	0.000		0	0.000	0	0.000	0.000	
SO3	S	0.58	0	0.000	0	0.000	0.000		19.81	4.264	19.67	4.234	4.249		0.21	0.045	0.19	0.041	0.043	
ZnO	Zn	0.09	0	0.000	0	0.000	0.000		0	0.000	0	0.000	0.000		0	0.000	0	0.000	0.000	
ZrO2	Zr	0	0		0				0		0				0		0		0.000	
P2O5	P	15.04	0.74	0.006	0.98	0.007	0.007		1.07	0.008	1.05	0.008	0.008		0.97	0.007	1.15	0.009	0.008	
As2O3	As	0.03																	0.000	
NiO	Ni	2.45	0	0.000	0	0.000	0.000		0	0.000	0	0.000	0.000		0	0.000	0	0.000	0.000	
F	F	0.03																	0.000	
Cl	Cl	0.06																	0.000	
B2O3	B		0.03		0.04				0.03		0.04				0.04		0.04		0.000	
CdO	Cd								0		0								0.000	
Sb2O3	Sb																		0.000	
Cs2O	Cs																		0.000	
HgO	Hg																		0.000	
SrO	Sr														0		0		0.000	
CaF2	Ca																		0.000	
	total	100																		

LVC-7			7 DAY						28 DAYS						91 DAYS					
Chemical	Element	Oxide	Sample C		Sample D				Sample C		Sample D				Sample C		Sample D			
		Wt%	ug/ml	NL (g/m^2)	ug/ml	NL (g/m^2)	Ave	pH	ug/ml	NL (g/m^2)	ug/ml	NL (g/m^2)	Ave	pH	ug/ml	NL (g/m^2)	ug/ml	NL (g/m^2)	Ave	pH
SiO2	Si	18.68	6.17	0.040	6.25	0.040	0.040	10.32	5.3	0.034	5.35	0.034	0.034	10.22	5.25	0.034	4.87	0.031	0.032	10.05
Al2O3	Al	13.83	13.06	0.089	12.95	0.088	0.089	10.31	13.54	0.093	13.7	0.094	0.093	10.23	13.5	0.092	13.82	0.094	0.093	10
Fe2O3	Fe	1.50	0	0.000	0.02	0.001	0.000		0	0.000	0	0.000	0.000		0.01	0.000	0.01	0.000	0.000	
CaO	Ca	21.53	47.63	0.077	47.77	0.078	0.078	10.32	52.83	0.086	53.26	0.087	0.086	10.23	53.09	0.086	54.68	0.089	0.088	10.03
Na2O	Na	0.53	10.05	1.290	10.25	1.316	1.303		13.32	1.710	13.54	1.738	1.724		16.88	2.167	17.88	2.295	2.231	
MgO	Mg	0.60	0	0.000	0	0.000	0.000		0	0.000	0	0.000	0.000		0	0.000	0.07	0.007	0.004	
K2O	K	0.66	25.27	3.162	24.97	3.125	3.144		39.43	4.934	39.6	4.956	4.945		55.37	6.929	56.14	7.276	7.103	
TiO2	Ti	0.18	0	0.000	0	0.000	0.000			0.000		0.000			0	0.000	0	0.000	0.000	
BaO	Ba	0.03	0.06	0.134	0.06	0.134	0.134		0.05	0.112	0.05	0.112	0.112		0.03	0.067	0.04	0.089	0.078	
Ce2O3	Ce	0.08	0	0.000	0	0.000	0.000		0	0.000	0	0.000	0.000		0	0.000	0	0.000	0.000	
Cr2O3	Cr	0.53	0.54	0.075	0.57	0.079	0.077		0.66	0.092	0.67	0.093	0.093		0.72	0.100	0.79	0.110	0.105	
CuO	Cu	0.00	0						0		0				0.02		0.01			
MnO	Mn	0.06	0	0.000	0	0.000	0.000		0	0.000	0	0.000	0.000		0	0.000	0	0.000	0.000	
PbO	Pb	0.00	0		0				0		0				0		0			
SO3	S	0.00	0.6		0.68				0.76		0.78				0.85		0.93			
ZnO	Zn	0.00	0		0				0		0				0		0			
ZrO2	Zr	17.10	0	0.000	0	0.000	0.000		0	0.000	0	0.000	0.000		0	0.000	0	0.000	0.000	
P2O5	P	0.00	0		0				0		0				0		0			
As2O3	As	0.00	0		0															
NiO	Ni	0.08	0	0.000	0	0.000	0.000		0	0.000	0	0.000	0.000		0	0.000	0	0.000	0.000	
F	F	0.00																		
Cl	Cl	0.00																		
B2O3	B	0.23	18.09	12.944	18.05	12.916	12.930		24.84	17.774	25.24	18.060	17.917		29.89	21.388	31.65	22.647	22.017	
CdO	Cd	0.04	0	0.000	0.02	0.030	0.015		0	0.000	0	0.000	0.000		0	0.000	0	0.000	0.000	
Sb2O3	Sb	0.03																		
Cs2O	Cs	0.23																		
HgO	Hg	0.04																		
SrO	Sr	0.60							1.62	0.160	1.64	0.162	0.161		1.02	0.101	1.01	0.100	0.100	
CaF2	Ca	25.58																		
	total	100.08																		

LVC-8			7 DAY						28 DAYS						91 DAYS					
Chemical	Element	Oxide	Sample C		Sample D				Sample C		Sample D				Sample C		Sample D			
		Wt%	ug/ml	NL (g/m^	ug/ml	NL (g/m^	Ave	pH	ug/ml	NL (g/m^	ug/ml	NL (g/m^	Ave	pH	ug/ml	NL (g/m^	ug/ml	NL (g/m^	Ave	pH
SiO2	Si	16.68	10.52	0.07	10.67	0.07	0.07	9.47	11.13	0.07	10.84	0.07	0.07	9.01	11.33	0.07	11.24	0.07	0.07	8.76
Al2O3	Al	58.29	9.72	0.02	9.95	0.02	0.02	9.30	10.44	0.02	10.13	0.02	0.02	8.98	10.37	0.02	10.29	0.02	0.02	8.71
Fe2O3	Fe	1.47	0.00	0.00	0.00	0.00	0.00		0.00	0.00	0.00	0.00	0.00		0.01	0.00	0.01	0.00	0.00	
CaO	Ca	5.52	3.86	0.02	3.80	0.02	0.02	9.39	2.41	0.02	2.35	0.01	0.02	9.00	2.57	0.02	2.52	0.02	0.02	8.74
Na2O	Na	0.54	5.42	0.68	5.55	0.69	0.68		7.72	0.96	7.86	0.98	0.97		9.35	1.17	9.38	1.17	1.17	
MgO	Mg	15.60	0.88	0.00	0.89	0.00	0.00		0.88	0.00	0.89	0.00	0.00		0.84	0.00	0.86	0.00	0.00	
K2O	K	0.81	0.00	0.00	0.00	0.00	0.00		1.70	0.18	1.41	0.15	0.16		3	0.31	3.2	0.33	0.32	
TiO2	Ti	0.18	0.00	0.00	0.00	0.00	0.00			0.00		0.00			0	0.00	0	0.00	0.00	
BaO	Ba	0.03	0.00	0.00	0.00	0.00	0.00		0.00	0.00	0.00	0.00	0.00		0	0.00	0	0.00	0.00	
Ce2O3	Ce	0.03	0.00	0.00	0.00	0.00	0.00		0.00	0.00	0.00	0.00	0.00		0	0.00	0.04	0.08	0.04	
Cr2O3	Cr	0.12	0.00	0.00	0.00	0.00	0.00		0.00	0.00	0.00	0.00	0.00		0	0.00	0	0.00	0.00	
CuO	Cu	0.00	0.00		0.00				0.00		0.00				0		0			
MnO	Mn	0.06	0.00	0.00	0.00	0.00	0.00		0.00	0.00	0.00	0.00	0.00		0	0.00	0	0.00	0.00	
PbO	Pb	0.00	0.00		0.00				0.00		0.00				0		0			
SO3	S	0.00	0.00		0.11				0.00		0.08				0.1		0.1			
ZnO	Zn	0.00	0.00		0.00				0.00		0.00				0		0			
ZrO2	Zr	0.12	0.00	0.00	0.00	0.00	0.00		0.00	0.00	0.00	0.00	0.00		0	0.00	0	0.00	0.00	
P2O5	P	0.00	0.00		0.00				0.12		0.12				0.12		0.12			
As2O3	As	0.00	0.00		0.00															
NiO	Ni	0.06	0.00	0.00	0.00	0.00	0.00		0.00	0.00	0.00	0.00	0.00		0	0.00	0	0.00	0.00	
F	F	0.00																		
Cl	Cl	0.00																		
B2O3	B	0.24	0.72	0.48	0.70	0.47	0.48		0.60	0.40	0.55	0.37	0.39		0.64	0.43	0.62	0.42	0.42	
CdO	Cd	0.03	0.00	0.00	0.00	0.00	0.00		0.00	0.00	0.00	0.00	0.00			0.00		0.00		
Sb2O3	Sb	0.03								0.00		0.00				0.00		0.00		
Cs2O	Cs	0.03								0.00		0.00				0.00		0.00		
HgO	Hg	0.03								0.00		0.00				0.00		0.00		
SrO	Sr	0.03	0.46	0.91	0.45	0.89	0.90		0.36	0.71	0.35	0.69	0.70		0.34	0.67	0.33	0.65	0.66	
CaF2	Ca	0.24		0.00		0.00				0.00		0.00				0.00		0.00		
	total	100.11								0.00		0.00				0.00		0.00		

LVC-9			7 DAY						28 DAY						91 DAY					
Chemical	Element	Oxide	Sample C		Sample D				Sample C		Sample D				Sample C		Sample D			
		Wt%	ug/ml	NL (g/m^2)	ug/ml	NL (g/m^2)	Ave	pH	ug/ml	NL (g/m^2)	ug/ml	NL (g/m^2)	Ave	pH	ug/ml	NL (g/m^2)	ug/ml	NL (g/m^2)	Ave	pH
SiO2	Si	33.35	14	0.045	14.09	0.045	0.045	9.06	13.66	0.044	13.95	0.045	0.044	8.6	14.53	0.047	14.35	0.046	0.046	8.4
Al2O3	Al	42.89	7.17	0.016	7.32	0.016	0.016	8.98	6.22	0.014	6.5	0.014	0.014	8.57	6.5	0.014	6.48	0.014	0.014	8.37
Fe2O3	Fe	2.78	0.02	0.001	0.01	0.000	0.000		0	0.000	0	0.000	0.000		0.01	0.000	0.01	0.000	0.000	
CaO	Ca	6.48	2.58	0.014	2.56	0.014	0.014	9.02	2.3	0.012	2.32	0.013	0.012	8.585	2.57	0.014	2.55	0.014	0.014	8.385
Na2O	Na	0.76	2.44	0.216	2.47	0.219	0.218		2.52	0.223	2.59	0.230	0.227		3.23	0.288	3.09	0.274	0.280	
MgO	Mg	11.2	1.05	0.006	1.06	0.006	0.006		1.09	0.006	1.09	0.006	0.006		1.16	0.006	1.16	0.006	0.006	
K2O	K	1.37	0	0.000	0	0.000	0.000		1.32	0.080	1.12	0.068	0.074		2.02	0.122	2.39	0.145	0.133	
TiO2	Ti	0.35	0	0.000	0	0.000	0.000		0	0.000	0	0.000	0.000		0	0.000	0	0.000	0.000	
BaO	Ba	0.05	0	0.000	0.16	0.179	0.089		0	0.000	0	0.000	0.000		0	0.000	0	0.000	0.000	
Ce2O3	Ce	0.02	0	0.000	0	0.000	0.000		0	0.000	0	0.000	0.000		0	0.000	0	0.000	0.000	
Cr2O3	Cr	0.08	0	0.000	0	0.000	0.000		0	0.000	0	0.000	0.000		0	0.000	0	0.000	0.000	
CuO	Cu	0	0		0				0		0				0		0			
MnO	Mn	0.07	0	0.000	0	0.000	0.000		0	0.000	0	0.000	0.000		0	0.000	0	0.000	0.000	
PbO	Pb	0	0		0				0	0.000	0	0.000	0.000		0		0			
SO3	S	0	0		0				0		0				0		0.09			
ZnO	Zn	0	0		0				0	0.000	0	0.000	0.000		0		0			
ZrO2	Zr	0.08	0	0.000	0	0.000	0.000		0	0.000	0	0.000	0.000		0	0.000	0	0.000	0.000	
P2O5	P	0	0.09		0.08				0.1		0.1				0.11					
As2O3	As	0	0		0															
NiO	Ni	0.04	0	0.000	0	0.000	0.000		0	0.000	0	0.000	0.000		0	0.000	0	0.000	0.000	
F	F	0																		
Cl	Cl	0																		
B2O3	B	0.16	0.15	0.151	0.16	0.161	0.156		0.13	0.131	0.13	0.131	0.131		0.15	0.151	0.15	0.151	0.151	
CdO	Cd	0.02	0.01	0.029	0	0.000	0.014		0	0.000	0	0.000	0.000		0	0.000	0	0.000	0.000	
Sb2O3	Sb	0.05																		
Cs2O	Cs	0.02																		
HgO	Hg	0.02																		
SrO	Sr	0.02	0.12	0.355	0.12	0.355	0.355		0.1	0.296	0.1	0.296	0.296		0.1	0.296	0.1	0.296	0.296	
CaF2	Ca	0.16																		
	total	99.97																		

LVC-10 Q			7 DAY						28 DAY						91 DAY					
Chemical	Element	Oxide	Sample C		Sample D				Sample C		Sample D				Sample C		Sample D			
		Wt%	ug/ml	NL (g/m^2)	ug/ml	NL (g/m^2)	Ave	pH	ug/ml	NL (g/m^2)	ug/ml	NL (g/m^2)	Ave	pH	ug/ml	NL (g/m^2)	ug/ml	NL (g/m^2)	Ave	pH
SiO2	Si	44.79	63.99	0.153	63.58	0.152	0.152	10.62	72.92	0.174	72.86	0.174	0.174	10.88	75.01	0.179	76.19	0.182	0.180	10.97
Al2O3	Al	35	53.26	0.144	52.23	0.141	0.142	10.64	59.67	0.161	59.74	0.161	0.161	10.88	60.89	0.164	62.15	0.168	0.166	10.96
Fe2O3	Fe	0	0.15		0.15				0.11		0.11				0.12		0.12			
CaO	Ca	0	0		0			10.63	0		0			10.88	0.14		0.13			10.965
Na2O	Na	18	75.64	0.283	74.95	0.281	0.282		99.43	0.372	99.37	0.372	0.372		119.95	0.449	122.57	0.459	0.454	
MgO	Mg	0.33	0	0.000	0	0.000	0.000		0	0.000	0	0.000	0.000		0.14	0.026	0.13	0.024	0.025	
K2O	K	0.33	0	0.000	0	0.000	0.000		0	0.000	0	0.000	0.000		1.46	0.266	1.05	0.192		
TiO2	Ti	0	0.01		0.01				0		0				0.02		0.02			
BaO	Ba	0	0		0				0		0				0		0			
Ce2O3	Ce	0	0		0				0		0				0		0			
Cr2O3	Cr	0.04	0.04	0.073	0.04	0.073	0.073		0.04	0.073	0.05	0.091	0.082		0.05	0.091	0.05	0.091	0.091	
CuO	Cu	0	0		0				0		0				0.01		0			
MnO	Mn	0.01	0	0.000	0	0.000	0.000		0	0.000	0	0.000	0.000		0	0.000	0	0.000	0.000	
PbO	Pb	0	0		0				0		0				0		0			
SO3	S	0.32	0.21	0.082	0.21	0.082	0.082		0.12	0.047	0.11	0.043	0.045		0.18	0.070	0.16	0.062	0.066	
ZnO	Zn	0	0		0				0		0				0.01		0.01			
ZrO2	Zr	0.01	0.01	0.068	0.01	0.068	0.068		0.01	0.068	0.01	0.068	0.068		0.02	0.135	0.02	0.135	0.135	
P2O5	P	1.18	1.03	0.100	1.05	0.102	0.101		1.24	0.120	1.25	0.121	0.121		1.19	0.116	1.22	0.118	0.117	
As2O3	As	0	0		0															
NiO	Ni	0	0.02		0.02				0		0				0.02		0.02			
F	F	0.21																		
Cl	Cl	0.09																		
B2O3	B	0	0.03		0.03				0.02		0.02				0.03		0.03			
CdO	Cd	0	0		0				0		0				0		0			
Sb2O3	Sb	0																		
Cs2O	Cs	0																		
HgO	Hg	0																		
SrO	Sr	0	0		0				0		0				0		0			
CeF2	Ce	0													0.14		0.13			
Bi2O3	Bi	0.01	0	0.000	0	0.000	0.000		0	0.000	0	0.000	0.000		0.06	0.350	0	0.000	0.175	
Nd2O3	Nd	0.01	0	0	0.02	0.195	0.097		0.02	0	0.02	0	0.000		0.07	0	0.06	0	0.000	
	total	99.99																		

LVC-10 HT			7 DAY						28 DAYS						91 DAYS					
Chemical	Element	Oxide	Sample C		Sample D				Sample C		Sample D				Sample C		Sample D			
		Wt%	ug/ml	NL (g/m^2)	ug/ml	NL (g/m^2)	Ave	pH	ug/ml	NL (g/m^2)	ug/ml	NL (g/m^2)	Ave	pH	ug/ml	NL (g/m^2)	ug/ml	NL (g/m^2)	Ave	pH
SiO2	Si	44.79	65.39	0.156	64.32	0.153	0.155	9.85	73.34	0.175	74.04	0.177	0.176	10.16	74.87	0.179	75.13	0.179	0.179	10.04
Al2O3	Al	35	56.42	0.152	55.58	0.150	0.151	9.93	64.88	0.175	64.73	0.175	0.175	10.18	65.33	0.176	66.01	0.178	0.177	10.03
Fe2O3	Fe	0	0.06		0.08				0.04		0.05				0.06		0.07			
CaO	Ca	0	0		0			9.89	0		0			10.17	0.13		0.19			10.035
Na2O	Na	18	59.66	0.223	58.86	0.220	0.222		70.4	0.264	70.21	0.263	0.263		74.56	0.279	76.24	0.285	0.282	
MgO	Mg	0.33	0	0.000	0	0.000	0.000		0	0.000	0	0.000	0.000		0	0.000	0	0.000	0.000	
K2O	K	0.33	0	0.000	0.32	0.058	0.029		0	0.000	0	0.000	0.000		0	0.000	0	0.000	0.000	
TiO2	Ti	0	0		0										0.01		0			
BaO	Ba	0	0.01		0.01				0		0				0		0			
Ce2O3	Ce	0	0		0										0		0			
Cr2O3	Cr	0.04	0.02	0.037	0.02	0.037	0.037		0	0.000	0	0.000	0.000		0	0.000	0	0.000	0.000	
CuO	Cu	0	0.01		0				0		0				0.01		0.01			
MnO	Mn	0.01	0.01	0.065	0.01	0.065	0.065		0	0.000	0	0.000	0.000		0	0.000	0	0.000	0.000	
PbO	Pb	0	0		0				0		0				0		0			
SO3	S	0.32	0.59	0.230	0.67	0.261	0.246		0.44	0.172	0.38	0.148	0.160		0.41		0.5			
ZnO	Zn	0	0		0				0		0				0		0			
ZrO2	Zr	0.01	0.01	0.068	0	0.000	0.034		0	0.000	0	0.000	0.000		0	0.000	0	0.000	0.000	
P2O5	P	1.18	0.98	0.095	0.97	0.094	0.095		1.19	0.116	1.13	0.110	0.113		1.19	0.116	1.2	0.117	0.116	
As2O3	As	0	0		0															
NiO	Ni	0	0		0				0		0				0.02		0.02			
F	F	0.21								0.000		0.000								
Cl	Cl	0.09																		
B2O3	B	0	0.06		0.06				0.07		0.05				0.06		0.07			
CdO	Cd	0	0		0				0		0				0		0			
Sb2O3	Sb	0																		
Ce2O	Ce	0																		
HgO	Hg	0																		
SrO	Sr	0	0.01		0				0		0				0		0			
CeF2	Ce	0																		
Bi2O3	Bi	0.01	0	0.000	0	0.000	0.000		0	0.000	0	0.000	0.000		0	0.000	0	0.000	0.000	
Nd2O3	Nd	0.01	0	0.000	0	0.000	0.000		0	0	0	0	0.000		0.02	0.117	0.02	0.117	0.117	
	total	99.99																		

LVC-11 (acmite)			7DAY					
Chemical	Element	Oxide	Sample C		Sample D			
		Wt %	ug/ml	NL (g/m^2)	ug/ml	NL (g/m^2)	Ave	pH
SiO2	Si	50.96	215.68	0.452	220.07	0.461	0.457	10.76
Al2O3	Al	0.95	0.47	0.047	0.47	0.047	0.047	10.80
Fe2O3	Fe	33.40	10.57	0.023	14	0.030	0.026	
CaO	Ca	0.00	0.22		0.21			10.78
Na2O	Na	12.46	198.94	1.076	204.38	1.105	1.091	
MgO	Mg	0.00	0		0			
K2O	K	0.33	0	0.000	0	0.000	0.000	
TiO2	Ti	0.00						
BaO	Ba	0.00	0		0			
Ce2O3	Ce	0.00	0		0			
Cr2O3	Cr	0.04	0	0.000	0	0.000	0.000	
CuO	Cu	0.00	0		0			
MnO	Mn	0.01	0	0.000	0	0.000	0.000	
PbO	Pb	0.00	0		0			
SO3	S	0.32		0.000		0.000	0.000	
ZnO	Zn	0.00	0		0			
ZrO2	Zr	0.00	0	0.000	0	0.000	0.000	
P2O5	P	1.20	7.3	0.697	7.07	0.675	0.686	
As2O3	As	0.00						
NiO	Ni	0.00	0		0			
F	F	0.22						
Cl	Cl	0.09						
B2O3	B	0.00	0.09		0.21			
CdO	Cd	0.00	0		0			
Sb2O3	Sb	0.00						
Cs2O	Cs	0.00						
HgO	Hg	0.00						
SrO	Sr	0.00	0		0			
CaF2	Ca	0.00						
Bi2O3	Bi	0.01	0	0.000	0	0.000	0.000	
Nd2O3	Nd	0.01	0	0.000	0	0.000	0.000	
	total	100.01						
LVC-11HT (acmite)			7 DAY					
Chemical	Element	Oxide	Sample C		Sample D			
		Wt %	ug/ml	NL (g/m^2)	ug/ml	NL (g/m^2)	Ave	pH
SiO2	Si	50.96	161.53	0.339	162.36	0.340	0.340	11.29
Al2O3	Al	0.95	8.61	0.856	8.59	0.854	0.855	11.22
Fe2O3	Fe	33.40	13.08	0.028	12.28	0.026	0.027	
CaO	Ca	0.00	0.18		0.19			11.26
Na2O	Na	12.46	214.48	1.160	214.22	1.159	1.159	
MgO	Mg	0.00	0		0			
K2O	K	0.33	1.93	0.485	1.46	0.367	0.426	
TiO2	Ti	0.00						
BaO	Ba	0.00	0		0			
Ce2O3	Ce	0.00	0		0			
Cr2O3	Cr	0.04	0	0.000	0	0.000	0.000	
CuO	Cu	0.00	0.01		0.01			
MnO	Mn	0.01	0.01	0.090	0.01	0.090	0.090	
PbO	Pb	0.00	0		0			
SO3	S	0.32		0.000		0.000	0.000	
ZnO	Zn	0.00	0		0			
ZrO2	Zr	0.00	0	0.000	0	0.000	0.000	
P2O5	P	1.20	12.71	1.214	12.98	1.239	1.226	
As2O3	As	0.00						
NiO	Ni	0.00	0		0			
F	F	0.22						
Cl	Cl	0.09						
B2O3	B	0.00	0.16		0.15			
CdO	Cd	0.00	0		0			
Sb2O3	Sb	0.00						
Cs2O	Cs	0.00						
HgO	Hg	0.00						
SrO	Sr	0.00	0		0			
CaF2	Ca	0.00						
Bi2O3	Bi	0.01	0.07	0.799	0.07	0.799	0.799	
Nd2O3	Nd	0.01	0.05	0.241	0.04	0.193	0.217	
	total	100.01						

LVC-12(LLW/TiO2)			7 DAY					
Chemical	Element	Oxide	Sample C		Sample D			
		Wt %	ug/ml	NL (g/m^2)	ug/ml	NL (g/m^2)	Ave	pH
SiO2	Si	38.77	68.52	0.189	69.25	0.191	0.190	10.91
Al2O3	Al	32.89	67.95	0.195	68.46	0.197	0.196	10.68
Fe2O3	Fe	0.00	0.06	1.208	0.06	1.208	1.208	
CaO	Ca	0.00	0.21		0.22			10.80
Na2O	Na	20.00	97.38	0.328	97.44	0.328	0.328	
MgO	Mg	0.00	0.02		0.02			
K2O	K	0.33	0	0.000	0	0.000	0.000	
TiO2	Ti	6.12	7.48	0.510	6.76	0.461	0.486	
BaO	Ba	0.00	0		0			
Ce2O3	Ce	0.00	0		0			
Cr2O3	Cr	0.04	0.06	0.123	0.06	0.123	0.123	
CuO	Cu	0.00	0		0			
MnO	Mn	0.01	0.02	0.182	0.02	0.182	0.182	
PbO	Pb	0.00	0		0.09			
SO3	S	0.32		0.000		0.000		
ZnO	Zn	0.00	0.25		0.26			
ZrO2	Zr	0.00	0.03	0.456	0	0.000	0.228	
P2O5	P	1.19	1.97	0.190	1.98	0.191	0.190	
As2O3	As	0.00						
NiO	Ni	0.00	0		0			
F	F	0.21						
Cl	Cl	0.09						
B2O3	B	0.00	0.02		0.02			
CdO	Cd	0.00	0		0			
Sb2O3	Sb	0.00						
Cs2O	Cs	0.00						
HgO	Hg	0.00						
SrO	Sr	0.00	0		0.01			
CaF2	Ca	0.00						
Bi2O3	Bi	0.01	0	0.000	0	0.000	0.000	
Nd2O3	Nd	0.01	0.03	0.146	0.06	0.292	0.219	
	total	100.00						
LVC-12HT			7 DAY					
Chemical	Element	Oxide	Sample C		Sample D			
		Wt %	ug/ml	NL (g/m^2)	ug/ml	NL (g/m^2)	Ave	pH
SiO2	Si	38.77	23	0.063	22.92	0.063	0.063	9.43
Al2O3	Al	32.89	55.34	0.159	54.12	0.155	0.157	9.43
Fe2O3	Fe	0.00	0.02	0.403	0.02	0.403	0.403	
CaO	Ca	0.00	0.19		0.21			9.43
Na2O	Na	20.00	186.62	0.629	182.97	0.617	0.623	
MgO	Mg	0.00	0		0			
K2O	K	0.33	0	0.000	0	0.000	0.000	
TiO2	Ti	6.12	0.15	0.010	0.16	0.011	0.011	
BaO	Ba	0.00	0		0			
Ce2O3	Ce	0.00	0		0			
Cr2O3	Cr	0.04	0	0.000	0	0.000	0.000	
CuO	Cu	0.00	0		0			
MnO	Mn	0.01	0.01	0.091	0.01	0.091	0.091	
PbO	Pb	0.00	3.8		3.7			
SO3	S	0.32		0.000		0.000		
ZnO	Zn	0.00	0.01		0.01			
ZrO2	Zr	0.00	0.02	0.304	0.03	0.456	0.380	
P2O5	P	1.19	0	0.000	0.09	0.009	0.004	
As2O3	As	0.00						
NiO	Ni	0.00	0		0			
F	F	0.21						
Cl	Cl	0.09						
B2O3	B	0.00	0.93		0.93			
CdO	Cd	0.00	0		0			
Sb2O3	Sb	0.00						
Cs2O	Cs	0.00						
HgO	Hg	0.00						
SrO	Sr	0.00	0		0			
CaF2	Ca	0.00						
Bi2O3	Bi	0.01	0	0.000	0	0.000	0.000	
Nd2O3	Nd	0.01	0.05	0.243	0.05	0.243	0.243	
	total	100.00						

LVC-13 (LLW)			7 DAY					
Chemical	Element	Oxide	Sample C		Sample D			
		Wt %	ug/ml	NL (g/m^2)	ug/ml	NL (g/m^2)	Ave	pH
SiO2	Si	44.89	70.45	0.168	70.42	0.168	0.168	10.80
Al2O3	Al	32.89	59.53	0.171	59.37	0.171	0.171	10.70
Fe2O3	Fe	0.00	0.08	1.610	0.62	12.478	7.044	
CaO	Ca	0.00	0.19		0.18			10.75
Na2O	Na	20.00	92.08	0.310	89.02	0.300	0.305	
MgO	Mg	0.00	0		0			
K2O	K	0.33	0	0.000	0	0.000	0.000	
TiO2	Ti	0.00	0.01		0.01			
BaO	Ba	0.00	0		0			
Ce2O3	Ce	0.00	0		0			
Cr2O3	Cr	0.04	0.07	0.143	0.07	0.143	0.143	
CuO	Cu	0.00	0		0			
MnO	Mn	0.01	0	0.000	0.01	0.091	0.045	
PbO	Pb	0.00	0		0			
SO3	S	0.32		0.000		0.000		
ZnO	Zn	0.00	0.27		0.28			
ZrO2	Zr	0.00	0.02	0.304	0.02	0.304	0.304	
P2O5	P	1.19	1.72	0.166	1.72	0.166	0.166	
As2O3	As	0.00						
NiO	Ni	0.00	0		0			
F	F	0.21						
Cl	Cl	0.09						
B2O3	B	0.00	0.02		0			
CdO	Cd	0.00	0		0			
Sb2O3	Sb	0.00						
Cs2O	Cs	0.00						
HgO	Hg	0.00						
SrO	Sr	0.00	0		0			
CaF2	Ca	0.00						
Bi2O3	Bi	0.01	0		0			
Nd2O3	Nd	0.01	0.03	0.146	0.05	0.243	0.195	
	total	100.00						
LVC-13HT			7 DAY					
Chemical	Element	Oxide	Sample C		Sample D			
		Wt %	ug/ml	NL (g/m^2)	ug/ml	NL (g/m^2)	Ave	pH
SiO2	Si	44.89	15.3	0.036	15.17	0.036	0.036	9.07
Al2O3	Al	32.89	22.79	0.065	22.53	0.065	0.065	9.07
Fe2O3	Fe	0.00	0.02	0.403	0.02	0.403	0.403	
CaO	Ca	0.00	0.28		0.15			9.07
Na2O	Na	20.00	120.54	0.406	120.48	0.406	0.406	
MgO	Mg	0.00	0		0			
K2O	K	0.33	0	0.000	0	0.000	0.000	
TiO2	Ti	0.00	0.02		0.02			
BaO	Ba	0.00	0		0			
Ce2O3	Ce	0.00	0		0			
Cr2O3	Cr	0.04	2.25	4.600	2.33	4.764	4.682	
CuO	Cu	0.00	0		0			
MnO	Mn	0.01	0.02	0.182	0.02	0.182	0.182	
PbO	Pb	0.00	0		0			
SO3	S	0.32		0.000		0.000		
ZnO	Zn	0.00	0.01		0			
ZrO2	Zr	0.00	0.07	1.065	0.07	1.065	1.065	
P2O5	P	1.19	48.27	4.650	47.82	4.607	4.629	
As2O3	As	0.00						
NiO	Ni	0.00	0		0			
F	F	0.21						
Cl	Cl	0.09						
B2O3	B	0.00	0.19		0.19			
CdO	Cd	0.00	0		0			
Sb2O3	Sb	0.00						
Cs2O	Cs	0.00						
HgO	Hg	0.00						
SrO	Sr	0.00	0		0			
CaF2	Ca	0.00						
Bi2O3	Bi	0.01	0.1	1.151	0.09	1.036	1.094	
Nd2O3	Nd	0.01	0.05	0.243	0.04	0.195	0.219	
	total	100.00						

LVC-14			7 DAY						28 DAY						91 DAY					
Chemical	Element	Oxide	Sample C		Sample D				Sample C		Sample D				Sample C		Sample D			
		Wt %	ug/ml	NL (g/m^2)	ug/ml	NL (g/m^2)	Ave	pH	ug/ml	NL (g/m^2)	ug/ml	NL (g/m^2)	Ave	pH	ug/ml	NL (g/m^2)	ug/ml	NL (g/m^2)	Ave	pH
SiO2	Si	6.67	4.56	0.073	4.53	0.073	0.073	9.37	4.19	0.067	4.21	0.067	0.067	9.20	36.72	0.588	3.737	0.060	0.324	8.95
Al2O3	Al	37.19	16.71	0.042	16.33	0.041	0.042	9.37	17.76	0.045	17.47	0.044	0.045	9.17	62.644	0.159	20.53	0.052	0.106	9.06
Fe2O3	Fe	2.72	0	0.000	0	0.000	0.000		0.02	0.001	0.02	0.001	0.001		4.701	0.124	0.012	0.000	0.062	
CaO	Ca	17.57	26.2	0.052	25.66	0.051	0.052	9.37	29.2	0.058	28.65	0.057	0.058	9.19	120.931	0.241	29.303	0.058	0.150	9.01
Na2O	Na	0.414	6.35	1.034	6.19	1.008	1.021		6.76	1.100	6.56	1.068	1.084		16.989	2.765	9.764	1.589	2.177	
MgO	Mg	0.24	0.23	0.079	0.25	0.086	0.083		0.1	0.035	0.11	0.038	0.036		0.964	0.333	0.008	0.003	0.168	
K2O	K	0.369	1.02	0.229	1.66	0.373	0.301		2.62	0.634	3.07	0.690	0.662		4.205	0.945	1.812	0.407	0.676	
TiO2	Ti	0.07							0		0				0.235		0			
BaO	Ba	0.01	0.02	0.112	0.02	0.112	0.112		0.02	0.112	0.02	0.112	0.112		0.191	1.066	0.006	0.033	0.550	
Ce2O3	Ce	0.073	0	0.000	0	0.000	0.000		0	0.000	0	0.000	0.000		0.027	0.022	0	0.000	0.011	
Cr2O3	Cr	0.466	0.08	0.013	0.09	0.014	0.013		0.1	0.016	0.08	0.013	0.014		0.099	0.016	0.111	0.017	0.016	
CuO	Cu	0	0		0				0.01		0.01				0.016		0.001			
MnO	Mn	0.054	0	0.000	0	0.000	0.000		0	0.000	0	0.000	0.000		0.089	0.106	0.001	0.001	0.054	
PbO	Pb	0	0		0				0		0				0		0			
SO3	S	0	0		0				0.17		0.17				0.275		0.183			
ZnO	Zn	0	0		0				0		0				0		0			
ZrO2	Zr	13.284	0	0.000	0	0.000	0.000		0	0.000	0	0.000	0.000		2.056	0.010	0	0.000	0.005	
P2O5	P	0	0.16		0.15				0		0				2.216		0.095			
As2O3	As	0																		
NiO	Ni	0.088	0	0.000	0	0.000	0.000		0	0.000	0	0.000	0.000		0.036	0.026	0.008	0.006	0.016	
F	F	0																		
Cl	Cl	0																		
B2O3	B	0.294	8.05	4.408	8.11	4.441	4.425		8.6	4.709	8.42	4.611	4.660		16.429	8.997	10.983	6.014	7.506	
CdO	Cd	0.044	0	0.000	0	0.000	0.000		0	0.000	0	0.000	0.000		0.004	0.005	0	0.000	0.003	
Sb2O3	Sb	0.01		0.000		0.000				0.000		0.000				0.000		0.000		
Ce2O	Ce	0.189		0.000		0.000				0.000		0.000				0.000		0.000		
HgO	Hg	0.044		0.000		0.000				0.000		0.000				0.000		0.000		
SrO	Sr	0.479		0.000		0.000			1.6	0.198	1.55	0.191	0.194		4.117	0.508	1.101	0.136	0.322	
CaF2	Ca	19.898		0.000		0.000				0.000		0.000				0.000		0.000		
Bi2O3	Bi	0	0		0				0		0				0.04		0.007			
Nd2O3	Nd	0	0.06		0.07				0.1		0.11				0.006		0.055			
	total	100.19																		

LVC-15			7 DAY						28 DAY						91 DAY					
Chemical	Element	Oxide	Sample C		Sample D				Sample C		Sample D				Sample C		Sample D			
		Wt %	ug/ml	NL (g/m^2)	ug/ml	NL (g/m^2)	Ave	pH	ug/ml	NL (g/m^2)	ug/ml	NL (g/m^2)	Ave	pH	ug/ml	NL (g/m^2)	ug/ml	NL (g/m^2)	Ave	pH
SiO2	Si	6.67	6.63	0.106	6.53	0.105	0.105	8.73	6.26	0.100	6.25	0.100	0.100	8.66	6.225	0.100	6.159	0.099	0.099	8.58
Al2O3	Al	31.87	10.64	0.032	10.73	0.032	0.032	8.70	1.65	0.005	10.61	0.031	0.018	8.65	11.486	0.034	11.693	0.035	0.034	8.52
Fe2O3	Fe	2.70	0	0.000	0	0.000	0.000		0.01	0.000	0	0.000	0.000		0	0.000	0	0.000	0.000	
CaO	Ca	15.99	12.23	0.027	12.38	0.027	0.027	8.72	13.3	0.029	13.28	0.029	0.029	8.66	14.536	0.032	15.259	0.033	0.033	8.55
Na2O	Na	0.379	4.34	0.772	4.64	0.825	0.798		4.7	0.836	4.71	0.838	0.837		6.113	1.087	6.979	1.241	1.164	
MgO	Mg	0.24	0.47	0.162	0.46	0.159	0.161		0.5	0.173	0.49	0.169	0.171		0.52	0.180	0.543	0.188	0.184	
K2O	K	0.3515	2.12	0.500	1.57	0.370	0.435		2.93	0.691	2.89	0.682	0.686		2.8	0.660	3.015	0.711	0.686	
TiO2	Ti	10.07		0.000		0.000			0	0.000	0	0.000	0.000		0.002	0.000	0.004	0.000	0.000	
BeO	Be	0.01	0.01	0.056	0.01	0.056	0.056		0.01	0.056	0.01	0.056	0.056		0.007	0.039	0.008	0.045	0.042	
Ce2O3	Ce	0.0655	0	0.000	0	0.000	0.000		0	0.000	0	0.000	0.000		0.026	0.023	0.029	0.026	0.025	
Cr2O3	Cr	0.421	0	0.000	0	0.000	0.000		0	0.000	0	0.000	0.000		0.01	0.002	0.01	0.002	0.002	
CuO	Cu	0	0		0				0.01	0.000	0.01	0.000	0.000		0.006	0.000	0.006	0.000	0.000	
MnO	Mn	0.049	0	0.000	0	0.000	0.000		0	0.000	0	0.000	0.000		0.001	0.001	0.001	0.001	0.001	
PbO	Pb	0	0		0				0	0.000	0	0.000	0.000		0.015	0.000	0.013	0.000	0.000	
SO3	S	0	0		0.09				0.18		0.2				0.234		0.277			
ZnO	Zn	0	0		0				0	0.000	0	0.000	0.000		0	0.000	0	0.000	0.000	
ZrO2	Zr	12.134	0	0.000	0	0.000	0.000		0	0.000	0	0.000	0.000		0	0.000	0	0.000	0.000	
P2O5	P	0	0.23		0.19				0		0				.088	0.000	0.11	0.000	0.000	
As2O3	As	0																		
NiO	Ni	0.078	0	0.000	0	0.000	0.000		0	0.000	0	0.000	0.000		0.009	0.007	0.011	0.009	0.008	
F	F	0																		
Cl	Cl	0																		
B2O3	B	0.259	3.12	1.939	3.3	2.051	1.995		3.21	1.995	3.31	2.058	2.026		4.062	2.525	4.469	2.778	2.651	
CdO	Cd	0.039	0	0.000	0	0.000	0.000		0	0.000	0	0.000	0.000		0.002	0.003	0.002	0.003	0.003	
Sb2O3	Sb	0.01		0.000		0.000			0	0.000	0	0.000	0.000			0.000		0.000		
Ce2O	Ce	0.1715		0.000		0.000				0.000		0.000				0.000		0.000		
HgO	Hg	0.039		0.000		0.000				0.000		0.000				0.000		0.000		
SrO	Sr	0.4365		0.000		0.000			0.75	0.102	0.75	0.102	0.102		0.843	0.114	0.877	0.119	0.116	
CeF2	Ce	18.173		0.000		0.000				0.000		0.000				0.000		0.000		
Bi2O3	Bi	0	0		0				0		0				0.018		0.018			
Nd2O3	Nd	0	0.07		0.05				0.08		0.08				0.067		0.071			

LVC-16Q			7 DAY						28 DAY					
Chemical	Element	Oxide	Sample C		Sample D				Sample C		Sample D			
		Wt %	ug/ml	L (g/m^2	ug/ml	L (g/m^2	Ave	pH	ug/ml	L (g/m^2	ug/ml	L (g/m^2	Ave	pH
SiO2	Si	34.42	19.42	0.060	16.64	0.052	0.056	7.35	20.13	0.062	25.76	0.080	0.071	7.22
Al2O3	Al	9.39	10.76	0.108	9.8	0.099	0.103	7.38	5.32	0.054	6.96	0.070	0.062	7.27
Fe2O3	Fe		0.22		0.39				1.44		0.95			
CaO	Ca		0		0			7.37	1.05		0.89			7.25
Na2O	Na		10.81		12.88				23.47		22.15			
MgO	Mg		0		1.05				1.49		0.78			
K2O	K		17.17		30.54				32.1		14.46			
TiO2	Ti		0.08		0.14				0.09		0.07			
BaO	Ba		0.14		0.15				9		0.07			
Ce2O3	Ce		0.44		0.75				0.89		0.39			
Cr2O3	Cr		0		0				0.53		0.32			
CuO	Cu		0.07		0.12				0.12		0.06			
MnO	Mn		0		0				0.06		0.03			
PbO	Pb		0		0				0.99		0.47			
SO3	S		0		0				1.54		0.89			
ZnO	Zn		0		0				0		0.09			
ZrO2	Zr		0		0.21				0.14		0.08			
P2O5	P	16.19	673.75	0.23	674.52	0.23	0.230		931.65	0.23	985.9	0.23	0.230	
As2O3	As													
NiO	Ni		0		0.22				0.45		0.27			
F	F													
Cl	Cl													
B2O3	B		0.24		0.25				0.16		0.11			
CdO	Cd		0		0				0.06		0.03			
Sb2O3	Sb													
Cs2O	Cs	35	1536	2.591	1812	3.056	2.823		3012.5	5.081	2937.5	4.954	5.017	
HgO	Hg													
SrO	Sr		0		0				0		0.02			
CaF2	Ca													
Bi2O3	Bi								0		0.3			
Nd2O3	Nd		0.52		0.94				1.14		0.51			
Li2O	Li	5	187.83	4.044	139.14	2.996	3.520		185.14	3.986	239.11	5.148	4.567	
	total	100.00												

LVC-16HT			7 DAY						28 DAY					
Chemical	Element	Oxide	Sample C		Sample D				Sample C		Sample D			
		Wt %	ug/ml	L (g/m^2	ug/ml	L (g/m^2	Ave	pH	ug/ml	L (g/m^2	ug/ml	L (g/m^2	Ave	pH
SiO2	Si	34.42	28.56	0.089	28.54	0.089	0.089	9.92	45.4	0.141	33.33	0.103	0.122	10.06
Al2O3	Al	9.39	12.95	0.130	13.01	0.131	0.131	9.65	14.83	0.149	13.23	0.133	0.141	9.95
Fe2O3	Fe		0.16		0.12				0.13		0.95			
CaO	Ca		0		0.13			9.79	0.39		0.83			10.01
Na2O	Na		2.99		2.81				2.8		3.34			
MgO	Mg		1.04		0.52				0.17		0.82			
K2O	K		31.47		14.55				3.15		18.16			
TiO2	Ti		0.07		0.05				0.02		0.04			
BaO	Ba		0.04		0.03				0.03		0.06			
Ce2O3	Ce		0.83		0.37				0.09		0.52			
Cr2O3	Cr		0		0				0.04		0.31			
CuO	Cu		0.11		0.06				0.02		0.06			
MnO	Mn		0		0				0		0.04			
PbO	Pb		0		0				0		0.5			
SO3	S		0		0				0		0.91			
ZnO	Zn								0		0.07			
ZrO2	Zr		0		0				0.02		0.06			
P2O5	P	16.19	235.42	0.23	247.66	0.23	0.230		275.28	0.23	243.04	0.23	0.23	
As2O3	As													
NiO	Ni		0.21		0.13				0.06		0.27			
F	F													
Cl	Cl													
B2O3	B		0.21		0.11				0.04		0.08			
CdO	Cd		0		0				0.01		0			
Sb2O3	Sb													
Cs2O	Cs	35	490.8	0.828	498	0.840	0.834		505	0.852	518.75	0.875	0.86	
HgO	Hg													
SrO	Sr		0		0				0.01		0			
CaF2	Ca													
Bi2O3	Bi		0		0				0.08		0			
Nd2O3	Nd		1.01		0.46				0.12		0.65			
Li2O	Li	5	87.31	1.880	92.83	1.999	1.939		127.97	2.755	103.11	2.220	2.49	
	total	100.00												

LVC-17Q			7 DAY						28 DAY					
Chemical	Element	Oxide	Sample C		Sample D				Sample C		Sample D			
		Wt %	ug/ml	L (g/m^2	ug/ml	L (g/m^2	Ave	pH	ug/ml	L (g/m^2	ug/ml	L (g/m^2	Ave	pH
SiO2	Si	38.46	287.23	0.798	276.07	0.767	0.782	11.85	292.19	0.812	342.53	0.952	0.882	11.99
Al2O3	Al	16.12	115.58	0.677	110.74	0.649	0.663	11.82	11.78	0.069	11.24	0.066	0.067	11.94
Fe2O3	Fe		0.12		0.13				1.14		1.19			
CaO	Ca		0		0			11.84	0.82		0.87			11.97
Na2O	Na		6.26		6.09				56.56		56.32			
MgO	Mg		0.31		0.45				0.85		0.92			
K2O	K		8.57		13.36				21.04		23.8			
TiO2	Ti		0.02		0.03				0.1		0.11			
BaO	Ba		0		0.02				0.05		0.05			
Ce2O3	Ce		0.24		0.34				0.53		0.59			
Cr2O3	Cr		0		0				0.45		0.47			
CuO	Cu		0.04		0.05				0.06		0.07			
MnO	Mn		0		0				0.04		0.04			
PbO	Pb		0		0				0.42		0.46			
SO3	S		0.64		0.61				12.71		12.9			
ZnO	Zn		0		0				0.1		0.09			
ZrO2	Zr		0		0				0.06		0.06			
P2O5	P		0.56		0.53				0		0			
As2O3	As													
NiO	Ni		0		0.11				0.3		0.32			
F	F													
Cl	Cl													
B2O3	B		0.11		0.12				0.24		0.27			
CdO	Cd		0		0				0.04		0.04			
Sb2O3	Sb													
Cs2O	Cs	35.42	385.2	1.162	384	1.158	1.160		4200	12.668	4262.5	12.857	12.763	
HgO	Hg													
SrO	Sr		0		0									
CaF2	Ca													
Bi2O3	Bi		0		0				0.32		0.36			
Nd2O3	Nd		0.33		0.47				0.7		0.77			
Li2O	Li	10	310.36	3.341	292.35	3.147	3.244		913.24	9.831	951.61	10.244	10.037	
	total	100.00												

LVC-17HT			7 DAY						28 DAY					
Chemical	Element	Oxide	Sample C		Sample D				Sample C		Sample D			
		Wt %	ug/ml	L (g/m^2	ug/ml	L (g/m^2	Ave	pH	ug/ml	L (g/m^2	ug/ml	L (g/m^2	Ave	pH
SiO2	Si	38.46	265.45	0.737	473.06	1.314	1.026	11.68	566.97	1.575	239.61	0.666	1.120	11.75
Al2O3	Al	16.12	118.57	0.695	344.83	2.021	1.358	11.65	341.66	2.002	105.89	0.621	1.312	11.75
Fe2O3	Fe		0.17		0.52				1.53		0.92		0.000	
CaO	Ca		0		0.52			11.67	1.54		0.82		0.000	11.75
Na2O	Na		11.93		13.82				27.83		16.28		0.000	
MgO	Mg		0.47		0.52				0.85		0.82		0.000	
K2O	K		13.92		13.82				16.99		19.05		0.000	
TiO2	Ti		0.04		0.09				0.1		0.05		0.000	
BaO	Ba		0.02		0.04				0.06		0.04		0.000	
Ce2O3	Ce		0.38		0.37				0.48		0.52		0.000	
Cr2O3	Cr		0		0				0.44		0.31		0.000	
CuO	Cu		0.06		0.07				0.08		0.07		0.000	
MnO	Mn		0.02		0.03				0.06		0.04		0.000	
PbO	Pb		0		0				0		0		0.000	
SO3	S		3.2		3.45				7.15		4.55		0.000	
ZnO	Zn		0		0				0.13		0.13		0.000	
ZrO2	Zr		0		0.06				0.07		0.06		0.000	
P2O5	P		6.99	0.23	7.47	0.23	0.230		11.11	0.23	6.67	0.23	0.230	
As2O3	As												0.000	
NiO	Ni		0.13		0.19				0.38		0.26		0.000	
F	F												0.000	
Cl	Cl												0.000	
B2O3	B		0.2		0.23				0.3		0.19		0.000	
CdO	Cd		0		0				0.09		0.04		0.000	
Sb2O3	Sb												0.000	
Cs2O	Cs	35.42	40.68	0.068	850.8	1.418	0.743		495	0.825	93.63	0.156	0.490	
HgO	Hg												0.000	
SrO	Sr		0		0.02				0.03		0		0.000	
CaF2	Ca												0.000	
Bi2O3	Bi		0		0.4				0.46		0.35		0.000	
Nd2O3	Nd		0.48		0.52				0.67		0.68		0.000	
Li2O	Li	10	182.71	1.967	309.46	3.331	2.649		419.07	4.511	198.25	2.134	3.323	
	total	100.00												

Distribution

No. of Copies

Offsite

2 DOE/Office of Scientific and Technical Information

G.C.S. Ordaz
U.S. Department of Energy
Office of Science and Technology
Germantown, MD 29874

M. J. Steindler
Argonne National Laboratory
Bldg. 205
9700 S. Cass Avenue
Argonne, IL 60439-4837

J. K. Bates
Argonne National Laboratory
Bldg. 205
9700 S. Cass Avenue
Argonne, IL 60439-4837

J. C. Cunnane
Argonne National Laboratory
Bldg.205
9700 S. Cass Avenue
Argonne, IL 60439-4837

C. M. Jantzen
Westinghouse Savannah River Co.
Savannah River Technology Center
Bldg 707-C, P.O. Box 616
Aiken, SC 29808

I. L. Pegg
The Catholic University of America
Vitreous State Laboratory
620 Michigan Avenue, N.E.
Washington, DC 20064

D. F. Bickford
Westinghouse Savannah River Co.
Savannah River Technology Center
Bldg 707-C, P.O. Box 616
Aiken, SC 29808

A. Barkatt
The Catholic University of America
Chemistry Department
620 Michigan Avenue, N.E.
Washington, DC 20064

Rod Ewing
Dept Nuclear Engineering and
Radiological Sciences
The University of Michigan
2355 Bonisteel Boulevard
Ann Arbor, Michigan 48109-2104

L. Wang
Dept Nuclear Engineering and
Radiological Sciences
The University of Michigan
2355 Bonisteel Boulevard
Ann Arbor, Michigan 48109-2104

W. Lutze
University of New Mexico
Department of Chemical and Nuclear
Engineering, Farris Engineering Center
Room 209
Albuquerque, NM 87131-1341

D. M. Strachan
Argonne National Laboratory
Chemical Technology Division
9700 S. Cass Avenue
Argonne, IL 60439-4837

D. Clark
University of Flordia
Dept of MSE
136 MAE, PO Box 116400
Gainesville, FL 32611-6400

W. Gong
University of New Mexico
Farris Engineering Center
Room 209
Albuquerque, NM 87131-1341

No. of Copies

Onsite

4 **DOE Richland Operations Office**

T. L. Aldridge, K8-50
R.A. Pressentin, K8-50
S.N Saget, K8-50
D. A. Brown, K8-50

16 **Pacific Northwest National Laboratory**

B. C. Bunker, K2-45
X. Feng, P8-37 (5)
M. Gong, P7-41
J. Vienna, P-8-37
H. Li, P8-37
Joe Perez, P7-41
P. Hrma, P8-37
Technical Report Files (5)